Developing Mass Transfer Based Model for Predicting VOCs Emission from Building Materials

LI Feng

Department of Building Services Engineering,
The Hong Kong Polytechnic University

A thesis submitted in partial fulfillment of the requirements for the Degree of Doctor of Philosophy

January, 2006

Certificate of Originality

I hereby declare that this thesis is my own work and that, to the best of my knowledge and belief, it reproduces no material previously published or written, nor material that has been accepted for the award of any other degree or diploma, except where due acknowledgement has been made in the text.

LI Feng

Department of Building Services Engineering
The Hong Kong Polytechnic University
Hong Kong SAR, China
January, 2006

Abstract

Abstract of thesis entitled: Developing Mass Transfer Based Model for Predicting VOCs Emission from Building Materials

Submitted by : LI Feng

For the degree of : Doctor of Philosophy

at The Hong Kong Polytechnic University in January, 2006.

Modern people spend most of their time indoors. Many of them do not realize that the air they breathe indoors may be more polluted than the air they breathe outdoors. There are a variety of sources of indoor air pollution. Building interior materials have been identified as significant indoor VOC (Volatile Organic Compounds) sources. It has been demonstrated that inhalation of VOC may cause a variety of adverse health effects.

Selecting low-emission building products is a more cost-effective solution to improve indoor air quality (IAQ), compared with ventilation method which is energy-intensive in both cold and hot, humid climates. Current standards only require that the VOCs emission rate profile be documented. The problem is that the emission rate thus obtained is test-condition specific, and can only be used to compare and rank the emission strengths between the tested samples under the specific test conditions, but cannot be extended to predict the VOCs concentrations in a real building. To evaluate the actual impact of a particular material on indoor VOCs concentration, modeling methods based upon mass transfer theories are required.

A simplified yet physically-based model is developed to predict VOCs emissions from wet materials like paints. To validate the proposed model, the European standard emission test cell called field and laboratory emission cell (FLEC) is

adopted, in view of its low cost and good repeatability, and potential to be adopted as a standard in Asia. Locally bought water-based emulsion paint is tested in the FLEC, and experimental results agree well with the model predictions. The proposed model is easy to scale up because the parameters involved have distinct physical meanings.

Regarding dry building materials, very few data on the key parameters, particularly the diffusion and sorption parameters, are available now. Different methods have been developed for the experimental determination of these parameters for a variety of VOC/material combinations, but large discrepancies exist due to the limitations of the test methods and data analysis techniques. In this study, FLEC is used to inversely determine the model parameters required for dry building materials, and also to validate the model.

Fundamental mass-transfer method is applied to analyze the VOCs emission processes in a standard test cell for dry building materials and then an inverse method is developed and utilized to analyze the recorded FLEC exhaust VOCs concentration profiles to determine the corresponding mass transfer parameters. The inverse parameter estimation method developed in this research is solved by the well-known Levenberg-Marquardt (LM) optimization algorithm and allows accurate determination of several parameters simultaneously. The inverse method is validated regarding the uniqueness, stability and accuracy by using synthetically generated series-of-measurements. Then real measured data for selected VOCs/materials are processed using the proposed method. The VOCs/material properties identified in this way are independent of test conditions.

Another important parameter to be determined is the VOCs initial condition within the material which is very likely to be non-uniform. To date, there is only one

reported experimental method, which requires special equipments. However, the reported method was destructive to the test sample and possible loss of VOCs might occur during sample preparation and analysis. Further, the obtained VOCs distribution within the material was in a discrete form. In this research, an inverse function estimation method - conjugate method of minimization with the adjoint problem, in conjunction with an environmental chamber or the non-destructive test facility - FLEC, is developed to figure out the VOCs' initial condition within the dry building material. The proposed method can be non-destructive to the test material if using FLEC and the distribution obtained is in a continuous form.

On the basis of a single component multi-layer model, a comprehensive VOCs source/sink model is developed and applied to predict the level of VOCs concentration, so that proper selection criteria can be set up based upon the health impact, and applicable IAQ control strategies can be evaluated. Unlike existing models, the comprehensive model developed in this research takes various conditions into consideration and thus can handle different building scenarios. Currently, the model can deal with different ventilation modes, multi-component and multi-layer material, porous/non-porous materials, non-uniform initial VOCs distributions, and transient outdoor air VOCs concentration. It can be used as a decision-making tool for assessing the impact of material emissions on indoor air quality under various ventilation conditions.

Publications arising from the thesis

I. Papers in Refereed Journals

- **Feng Li**, Jianlei Niu, Lizhi Zhang, 2006. A physically-based model for prediction of VOCs emissions from paint applied to an absorptive substrate. ***Building and Environment*** Vol. 41, No.10, pp. 1317-1325. (based on Chapter 3)

- **Feng Li** and Jianlei Niu, 2005. Simultaneous estimation of VOCs diffusion and partition coefficients in building materials via inverse analysis. ***Building and Environment*** Vol. 40, No.10, pp. 1366-1374. (based on Chapter 4)

- **F. Li** and J. L. Niu, 2005. An inverse technique to determine volatile organic compounds diffusion and partition coefficients in dry building material. ***Heat and Mass Transfer*** Vol. 41, No. 9, pp. 834-842. (based on Chapter 4)

- **Feng Li** and Jianlei Niu, 2005. An inverse approach for estimating the initial distribution of volatile organic compounds in dry building material. ***Atmospheric Environment*** Vol. 39, No. 8, pp. 1447-1455. (based on Chapter 5)

II. Papers in Refereed Conferences

- **F. Li** and J.L. Niu, Further Development of a Single-Zone Multi-component Multi-layer Model for Characterizing VOCs Source/Sink Behaviors in a Room. ***Healthy Buildings 2006***, vol. 4, pp. 95-98, 4-8 June, 2006, Lisboa, Portugal. (Based on Chapter 7)

- **F Li** and JL Niu, Determination of VOCs Diffusion and Partition Coefficients in Dry Building Material from Time-dependent Sorption Data. ***Proceedings of the 10th International Conference on Indoor Air Quality and Climate: Indoor Air 2005***, vol. 3, pp. 2701-2706, 4-9 September 2005, Beijing, P.R. China. (based on Chapter 4)

- **F Li** and JL Niu, Numerical Simulation of VOCs Emissions from Multi-Layer Porous/Non-porous Building Material Assemblies. ***Proceedings of the 10th International Conference on Indoor Air Quality and Climate: Indoor Air 2005***,

vol. 3, pp. 2707-2712, 4-9 September 2005, Beijing, P.R. China. (based on Chapter 6)

- **F. Li** and J. L. Niu, Evaluating the Impacts of Some Major Factors on Indoor VOCs Concentration Following Application of the Paint. ***Joint Symposium 2005 New Challenges in Building Services***, pp. 43-50, 15 November 2005, Hong Kong. (based on Chapter 3)

III. Manuscripts in Progress

Feng Li and Jianlei Niu, Control of volatile organic compounds in indoor environment: development of an integrated mass-transfer-based model and its application. [Submitted to ***Atmospheric Environment***] (Based on Chapter 7)

Acknowledgements

I must express my grateful thanks to my Chief Supervisor, Dr. Niu Jianlei, and my Co-supervisor, Prof. Chan Wai-tin, Daniel, from the Department of Building Services Engineering, The Hong Kong Polytechnic University, for their readily available supervisions, valuable suggestions, patient guidances, continuous helps and encouragements throughout the course of the work.

I highly appreciate senior technician Mr. Lau Wai-pang and technician Mr. Hung Kit in the department, for their assistance in laboratory work. Thanks also go to Mr. Chu Chi Man, a part-time student from the BSE department for measuring TVOC concentration data. Useful discussions with Prof. Luo Rui from Tsinghua University, and Prof. Zhang Lizhi from South China University of Technology, are highly appreciated.

Finally I would like to express my deepest appreciation to my family and my beloved wife, Li Dan, for their love, encouragement, moral support and understanding.

Table of Contents

List of Figures

List of Tables

Nomenclature

Variable	Description	Unit
C_{ad}	Adsorbed phase concentration	kg m^{-3}
C_g	Gas phase concentration in the pores	kg m^{-3}
K_p	Partition coefficient	
C_{ad}^0	Surface concentration corresponding to complete coverage by a single monolayer	kg m^{-3}
K_L	Langmuir constant	
C_{sat}	Gas phase concentration corresponding to saturated condition	kg m^{-3}
K_{BET}	BET constant	
K_F , n	Fitting parameters of Freundlich model	
r_p	Pore radius	m
D_{AB}	Molecular diffusivity	m^2 s^{-1}
T	Temperature	^{o}C
$D_{K,A}$	Knudsen diffusivity	m^2 s^{-1}
D_c	Combined diffusivity in the transition regime	m^2 s^{-1}
D	Gas phase diffusivity	m^2 s^{-1}
J	Diffusive flux	kg m^{-3} s^{-1}
K_s	Sorption coefficient	
$D_{e,g}$	Effective gas-phase diffusivity	m^2 s^{-1}
$D_{e,s}$	Effective surface diffusivity	m^2 s^{-1}
C_{in} , C_{OA}	VOCs concentration in the supply air	kg m^{-3}
Q	Airflow rate	ml min^{-1}
V	Volume	m^3
A	Area	m^2
E	Emission factor	mg m^{-2} h^{-1}
N , ACH	Air change rate	h^{-1}
C_a	VOCs concentration in bulk chamber/room air	kg m^{-3}

C_{as}	VOCs concentration in the boundary layer air	kg m^{-3}
L	Loading factor: ratio of nominal material surface area to the chamber/room volume	m^2 m^{-3}
k_g , h_m	Mean convective mass transfer coefficient	m s^{-1}
K_e	Paint film-air equilibrium constant	m
M	VOCs mass per unit area of the wet film	kg m^{-2}
M_0	Initial VOCs mass per unit area of the wet film	kg m^{-2}
D_s	Diffusivity of the substrate material	m^2 s^{-1}
K_{sa}	Substrate-air partition coefficient	
C_s	VOCs concentration in the substrate	kg m^{-3}
C_{s0}	Initial VOCs concentration in the substrate	kg m^{-3}
D_m	Material phase diffusivity	m^2 s^{-1}
K_{ma}	Material-air partition coefficient	
C_m	VOCs concentration in the material	kg m^{-3}
C_{m0}	Initial VOCs concentration in the material	kg m^{-3}
Re	Reynolds number	
Sc	Schmidt number	
Sh	Sherwood number	
u_m	Mean air velocity of the air over the material	m s^{-1}
$\boldsymbol{S}$	Objective functional	
J(P)	Sensitivity matrix	
$\mathbf{Y_{exa}}$	Generated errorless measurements	kg m^{-3}
f	Recirculation air fraction	
E_f	Efficiency of the in-duct filter	
CADR	Clean air delivery rate of a portable air cleaner	l s^{-1}
D_a	Diffusivity of VOCs in air	m^2 s^{-1}
a_T , a_{FA} , a_I , a_P , a_N , a_S , a_Z , a_B	Coefficients in discretized equations	

Greek symbols

β	Search step size	
λ	Mean free path	m
ε	Porosity	
δ	Constrictivity	
τ	Tortuosity	
υ	Kinematic viscosity of the air	$m^2\ s^{-1}$
$\boldsymbol{\omega}$	Random variable	
σ	Standard deviation of the measurement errors	
$\nabla\mathcal{S}$	Gradient of the objective functional	
$\lambda(x,t)\,,\lambda_a(t)$	Lagrange multipliers	
γ	Conjugate coefficient	
ρ	Density	$kg\ m^{-3}$

Superscripts

T	Transpose
k	Iterative number
0	Denotes the known values at the last time step

Subscripts

i, j, k	i^{th} component, j^{th} layer, k^{th} node
0	Denotes initial conditions

Chapter 1
Introduction

1.1 Sources of Indoor Air Pollution

Although most people take it for granted that their homes, workplaces, and schools are safe places to stay, recent scientific evidences show that there are various sources of indoor air pollution. Figure 1.1 shows the schematic drawing of potential sources of pollution in a typical office building.

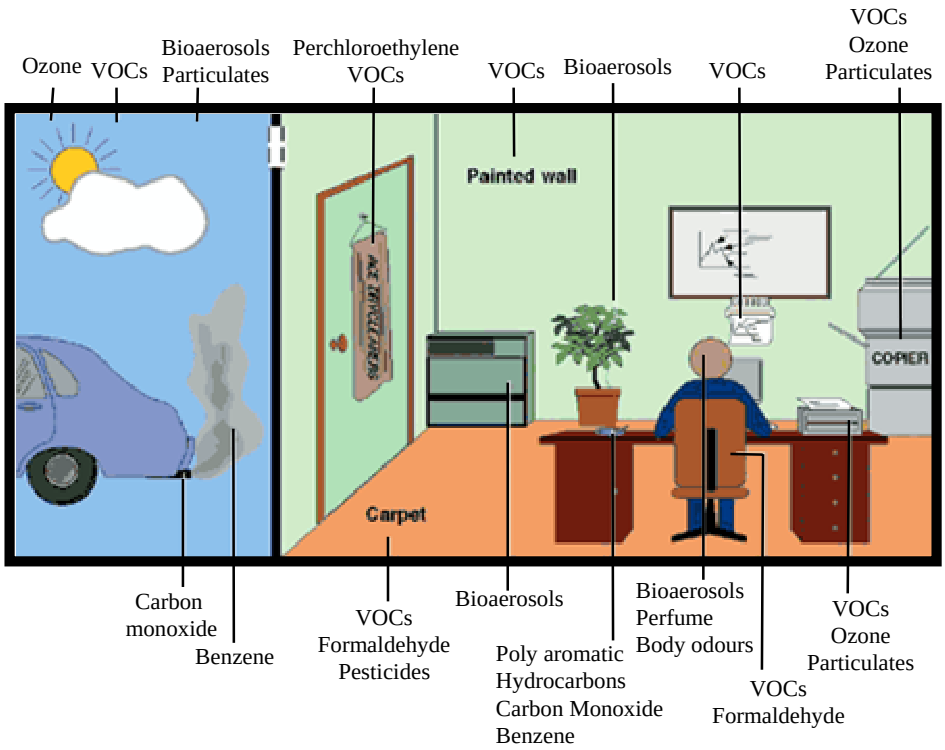

Figure 1.1 Primary sources of indoor air pollution in a typical office building [extracted from: (EPA, 1994)]

The primary sources come from: outdoor air (e.g. vehicle exhaust); building, construction, furnishing materials and equipments (e.g. carpet, paint, copier and computer); building occupants and activities (e.g. smoking); inadequate building design and maintenance (e.g. HVAC system).

Furthermore, the U.S. Environmental Protection Agency (EPA) demonstrates that air within homes and other buildings may be much more polluted than the air outside. The U.S. EPA also estimates that indoor levels of pollutants can be two to five times higher (EPA, 1994) (and occasionally more than 100 times higher) than outdoor levels. A recently experimental study conducted by Zhu et al. (2005) also confirmed that the I/O ratios of selected VOCs in residential air in the city of Ottawa, Canada were greater than 1 for virtually all analytes and were as high as 150.

1.2 Time Budget People Spend Indoors

Figure 1.2 shows the mean percentage of time the U.S. National Human Activity Pattern Survey (NHAPS) respondents spent in six different locations on the diary day.

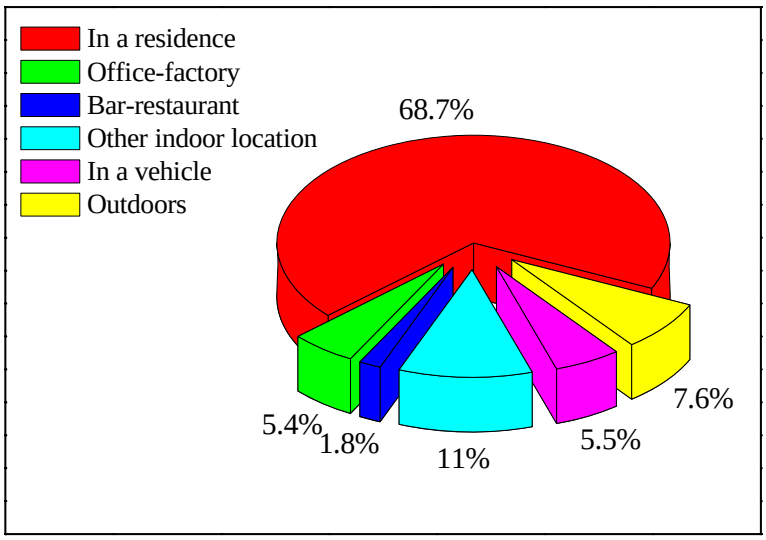

Figure 1.2 Pie chart showing the mean percentage of time the NHAPS respondents spent in six different locations on the diary day (weighted) [extracted from: (Klepeis et al., 2001)]

This survey was conducted by the University of Maryland Survey Research Center with support from U.S. EPA. The survey via telephone interviewing began in late

September 1992, ended on October 1, 1994. NHAPS respondents reported spending an average of 86.9% of their time in enclosed buildings (Klepeis et al., 2001).

Regarding Hong Kong, in the period between April and August, 1998, Chau et al. also conducted a survey to investigate the time spending pattern for the Hong Kong people. A random population survey sample was drawn from the 1998 residential telephone directory in Hong Kong, with a 7-day recall questionnaire survey used for collecting time diaries of surveyed subjects (Chau et al., 2002). The results illustrated in Figure 1.3 show that Hong Kong people spend an average of 89% of their time in indoor environments.

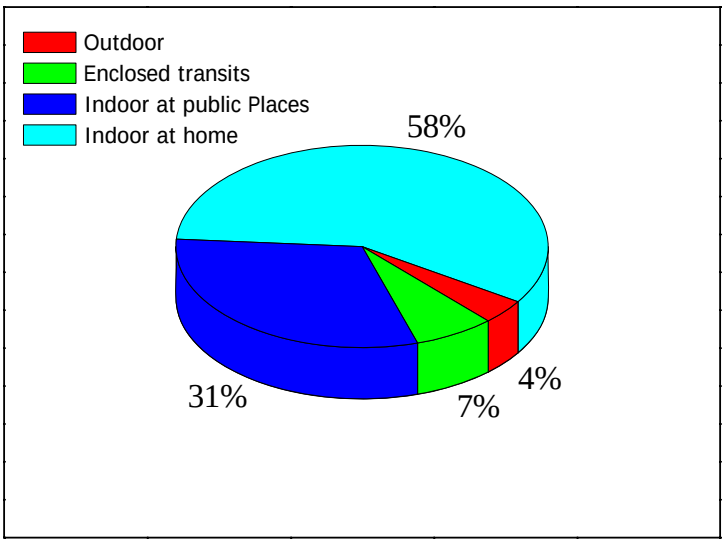

Figure 1.3 Percentage of time spent in major locations by Hong Kong people [extracted from: (Chau et al., 2002)]

Although the time people spend indoors may vary from region to region, people to people, and season to season, generally speaking, the **American Lung Association** estimates most people spend 60-90% of their time indoors.

1.3 Sick Building Syndrome (SBS) and Building Related Illnesses (BRI)

High indoor concentrations, coupled with the fact that people spend a large fraction of time indoors (Zhang and Smith, 2003), there have been an increasing number of studies (Molhave, 1989; Molhave, 1991; Mendell, 1993; Wieslander et al., 1996; Knudsen et al., 1999; Fanger, 2000; Klepeis et al., 2001; Seppanen and Fisk, 2002; Mendell, 2003; Bako-Biro et al., 2004; Engvall et al., 2005; Mendell and Heath, 2005) focusing on discomfort or illnesses arising from indoor environments. Such problems are generally divided into the following categories: sick building syndrome (**SBS**) and building related illnesses (**BRI**).

"The term 'sick building syndrome' (SBS) is used to describe situations in which building occupants experience acute health and comfort effects that appear to be linked to time spent in a building, but no specific illness or cause can be identified. The complaints may be localized in a particular room or zone, or may be widespread throughout the building" (EPA, 1994).

"The term 'building related illness' (BRI) is used when symptoms of diagnosable illness are identified and can be attributed directly to airborne building contaminants" (EPA, 1994).

1.4 Building Materials and Volatile Organic Compounds (VOCs)

Recent scientific studies show that many materials used in buildings, either as structural materials or as furnishings, are the main sources of indoor air pollution, due to their large surface areas and their permanent exposure to indoor air (Haghighat and Donnini, 1993; EPA, 1994). Table 1.1 summarizes some common

materials and their possible emissions, as well as the health effects of the emitted pollutants.

It is believed that a major contributory factor to SBS is the presence of chemicals such as volatile organic compounds (VOCs) and formaldehyde in indoors (Oliver and Shackleton, 1998), particularly in new or newly renovated buildings, which often have substantial amounts of building and furnishing materials that emit VOCs. Organic compounds in indoor air are extremely diverse. Although most occur in extremely low concentrations, impact on health can be significant and some may be carcinogenic. More than 350 VOCs have been recorded at concentrations exceeding 1 ppb in indoors (Jones, 1999).

Table 1.2 shows the World Health Organization (WHO) classification of organic compounds (WHO, 1986). The class of VOCs is organic compounds with boiling points from 50 to 100°**C** up to 240-260°**C** depending on the sampling and analytical techniques. They comprise a range of substances including alkanes, alkenes, aromatic hydrocarbons, chlorinated hydrocarbons, esters and alcohols (derived in part from microbiological sources), aldehydes and ketons (many from precursor terpene compounds and fatty acids) (Ellacott and Reed, 1999).

VOCs are volatile at normal room temperatures, and whose vapors are readily inhaled. Inhalation of VOCs may have adverse health effects. Acute symptoms of VOC exposure can be: eye irritation/watering, nose irritation, throat irritation, headaches, nausea/vomitting, dizziness, asthma exacerbation. Chronic symptoms are: cancer, liver damage, kidney damage, central nervous system damage (EPA, 1994).

Table 1.1 Interior materials and their pollutant emissions and health concerns [modified from: (Niu and Burnett, 2001)]

Materials	Pollutants emitted	Contributed indoor concentrations	Health effects
Earth-derived materials- brick, concrete, and titles	radon	ventilation rate-dependent, up to 1000 Bq m^{-3}	lung cancer, particularly for smokers
Asbestos-fire-proofing materials	asbestos fibers		lung disease: asbestosis, cancer
Adhesives, sealants, and architectural coating, paintings	variety of VOCs	usually at parts-per-billion levels, unusually high concentrations occur	species-dependent, likely causes of SBS
Particleboard and plywood	formaldehyde	parts-per-billion to parts-per-million levels	membrane irritation, suspected carcinogens
Carpet, resilient flooring, and wall covering	variety of VOCs	usually at parts-per-billion levels	species-dependent, likely causes of SBS
Insulations, acoustical ceiling tile, and furnishing	VOCs, particulate contaminants		cardiovascular and respiratory diseases and lung cancer

Table 1.2 WHO classifications of organic compounds [modified from: (WHO, 1986)]

Abbreviation	**Description**	**Boiling point range ($^{o}C^{*}$)**	**Sampling method typically used in field studies**
VVOC	Very volatile (gaseous) organic compounds	< 0 to 50-100	Batch sampling adsorption on charcoal
VOC	Volatile organic compounds	50-100 to 240-260	Adsorption on Tenax, carbon molecular black or charcoal
SVOC	Semivolatile organic compounds	240-260 to 380-400	Adsorption on polyurethane foam or XAD-2
POM	Organic compounds associated with particulate matter or particulate organic matter	> 380	Collection on filters

*Polar compounds appear at the higher end of the range.

The impact of increased consciousness about our indoor environment has created a demand for low-emitting (healthy) building materials (Zhang and Niu, 2003c). However, basically there are few emission-free building materials, except glasses or stainless steels. The emission rates and the number of compounds emitted can vary by a magnitude of several orders among different common interior materials even within the same category of products, and different countries have different sets of rules on testing and labeling the indoor climate (Niu and Burnett, 2001). There is a great need of standardized VOCs emission test methods as well as accurate mathematical modeling tools to aid in selecting healthier materials and evaluating and implementing proper indoor air quality control strategies.

1.5 The Purposes

The aim of this research is therefore to develop mathematical models that can be used to estimate indoor VOCs concentrations originating from emissions from building materials in their actual use conditions. To this end, a comprehensive physical model will be developed that explicitly includes the effects of sorption/desorption, diffusion, and convection mass transfer processes, as well as the ventilation strategies. The European standard emission test cell, called the field and laboratory emission cell (FLEC) will be used to experimentally determine the material properties, and to help to validate the developed models.

1.6 The Key Issues and the Problems Being Addressed

The key issues are: 1) Adverse health effects, as reflected as sick building syndrome (SBS), defined by the WHO or EPA, are related to indoor air pollution; 2) IAQ control by outdoor air ventilation is energy-intensive in both cold and hot-humid

climates; 3) IAQ improvements by proper selection of building interior materials, and pre-occupancy “flush-out” after construction and renovation are more cost-effective engineering solutions. To realize this strategy, characterizing VOCs emissions from building materials is essential. Existing methods for this use can be classified into three categories: 1) specifying and limiting VOCs content contained in the material, 2) testing and limiting the area-specific emission rates as found in a standard test chamber or test cell, and 3) predicting the VOCs concentration via mass balance and mass transfer modeling. In nature, these three methods are related to each other. However, there is still a lack of such links between these methods, which is the key issue being addressed in this research. In particular, the emission test cell method, one of the two European standard methods, is most likely to be introduced into Asian countries due to its low cost and good repeatability.

1.7 Outcomes and Significances

A comprehensive model capable of simulating indoor VOCs concentrations in the presence of various building materials will be established. Methods of determining required model input parameters will be developed to make the model applicable. The significance of the model is that the effects of potential IAQ management strategies like pre-occupancy ‘flush-out’ or lead-time provision of ventilation etc. can be quantitatively estimated, with the potential health impacts assessed at the same time. The results can also be fed back to the manufacturers for reformulation of the related products. This will eventually lead to improved IAQ, reduced energy consumption and reduced adverse impacts on people’s health and productivity.

1.8 Thesis Structure

The thesis begins with a brief introduction of the backgrounds of the indoor air pollution, the purposes, the key issues, potential outcomes and significances of the research. The outline of the thesis is presented at the end of this chapter.

Chapter 2 presents a critical review on the classification of building materials, the mechanisms of mass transfer, the experimental and modeling approaches for characterizing the source/sink behaviors of VOCs in building materials, as well as the methods of determining key model parameters. Special attention is paid to modeling approaches and methods of parameter determination.

In Chapter 3, a simplified mass transfer theory based model for predicting VOCs emissions from wet materials like paints applied on substrate material is developed. The major factors that have substantial impacts on the emission behavior of VOCs from the wet material are demonstrated through a series of simulations utilizing the proposed model. Proper strategies for controlling the indoor VOCs concentration are proposed and discussed.

In Chapter 4, a so-called inverse method for the determination of the diffusion and partition coefficients is developed. The proposed method is firstly validated and assessed through parametric studies, then two experimental methods capable of obtaining the required concentration data are presented - one is VOCs emission test in a FLEC, and the other is sorption test in a FLEC. The real measurements are then utilized to obtain the corresponding emission parameters via inverse analyses.

Chapter 5 discusses a realistic problem: the VOCs initially containing in dry building materials are seldom uniformly distributed. However, previous models usually

assume a uniform initial condition. This simplification will cause large error for short-term predictions. In this chapter, a model that can handle non-uniform initial condition is developed. Meanwhile, an inverse function estimation method is therefore developed to figure out how VOCs are initially distributed within a dry building material.

Building materials usually exist in composite forms, such as wall or floor assemblies, etc. In Chapter 6, a model is developed to predict VOCs emissions from a multi-layer material assembly. The individual layers of materials can be either porous or non-porous materials. The model explicitly takes ventilation strategy into consideration.

Then a more realistic situation is under consideration - i.e. a real room composed of different components (side walls, floor and ceiling). Based on the single component multi-layer model developed in the previous chapter, Chapter 7 extends the model into a multi-component multi-layer multi-phase model. A variety of ventilation strategies are evaluated by utilizing the proposed model.

Chapter 8 summaries the main conclusions and achievements of the researches reported in this thesis and gives recommendations for future application and research work in the related areas.

Chapter 2
Literature Review

2.1 Classification of Building Materials

2.1.1 Classification according to Physical States

According to the physical states at room temperature a variety of building materials in indoors can be divided into two categories: **wet materials** and **dry materials**.

2.1.1.1 Wet Material

Wet materials usually exist in fluid form before they are applied and exhibit a particular curing stage from wet, to partially wet and dry after applications. Paints, varnishes, wood stains, adhesives, caulks, and sealants etc. are typical materials in this category. Wet materials are typically characterized by very high initial emissions followed by much lower emissions (Low et al., 1998; Guo and Murray, 2000; Sparks, 2001). This is because most solvents and other chemicals within wet materials are at or near the surface of the material and thus have emission bursts during and after application.

2.1.1.2 Dry Material

It is no doubt that the majority of indoor building materials are **dry materials**, such as wall assembly (concrete, brick, and wallpaper etc), floor coverings (carpet, vinyl flooring, linoleum and wood flooring etc.) and ceiling materials (gypsum board and acoustics tile, etc.). These materials usually emit VOCs at low emission rates and the slow emissive periods last for several months to several years or even the entire life

of usage because the VOCs must migrate by diffusion from the deep within the materials to the surfaces before they can evaporate into the air.

2.1.2 Classification according to Microstructures

Dry building materials can be further classified into **non-porous materials** and **porous materials** according to the interior microstructures. Though most materials are to some extent porous and it is quite difficult to find or prepare a truly non-porous solid, some materials, for example, metals, glass, and hard plastics can be practically treated as homogenous systems, i.e., non-porous materials.

According to the International Union of Pure and Applied Chemistry (IUPAC) classification, pores are categorized as micropores, mesopores and macropores based on pore diameters as shown in Table 2.1:

Table 2.1 IUPAC pore size classification

Category	Pore diameter
micropores	$d < 20$ Å
mesopores	20 Å $< d <$ 500 Å
macropores	$d > 500$ Å

where the Ångström unit, Å, is used for the atomic scale. (1 nm = 10 Å)

Generally speaking, most of the typically used building materials are porous (even very porous) materials, such as wood, concrete, plaster, ceiling tiles, insulation, and wallboard (drywall, sheetrock, or gypsum board). Mass transfer mechanisms within porous materials are far more sophisticated than in non-porous materials. Table 2.2 shows the mean pore diameters and porosities of some typical building materials determined by Blondeau et al. (2003) from mercury intrusion porosimetry (MIP)

tests. It can be seen that the mean pore diameter varies greatly from material to material, even for the materials in the same category.

Table 2.2 Pore size and porosity of some typical building materials [extracted from: (Blondeau et al., 2003)]

Material	Porosity ε (%)	Mean pore diameter (μm) (Volume weighted)
Particle board	25.82	70.25
Aerated concrete	29.9	66.03
Solid concrete	10.4	0.96
Brick	17.1	1.98
Mortar	22.6	0.07
Gypsum board (From Denmark)	27.7	10.54
Gypsum board (From France)	29.5	1.41

2.1.3 Classification according to the Direction of VOCs' Migration

Building materials, which have been developed mainly from the viewpoint of construction and energy conservation, have been acknowledged as major VOC emission sources indoors (Girman et al., 1986; Wallace et al., 1987; Clausen et al., 1991; Chang and Guo, 1992; Salthammer, 1997; Yu and Crump, 1998; Cox et al., 2002; Zhang et al., 2002a; Afshari et al., 2004).

Evidence from a variety of investigations and systematic studies suggests that building materials can also affect the transport and removal of indoor VOCs by adsorption and desorption (Colombo et al., 1993; Chang et al., 1998; Jørgensen and Bjørseth, 1999; Meininghaus et al., 2000b; Tiffonnet et al., 2002; Elkilani et al., 2003). The re-emission of adsorbed VOCs can dramatically elevate VOCs concentration in the indoor environment for months or years after a source event.

If the VOCs concentration in the building material is much higher than that in indoor air, VOCs will emit to the indoor air due to the concentration gradient; the material is then regarded as a source. On the contrary, when the VOCs concentration in the material is much lower than that in indoor air, VOCs will be adsorbed onto/into material, the material is now considered as a sink; and later, when the indoor VOCs concentration decreases because of dilution and is lower than that in the material, the adsorbed VOCs will be re-emitted from the material, and the material becomes a source material. Figure 2.1 illustratively shows the interaction of source material and sink material with indoor air.

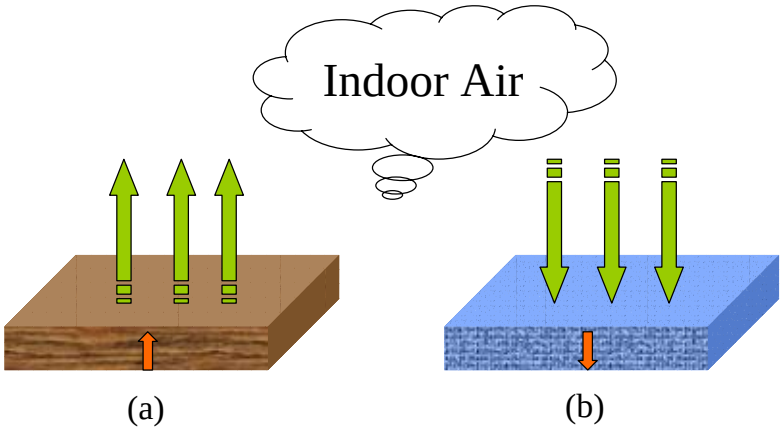

Figure 2.1 (a) Source material; (b) Sink material

2.2 Mass Transport Mechanisms

Sorption and diffusion are two major processes that play important roles in the overall VOCs transport, where sorption describes the interactions between gas molecules and the material surface (not limited to the physical surfaces, including pore surfaces for porous materials), and diffusion describes the rate of gas passage through the material. Qualitative and quantitative analysis of the involvement of these steps is required to understand the overall mass transport mechanisms.

2.2.1 Sorption Theory

Adsorption is a process where molecules from the gas phase or from solution bind in a condensed layer on a solid or liquid surface. The molecules that bind to the surface are called adsorbate while the substance that holds the adsorbate is called adsorbent. Desorption is used to denote the reverse phenomenon of adsorption, i.e. removal of the molecules from the surface (Masel, 1996).

2.2.1.1 Physisorption and Chemisorption

Adsorption at solid-gas or solid-liquid interfaces is often categorized as being by physisorption or chemisorption. Physisorption is generally thought to arise from three types of forces (i.e. Van der Waals forces, electrostatic forces, and solvent ordering and the hydrophobic 'force') between the adsorbent (e.g., a surface) and the adsorbate (the adsorbing molecule), while chemisorption is thought to result from the actual formation of a chemical bond, such as a covalent bond, between the surface and the adsorbate (Masel, 1996). Physisorption permits the formation of multi-layers on the adsorbent surface and is expected to be reversible, while chemisorption should only result in a monolayer of adsorbate molecules on the surface since a chemical bond is required and thus is usually irreversible (Masel, 1996).

People usually distinguish between two fundamentally different types of adsorption: multi-layer adsorption, where there are several layers of the adsorbate on the surface of the adsorbent, and monolayer adsorption where all the adsorbate is held in close proximity to the solid. Both types of adsorption are illustrated in Figure 2.2 (Masel, 1996). Multilayer adsorption is basically a condensation process; attractive interactions between adsorbate molecules cause gases to condense into a liquid-like

film on top of the molecules in the first monolayer. Monolayer adsorption is usually dominated by the direct interactions between the adsorbate and the surface.

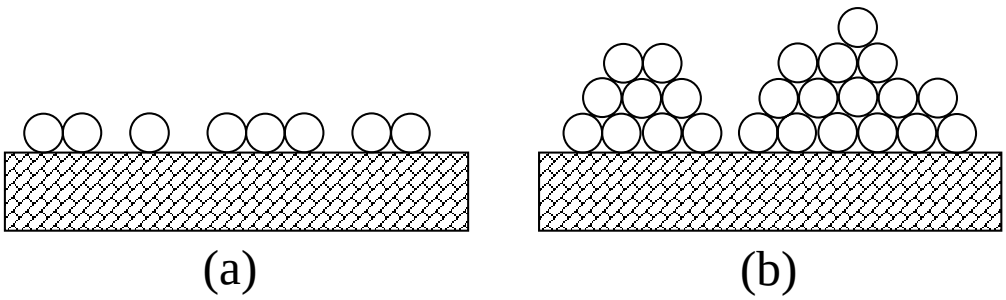

Figure 2.2 (a) monolayer adsorption; (b) multilayer adsorption

2.2.1.2 Sorption Isotherm

An adsorption isotherm gives the relationship between the concentration of contaminant and the amount of that contaminant that will be adsorbed at equilibrium on the adsorbent at a given temperature and pressure. In functional notation, the adsorption isotherm can be expressed as: $C_{ad} = f(C_g)$, at a certain temperature and pressure. In 1945, Brunauer (1945) proposed that one can classify the different kinds of behavior seen during the adsorption of gases on solids into one of the five general forms shown in Figure 2.3.

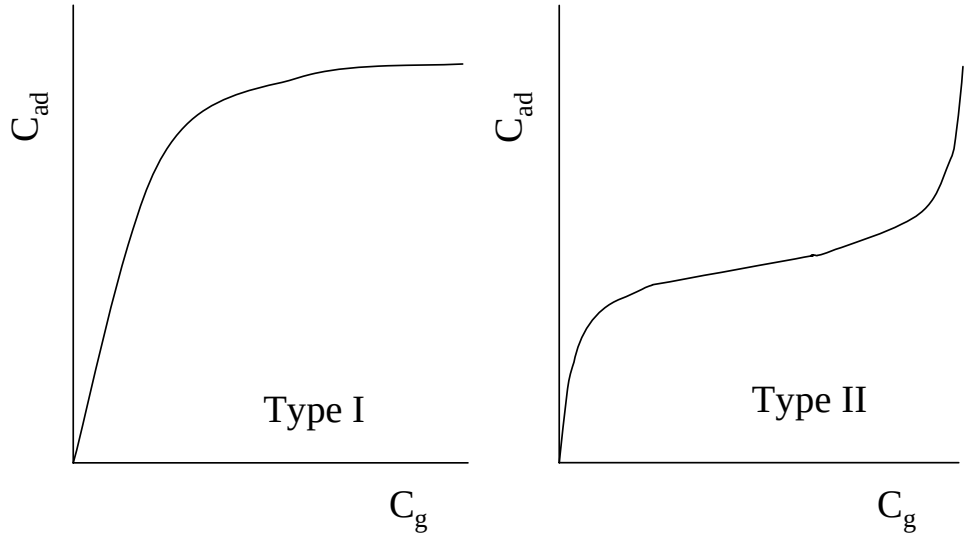

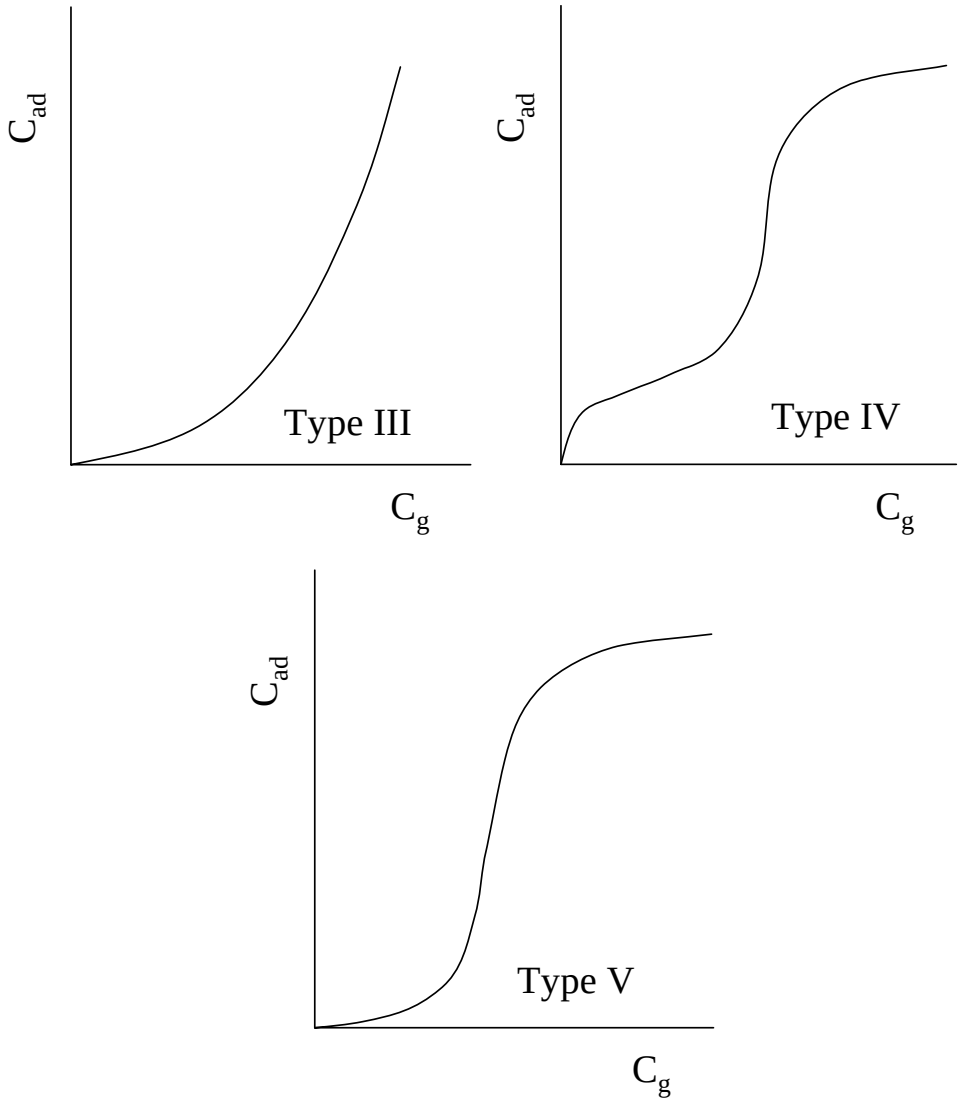

Figure 2.3 The five types of adsorption isotherms described by Brunauer [extracted from: (Brunauer, 1945)]

With flat surface one usually observes one of the two types of adsorption isotherms: Type I isotherm where the amount of gas increases with increasing air-phase concentration and then saturates at about a monolayer coverage, and type II isotherm where the amount adsorbed increases with increasing air-phase concentration, starts to level off, and then starts to grow again at higher air-phase concentration. Type I isotherms are characteristic of monolayer adsorption. Similar isotherms also arise if the adsorbent has very small pores that all fill up at once. Type II isotherms are characteristic of multilayer adsorption. Occasionally, one observes a so-called type

III adsorption isotherm where initially there is very little adsorption. However, once a small droplet or island of adsorbate nucleates on the surface, additional adsorption occurs more easily because of strong adsorbate-adsorbate interactions. Brunauer (1945) also defined a type IV and a type V adsorption isotherm. The type IV and type V isotherms usually occur when multi-layers of gas adsorb onto the surface of the pores in a porous solid. Initially, the adsorption looks like a type II or a type III adsorption, but eventually the adsorbed layer gets so thick that it fills up the pores. As a result, no more gas can adsorb and the isotherm saturates (Masel, 1996).

Several types of isotherms have been useful in indoor VOCs modeling, in explaining experimental adsorption/desorption data, and in characterizing surfaces: Linear, Langmuir, BET, and Freundlich isotherms. The first three isotherms have theoretical bases, while the last one is empirical (Axley, 1991).

2.2.1.2.1 Linear Isotherm

This is the simplest model describing sorption phenomena. The adsorption isotherm is defined by a linear relationship:

$$C_{ad} = K_p C_g \tag{7.1}$$

where K_p is partition coefficient.

This model may be expected to be appropriate for cases of physical adsorption of gases at very low concentrations (e.g., indoor air concentration level) on homogeneous surfaces with ample sites available for adsorption (Axley, 1991), and yet has been widely used in modeling indoor VOCs concentration (Little et al., 1994; Low et al., 1998; Cox et al., 2002; Kumar and Little, 2003a; Xu and Zhang, 2003;

Zhang and Niu, 2003c; Xu and Zhang, 2004; Zhang and Niu, 2004; Li and Niu, 2005a).

2.2.1.2.2 Langmuir Model

In a series of papers between 1913 and 1918, Langmuir derived a simple model for an adsorption isotherm which is still in use today (Axley, 1991; Clark, 1996; Masel, 1996). The Langmuir model describes adsorption in which the adsorbates accumulate on limited adsorption sites in a single layer. The Langmuir model may be expressed as:

$$C_{ad} = \frac{C_{ad}^{0} K_L C_g}{1 + K_L C_g} \tag{7.2}$$

where C_{ad}^{0} is the surface concentration corresponding to complete coverage by a single monolayer, and K_L is the Langmuir constant. Actually, when C_g is low enough (i.e., $K_L C_g \ll 1$ and $1 + K_L C_g \approx 1$), the Langmuir model becomes a linear one: $C_{ad} = C_{ad}^{0} K_L C_g$. Under this circumstance, $C_{ad}^{0} K_L \approx K_p$ (Axley, 1991).

2.2.1.2.3 BET Model

Another well-known adsorption isotherm is the BET (Brunauer, Emmet, and Teller) isotherm that accounts for the possibilities of multilayer adsorption (Axley, 1991; Clark, 1996; Masel, 1996). It takes the following form:

$$C_{ad} = \frac{C_{ad}^{0} K_{BET} \dfrac{C_g}{C_{sat}}}{\left(1 - \dfrac{C_g}{C_{sat}}\right)\left(1 - \dfrac{C_g}{C_{sat}} + K_{BET} \dfrac{C_g}{C_{sat}}\right)} \tag{7.3}$$

where C_{ad}^{0} is monolayer adsorbent concentration, K_{BET} is BET constant, C_{sat} is the air-phase concentration corresponding to saturated conditions. It is interesting that the BET model also approximates the linear model for very low concentrations of adsorbate in gas-phase (i.e., $\frac{C_g}{C_{sat}} \ll 1$ and $K_{BET}\frac{C_g}{C_{sat}} \ll 1$):

$$C_{ad} = C_{ad}^{0} K_{BET} \frac{C_g}{C_{sat}} \tag{7.4}$$

Under this circumstance, $\frac{C_{ad}^{0} K_{BET}}{C_{sat}} \approx K_p$ (Axley, 1991).

2.2.1.2.4 Freundlich Model

The Freundlich model is an important multi-site adsorption isotherm for rough surfaces. It is used to fit data rather than to verify an adsorption mechanism (Axley, 1991; Clark, 1996; Masel, 1996). The model takes the following form:

$$C_{ad} = K_F C_g^{1/n} \tag{7.5}$$

where K_F is a fitting parameter related to the capacity of the adsorbent material to adsorb the adsorbate (the higher the K_F value, the more material potentially adsorbed) and n is the other fitting parameter related to the affinity of the adsorbate for the surface (the smaller the n value, the greater the affinity of the adsorbate for the surface) (Clark, 1996).

2.2.2 Diffusion Theory

2.2.2.1 Types of Diffusion

Several distinct diffusion mechanisms may operate singularly or simultaneously in porous materials (Gunnarsen et al., 1994; Xi et al., 1994; Blondeau et al., 2003; Lee

et al., 2005): they are molecular diffusion, Knudsen diffusion, transition diffusion and surface diffusion, as demonstrated in Figure 2.4. Viscous flow through a porous material, which is driven by the difference in the total pressure across the porous solid, is excluded in this review since it can be generally negligible for building materials in indoor environments (Lee et al., 2005).

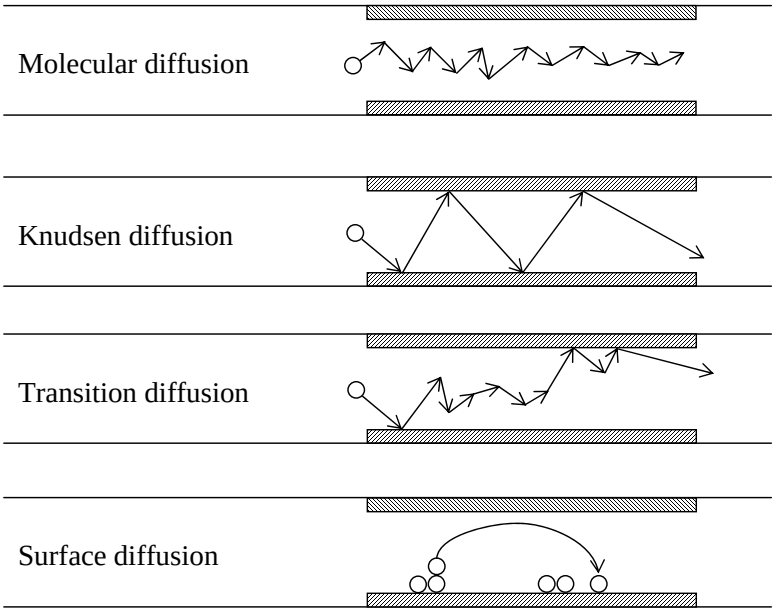

Figure 2.4 Different types of diffusion involved in building materials [modified from: (Gudmundsson, 2003)]

Consider a one-dimensional diffusion problem in a single straight cylindrical pore of radius r_p and length L through which binary gaseous diffusion of components A and B occurs under isobaric conditions. The mean free path of species A can be estimated by:

$$\lambda = \frac{3.2\mu}{P}\left(\frac{RT}{2\pi M_A}\right) \tag{7.6}$$

where λ is the mean free path (m), μ, the dynamic viscosity of the air (kg m^{-1} s^{-1}), P, the pressure (Pa), R, the universal gas constant (J mol^{-1} K^{-1}), T, temperature (K), and M_A molecular weight (kg mol^{-1}).

2.2.2.1.1 Molecular Diffusion

Molecular diffusion occurs when the mean free path is relatively short compared to the pore size ($r_p/\lambda \gg 10$), and the collisions between gaseous molecules are predominant. Molecular diffusion controls the transport mechanism in macropores of porous materials. The molecular diffusion coefficient of species A in the air can either be experimentally determined or calculated utilizing empirical relationships. For example, the Fuller-Schettler-Giddings (FSG) method for gas phase diffusion (Clark, 1996):

$$D_{AB} = \frac{10^{-3} T^{1.75} \sqrt{1/M_A + 1/M_B}}{P(V_A^{1/3} + V_B^{1/3})^2} \tag{7.7}$$

where, D_{AB} is the molecular diffusivity (cm^2 s^{-1}), T, temperature (K), P, pressure (atm), M_A, molar mass of species A (g mol^{-1}), M_B, the molar mass of the air (28.97 g mol^{-1}, at 1 atm, 20 ^{o}C), V_A, the molar volume of species A (cm^3 mol^{-1}), and V_B, the molar volume of the air (20.1 cm^3 mol^{-1}, at 1atm, 20 ^{o}C).

2.2.2.1.2 Knudsen Diffusion

Knudsen diffusion occurs when the mean free path of the diffusing molecular is relatively long compared to the pore size ($r_p/\lambda \ll 0.1$), so the molecules collide more frequently with the pore wall than with each other. Knudsen diffusion is dominant in mesopores of porous materials. In the Knudsen regime, the flux of the component A is unaffected by the presence of the other species, and the Knudsen diffusivity can be calculated using (Park and Do, 1996):

$$D_{K,A} = \frac{2}{3} r_p \sqrt{\frac{8RT}{\pi M_A}} \tag{7.8}$$

where, M_A is the molecular weight of species A, and T, the temperature in Kelvin.

2.2.2.1.3 Transition Diffusion

Transition diffusion may occur in a wide range of conditions under which both Knudsen and molecular diffusion are significant. Both wall collisions and intermolecular collisions contribute to the diffusional resistance and the effective diffusivity depends on the Knudsen and molecular diffusivities, as well as the concentration. In the transition regime, the combined diffusivity can be calculated by (Park and Do, 1996):

$$\frac{1}{D_c} = \frac{1}{D_{AB}}\left(1 - \left(1 + \sqrt{\frac{N_B}{N_A}}\right) y_A\right) + \frac{1}{D_{K,A}} \tag{7.9}$$

where, N_A, N_B are the diffusion flux of component A, B respectively, y_A, the mole fraction of A. For equimolar counterdiffusion ($N_A = -N_B$) and also for dilute system ($y_A \ll 1$), equation (7.9) reduces to:

$$\frac{1}{D_c} = \frac{1}{D_{AB}} + \frac{1}{D_{K,A}} \tag{7.10}$$

The magnitude of the diffusivity ratio $D_{AB}/D_{K,A}$ dictates the controlling diffusion mechanism in the porous medium. If the ratio is very small, the molecular diffusion is the controlling mechanism. Otherwise, if the ratio is very large, Knudsen diffusion is the controlling mechanism.

2.2.2.1.4 Surface Diffusion

Surface diffusion usually occurs in micropores. The adsorbed adsorbate molecules never escape the force field of the pore surface and may hop from one site to another

through interactions between the surface and molecules. Surface diffusion depends on the concentration and on the rates of adsorption and desorption. The diffusive flux due to surface diffusion increases with increasing sorption (Park and Do, 1996). In the filed of indoor VOCs emission and sorption, the surface diffusion can usually be ignored.

2.2.2.2 Diffusion in Porous Material

In this part, equations describing gas phase diffusion in porous material are derived step by step based on the Fick's first and second laws (Clark, 1996; Choy and Reible, 2000). The reduction of diffusion resulted from porosity, sorption, constrictivity, tortuosity and contribution to diffusion resulted from surface diffusion are considered.

2.2.2.2.1 Diffusion in Free Phase

The steady state and transient diffusion are often described with Fick's first and second laws (Crank, 1975), respectively:

$$J = -D\frac{\partial C}{\partial x} \tag{7.11}$$

$$\frac{\partial C}{\partial t} = -\frac{\partial J}{\partial x} \tag{7.12}$$

where J is the flux, D, the diffusivity, C, the tracer concentration, x, the distance and t, the time, the negative sign indicates that the direction of the contaminant movement is in the direction of decreasing concentration as Figure 2.5 shows.

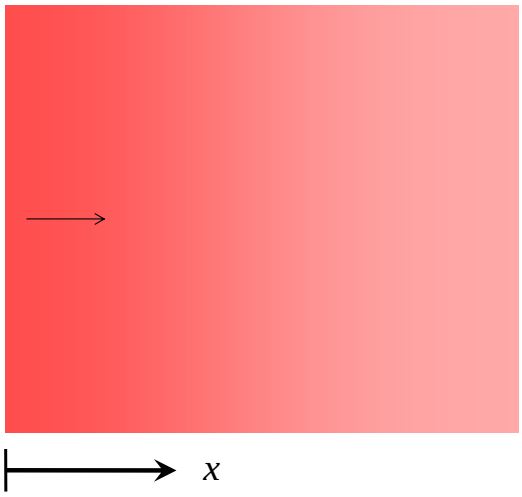

Figure 2.5 Diffusion in free phase

2.2.2.2.2 Reduction of Diffusion Due to Porosity

Considering diffusion through a bundle of straight tubes shown in Figure 2.6, the diffusive flux is partially blocked by the solid matrix (Peter, 1998), thus:

$$J = -\varepsilon D \frac{\partial C_g}{\partial x} \tag{7.13}$$

$$\varepsilon \frac{\partial C_g}{\partial t} = -\frac{\partial J}{\partial x} \tag{7.14}$$

where ε ($0 \le \varepsilon \le 1$) is porosity, and C_g gas phase concentration.

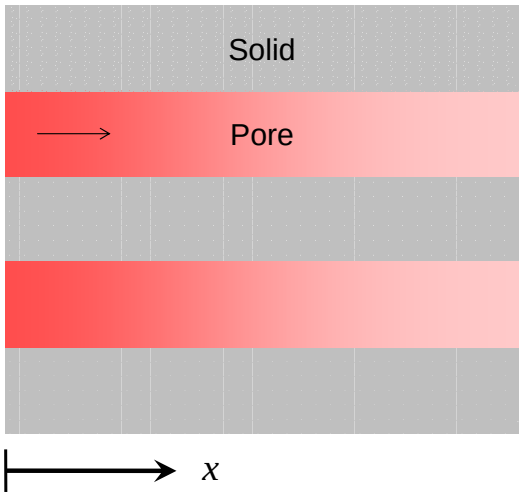

Figure 2.6 Reduction of diffusion due to porosity

2.2.2.2.3 Reduction of Diffusion Due to Sorption

During diffusion through the porous media, the diffusing molecules can adsorb to the pore surface as shown in Figure 2.7. This phenomenon will tend to slow the mass transfer through the porous medium (Clark, 1996).

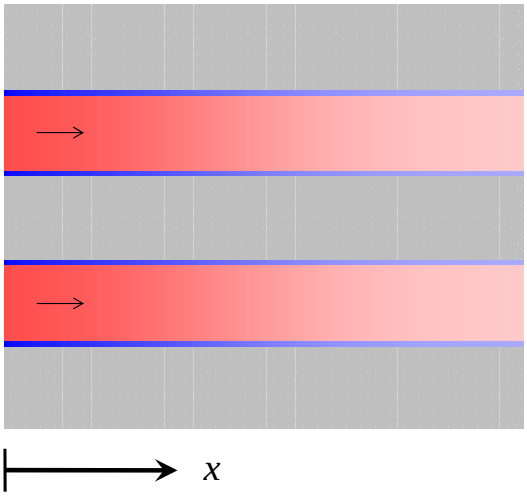

Figure 2.7 Reduction of diffusion due to sorption

If the sorption follows a linear isotherm and the physical process of sorption at an internal site is fast compared to the diffusion process (local equilibrium), then relationship between the adsorbed-phase concentration and the gas-phase concentration can be expressed as:

$$C_{ad} = K_s C_g \tag{7.15}$$

where K_s is the sorption coefficient.

The equation for diffusive flux J remains the same as equation (7.13), while the transient diffusion equation becomes:

$$\varepsilon \frac{\partial C_g}{\partial t} + \frac{\partial C_{ad}}{\partial t} = -\frac{\partial J}{\partial x} \tag{7.16}$$

Substituting equation (7.15) into equation (7.16) results in:

$$(\varepsilon + K_s)\frac{\partial C_g}{\partial t} = -\frac{\partial J}{\partial x} \tag{7.17}$$

2.2.2.2.4 Reduction of Diffusion Due to Constrictions

Practically, as Figure 2.8 shows, the cross sectional area varies along a pore. The most constricted parts of the pores limit the diffusive flux, resulting in that the entire pore volume cannot be effectively used for transport (Peter, 1998). Such that:

$$J = -\varepsilon\delta D\frac{\partial C_g}{\partial x} \tag{7.18}$$

$$(\varepsilon + K_s)\frac{\partial C_g}{\partial t} = -\frac{\partial J}{\partial x} \tag{7.19}$$

where δ is constrictivity ($0 < \delta \leq 1$).

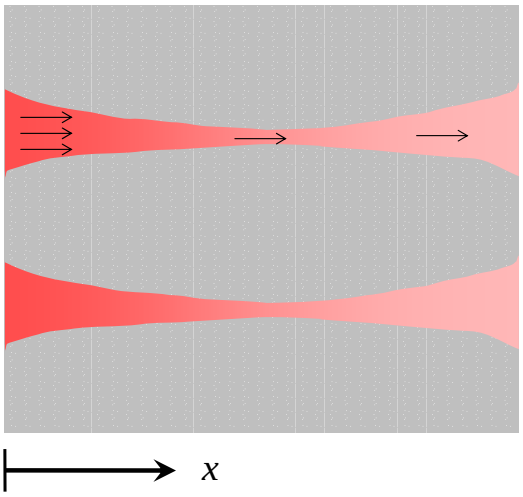

Figure 2.8 Reduction of diffusion due to constrictions

2.2.2.2.5 Reduction of Diffusion Due to Tortuosity

The pores are usually tortuous and species diffusing cannot take the shortest route, as shown in Figure 2.9. It is thus necessary to account for the additional slowing of diffusion caused by the tortuosity of the diffusion path (Peter, 1998). The diffusion equations become:

$$J = -\frac{\varepsilon\delta}{\tau^2} D \frac{\partial C_g}{\partial x} \tag{7.20}$$

$$(\varepsilon + K_s)\frac{\partial C_g}{\partial t} = -\frac{\partial J}{\partial x} \tag{7.21}$$

where $\tau = L_c/L \geq 1$ is the tortuosity.

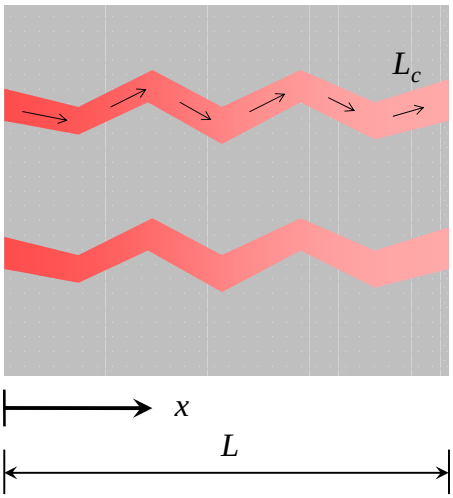

Figure 2.9 Reduction of diffusion due to tortuosity

It is a common practice to describe the diffusion mechanism of gas in pores in terms of the effective diffusivity. Define the effective diffusivity for gas-phase diffusion as $D_{e,g} = \frac{\varepsilon\delta}{\tau^2} D$, and then the transient diffusion equation becomes:

$$(\varepsilon + K_s)\frac{\partial C_g}{\partial t} = D_{e,g} \frac{\partial^2 C_g}{\partial x^2} \tag{7.22}$$

2.2.2.2.6 Effect of surface diffusion

In case the surface diffusion plays an important role in the overall mass transport, the diffusion equation should then take surface diffusion into account and can be described as:

$$(\varepsilon + K_s)\frac{\partial C_g}{\partial t} = D_{e,g} \frac{\partial^2 C_g}{\partial x^2} + D_{e,s} \frac{\partial^2 C_{ad}}{\partial x^2} \tag{7.23}$$

where C_{ad} is the adsorbed phase concentration and $D_{e,s}$ the effective surface diffusion coefficient.

Then an expression for the total transient matrix diffusion is obtained:

$$(\varepsilon + K_s)\frac{\partial C_g}{\partial t} = (D_{e,g} + K_s D_{e,s})\frac{\partial^2 C_g}{\partial x^2} \tag{7.24}$$

However, due to the mobility of molecules in the adsorbed phase is generally much slower than in the gas phase and the surface diffusivities are typically several orders of magnitude smaller than molecular and Knudsen diffusivities (Lee et al., 2005). It is reasonable to neglect the surface diffusion in the field of indoor air quality modeling like most modelers do in practice.

2.3 Experimental Methods for Characterizing Source/Sink Behaviors

Since building materials are the sources/sinks of VOCs in indoor environments, low-emitting or green building materials are expected to be used to attain good indoor air quality. To characterize material emission/sorption behaviors and obtain reliable data, systems and devices are continuously being developed and improved (Little and Hodgson, 1996).

2.3.1 Typical Source Testing Methods

Some typically used methods for the determination of VOCs contents or emissions in/from indoor building materials are presented.

2.3.1.1 Laboratory Studies

Static headspace analysis is used to determine emission composition of materials. A sample of material is placed in a small airtight container made of inert emission-free

material. Samples of the air inside the container are taken and analyzed by gas chromatography (GC) with mass spectrum (MS) thereafter to quantify the compounds emitted from the material.

Direct thermal desorption (DTD) (McCrillis et al., 1999) and fluidized-bed desorption (FBD) methods (Cox et al., 2001a) are used to determine the initial solid-phase VOCs concentration within the building materials.

The concentration measured by FBD is much lower than that of by DTD method. The reasons are: in the FBD method, the extraction is completed under room temperature, while in the DTD method, the extraction is conducted at much higher temperature (above the T_g - the temperature at which an inflection point in the free volume versus temperature curve occurs.). Below the glass transition temperature, one fraction of the diffusant population is considered mobile, while the other is considered partially immobilized. Therefore, concentration determined by FBD approximates the mobile portion of VOCs, while concentration determined by DTD represents the total VOCs initially present in the material (McCrillis et al., 1999). In view of this point, FBD method is advantageous over DTD method because the conditions in FBD method resemble those in which the material would be installed in an indoor environment (Cox et al., 2001a).

Since the headspace analysis can only provide emission composition and does not provide dynamic behavior of emissions with respect to time, dynamic chamber tests should be carried out to provide such information. By conducting the dynamic chamber tests, various building materials can be ranked according to their emission profiles; various models can be evaluated utilizing the obtained test data; the impact

of environmental conditions on emission can be investigated. Both FLEC/small-scale chambers and full-scale chambers are commonly used to conduct these tests.

2.3.1.2 Dynamic Chamber Studies

Since 1991, the Field and Laboratory Emission Cell (FLEC) has been used worldwide for emission testing of building products due to its reliability, flexibility, fast response, and low cost etc. It allows in-situ testing of emissions from surfaces. Two European standards for operation of emission cells like the FLEC (NORDTEST-1177-94 and EN 13419-2) have been available for some time. And one international standard (ISO 16000-10) “Determination of the emission of volatile organic compounds from building products and furnishing - Emission test cell method” is at its approval stage. More recently, the American Society for Testing and Materials (ASTM) has also approved a new standard, D 7143-05 “Emission Cells for the Determination of Volatile Organic Emissions from Indoor Materials/Products”, for emission cells.

The FLEC is made of hand-polished, acid resistant stainless steel to minimize the sink effect. The internal cavity of the FLEC is designed to be like the mouth of a trumpet to optimize the air velocity over the test specimen surface. In contrast to conventional chambers, the FLEC is placed on the surface of the emission source to be tested, and the test material becomes the bottom part of the cell. The FLEC air control unit controls the flowrate and RH of air stream supplied to FLEC cell. The clean air is introduced into two diagonally positioned inlets at the perimeter of the cell and then distributed by a channel following the perimeter, from where the air is distributed over the surface of the test material. Finally, the air containing emitted

VOCs exits the cell through the center of the trumpet. Detailed information on the FLEC can be found in (Wolkoff et al., 1993).

Small-scale chambers (a few liters to 5 m^3) (ASTM, 1990) are also often used, for example, Colombo et al., (1990) determined VOCs emissions from particle board with carpet, gypsum board with wallpaper and plywood with polyurethane lacquer using two small chambers (0.45 m^3).

Table 2.3 demonstrates the comparison of technical parameters and discussion of performance data of FLEC cell and small chamber.

Table 2.3 Technical parameters and discussion of performance data of FLEC cell and small chamber [modified from: (Wolkoff, 2001)]

Parameter	FLEC	Chamber (< 1 m^3)	Impact of difference
Air change rate (h^{-1})	~ 350-2400	Typically 0.5-1.0	Not significant.
Air supply (L/min)	0.2-1.4	0.5-20	More cheaper to run tests using cells
Air velocity (m/s)	0.007-0.05	> 0.1-0.3	Results in different SER_A for evaporative emissions
Sample area	177 cm^2	~200-1000 cm^2	Cells more likely to require repeat tests on inhomogeneous materials
Volume	35 ml.	20 L to 1 (5) m^3	No still air in cell - minimizes sink effects
Loading (m^2/m^3)	510	0.5-20	Counter balances diff. in exchange rate
Air distribution	Slightly uneven	Uneven	Little impact on dry materials
Equilibration time	Minutes	Hours-days	Cells allow higher experimental throughput
Cost	Inexpensive	Inexpensive to expensive	Cells consume less ultra clean air
Edge effects	Negligible	Necessary to seal	
On-site measurement	Feasible	Difficult	Cells can be used for on-site measurement, more flexible.
Cleaning	Easy	Easy to cumbersome	

However, the small volume of FLEC or small-scale chamber limits the measurement of large materials (such as whole sets of furniture, equipments, etc.) and the evaluation of the application phase of the coating process (the emission rate during the application of paints and coatings using brushing, spraying, rolling, etc. is higher than the rate during the drying period). Large chamber is expected to be able to overcome these limitations.

A large chamber (>5 m^3) (ASTM, 1990) usually consists of a full-size stainless steel room and an HVAC system (e.g., fan, ducts, dampers, coils, etc.) with stainless steel components, which is expected to overcome the limitations of small-scale chamber. In comparison with small chambers, the large chamber can handle not only large materials, application phase of coating process, but occupant activities (e.g. smoking). For example, Hodgson et al. (1993) measured VOCs emissions from four carpets in a 20 m^3 environmental chamber. Leovic et al. (1998) developed a large chamber emission test method for measuring indoor air emissions from office equipment and the method was evaluated and revised by testing four photocopiers in different labs.

It should be pointed out that the cost of the large chamber test is relatively high because of its large volume. The environmental conditions in large chamber are not easy to be precisely controlled, for example, the air in the large chamber is difficult to be fully mixed, and thus air samples are usually collected at one or more locations in the chamber instead of solely in the outlet flow.

2.3.1.3 Field Studies

Although dynamic chamber studies are useful for determining emission/sorption rates of indoor building materials under controlled conditions, they can not fully reflect the actual situations in real buildings. Conditions in actual buildings are far

more complicated than in chambers because of the presence of a variety of different building materials, occupant activities, HVAC system and other potential affecting factors. Full-scale studies provide opportunities to validate the chamber data and evaluate factors such as operation mode of HVAC system, occupant activities, etc. (Little and Hodgson, 1996).

2.3.2 Typical Sink Testing Methods

The recognition of and research on the sink effects lag behind the source testing work, but increased awareness of the negative impacts of the sink effect has led to numerous extensive investigations since the late 1980s. The methods used to evaluate the adsorptive and desorptive behavior are similar to the source characterization methods described above (Tichenor, 1996). Dynamic small chambers are commonly used to evaluate the sink rates of indoor building materials.

Berglund et al. (1989) reported that organic compounds adsorbed on building materials in a seven-year-old preschool were re-emitted when placed in a small environmental test chamber ventilated with clean air. Kjaer and Nielsen (1991) investigated adsorption and desorption of toluene and 2-butoxyethanol on nylon and wool fibers from textile floor coverings and found that the extent of the adsorption and desorption have an outstanding influence on indoor air quality. Tichenor et al. (1991) demonstrated the adsorption to and re-emission from five materials: carpet, painted wallboard, ceiling tile, window glass, and upholstery for two typical indoor VOCs tetrachhethyhe and ethylbenzene. Neretnieks (1993) investigated sink effects by placing a PVC flooring material as a primary emission source in a system where materials such as wood, paint, cloth, chipboard, and cellulose were present. The results show that the mechanism of adsorption/re-emission of volatiles may extend

the time of residence in an indoor system considerably. Trikkonen and Saarela (1997) tested five surface materials (pine wood plank treated with solvent based wood treating wax, spruce panel treated with coconut oil-based wood treating agent, wood fiber wall board painted with water-based linseed oil and resin emulsion paint, gypsum board painted with tixotropic paint with vegetable oil and casein based binder, brichplyed MDF board primed with water-based resin and finished with hot wax, house door finished with natural oils-based wax) in small chambers to determine the VOCs emissions, meanwhile, the emissions from corresponding surfaces in full scale building were in-situ determined using FLEC, by comparing the emissions profiles the sink effect was clearly demonstrated. Chang et al. (1998) evaluated the sink effects of a carpet and a gypsum board with four VOCs: propylene glycol, ethylene glycol, 2-(2-butoxyethoxy)ethanol (BEE), and Texanol - representing the major VOCs emitted from a latex paint. The results indicate that the sorption capacity of common indoor materials for the four VOCs is unusually high; the re-emission process is relatively slow and can result in chronic and low-level exposure to the VOCs after painting interior walls and surfaces. Continuous experimental work on sink effects has been in progress, such as (Colombo et al., 1993; Chang and Guo, 1994; De Bortoli et al., 1996; Kephalopoulos et al., 1996; Little and Hodgson, 1996; Trikkonen and Saarela, 1997; Chang et al., 1998; Van Der Wal et al., 1998; An et al., 1999; Bouhamra and Elkilani, 1999; Jørgensen and Bjørseth, 1999; Jørgensen et al., 1999; Kirchner et al., 1999; Meininghaus et al., 1999; Zhang et al., 1999; Meininghaus et al., 2000a; Meininghaus et al., 2000b; Won et al., 2000; Won et al., 2001b; Yang et al., 2001c; Tiffonnet et al., 2002; Zhang et al., 2002a; Zhang et al., 2002b; Elkilani et al., 2003; Popa and Haghighat, 2003; Silva et al., 2003; Zhang et al., 2003; Zhao et al., 2003; Singer et al., 2004; Zhao et al., 2004),

test facilities vary among environmental chamber, microbalance, Climpaq and FLEC. A variety of typical building materials and common indoor VOCs have been tested; limited corresponding sorption data have been available. It has been revealed that the amount of adsorbed mass depends on several parameters, such as temperature, relative humidity, chemical nature and gas phase concentration of the VOCs, and VOCs/material properties like chemical structure, pore size, or specific surface area (Meininghaus et al., 2000b).

Full-scale chamber studies or test house studies are usually used to validate the small-scale chamber derived sink rates (Tichenor, 1996), for example, the scale-up experiments done by Won et al. (2001b) demonstrated the validity of using surface sink model to characterize sink behaviors of three chemicals (cyclohexane, toluene, and ethylbenzene) on three materials (carpet system, pad, and virgin gypsum board).

2.4 Modeling Approaches for Characterizing Source/Sink Behaviors

The costs of dynamic chamber tests could be very high because characterization of emission/sorption patterns requires multiple samples over time, and expensive, well controlled facilities (e.g., chemical analysis system, ATD-GC/MS), a tremendous amount of time and resources can be saved if the source/sink behavior can be accurately modeled and predicted. There have been increasing interests in developing mathematical models to predict the emission/sorption characteristics of building materials. Models have been advancing from the statistical models to the recently popular mass transfer based models.

2.4.1 Modeling VOCs Transfer in Room Air

Before reviewing detailed VOCs emission/sorption models for indoor building materials, it is necessary firstly to have a look at how the VOCs in the indoor air are dealt with. Conventionally, VOCs transfer in the room air can be described and modeled by well-mixed models, zonal models, or CFD models depending on the assumptions made on the extent of VOCs mixing with air (Haghighat et al., 2005).

2.4.1.1 Well-mixed Model

The well-mixed model is the simplest one which treats the room air as a homogenous single zone and assumes that the VOCs is instantaneously and completely mixed with the room air (Haghighat et al., 2005). This simplified model does not care about the air flow pattern and how the VOCs are distributed in the room, it aims to have a general idea on the level of the indoor VOCs concentration. A basic mass balance equation for the VOCs in the room can be written as:

$$V\frac{dC_a}{dt} = Q(C_{in} - C_a) + A \cdot R(t) - A \cdot S(t) \tag{7.25}$$

where V is the volume of the room (m^3), C_a the VOCs concentration in the room (kg m^{-3}), Q the supply air flow rate (m^3 s^{-1}), C_{in} the VOCs concentration in the supply air, A the surface area of the material (s^2), $R(t)$ the emission rate from the building materials (kg m^{-2} s^{-1}), and $S(t)$ the sorption rate to the building materials (kg m^{-2} s^{-1}).

2.4.1.2 Zonal Model

In zonal models, a room is usually divided into a small number of zones. VOCs in each zone are assumed to be uniform. Heat and mass transfer between zones is

through zone interfaces. Mass balance and heat balance equations are applied to the individual zones. Different zonal models distinguish themselves in terms of modeling the airflow and the driving forces. For instance, Huang (2003) developed a zonal model which applied an empirical power law to calculate the air flow rate across the zone interfaces (Haghighat et al., 2005).

2.4.1.3 CFD Model

In 1974, Nielsen (1974) conducted a research to investigate the indoor air flow by means of computational fluid dynamics (CFD). Since then, CFD became a popular tool to conduct IAQ study, for example, Topp et al. (2001) studied the influence of local airflow on the pollutant emission from indoor building surfaces. Other researchers (Murakami et al., 2001; Yang and Chen, 2001; Haghighat and Huang, 2003; Murakami et al., 2003; Zhang and Niu, 2003b) also did some extensive researches by means of CFD. In this method, the conservation equations for continuity, momentum, energy, and VOC transport should be solved. Considering the VOCs emission/sorption has a negligible effect on air flow and heat transfer, the first three conservation equations are first solved and the steady-state air flow and temperature distributions obtained are then incorporated into the VOCs mass transfer equations for calculating indoor VOCs distribution.

The CFD method is obviously mathematically the most complex of the three methods described above. Not to mention the huge computation loads and long computation time required, the CFD method generally requires a specialist operator to perform the modeling (Ellacott and Reed, 1999) because the accuracy of the simulation results heavily depends on the user's experiences and skills (Haghighat et al., 2005). Although the zonal model is somewhat simpler than CFD model, it is still

more complicated than the well-mixed model. Actually, users are not usually interested in excessively detailed results (such as air flow and VOCs distributions) obtained from zonal models or CFD models; they may take more care of the overall level of the contaminant concentration. If the level is below the recommended level, that's enough. For these reasons, the well-mixed model has been widely used.

2.4.2 Building Material VOCs Source Models

2.4.2.1 Empirical Source Models

2.4.2.1.1 First-order Decay Model

This kind of models is based solely on the observations and statistical analysis of emission data obtained from chamber tests. Among these, the first-order decay model is the simplest and most widely used, and many others are derived from it. The main assumption made is that the emission rate is proportional to the mass of VOCs remaining in the material (Clausen et al., 1991; Chang and Guo, 1992; Clausen, 1993; Little and Hodgson, 1996):

$$E = -\frac{dM}{dt} = E_0 e^{-kt} \tag{7.26}$$

where E is emission factor (mg m^{-2} h^{-1}), M amount of VOCs remaining in the source (mg m^{-2}), E_0 initial emission factor (mg m^{-2} h^{-1}), k first-order decay rate constant (h^{-1}), and t time (h). The first-order decay model is fully defined by the parameters E_0 and k. This model has been used to fit emission curves of many materials, especially wet and semi-dry materials. In general, sources with decay constants larger than 0.2 h^{-1} are limited by gas-phase mass transfer (evaporation), and those with decay constants smaller than 0.01 h^{-1} are limited by source-phase mass transfer (diffusion). Products such as wood stain, varnish, floor wax, and liquid nails

are examples of gas-phase-limited sources. Products such as carpet, linoleum, and aged paint are examples of source-phase-limited sources (Sparks, 2001).

2.4.2.1.2 Dual First-order Decay Model

However, it is found that the first-order decay models often fit the short-term emissions data very well, but almost always underestimate the long-term emissions (Guo, 2002), especially for a source with high initial emission rate that decays rapidly and followed by a slower emission rate that lasts for a long time (Sparks, 2001).

To overcome this problem, two first-order decay terms can be combined (Chang and Guo, 1992; Chang et al., 1997; Brown, 1999; Guo and Murray, 2000; Guo et al., 2000; Zhao et al., 2003):

$$E = E_1 e^{-k_1 t} + E_2 e^{-k_2 t} \tag{7.27}$$

The first term and the second term in the above equation represent the fast emissions and the slow emissions, respectively. In some cases, a sum of three or more exponential decay rates is used to describe the overall emission rate (Sparks, 2001).

2.4.2.1.3 Power law model

Zhu et al. (1999a; 1999b) developed a power law model:

$$R = \frac{a}{t^b} \tag{7.28}$$

for describing VOCs emissions from wood-based panels under dynamic chamber test. They compared the performance of a power law model and a first-order decay model and found that the power law model is a better choice than the first-order decay model for describing emission characteristics for short-term (less than 100 h)

experimental data and is also more superior in predicting long-term (up to 900 h) emission factors (Zhu et al., 1999a).

However, this model is also a pure data-fitting because its parameters *a* and *b* do not have any physical meanings.

2.4.2.1.4 Second-order Decay Model

Another approach to take into account both short and long-term emissions is to use higher-order decay models, such as the second-order decay model (Guo et al., 1996; Little and Hodgson, 1996; McCrillis et al., 1999):

$$E = \frac{E_0}{1 + ktE_0} \tag{7.29}$$

This model has been applied to many sources that feature strong emissions in the early stage, followed by long-lasting, low-level emissions (Guo, 2002). However, the shortcoming of this model lies in that it is not useful beyond the time frame of the test, because it allows for infinite emissions (McCrillis et al., 1999) - a consequence that is physically impossible (Guo, 2002).

2.4.2.1.5 Combined First-order Decay Model and Diffusion Model

Guo et al. (1996) developed an empirical model that could predict individual VOCs emissions from latex paint applied to porous materials such as gypsum board. This model is a combination of the first-order decay model and a diffusion model with an additional adjustment factor and intends to account for both short-term and long-term emissions. The model is:

$$E = M_{v0} k_1 e^{-k_1 t} + (1 - e^{-k_1 t})^2 \frac{f_{D1} M_{D0} e^{-2 f_{D1} \sqrt{t}}}{\sqrt{t}} \tag{7.30}$$

$$M_{T0} = M_{v0} + M_{D0} \tag{7.31}$$

where M_{v0} is the initial mass per unit area for evaporation, k_1, the first-order decay constant, $(1-e^{-k_1 t})^2$, the adjustment factor (it is easy to see that, this factor only has an effect in a short period of time and will quickly approach 1 afterwards), $f_{D1} = \frac{0.632\sqrt{D}}{b}$, the diffusion constant, M_{D0}, the initial mass per unit area for diffusion, and M_{T0}, the total emittable mass per unit area applied.

There are many other empirical models, although the majority of them are simple and usually fit test data well, they can not provide a description of the physical processes associated with the emission processes, and the parameters used in the models generally have no distinct physical meanings and are determined by fitting experimental data to a predefined model - thus they are test-conditions dependent, which makes this type of models difficult to scale up. These limitations urge researchers to develop a new generation of models which are based on fundamental mass transfer theories.

2.4.2.2 Mass Transfer Based Source Models

Models based on mass transfer theories are more attractive than empirical models due to their explicit physical definitions. The fundamentals of mass transfer processes include diffusion within the material as the result of concentration gradient (pressure or temperature gradient is generally neglected in modeling VOCs emissions from indoor building materials), and surface emission between the material and the overlaying air as a consequence of evaporation, convection and diffusion.

2.4.2.2.1 Evaporation Controlled Models

For wet materials such as paints or wood stains, the concentration dependent diffusion coefficients are very difficult to be determined, and studies show that the surface emission usually dominates the emission process. Therefore most of the previous emission source models for wet materials focused on the evaporation dominant stage. The Vapor pressure and Boundary layer (VB) model is an example:

$$E = k_g \left(C_{v0} \frac{M_T}{M_{T0}} - C \right) \tag{7.32}$$

where k_g is the gas phase mass transfer coefficient, C_{v0} , the initial vapor concentration at the interface, M_{T0} , the amount of initial TVOC applied in the material, M_T , the amount of emittable TVOC concentration remaining in the material, and C , TVOC concentration in the bulk air.

This model developed by Tichenor et al. (1993) is a simple mass transfer model for predicting TVOC emissions from oil-based indoor coating materials. The model considers emission as a pure evaporation process and neglects internal diffusion. It assumes that as the coated surface ages the total vapor pressure at surface decreases gradually and is assumed to be proportional to the amount of TVOC remaining in the source. This assumption has been validated by Sparks et al. (1996). It has been found that the VB model predicts short-term TVOC concentration well, but underestimates the long-term TVOC emissions (Low et al., 1998).

The VBX model (Leovic et al., 1998; Guo et al., 1999) is an extension of VB model which allows to predict individual VOCs emissions. The VBX model is in the form of:

$$E_i = k_{gi}\left(C_{vi}\frac{M_i \cdot MW_T}{M_T \cdot MW_i} - C_i\right) \tag{7.33}$$

where E_i is the emission rate of i_{th} component, k_{gi}, the gas phase mass transfer coefficient of i_{th} component, C_{vi}, the gas phase concentration of i_{th} component, M_i, the amount of i_{th} component remaining in the material, MW_T, the average molecular weight of TVOC, MW_i, the molecular weight of i_{th} component, and C_i, the concentration of i_{th} component in bulk air. The model parameters can be estimated from the product formulation data (Guo et al., 1999). This model must be used with VB model in order to calculate the amount of TVOC remaining in the source (Guo, 2002).

2.4.2.2.2 Diffusion Controlled Models

It has been well demonstrated that emission from many sources, especially from those dry building materials are dominant by diffusion process. Christiansson et al. (1993) developed a model for VOCs emissions from PVC flooring. The model is composed of two equations:

$$E = C_0\sqrt{\frac{D}{\pi t}} \tag{7.34}$$

$$E = \frac{2C_0 D}{x}\mathrm{e}^{-\frac{D\pi^2 t}{4x^2}} \tag{7.35}$$

The first equation is for the first 50% of the VOCs mass in the material, and the second equations is for the last 45% of the VOCs mass. But the authors did not mention which equation to use for the mass between 50% and 55% (Guo, 2002).

Yang et al. (1998) developed an analytical model for the prediction of long-term VOC emissions from SBR bitumen-backed carpet based on the parameters obtained from the short-term CFD simulation. This model assumes that the diffusion coefficient in the solid is very small and therefore the emission is dominated solely by internal diffusion of the carpet polymer and the mass transfer resistance in the solid-air boundary layer is negligible. Further, when calculating the VOCs distribution in the carpet, the VOCs concentration at the material surface is assumed to be zero in comparison with much higher concentration within carpet. The average emission rate between t_1 to t_2 is then given by:

$$R_{12} = \frac{3600 M_0 (M_2 / M_0 - M_1 / M_0)}{t_2 - t_1} \tag{7.36}$$

where, $\frac{M}{M_0} = 1 - \sum_{i=0}^{\infty} \frac{2}{B} \mathrm{e}^{-BF_o}$, $B = \left[(i + 1/2)\pi\right]^2$, $F_o = Dt/b^2$. It should be noted that the assumptions made in developing this model makes it only applicable to predict emissions that last at least several months (Yang et al., 1998).

Little et al. (1994) developed a model including a material-air partition coefficient *K* and assuming an instant equilibrium between the air and the material surface. This analytical model uses the following equation to calculate the VOCs concentration in the material:

$$C_m(z,t) = 2C_0 \sum_{n=1}^{\infty} \frac{e^{-D_s q_n^2 t (h - k_0 q_n^2)} \cos(q_n x)}{\left[z(h - k_0 q_n^2)^2 + q_n^2 (z - k_0) + h \right] \cos(q_n z)} \tag{7.37}$$

where $h = \frac{Q}{SD_s K}$, $k_0 = \frac{V}{SK}$, $q_n \tan(q_n z) = h - k_0 q_n{}^2$. It was initially developed for VOC emissions from new carpet backing, but later work has shown that it can also be applied to other dry sources such as vinyl flooring (Little and Hodgson, 1996; Cox

et al., 2002) and decking wood etc. (James and Yang, 2005). Recently, based on this model, Kumar and Little (2003a) developed a double-layer analytical model which allows non-uniform initial material-phase concentrations in each of the two layers and a transient influent gas-phase concentration to be considered. The weakness of these models lie in neglecting the convective mass transfer resistance, resulting in over-estimated early stage emissions for solid material with large diffusion coefficient (Xu and Zhang, 2003; Lee et al., 2005).

2.4.2.2.3 Combined Evaporation and Diffusion Models

Researchers have been putting numerous efforts in developing models capable of characterizing the entire emission processes. Sparks et al. (1999a) attempted to combine the VB model and the diffusion-controlled model to describe the VOCs emissions from latex paint. The combined model has three parts: the VB model for the gas-phase limited emissions; the diffusion-limited emissions; and an adjustment term for the transition. The full model is:

$$R = k_g \left(C_{v0} \frac{M_v}{M_{v0}} - C \right) + \left(1 - \frac{M_v}{M_{v0}} \right)^2 \frac{f_{D1} M_D}{\sqrt{t}} \tag{7.38}$$

The model has proven to provide an excellent description of short-term and long-term (>200 days) latex paint emissions (Sparks et al., 1999b). However, the use of empirical factor limits the general applicability of this model. Further, the above model fails to consider the impact of substrates on emissions (Yang et al., 2001b).

It has been evidenced that the VOCs emissions from wet materials are governed by mass transfer in four different layers: the material film, the substrate, the material-air interface, and the air phase. Several models (Yang et al., 2001a,b; Haghighat and Huang, 2003; Zhang and Niu, 2003a,c) based on the corresponding fundamental

mass transfer mechanisms have been developed. The mass transfer emission models for wet materials differ from those for dry materials in the VOCs diffusion coefficient D_m. Various previous studies have demonstrated that the VOCs emissions from wet materials are characterized with high initial emission rate and fast decay, followed by low emission rate and slow decay (Guo and Murray, 2000). That means the VOCs concentration within wet material is extremely high when the material is freshly applied or partially dry. Under this circumstance, the dependency of the diffusion coefficient on the concentration $D_m = D_{m,wet} = f(C_m)$ must be taken into consideration. When the applied material film is totally dry, the majority of the VOCs containing in the film have emitted, VOCs concentration in the material is relatively low and until now the diffusion coefficient can be considered as concentration independent, i.e. $D_m = D_{m,dry} = \text{Constant}$. The core part of these models is the diffusion equation describing VOCs diffusion within the material film:

$$\frac{\partial C_m}{\partial t} = \frac{\partial}{\partial x}\left(D_m \frac{\partial C_m}{\partial x} \right) \tag{7.39}$$

Due to the difficulty in theoretical or experimental determination of D_m for wet materials, a third-power empirical equation (Yang et al., 2001a,b; Zhang and Niu, 2003a,c) $D_m = D_{m0,wet}\left(\frac{C_m}{C_{m0,wet}} \right)^3$, was used to describe the dependence of D_m on C_m, where $D_{m0,wet}$ is the initial diffusion coefficient in the wet film, and $C_{m0,wet}$, the initial VOCs concentration in the wet film. However, the third-power empirical equation may not be valid when the film is totally dry (Haghighat and Huang, 2003), because when C_m is very small, $(C_m / C_{m0,wet})^3$ approaches zero. In order to overcome this problem, a second-power empirical equation was proposed (Haghighat and Huang,

2003) $D_m = D_{m0,wet}\left(\frac{C_m}{C_{m0,wet}}\right)^2 + D_{m,dry}\left(1-\left(\frac{C_m}{C_{m0,wet}}\right)^2\right)$, where $D_{m,dry}$ is the VOCs diffusion coefficient of the dried material film. However, both of the empirical equations used weaken the physical foundations of the models.

The latest models developed for VOCs emissions from dry materials (Yang et al., 2001d; Huang and Haghighat, 2002; Xu and Zhang, 2003; Zhang and Xu, 2003; Deng and Kim, 2004a; Xu and Zhang, 2004) or dry material assemblies (Zhang and Niu, 2004; Li et al., 2005) usually assume that building material is a homogenous medium and VOCs exist within the material only in a material phase. So these models all belong to the so-called **one-phase models** or **continuum models**. They are very similar to the above discussed models for wet materials but are simpler due to the constant diffusion coefficient employed.

Actually, as described earlier, building materials are often porous mediums - consisting of pores and solid parts (Peter, 1998; Blondeau et al., 2003) and VOCs existing within the material are in a gas phase and an adsorbed phase (Murakami et al., 2001; Tiffonnet et al., 2002; Lee et al., 2003; Haghighat et al., 2005; Lee et al., 2005). Utilizing the knowledge of mass transfer in porous medium introduced earlier, the main part of a **multi-phase model** is straightforward:

$$(\varepsilon + K)\frac{\partial C_g}{\partial t} = (D_{e,g} + KD_{e,s})\frac{\partial^2 C_g}{\partial x^2} \tag{7.40}$$

A summary of the features and limitations of the mass transfer based source models and the type of material that they are applicable to is presented in Table 2.4.

Table 2.4 Summary of the features and limitations of the mass transfer based source modes and the type of material they are applicable to

Model		Features	Limitiations	Type of material
Evaporation controlled model	Tichenor et al. (1993) VB model	● VOC equilibrium vapor pressure is characteristic of product and is independent of the amount of coating applied ● Total vapor pressure at surface is assumed to be proportional to the amount of TVOC remaining in the source ● The average gas phase diffusivity of solvent molecules can be represented by the diffusivity of the most abundant component in the solvent mixture.	● Underestimates the long-term TVOC emissions ● Difficult to determine boundary layer thickness	Wet material
	Guo et al (1999) VBX model	● Extension of VB model ● Can be used to predict individual VOC emission	● Underestimates the long-term emissions	
Diffusion controlled model	Christiansson et al. (1993)	● Only diffusion controls the release	● Did not indicate how to deal with the mass between 50% and 55%	Dry material
	Yang et al. (1998)	● Emission is solely determined by internal diffusion ● Zero material surface concentration assumed	● Only applicable to predict long-term emissions	
	Little et al. (1994)	● Instant equilibrium between gas-phase and material surface concentrations	● Convective resistance neglected ● Overestimation of the early stage data	

Combined evaporation and diffusion model	Sparks et al. (1999a)	● A VB model for evaporation controlled emission ● A diffusion-limited emissions ● An adjustment term for the transition	● Empirical term limits the general applicability ● No consideration of substrate effect	Wet material
	Yang et al. (2001b)	● Diffusion coefficient dependent on concentration ● Third-power equation used	● No validation of the equation ● Physical foundation weakened	
	Haghighat and Huang (2003)	● Diffusion coefficient dependent on concentration ● Second-power equation used	● No validation of the equation ● Physical foundation weakened	
	Deng and Kim (2004a)	● Homogeneous material ● VOCs only in material-phase	● Can not provide insight into inherent mass transfer processes in porous materials	Dry material
	Tiffonnet et al. (2002)	● Solid and void overlapping ● VOCs exist in gas-phase and adsorbed-phase	● Detailed model is not developed	
	Zhang and Niu (2004)	● Homogeneous material ● VOCs only in material-phase ● Whole room scenario	● Can not provide insight into inherent mass transfer processes in porous materials	Dry material assemblies

2.4.3 Building Material VOCs Sink Models

In order to model the real scenarios in indoor environment, special attention should be paid to one more important phenomenon, i.e., the so-called sink effect. It has been revealed that the amount of adsorbed mass depends on several parameters, such as temperature, relative humidity, chemical nature and gas phase concentration of the VOCs, and VOCs/material properties like chemical structure, pore size, or specific surface area (Meininghaus et al., 2000b).

The sink effect, i.e., adsorption and desorption of VOCs by indoor materials like wall coverings, furniture, or floorings, can have a significant impact on indoor air quality by changing their dynamic behavior (Meininghaus et al., 2000b). Sorptive interactions may lead to reductions in peak concentrations of VOCs and hence reductions in occupant inhalation exposures to high level of concentrations. However, sorption may also lead to significant increases in chemical retention time within a building and subsequent re-emission over prolonged time periods (Won et al., 2000). Therefore, in view of the significant impact of building materials on indoor concentrations of VOCs, an accurate characterization of sink effect of VOCs in building materials is in great need of.

2.4.3.1 Empirical Sink Models

Traditionally, sorption is viewed as a solely surface phenomenon: the adsorption and desorption processes occur simultaneously. Tichenor et al. (1991) developed a **one-sink** model to describe the sorption at the indoor surfaces. This model was derived from the Langmiur isotherm. In this model, the adsorption rate is proportional to the concentration in the chamber $k_a C$ (k_a is adsorption rate constant), the desorption

rate is proportional to the mass adsorbed by the sink surface $k_d M$ (k_d is desorption rate constant). The model can be described by a mass balance equation at the sink surface in a small chamber:

$$\frac{dM}{dt} = k_a C - k_d M \tag{7.41}$$

This model has been widely used by many researchers (Chang and Guo, 1994; Chang et al., 1998; Yu and Crump, 1998; An et al., 1999; Bouhamra and Elkilani, 1999; Jørgensen and Bjørseth, 1999; Jørgensen et al., 1999; Won et al., 2000, , 2001a; Elkilani et al., 2003) to study the sink effect, and has proven to be applicable to many indoor sinks. Won et al. (2001b) further conducted scale-up experiments to validate this surface sink model. Three materials (carpet system, pad, and virgin gypsum board) were exposed to three chemicals (cyclohexane, toluene, and ethylbenzene) in a large-scale experimental chamber (10.4 m^3). Measured concentrations were compared to predicted data, which were calculated from sorption coefficients estimated from small-scale chamber experiments. In general, the predicted concentrations were in good agreement with the measured concentrations. Won et al. (2001b) concluded that the surface sink model can successfully describe the sorptive sinks in the large-scale laboratory chamber along with sorption coefficients obtained from small-scale experiments.

However, Tichenor et al. (1991) pointed that Langmuir kinetics apply to relatively flat, smooth surfaces (e.g., ceiling tile, wallboard), but may be inappropriate for more complex surfaces (e.g., carpet and upholstery). So that a commonly expressed disadvantage with the one-sink model is that it has a problem characterizing the ‘tail’ of the desorption curve from complex materials (e.g., fleecy materials such as carpet)

(Jørgensen et al., 2000). For complex materials, the relatively slow in-material diffusion may be significant and thus can not be neglected.

In order to overcome this problem, De Bortoli et al. (1996) tried to characterize sorption processes with two sinks - a 'fast' sink (the rate constants k_3 and k_4) and a 'slow' sink (the rate constants k_5 and k_6). Although the use of 'slow' sink makes the two-sink model fit most experimental data very efficiently, the model does not provide a complete physical description of the real adsorption processes (De Bortoli et al., 1996).

Later, Jørgensen et al. developed a **sink-diffusion** model (Jørgensen et al., 2000), which is modified from the Tichenor's one-sink model by taking into account Fickian-like diffusion into the material. The model is in the form of:

$$\frac{dM_1}{dt} = k_a C - k_d M_1 - k_{diff}(M_1 - M_2) \tag{7.42}$$

$$\frac{dM_2}{dt} = k_{diff}(M_1 - M_2) \tag{7.43}$$

where M_1 is the VOCs mass in the surface sink, M_2 the VOCs mass in the interior sink, and k_{diff} the effective mass transfer coefficient between surface and interior sinks. This model has been shown to give better descriptions of the desorption curve in the cases with strong sorption effect (nylon carpet) in comparison with the one-sink model (Jørgensen et al., 2000).

However, the linear concentration gradient assumption used to quantify diffusion between surface sink and interior sink results in the model does not fully represent the physical characteristics of a diffusion-controlled sink and necessitates to fitting of data to estimate parameter (Zhao et al., 2002). Further, obtaining more than two

parameters simultaneously by fitting to the concentration curve might lead to multiple solutions (Zhang et al., 2002a).

2.4.3.2 Mass Transfer Based Sink Models

2.4.3.2.1 Equilibrium Adsorption (EA) Model

Axley (1991) proposed a so called equilibrium adsorption model to characterize the sink effect. He assumed that the mass transport due to advection is much slow relative to both external and internal diffusion rates (i.e., diffusion, adsorption and desorption transport rates are instantaneous relative to the flow transport dynamics), then the air-phase concentration and the adsorbed phase concentration will be uniform and are at all times in equilibrium with each other. This assumption is valid when the adsorbate is well distributed in the zone, and the zone-air concentration is changing very slowly. Different equilibrium relationships (such as linear, Langmiur, BET and Freundlich isotherms introduced earlier) might be employed. For the simplest case, considering low VOCs concentrations indoors, the linear isotherm can be used:

$$C_s = K_p C_z \tag{7.44}$$

or

$$\frac{dC_s}{dt} = K_p \frac{dC_z}{dt} \tag{7.45}$$

where units for C_s is (mass adsorbate)/(mass adsorbent) and for C_z is (mass adsorbate)/(mass air), then the unit for K_p should be (mass air)/(mass adsorbent).

The mass balance equation for the whole system (zone air+adsobent) is:

$$m_z \frac{dC_z}{dt} + m_s \frac{dC_s}{dt} = (m_z + m_s K_p)\frac{dC_z}{dt} = W(C_{in} - C_z) + G_z + G_s \tag{7.46}$$

where, m_s, m_z are the mass of adsorbent and zone air, respectively. W is the air mass flow rate through the chamber or room. C_{in} is the inlet VOCs concentration, G_s, G_z are the VOCs generation rate in the zone air and adsorbent, respectively.

2.4.3.2.2 Boundary Layer Diffusion Controlled (BLDC) Model

Axley (1991) also noticed that "adsorption mass transport rates from the room air to solid (i.e., non-porous) adsorbents with reasonably smooth surfaces may be expected to be controlled by the rate at which a contaminant species diffuses from the bulk phase to the surface of the adsorbent". He further developed a sink model to take the boundary layer diffusion into consideration. The uniform adsorbed phase concentration is assumed to be at all times at equilibrium with the near surface air phase concentration:

$$C_s = K_p C_z^* \tag{7.47}$$

Based on the boundary layer theory, the mass transport rate from the bulk phase to the surface can then be expressed as:

$$W_s = h_m \rho A (C_z - C_z^*) = h_m \rho A \left(C_z - \frac{C_s}{K_p} \right) \tag{7.48}$$

where h_m is the average convective mass transfer coefficient over the adsorbent surface, ρ is the film density (average of the bulk and surface air density), A is the projected surface area of the adsorbent.

Then the mass balance for the zone air is:

$$W(C_z - C_{in}) + h_m \rho A \left(C_z - \frac{C_s}{K_p} \right) + m_z \frac{dC_z}{dt} = G_z \tag{7.49}$$

and for the adsorbent is:

$$-h_m \rho A\left(C_Z - \frac{C_s}{K_p}\right) + m_s \frac{dC_s}{dt} = G_s \tag{7.50}$$

2.4.3.2.3 Boundary Layer and Porous Diffusion (BLPD) Model: Multi-phase Sink Model

In cases the porous diffusion process plays an import role in the overall mass transport. Axley and Lorenzetti (1993) further developed a boundary layer and porous diffusion model. In this model, the adsorbent was sliced up into *n* control volumes to enable the modeling of porous diffusion transport (only gas phase diffusion, neglecting the surface and solid phase diffusion); the zone-air is supposed to occupy another individual control volume. Assume the pore air phase concentrations remain in equilibrium with the adsorbed phase concentrations (i.e., $C_{s,i} = f(C_{g,i})$, i=1,2, …n.).

The mass balance equations for the zone-air and individual slices can be written as:

Zone air:

$$m_z \frac{dC_z}{dt} = W(C_{in} - C_z) - h_m \rho A(C_z - C_{g,1}) + G_z \tag{7.51}$$

First slice:

$$A\Delta x_1\left(\rho\varepsilon + \rho_s \frac{\partial f}{\partial C_g}\right)\frac{dC_{g,1}}{dt} = h_m \rho A(C_z - C_{g,1}) - \left[\rho A \frac{D_{e,g}}{\Delta x_1}(C_{g,2} - C_{g,1})\right] \tag{7.52}$$

Internal slice:

$$\begin{aligned} A\Delta x_i\left(\rho\varepsilon + \rho_s \frac{\partial f}{\partial C_g}\right)\frac{dC_{g,i}}{dt} &= -\rho A \frac{D_{e,g}}{\Delta x_i}(C_{g,i} - C_{g,i-1}) \\ &\quad - \left[\rho A \frac{D_{e,g}}{\Delta x_1}(C_{g,i+1} - C_{g,i})\right] \end{aligned} \tag{7.53}$$

Bottom slice:

$$A\Delta x_n \left(\rho\varepsilon + \rho_s \frac{\partial f}{\partial C_g} \right) \frac{dC_{g,n}}{dt} = -\rho A \frac{D_{e,g}}{\Delta x_n} (C_{g,n} - C_{g,n-1}) \tag{7.54}$$

where ε is the porosity of the adsorbent, ρ_s the bulk density of the adsorbent, Δx_i the thickness of individual slice, $C_{g,i}$ the pore air phase concentration in individual slice, and $D_{e,g}$ the effective gas phase diffusivity of the adsorbent.

It can be observed that if Δx_i is small enough, equation (7.54) is equivalent to:

$$\left(\rho\varepsilon + \rho_s \frac{\partial f}{\partial C} \right) \frac{\partial C_g}{\partial t} = \rho D_{e,g} \frac{\partial^2 C_g}{\partial x^2} \tag{7.55}$$

Then it is clear that the BLPD model is a **multi-phase sink model** and is expected to be able to better characterize the sink effect. Lee et al. (2005) developed a similar model and obtained an analytical solution by assuming that the ambient VOCs concentration C_z is constant. However this is somewhat an oversimplification and may introduce uncertainties.

Axley and Lorenzetti (1993) also demonstrated the model selection criterion based on a three-part ratio:

$$W : h_m \rho A : \rho A D_{e,g} / b \tag{7.56}$$

where b is the total thickness of the material. When the last two terms are large relative to the first, then the **EA** model may be expected to be accurate; when the first two terms are of the same magnitude yet smaller than the third term, then the **BLDC** model may be expected to be accurate; and when the last term is small or of a similar magnitude to the other terms, then the complete **BLPD** model should be used.

2.4.3.2.4 Boundary Layer and Material-phase Diffusion Model: One-phase Sink Model

It should be noted that the diffusion process is more often described by ***one phase*** (i.e., material phase) diffusion for the sake of simplicity. And consequently the sorption is assumed to occur only at the projected surface of the material. For example, Yang et al. (2001c) developed a numerical sorption model based on the above simplifications. Little and Hodgson (1996) developed an analytical diffusion-controlled sink model by further neglecting the boundary layer convective mass transfer resistance. Zhao et al. also (2002) used this model to theoretically investigate the sink effect of a styrene butadiene rubber (SBR) backed carpet, vinyl flooring (VF), and a polyurethane foam (PUF) carpet in response to transient contaminant sources. Kumar and Little (2003a) further extended the model and obtained an analytical solution for characterizing the sink effect of double-layer dry building materials.

A summary of the assumptions, merits and limitations of the sink models described above is present in Table 2.5.

Table 2.5 Summary of assumptions, merits and limitations of different sink models

Models			Assumptions	Merits	Limitations
Empirical model		One sink model	● Sorption is viewed as a surface phenomenon ● Adsorption and desorption occur simultaneously	● Simple	● Inappropriate for complex surfaces ● Can not correctly characterize the 'tail' of the desorption curve from complex materials
		Two sinks model	● A 'fast' sink and a 'slow' sink	● Fits data better	● Can not provide a complete physical description of the real sorption processes ● More parameters to be fitted ● Possible of multiple solutions
		Sink-diffusion model	● Linear concentration gradient between surface sink and interior sink assumed	● Fits data better	● The model doesn't fully represent the physical processes ● Possible of multiple solutions
Mass transfer based model		Equilibrium adsorption model	● Air phase concentration and adsorbed phase concentration is uniform and are at all times in equilibrium.	● Simple	● Valid only when the adsorbate is well distributed in the zone and zone air concentration is changing very slowly.
		Boundary Layer Diffusion Controlled (BLDC) model	● Boundary layer diffusion controls the sorption processes	● Physically more reasonable	● Only valid for solid materials with reasonably smooth surfaces
	Multiphase	Boundary Layer and Porous Diffusion (BLPD) model	● Porous diffusion process plays an important role	● Better characterizes the sorption phenomena	● An addition parameter 'porosity' required
	One phase	Boundary Layer and Material-phase Diffusion (BLMD) model	● Material is a homogenous media ● VOCs exist only in a material-phase	● An simplification of BLDP model	● Can not provide insight into inherent mass transfer processes within the material

2.4.4 Integrated Source/Sink Models

In reality, a variety of building materials exist in the same indoor environment and it is known that building materials can act both as sources and sinks of indoor VOCs depending on the concentration gradient. It is necessary to have an integrated model that accounts for multi-layer multi-component situations of the materials so that accurate predictions of indoor VOCs concentration can be achieved. These models are quite similar to the latest versions of mass transfer theory based source or sink models, i.e., considering the convective mass transfer, surface (internal) partitioning, and diffusion in (porous) material, the major differences are the initial conditions of the models. Obviously, there should also be two types of these models: one-phase and multi-phase models. Analytical solutions are no longer easy to obtain, the system of the equations is usually numerically solved by means of finite difference method or finite volume method etc. Haghighat and Huang (2003) first developed an integrated one-phase source/sink model, and later Zhang and Niu (2004) did similar work. Up to date, an integrated multi-component multi-layer multi-phase source/sink model is still unavailable.

2.5 Determination of Model Parameters

In order to accurately characterize VOCs source/sink behaviors for indoor building materials, mass transfer based models are obviously more advantageous over empirical ones because they are easy to scale up. However, a number of parameters (such as diffusion coefficient, partition coefficient, mean convective mass transfer coefficient, and initial condition of the material) in this kind of models should be known or determined before the modeling can proceed. The more accurate parameters provided, the better model predictions fit the test results. The true

obstacles in the development and utilization of the models capable of simulating realistic building configurations are the lack of experimental data for the physical parameters involved in the models (Blondeau et al., 2003).

2.5.1 Determination of Diffusion and/or Partition Coefficients

Researches show that the concentration dependence on the coefficients may be neglected below a concentration ratio (a dimensionless ratio of the initial concentration of VOC to the material density) of 1%. For dry materials, the initial concentrations are generally very low, thus the ratio is well below the threshold 1%. The diffusion and partition coefficients for dry materials can then be considered as concentration independent (Yang et al., 2001b). So, when determining the properties of common indoor VOC/material combinations, special attention should be paid to ensure the VOC concentration within the range of or at most slightly higher than typical indoor VOC concentration, otherwise the parameters determined would not be representative for indoor use.

2.5.1.1 Packed Column Method

Borazzo et al. (1990) used a “packed column” method to determine the partition coefficient of fiber material. The idea is the retention time of VOC through a column packed with the material is related with its partition coefficient. By measuring the retention time of a test VOC, one can calculate its partition coefficient. The limitation of this method is that material has to be cut into small piece which may significantly change the material structure (Zhang et al., 2002a).

2.5.1.2 Wet Cup Method

The wet cup method has been used to measure water vapor diffusion coefficient with great success. Kirchner et al. (1999) adopted this method to measure the diffusion coefficient of *n*-octane and ethyl acetate for wallpaper with paste, acrylic paint on woodchip paper, gypsum board, solid concrete, aerated concrete, PVC floor covering, carpet with SBR backing, brick and acoustic tile. And later, Hansson and Stymne (2000) also used this method to determine the diffusion coefficient of toluene for gypsum board, medium density fiber board and wood particle board. The test material forms the lid of the cup containing a liquid VOC at saturation under controlled temperature and humidity conditions. The diffusion coefficients are determined using the information of weight loss recorded by a microbalance. Though simple, the main drawback of this method is the unrealistically high VOC concentration (saturation concentration of the test VOC, under this circumstance, the diffusion coefficient is usually dependent on the concentration) involved and thus will overestimate the diffusion coefficient (Haghighat et al., 2002).

2.5.1.3 Twin CLIMPAQ/FLEC Method

Kichner et al. (1999) and Meininghaus et al. (2000a) also measured the diffusion and sorption capacity of the two VOCs in eight building materials as stated in the above wet cup method by means of Chamber for Laboratory Investigations of Materials, Pollution and Air Quality (CLIMPAQ) method. A pair of CLIMPAQ (Gunnarsen et al., 1994) type chambers was used, the test material was placed between two CLIMPAQs. One of the CLIMPAQ (primary) was ventilated with constant concentration of contaminated air and the other (secondary) with clean air. When steady state reaches, the effective diffusion coefficient can be determined by:

$$D_{eff} = -\frac{m}{A}\frac{\Delta x}{\Delta C} = -\frac{Qd}{A}\frac{C_2}{C_2 - C_1} \tag{7.57}$$

where Q is the ventilation rate, d the thickness of test material, A the area of the material, C_1 steady state VOC concentration in primary CLIMPAQ, and C_2 steady state VOC concentration in secondary CLIMPAQ.

The sorption capacity S can be estimated based on the difference between VOC mass flow into the primary chamber ($\dot{m}_{i,in}$) and out of both primary ($\dot{m}_{i,prim}$) and secondary ($\dot{m}_{i,sec}$):

$$S = \frac{\sum_{i=1}^{n}\left[\dot{m}_{i,in} - (\dot{m}_{i,prim} + \dot{m}_{i,sec})\right]\cdot \Delta t_i}{\left(\frac{C_1 + C_2}{2}\right)} \tag{7.58}$$

The limitations of this method lie in that it is assumed that the concentration gradient in the material is linear and concentrations on the test materials' surfaces are the same as the chamber concentration at steady state.

The **twin FLEC method** developed by Meininghaus and Uhde (2002) is a variation of the twin **CLIMPAQ** method. In this method, two FLECs instead of CLIMPAQs were installed face-to-face, separated by the test specimen. The principles and method of data analysis are the same as those in twin CLIMPAQ method.

2.5.1.4 Diffusionmetric Method

Bodalal et al. (2000) developed a diffusionmetric method to determine the diffusion and partition coefficients of four VOCs (toluene, nonane, decane, undecane) for a backing material of a carpet specimen, four VOCs (ethyl benzene, nonane, decane, and undecane) for a floor tile and three VOCs (cyclohexene, ethylbenzene, and

decane) for plywood. Two identical chambers of 50 liters in volume were separated by the test specimen. The first chamber was initially at a VOCs concentration level of C_0, and an impermeable membrane prevented the VOCs contacting with the test specimen, the second chamber was initially at a zero VOCs concentration. When the test began, the membrane was broken and then VOCs diffused through the test specimen. VOCs concentrations in both chambers were periodically monitored. Fick's second law was used to describe the diffusion process, diffusion and partition coefficients could be inferred from the obtained concentration curves. They found that the values of diffusion coefficients for a given material were inversely proportional to the molecular weights of the VOCs, whereas the values of the partition coefficients were proportional to the vapor pressures of the VOCs. However, the boundary conditions they used:

$$C_m \big|_{x=0}(t) = K_{ma} C_1(t) \tag{7.59}$$

$$C_m \big|_{x=d}(t) = K_{ma} C_2(t) \tag{7.60}$$

are on the basis of neglecting convective mass transfer resistance. Where C_1 and C_2 are the chamber air concentration in the two chambers.

2.5.1.5 Twin compartment Method

Hansson and Stymne (2000) used a stainless steel chamber consisting of two cylindrical compartments (the first was flushed with contaminated air and the second with clean air) with test specimen placed in between them. The inlet compound - toluene concentration for the first compartment and the outlet concentration for both compartments were continuously recorded using a quadrupole mass spectrometer until a steady state was observed. A complex model with five parameters was used to describe the mass transport mechanisms, three of them (D , K_i and g) were

determined by fitting model to the experimental results, K_s was set equal to the value obtained in a previous study, K_g was guessed to reasonable values. Hence, there is a possibility of multi-solution (Haghighat et al., 2002).

2.5.1.6 Microbalance Method

Researchers also used dynamic microbalance to measure the material properties (Little and Hodgson, 1996; Cox et al., 2001b; Kumar and Little, 2003b; Zhao et al., 2004). In such a method, the specimen inside a small chamber was placed on a high-resolution microbalance. The chamber was flushed by contaminated air flow with a constant VOC concentration until equilibrium was established, and then the contaminated air was replaced by clean air and desorption period began. The weight of the specimen changes with elapsed time and was measured and recorded by a computer-based data-acquisition system. In this method the partition coefficient is usually determined by equilibrium parameters at the end of the adsorption period $K_{ma} = C_{m,e} / C_{a,e}$, where $C_{m,e}$ is the equilibrium concentration in the material which can be inferred from the weight difference between the start and end of adsorption period, $C_{a,e}$ is the equilibrium concentration in the chamber and can be determined by $C_{a,e} = E / Q$, where E is the constant VOC emission rate synthetically generated and Q is the airflow rate through the system. The diffusion coefficient is determined by fitting the diffusion model either to experimental adsorption or desorption data. This novel method is simple and cost-effective because no VOC sampling and analysis is needed. However, due to the range and detection limit of the microbalance, the test specimen must be cut into extremely thin pieces, which may significantly affect the surface characteristics of the test material (Zhang et al., 2002a) and the generated VOC concentration used is much higher than common indoor VOC

concentration level. Further, the diffusion model used neglects the convective mass transfer resistance. In addition, only one compound can be tested in one sorption test by using this method.

Other researchers (Meininghaus et al., 2000b) used the dynamic microbalance method with emphasis on investigating the adsorption isotherm. The test procedures are relatively simple: once an equilibrium state is reached, the equilibrium gas phase concentration in the chamber is sampled and quantified; the equilibrium material phase concentration is inferred from the mass increase of the test specimen. Then increase the inlet VOC concentration and let another equilibrium state to establish. Repeat the procedures for several inlet VOC concentration level, and plot the obtained data sets in a graph. If the adsorption isotherm follows a linear form, all the data should be approximately on a line, and the slope of the regression line is the partition coefficient according to the definition: $K_{ma} = C_{m,e} / C_{a,e}$. Meininghaus et al. (2000b) found linear or almost linear adsorption isotherms for most combinations of compounds (*n*-octane and *m*-xylene) and materials (wallpaper, carpet, acrylic paint, PVC flooring, aerated concrete, and gypsum board).

2.5.1.7 Static Chamber Method

Tiffonnet et al. (2002) developed a static chamber method to investigate the sorption isotherms of acetone on chipboard, acrylic paint, and the gypsum core of commercially available gypsum board. A cleaned test material was placed in a 46-liters stainless steel chamber and then the chamber was totally sealed. Known amount of liquid acetone was injected into the chamber and vaporized instantly due to its high volatility. A mixing fun in the chamber ensured that the acetone was fully mixed in the chamber air. The air samples in the chamber were taken and analyzed

every 5 min and then back to the chamber. When the air phase concentration would not change any more, equilibrium state was reached, and the equilibrium gas phase concentration was $C_{a,e}$. The equilibrium adsorbed phase concentration $C_{m,e}$ can be inferred from the difference of acetone mass between injected and in the chamber air at equilibrium state. Repeat the above procedures results in the adsorption isotherm.

The desorption isotherm can be determined as follow: at the final equilibrium state of adsorption period, a known volume of air in the chamber was pumped out and replaced by same volume of clean air, the system would reach a new equilibrium state. Record the gas phase concentration in the chamber and calculate the adsorbed phase concentration based on mass balance, and repeat the procedures to get several data sets. Tiffonnet et al. (2002) found that adsorption isotherms for acetone on acrylic paint is linear but is nonlinear on chipboard and gypsum board (even at common indoor concentration range). They also noticed that the adsorption and desorption isotherms of acetone on gypsum board are clearly distinct.

2.5.1.8 Dynamic One Chamber/FLEC Method

This method is commonly used and has two versions. The first one is dynamic emission test method (Little et al., 1994). A test material initially containing uniformly distributed VOCs was flushed with clean air in a chamber, and the air in the chamber was periodically sampled and analyzed. The diffusion coefficients of individual VOCs can be obtained by fitting the diffusion model to the experimental data, the partition coefficient can be separately determined by, for example, additional test of headspace analysis. The second one is the dynamic sorption test method (Zhang et al., 2002b,2003), which consists of an adsorption period and a

desorption period. The parameters can be determined from either the adsorption data or desorption data.

2.5.1.9 Porosimetry Test Method

Blondeau et al. (2003) developed a new method to assess diffusivities of ethyl acetate and *n*-octane in seven typical building materials (particle board, aerated concrete, solid concrete, brick, mortar, and two different types of gypsum bard). This method consists carrying out mercury intrusion porosimetry (MIP) tests to characterize the porous structure of the materials of interest, and then applying Carniglia's mathematical model to estimate the effective diffusivities of any gaseous species in these materials. The advantage of this method is that it only requires 1 to 2 h to determine the effective diffusivity of any gas in a given material. Some important information like the pore size distribution, total porosity, tortuosity factor and specific surface area etc. of the test material can also be determined, which provides the possibility of relating the diffusivity with the microstructure of building material. However, this method can not be applied to all building materials; according to the theory the methodology only applies to homogeneous materials. In addition, some materials cannot undergo MIP tests, either due to chemical incompatibilities or because they are not resistant enough to sustain high pressures. Finally, the partition coefficient of the building material can not be measured by this method.

Finally, a summary of merits and drawbacks of each method is presented in Table 2.6.

Table 2.6 Summary of merits and drawbacks of different methods

Method	Parameter(s)	Merits	Drawbacks
Packed column	K_{ma}	● Simple experimental procedure ● Simple calculation technique	● Small piece of test material required, which may change material structure
Wet cup	D_{eff}		● Unrealistically high VOC concentration used ● Possible overestimation of D_{eff} ● Only one compound in a test
Twin CLIMPAQ/FLEC	D_{eff}, S	● Controllable VOC concentration ● VOCs mixture can be used	● Long time to reach steady state ● Linear concentration gradient in the material assumed ● Material surface concentration equals to bulk air concentration assumed
Diffusionmetric	D_m, K_{ma}		● A variety of air samples required ● Convective resistance neglected in the model ● Possible of multiple solutions
Twin compartment	D_g, K_i, g		● Continuous constant VOC concentration source required ● Possible of multiple solutions
Microbalance	D_m, K_{ma}	● No need of air sampling	● Thin piece of test material required ● High VOC concentration used ● Only one compound in a test
Static chamber	Sorption isotherm	● Simple calculation technique	● Both microbalance and air samples required ● Can not determine diffusion coefficient ● Only one compound in a test
Dynamic one chamber or FLEC	D_m, K_{ma}	● Controllable VOC concentration ● VOCs mixture can be used	● A variety of air samples required ● Possible of multiple solutions
Porosimetry test	D_{eff}	● Only 1~2h required ● Provide porous material properties	● Special equipments required plus relatively complicated analysis procedure ● Not applicable to all building materials ● No consideration of possible interaction between VOC and material

2.5.2 Determination of Initial VOCs Concentration in the Material

The initial concentration in the material can be experimentally determined using the methods, such as extraction and direct thermal desorption or extraction and fluidized-bed desorption. The former can only be used to determine the mean total (mobile portion and immobile portion) initial VOCs concentration in the material while the latter also provides the possibility of determining the distribution of the mobile VOCs within the material.

2.5.3 Determination of Mean Convective Mass Transfer Coefficient

2.5.3.1 In an Environmental Chamber or a Room

In the field of indoor air quality, air flow passing building material surfaces is usually treated as flow parallel to a flat plate, and the mean convective mass transfer coefficient h_m is estimated from mass transfer correlations among Sherwood number (Sh), Reynolds number (Re) and Schmidt number (Sc):

For laminar flow ($Re < 500,000$)

$$Sh = 0.664 Sc^{1/3} Re^{1/2} \tag{7.61}$$

For turbulent flow ($Re > 500,000$)

$$Sh = 0.037 Sc^{1/3} Re^{1/5} \tag{7.62}$$

where $Sh = h_m l / D_a$, $Sc = v / D_a$, and $Re = u_m l / v$. u_m is the mean air velocity over the material surface (m s^{-1}), l is the characteristic length of the material (m), D_a is the compound diffusivity in air (m^2 s^{-1}), and v is the kinematic viscosity of the air (m^2 s^{-1}).

2.5.3.2 In the Field and Laboratory Emission Cell (FLEC)

Due to the unique geometry of the FLEC cell, Zhang and Niu (2003b) investigated mass transfer in the FLEC by means of both CFD and experiments. They used distilled water to substitute the emission surface. Mass transfer data were obtained by calculating humidity differences between the inlet and outlet of a gas stream flowing through the FLEC. They found that the Reynolds numbers for the flow in the FLEC cell are very small, e.g. Re=21 when Q=5 l/min, which is far below the critical Re_{cr} of 2000, so that the flow in the FLEC is thought to be laminar. They also found that the air will become saturated as it flows along the FLEC radius if the air flow rates are below 1000 ml/min. They finally formulated an experimental correlation using dimensionless group numbers:

$$Sh_m = 0.817 Re^{0.86} Sc^{0.68} \left(\frac{r_o - r_i}{2\delta} \right)^{-0.68} \tag{7.63}$$

where $r_o = 75\ mm$, r_i is the radial coordinate, $\delta = 1\ mm$ is the height of the air slit. This correlation can be used to estimate the mean convective mass transfer coefficient in the FLEC.

Chapter 3
A Physically-Based Model for Predicting VOCs Emissions from Paint Applied on an Absorptive Substrate

3.1 Introduction

VOCs emitted by building materials are recognized as major problems affecting human comfort, health, and productivity (Huang and Haghighat, 2002). They affect indoor air quality via several mass transfer mechanisms: 'Wet' materials like paints release VOCs mainly by evaporation, while VOCs in 'dry' materials like carpets become airborne via diffusion and surface convective processes. 'Wet' indoor coatings such as paints are widely used during remodeling and renovation in buildings, most of which are petroleum-based and thus emit a wide variety of VOCs (Yang et al., 2001b).

Increased awareness regarding the indoor air quality has created a demand for low-emitting (healthy) building materials (Zhang and Niu, 2003c). For VOCs emissions from petroleum-based materials, in the industry, product reformation makes it possible to change from solvent-based paints to water-based emulsion paints, and corresponding regulations in some regions restrict the VOCs contents of paints for indoor use. These have prompted several activities for standardized methods to characterize and quantify the emissions from building materials (Zhang and Niu, 2003c). The field and laboratory emission cell (FLEC) (CEC, 1998) is primary designed for the measurement of VOCs emissions from planar construction products and from applied paints or coatings. It has proved a convenient tool since its commercial introduction in the early 1990s, and has become European standard for

emission test. This study also uses FLEC to characterize and quantify VOCs emissions from paint.

In this research, a novel simple physically-based model for the prediction of VOCs emissions from paint is developed. Considering the fact that paint film is usually very thin, the present model assumes the VOCs concentration within the applied paint film is always uniform, i.e. the internal diffusion resistance in the paint film is negligibly small. It should be noted that this assumption may not hold when the paint film is totally dry. Meanwhile the substrate effect is considered so that the model can be generally applicable to circumstances of paints applied onto real substrates like particle board, gypsum board and plywood etc. The model can be used to predict both individual VOCs and TVOC emissions from paint. Since the model parameters have distinct physical meanings, the proposed model is easy to scale up.

3.2 Mathematical Model

3.2.1 Model Development

Figure 3.1 is a schematic representation of a paint film applied on a substrate and relevant mass transfer mechanisms.

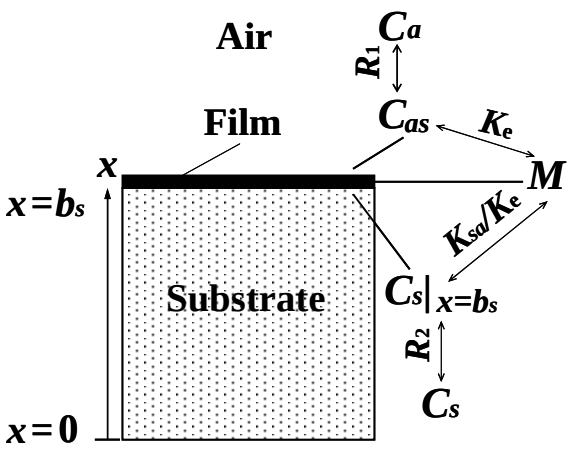

Figure 3.1 Schematic drawing of VOCs mass transfer from a paint film applied on a substrate

Several assumptions are made when developing the model. Firstly, although most of the natural substrates are porous materials, for the sake of simplicity, from macroscopic point of view, the substrate can be treated as homogenous. Secondly, the internal diffusion resistance in the wet thin paint film is negligible. Thirdly, VOCs concentration in the air near the paint film and substrate upper surface is always in equilibrium with the concentration in the film and substrate upper surface, respectively. Finally, the VOCs concentration in the emission cell is assumed to be uniform.

When clean air is supplied to the emission cell, the transient VOCs mass balance in the cell should be satisfied, which can be expressed by:

$$\frac{dC_a}{dt} = -NC_a + Lh_m(C_{as} - C_a) \tag{3.1}$$

where N is the air change rate (h^{-1}), L is the loading ration ($m^2\ m^{-3}$), h_m ($m\ s^{-1}$) is the mean convective mass transfer coefficient over the paint film, C_{as} ($kg\ m^{-3}$) is the VOCs concentration in the cell air near the paint film, and C_a ($kg\ m^{-3}$) is the VOCs concentration in the bulk air in the cell.

Assume that no mass flux is accumulated at the paint film/air interface, i.e. the mass flux out of the upper surface of the paint film is equal to the mass flux transferred through boundary layer diffusion to the bulk air in the cell. Therefore the following equation can be written:

$$R_1 = h_m (C_{as} - C_a) \tag{3.2}$$

where R_1 (kg m^{-2} s^{-1}) is the VOCs mass transfer rate out of the upper surface of the paint film.

Although Henry's law is valid only for low-solute concentrations, it can also be applied to a wide range of gases and VOCs of environmental interest (Clark, 1996). Thus at the film/air interface, Henry's law can be written as:

$$M = K_e C_{as} \tag{3.3}$$

where K_e (m) is the equilibrium constant, M (kg m^{-2}) is VOCs concentration in the thin paint film.

Because of the existence of the substrate, VOCs will first diffuse into the substrate, and later re-emit from the substrate. Let R_2 (kg m^{-2} s^{-1}) denote the VOCs mass flux of this portion. Transient mass balance in the paint film is then expressed as:

$$\frac{dM}{dt} = -R_1 + R_2 \tag{3.4}$$

At the paint film/substrate interface, equilibrium between the VOCs concentration in the paint film and the substrate surface VOCs concentration is assumed, as equation (3.5) describes:

$$C_s \Big|_{x=b_s} = \frac{K_{sa}}{K_e} M \tag{3.5}$$

where K_{sa} is the partition coefficient between the substrate and air.

VOCs transfer in the substrate mainly through diffusion, Fick's second law is often used to describe the transient diffusion process. Thus the VOCs diffusion in the substrate is governed by:

$$\frac{\partial C_s}{\partial t} = D_s \frac{\partial^2 C_s}{\partial x^2} \tag{3.6}$$

The boundary condition at the upper surface of the substrate is:

$$-D_s \frac{\partial C_s}{\partial x}\Big|_{x=b_s} = R_2 \tag{3.7}$$

The boundary condition at the lower surface of the substrate is:

$$-D_s \frac{\partial C_s}{\partial x}\Big|_{x=0} = 0 \tag{3.8}$$

The initial conditions for the paint film and substrate are given by equations (3.9) and (3.10) respectively:

$$M\big|_{t=0} = M_0 \tag{3.9}$$

$$C_s\big|_{t=0} = 0 \tag{3.10}$$

3.2.2 Model Parameters

The five key parameters of the present model are: mean convective mass transfer coefficient h_m, the equilibrium constant K_e between the paint film and air, the partition coefficient K_{sa} between the substrate and air, the diffusion coefficient D_s of the substrate, and initial VOCs mass per unit area of the paint film M_0.

The properties (K_{sa} and D_s) of the substrate are usually determined by emission/sorption experiments, related work can be found in (Bodalal et al., 2000; Cox et al., 2001b). There are already some published data available for a certain number of VOC/material combinations, which can be directly used because they are test-condition independent.

Regarding the mean convective mass transfer coefficient h_m over the paint film in the FLEC, a previous study (Zhang and Niu, 2003b) has summarized a formula to estimate its value. The formula shows the relationship among Sherwood number (Sh_m), Reynolds number (Re) and Schmidt number (Sc):

$$Sh_m = 0.817 Re^{0.86} Sc^{0.68} \left(\frac{r_o - r_i}{2\delta} \right)^{-0.68} \tag{3.11}$$

where $Sh_m = \frac{2h_m\delta}{D_a}$, $Re = \frac{2u_m\delta}{\nu}$ and $Sc = \frac{\nu}{D_a}$. δ is the height of air slit (m), u_m is the mean air velocity at the slit, ν is the kinematic viscosity of air ($m^2\ s^{-1}$) and D_a is the diffusivity of VOCs in air ($m^2\ s^{-1}$). The value of D_a for some VOCs can be readily found in (Rafson, 1998) or can be estimated using empirical approaches like FSG method (Clark, 1996). The formula given by FSG method is:

$$D_a = \frac{10^{-3} T^{1.75} \sqrt{M_r}}{p\left(V_A^{1/3} + V_{air}^{1/3}\right)^2} \tag{3.12}$$

where T is the absolute temperature (K), p is the pressure (atm), V_A and V_{air} are the molar volume of the VOC and the molar volume of the air (20.1 $cm^3\ mol^{-1}$), respectively. M_r is a function of the molar mass of the VOC and air:

$$M_r = \frac{m_A + m_{air}}{m_A m_{air}} \tag{3.13}$$

where m_A and m_{air} are the molar mass of the VOC and the molar mass of air (28.97 g mol^{-1}), respectively.

The initial VOCs mass per unit area of the paint film M_0 is often estimated from product formulation or can be experimentally determined, e.g. by using heat or

solvent extraction method. For emission tests it can simply be estimated by utilizing concentration curve obtained at the outlet of the chamber or cell.

There is only one parameter left, namely K_e to be determined. It can be obtained by fitting the present model to the experimental data. It should be pointed out that K_e is the property of VOC/paint combination, and thus is test-conditions independent. So this coefficient can also be used under other test conditions.

3.2.3 Model Solution

The system of equations (3.1) - (3.10) is closed. The model can be solved by using implicit finite volume method. A uniform grid system of the air-film-substrate structure is shown in Figure 3.2.

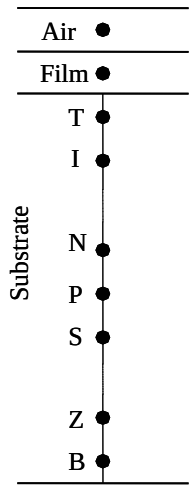

Figure 3.2 Schematic drawing of the grid system for the discretization of VOCs governing equations

One control volume (CV) standards for the air in the cell and the other CV represents coating film, the rest CVs are for the substrate. The grid T denotes the center of the boundary CV of the substrate near the coating film and the grid B denotes the center of the boundary CV of the substrate bottom, other grids denote the center of the

internal CVs of the substrate. The detailed discretization processes are shown as follow (where the superscript 0 denotes the known values at the last time step):

Substitute equations (3.2), (3.3), (3.5) and (3.7) into equation (3.4), and discretize the obtained new equation, after re-arrangement, one can get:

$$C_{ss} = \frac{\dfrac{M^0}{\Delta t} + h_m C_a + \dfrac{D_s}{\frac{1}{2}\Delta x} C_{s,T}}{\dfrac{K_e}{K_{sa}\Delta t} + \dfrac{h_m}{K_{sa}} + \dfrac{D_s}{\frac{1}{2}\Delta x}} \tag{3.14}$$

where C_{ss} is the substrate surface concentration.

Grid T:

Integrate equation (3.6) over the control volume T, one gets:

$$\Delta x\left(C_{s,T} - C_{s,T}^0\right) = \left[D_s \frac{C_{ss} - C_{s,T}}{\frac{1}{2}\Delta x} - D_s \frac{C_{s,T} - C_{s,I}}{\Delta x} \right] \Delta t \tag{3.15}$$

Substitute equation (3.14) into equation (3.15) and re-arrange the obtained new equation yields:

$$\left[\frac{\Delta x}{\Delta t} + \frac{D_s}{\frac{1}{2}\Delta x} + \frac{D_s}{\Delta x} - \frac{\dfrac{D_s}{\frac{1}{2}\Delta x}}{\dfrac{K_e}{K_{sa}\Delta t} + \dfrac{h_m}{K_{sa}} + \dfrac{D_s}{\frac{1}{2}\Delta x}} \cdot \frac{D_s}{\frac{1}{2}\Delta x} \right] C_{s,T} = \frac{\Delta x}{\Delta t} C_{s,T}^0 + \frac{\dfrac{D_s}{\frac{1}{2}\Delta x}}{\dfrac{K_e}{K_{sa}\Delta t} + \dfrac{h_m}{K_{sa}} + \dfrac{D_s}{\frac{1}{2}\Delta x}} \left(\frac{M^0}{\Delta t} + h_m C_a \right) + \frac{D_s}{\Delta x} C_{s,I} \tag{3.16}$$

The above equation can be written as:

$$a_T C_{s,T} = a_{FA} C_a + a_I C_{s,I} + a_T^0 C_{s,T}^0 + a_F^0 M^0 \tag{3.17}$$

where $a_T^0 = \frac{\Delta x}{\Delta t}$, $a_F^0 = \frac{\frac{D_s}{\frac{1}{2}\Delta x \Delta t}}{\frac{K_e}{K_{sa}\Delta t} + \frac{h_m}{K_{sa}} + \frac{D_s}{\frac{1}{2}\Delta x}}$, $a_{FA} = a_F^0 h_m \Delta t$, $a_I = \frac{D_s}{\Delta x}$ and

$$a_T = \frac{D_s}{\frac{1}{2}\Delta x}(1 - a_F^0 \Delta t) + a_I + a_T^0 .$$

Internal grids:

Integrate equation (3.6) over the internal control volumes yields:

$$\Delta x\left(C_{s,P} - C_{s,P}^0\right) = \left[D_s \frac{C_{s,N} - C_{s,P}}{\Delta x} - D_s \frac{C_{s,P} - C_{s,S}}{\Delta x}\right]\Delta t \tag{3.18}$$

The above equation can be re-written as:

$$a_P C_{s,P} = a_N C_{s,N} + a_S C_{s,S} + a_P^0 C_{s,P}^0 \tag{3.19}$$

where $a_N = a_S = \frac{D_s}{\Delta x}$, $a_P^0 = \frac{\Delta x}{\Delta t}$ and $a_P = a_N + a_S + a_P^0$.

Grid B:

Integrate equation (3.6) over the control volume B yields:

$$\Delta x\left(C_{s,B} - C_{s,B}^0\right) = \left[D_s \frac{C_{s,J} - C_{s,B}}{\Delta x} - 0\right]\Delta t \tag{3.20}$$

The above equation can be re-written as:

$$a_B C_{s,B} = a_Z C_{s,Z} + a_B^0 C_{s,B}^0 \tag{3.21}$$

where $a_Z = \frac{D_s}{\Delta x}$, $a_B^0 = \frac{\Delta x}{\Delta t}$ and $a_B = a_Z + a_B^0$.

Grid in the air:

Equation (3.1) can be discretized into:

$$\frac{C_a - C_a^0}{\Delta t} = -NC_a + Lh_m(C_{as} - C_a) \tag{3.22}$$

According to equations (3.3) and (3.5), we know that:

$$C_{ss} = K_{sa} C_{as} \tag{3.23}$$

Substitute equation (3.14) into equation (3.23), and then substitute the new equation into equation (3.22), after re-arrangement and re-writing, one can get:

$$a_A C_a = a_{FT} C_{s,T} + a_A^0 C_a^0 + a_{AF}^0 M^0 \tag{3.24}$$

where $a_A^0 = \dfrac{1}{\Delta t}$, $a_{AF}^0 = \dfrac{\dfrac{Lh_m}{K_{sa}\Delta t}}{\dfrac{K_e}{K_{sa}\Delta t} + \dfrac{h_m}{K_{sa}} + \dfrac{D_s}{\frac{1}{2}\Delta x}}$, $a_{FT} = a_{AF}^0 \dfrac{D_s}{\frac{1}{2}\Delta x}\Delta t$ and

$a_A = a_A^0 + N + Lh_m - a_{AF}^0 h_m \Delta t$.

Grid in the paint film:

Based on equations (3.5) and (3.14), it is easy to obtain:

$$M = \frac{\dfrac{1}{\Delta t} M^0 + h_m C_a + \dfrac{D_s}{\frac{1}{2}\Delta x} C_{s,T}}{\dfrac{1}{\Delta t} + \dfrac{h_m}{K_e} + \dfrac{K_{sa}}{K_e}\dfrac{D_s}{\frac{1}{2}\Delta x}} \tag{3.25}$$

These algebraic equations can be easily solved by the Tri-Diagonal Matrix Algorithm (TDMA). The concentration values at each CV at different time level can then be calculated.

3.3 Experimental Work

The Field and Laboratory Emission Cell (FLEC) is a 35 ml mini-environmental chamber; it is primarily designed for the measurement of VOCs emissions from planar construction products and from applied paints/coatings. Figure 3.3 is the description of an example of a FLEC.

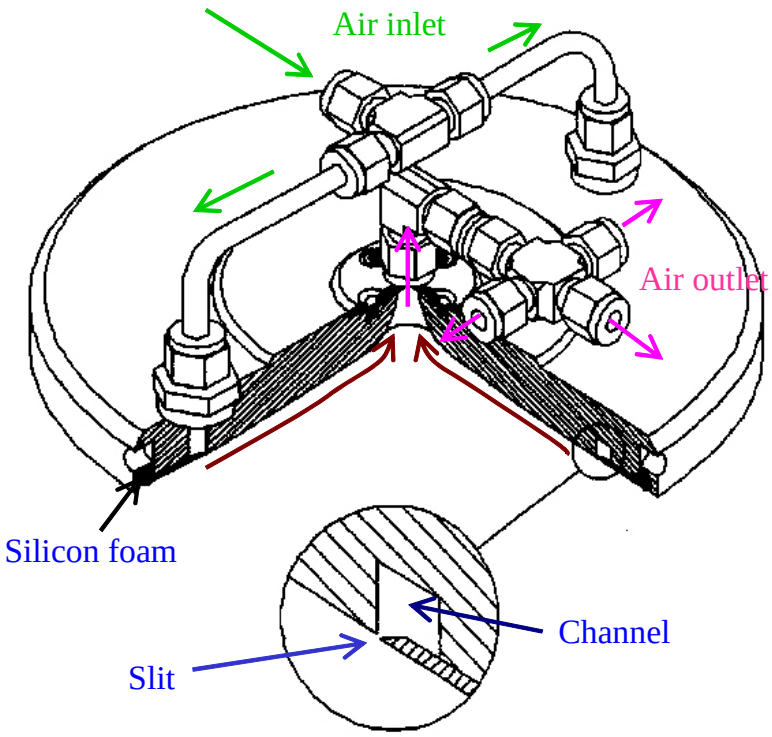

Figure 3.3 Description of an example of a FLEC

The top of the cell is 'sealed' onto the surface of the test material by an emission-free silicone rubber o-ring and the material itself becomes the bottom part of the chamber. Clean humidified air enters the cell from a narrow baffle around the inner perimeter of the cell and passes over the surface of the material. Then the air containing VOCs exits the cell through the outlet positioned at the center of the cell and is periodically pumped onto multi-sorbent tubes if necessary. More detailed information on FLEC can be found in (Wolkoff et al., 1995). Before carrying out an emission test, the cell is purged by VOCs-free air, which is generated by passing through a clean air system with particle filters and activated charcoal.

VOCs emission from commercially available water-based emulsion paint was tested with this European standard emission test method by our research group. The pictures of the test plate and application roller are shown in Figure 3.4.

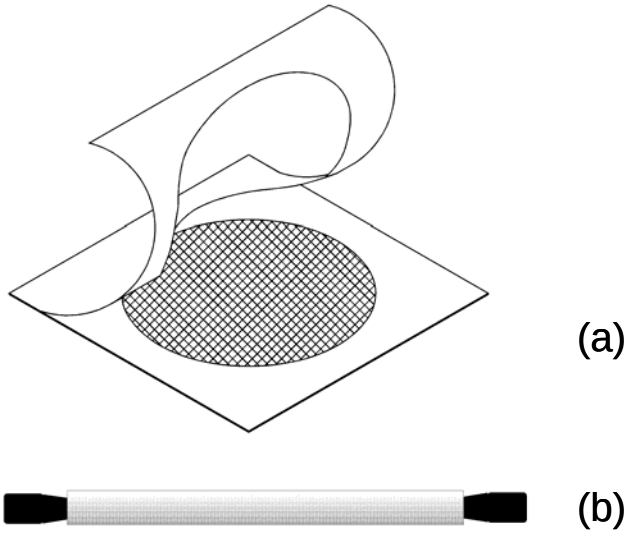

Figure 3.4 (a) FLEC test plate; (b) FLEC application roller

The paint test sample was prepared using the FLEC test plate (Part no. FL-0161). The test plate is 2 mm thick. A 0.08 mm thick paint film can be obtained by applying the paint to the hole on the plate and distribute it using the FLEC Application Roller (Part no. FL-0160). The defined application area is obtained by removing the foil from the plate, the application area is 177 cm^2 in this test.

The airflow through FLEC (Part no. FL-0001) was 509 ml/min, which was controlled and measured by an air pump (Part no. FL-1009) at the inlet of the FLCE, providing an air exchange rate of 873 h^{-1} and mean air velocity over the material surface of 0.02 m s^{-1}. Relative humidity of the supplied air to the FLEC was adjusted to 50±3% by FLEC air control unit (ACU) (Part no. FL-1000). The test was performed in an air conditioned lab, where the temperature was maintained at 23±1°C. Relative humidity and temperature of the air through the FLEC were continuously monitored by a built-in RH/T sensor in the air pump. The measuring accuracies were 2% for relative humidity, 0.2°C for temperature, and 2.5% for airflow rate, respectively.

The air samples at the outlet of the FLEC were collected on Tenax® TA sorbent tubes at a flowrate of 111ml/min. The sampling period for each sorbent tube was set in the range from 10-30 minutes with a shorter period at the start and a longer period after a few hours. The sampled tubes were desorbed in a thermal desorption system followed by gas-chromatography/mass-spectroscopy system according to the descriptions given in the U.S. Compendium Method TO-17.

3.4 Model Validation

In the present experimental study, water-based emulsion paint was applied on an aluminium substrate. Emission data obtained from the FLEC test system was used, on one hand to obtain model parameters, on the other hand to validate the present model. Because the substrate effect of aluminium is very weak and contributes little to the emission data, it is reasonable to neglect such weak substrate effect for this impermeable substrate. Under this circumstance, the model becomes simpler by setting R_2=0 in equation (3.4), then equations (3.1) - (3.4) are sufficient to describe VOCs transfer from paint/aluminium substrate system. Deng and Kim (2004b) used these equations to simulate VOCs emissions from carpet, they have given an analytical solution for the system of equations (3.1) - (3.4) (when R_2=0). The analytical solution reveals that C_a, M, and R_1 take the double exponential form. One exponential term stands for the fast decay, and the other accounts for slow decay.

The VOCs emission from paint is known to have three stages: (1) shortly after application when the material is still wet, this stage is evaporation controlled; (2) the material dries as emissions transition from evaporation controlled stage to internal diffusion controlled stage; (3) the material becomes relatively dry, this stage is dominated by internal diffusion. So, mathematically, the present model taking double

exponential form is more suitable to predict the VOCs emissions from wet materials than dry materials. It should be pointed out that unlike the empirical double exponential model, the present model has a strong, physically-based foundation, and thus is easy to scale up.

The 7 most abundant VOCs emissions from the water-based emulsion paint were 1-ethyl-3-methylbenzene, followed by 1,2,4-trimethylbenzene, n-hexane, 1,3,5-trimethylbenzene, propylbenzene, o-xylene and toluene. Totally there were 23 VOCs identified and quantified, besides the afore mentioned 7 dominant VOCs, the others are cyclohexane, benzene, heptane, octane, ethylbenzene, m-xylene, p-xylene, nonane, styrene, 1-methylethylbenzene, decane, 1,1-dimethylethylbenzene, 1-methylpropylbenzene, p-isopropyltoluene, butylbenzene, and undecane. All individual VOCs were summed up to find the emission data of TVOC. It was found that the sum of the amount of the seven major VOCs was about 85% of TVOC containing in the paint.

The measured initial VOC mass per unit area of the paint film and the model-derived parameter K_e for the seven VOCs are given in Table 3.1.

Table 3.1 Measured M_0 and model-derived K_e for the VOCs

VOC	M_0 (mg m^{-2})	K_e (m)
1-ethyl-3-methylbenzene	2154.96	1.55
1,2,4-trimethylbenzene	2039.10	1.90
n-hexane	1068.79	2.02
1,3,5-trimethylbenzene	1048.58	1.44
Propylbenzene	887.06	1.11
O-xylene	396.16	0.69
Toluene	357.92	1.24

Figure 3.5 - Figure 3.11 show the measured concentration-time data and corresponding model predicted concentration curves of the seven predominant VOCs.

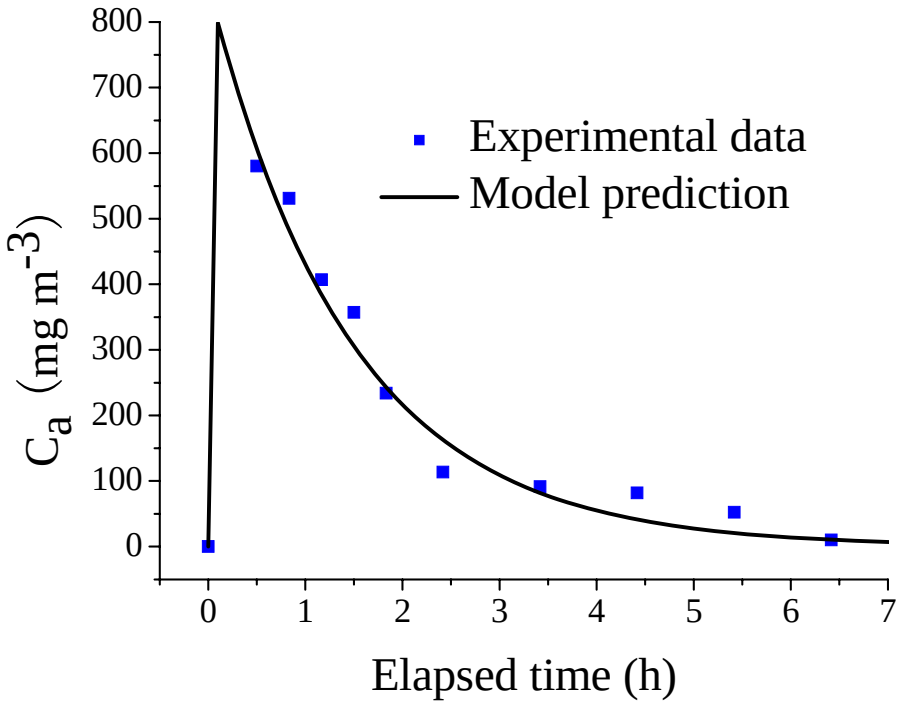

Figure 3.5 The 1-ethyl-3-methylbenzene concentration profile in the FLEC

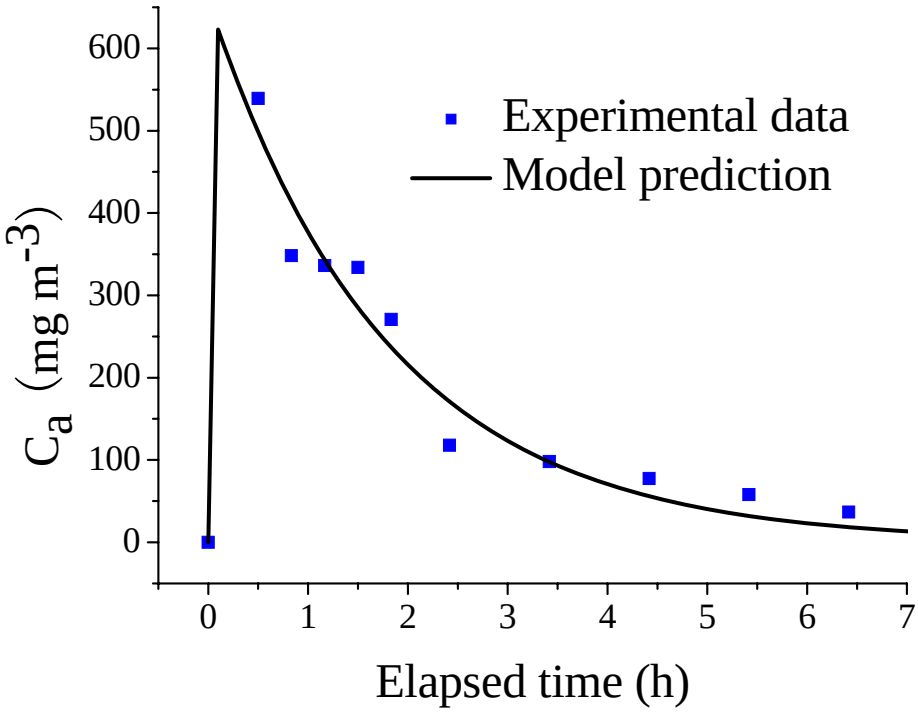

Figure 3.6 The 1,2,4-trimethylbenzene concentration profile in the FLEC

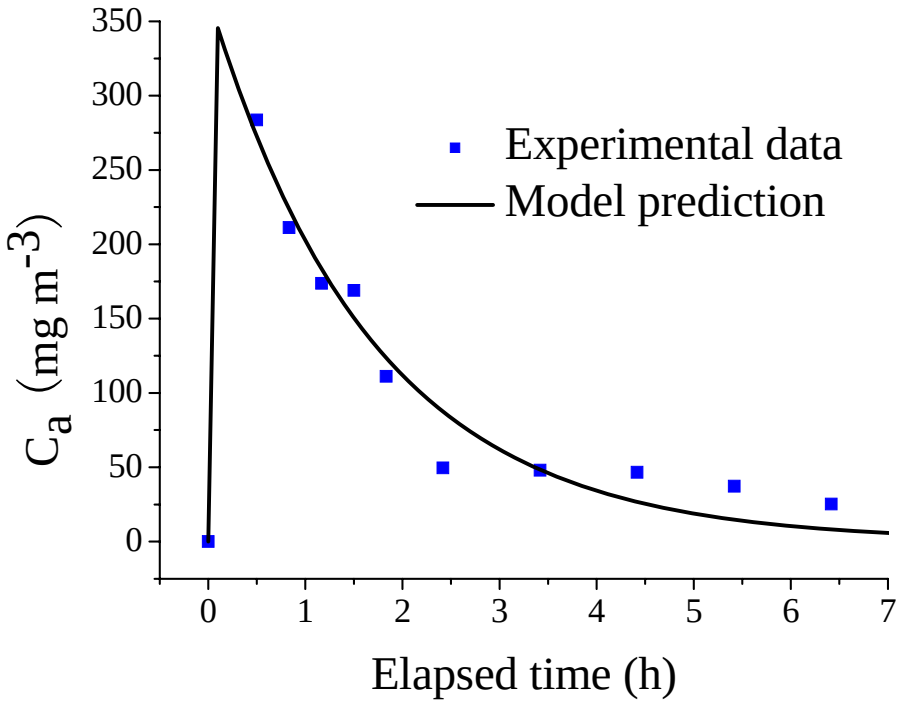

Figure 3.7 The n-hexane concentration profile in the FLEC

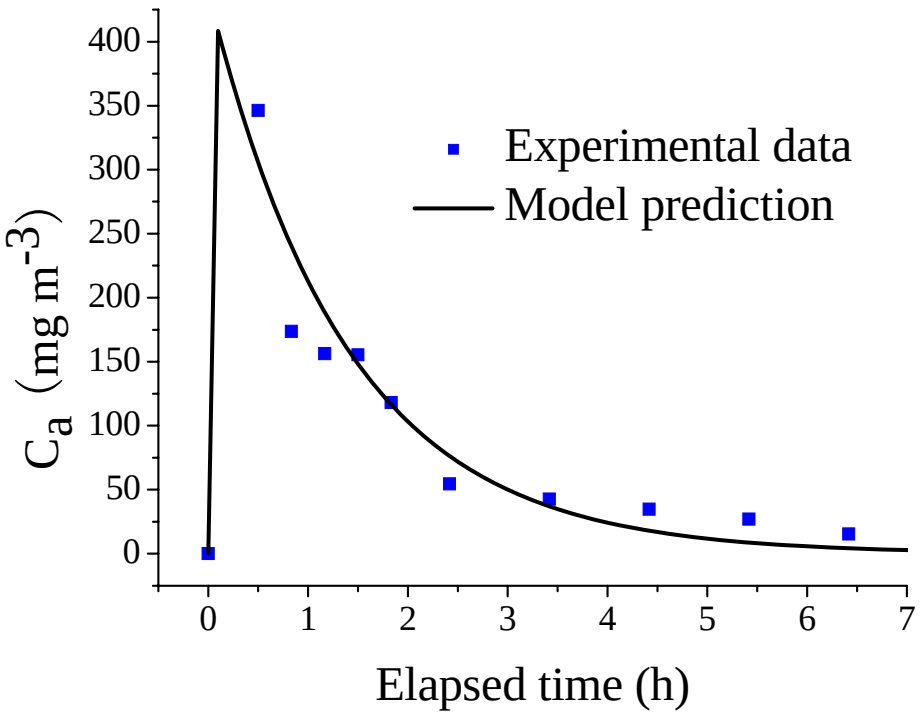

Figure 3.8 The 1,3,5-trimethylbenzene concentration profile in the FLEC

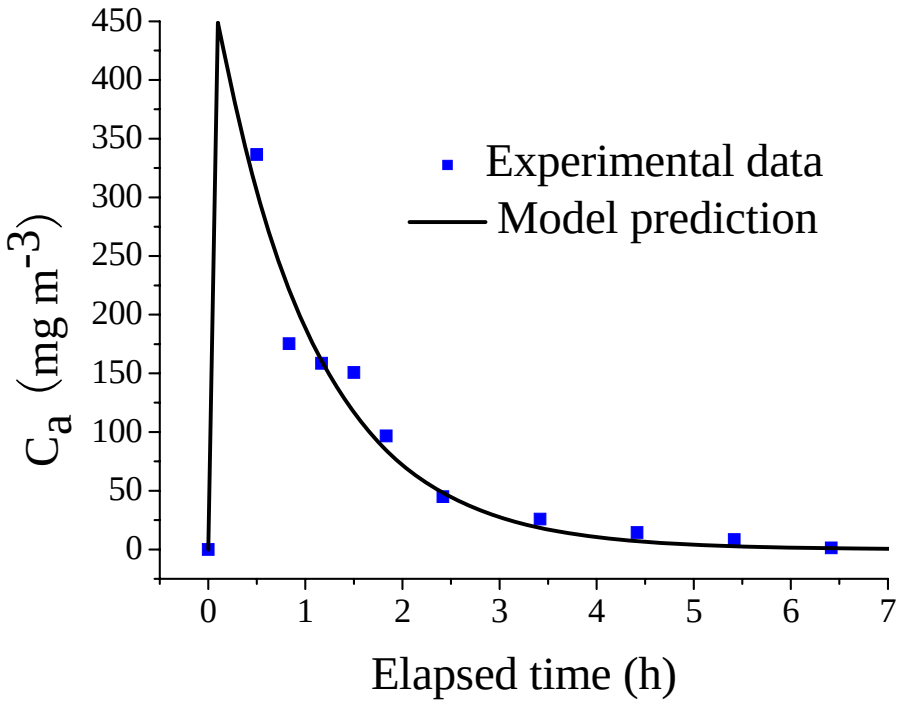

Figure 3.9 The propylbenzene concentration profile in the FLEC

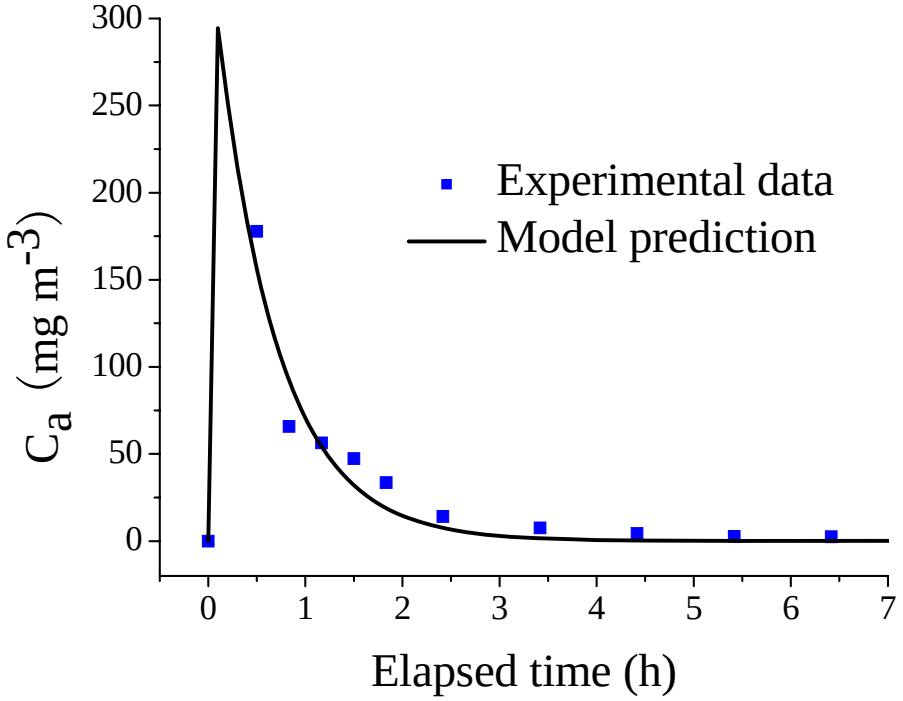

Figure 3.10 The o-xylene concentration profile in the FLEC

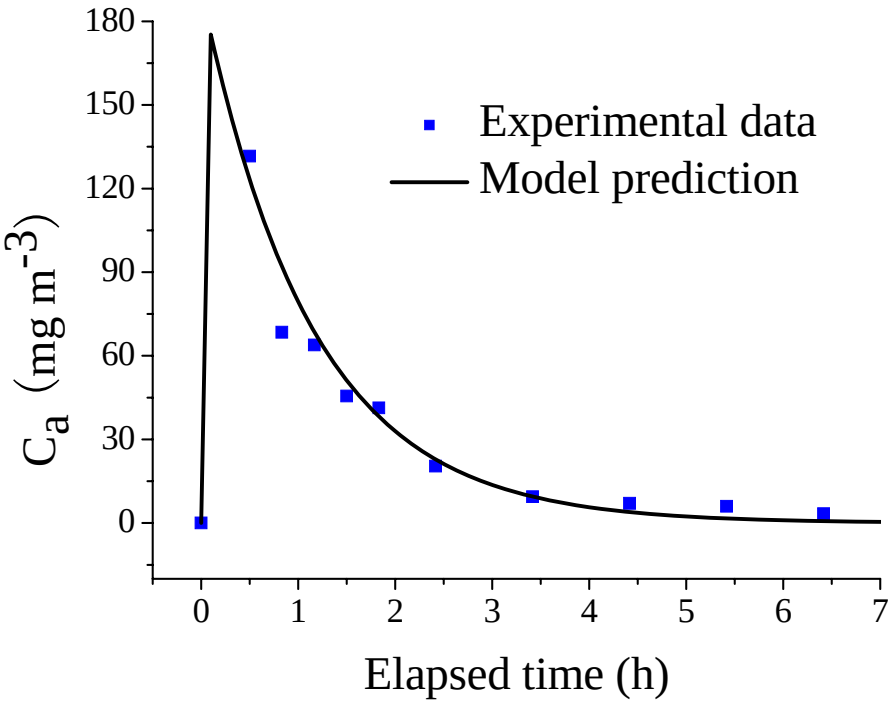

Figure 3.11 The toluene concentration profile in the FLEC

Results show that individual VOCs concentrations reach maximum immediately after the test starts. This is due to the high initial emission rate of paint, as well as the characteristic of the test cell system, i.e. small volume and extremely low sink effect. Luo and Niu (2004) demonstrated that the FLEC system has a fast dynamic response: the surface concentration can be represented without delay by the outlet concentration. Then the VOCs concentrations decay rapidly within the first 2~4 h, after that the concentrations of the VOCs change little and remain at low value, finally the concentration will reduce to undetectable level due to dilution.

Regarding TVOC, it is often assumed that the TVOC mixture has lumped properties of TVOC as if it is a single compound. The weighted average of the K_e values of the 7 dominant VOCs (weighting based on corresponding initial concentrations of the dominant VOCs) is considered to be able to represent K_e for TVOC (Tichenor et al., 1993; Yang, 1999), thus $K_{e,\mathrm{TVOC}}$ is estimated to be 1.59 m. The measured initial

TVOC concentration is 9448.77 mg m^{-2}. Then the TVOC concentration decay curve can be predicted by applying the proposed model, results are shown in Figure 3.12. Generally speaking, the model predictions agree well with the experimental measurements.

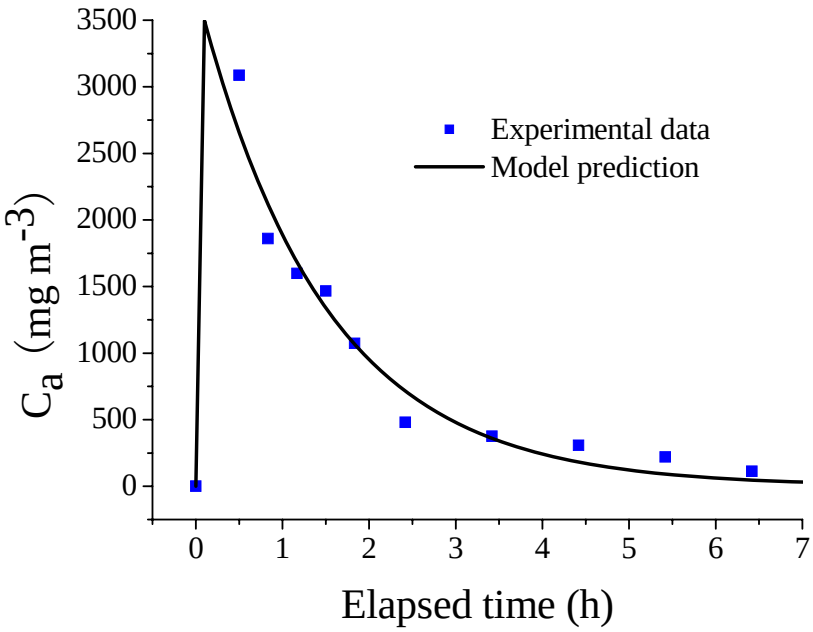

Figure 3.12 The TVOC concentration profile in the FLEC

3.5 Model Application

An office room with a floor area of 6×6=36 m^2 and a volume of 6×6×3=108 m^3 is considered here. The room temperature and relative humidity are 23°C and 50%, respectively. Assume that all the walls other than areas occupied by windows and doors are freshly painted with the same water-based emulsion, and the effective painted surface area is 4×6×3×90%=64.8 m^2. The paint is identical to that tested in section 3.3, and the applied film thickness is also 80 μm so that the parameters $M_{0,\mathrm{TVOC}}$ and $K_{e,\mathrm{TVOC}}$ determined can be directly adopted. For ease of investigation, the ceiling and floor in the room are assumed to be neither VOCs sources nor sinks.

In order to investigate various factors that may affect VOCs emission from paint, a variety of scenarios as shown in Table 3.2 are considered and simulated. Case 2 and 10 are two reference cases; the former one is a reference case of no substrate situation while the latter one is the reference case of with substrate situation. Only one parameter is changed for other cases compared with the corresponding reference case. And the reference value of air velocity above the paint film is assumed to be 0.15 m/s, which corresponds to common air velocity found indoors (Yang et al., 2001a). In case intermittent ventilation is employed, the HVAC system is assumed to operate during 8:00 AM~20:00 PM in working days and the air change rate (due to infiltration and exfiltration) during the off-work hours is assumed to be 0.2 h^{-1}. In all circumstances, the outdoor air is assumed to be free of VOCs and the air in the office is assumed to be well-mixed.

Table 3.2 The parameters of individual simulation cases

Case	Ventilation mode	u_m	M_0	D_s	K_{sa}
1	Continuous, 1ACH	0.05	9448.77	-	-
2	Continuous, 1ACH	0.15	9448.77	-	-
3	Continuous, 1ACH	0.3	9448.77	-	-
4	Continuous, 0.5ACH	0.15	9448.77	-	-
5	Continuous, 2ACH	0.15	9448.77	-	-
6	Continuous, 1ACH	0.15	3000	-	-
7	Continuous, 1ACH	0.15	12000	-	-
8	Continuous, 1ACH	0.15	9448.77	5×10^{-13}	6000
9	Continuous, 1ACH	0.15	9448.77	5×10^{-11}	6000
10	Continuous, 1ACH	0.15	9448.77	5×10^{-12}	6000
11	Continuous, 1ACH	0.15	9448.77	5×10^{-12}	600
12	Continuous, 1ACH	0.15	9448.77	5×10^{-12}	60
13	Continuous, 1ACH	0.15	9448.77	5×10^{-12}	60000
14	Intermittent, 1ACH/0.2ACH	0.15	9448.77	5×10^{-12}	6000

3.5.1 Effects of Mean Air Velocity

It is well demonstrated in Figure 3.13 that the air velocity over the paint film has significant impacts on indoor VOCs concentration. When the air change rate is maintained unchanged, increasing the air velocity results in an increased convective mass transfer coefficient between the paint film surface and the indoor air. It is noticed that the higher the air velocity, the higher the peak concentration, the lower the late stage concentration. The effect is more significant in early times than in late times. Many researchers have drawn the conclusion that the increased convective mass transfer coefficient results in an increased initial emission rate (when paint film is wet) and has less significant effect when the film is dry (Yang et al., 2001a), which is consistent with this finding.

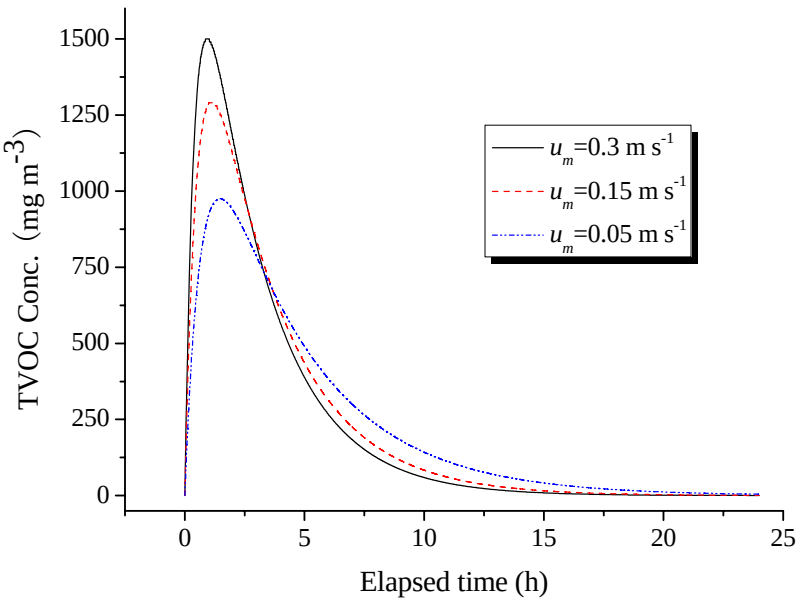

Figure 3.13 Effect of mean air velocity (Cases 1, 2 and 3)

3.5.2 Effects of Air Change Rate

Figure 3.14 shows the effect of air change rate on indoor VOCs concentration. The larger the air change rate, the lower the peak concentration, and the faster the concentration curve decays. This is straightforward because the larger the air change

rate is, the more amount of outdoor air passes through the office to dilute and flush out contaminants, and thus the lower the indoor concentration is. The effect is more significant for early time emissions - the evaporation-controlled emission period. In view of this point, it is recommended that the maximum amount of outside air should be provided after installation of VOCs emitting materials, in particular paint, for the maximum amount of time feasible (this process is also known as building flush-out).

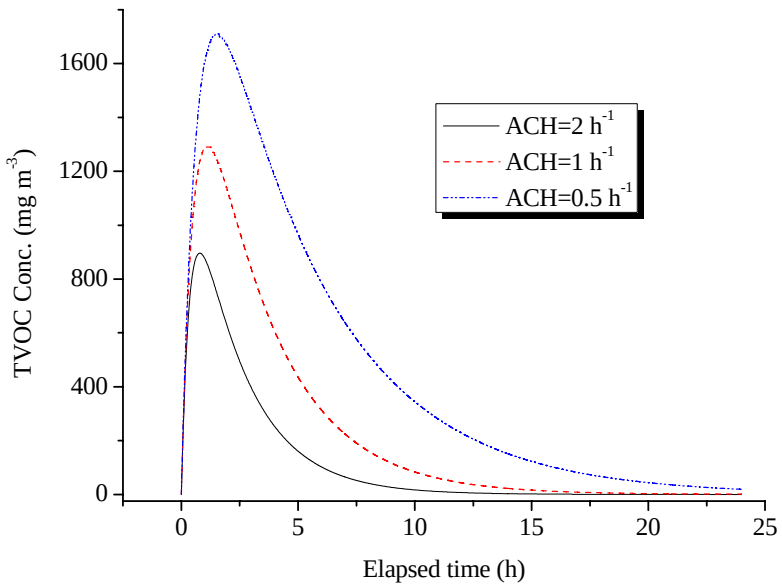

Figure 3.14 Effects of air change rate (Cases 2, 4 and 5)

3.5.3 Effects of Initial Source Strength

Figure 3.15 shows the effect of initial VOCs source strength on indoor VOCs concentration. It is clear that lower initial source strength results in lower indoor VOCs concentration. That means VOCs emissions reduction may be achieved by source reduction or source removal. Practically speaking, using of low emission materials or so-called green materials is the most cost effective way to achieve better indoor air quality compared with other means.

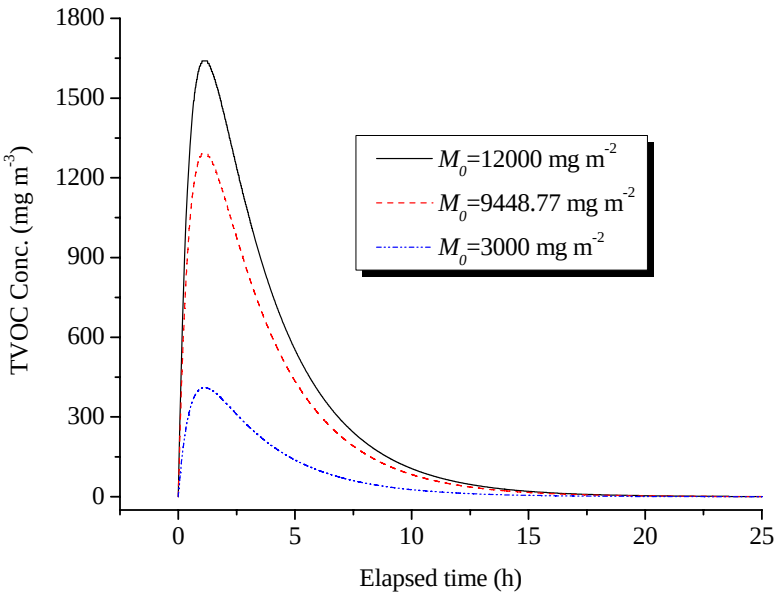

Figure 3.15 Effects of initial source strength (Cases 2, 6 and 7)

3.5.4 Effects of Substrate

Figure 3.16 illustrates the effect of substrate on indoor VOCs concentration.

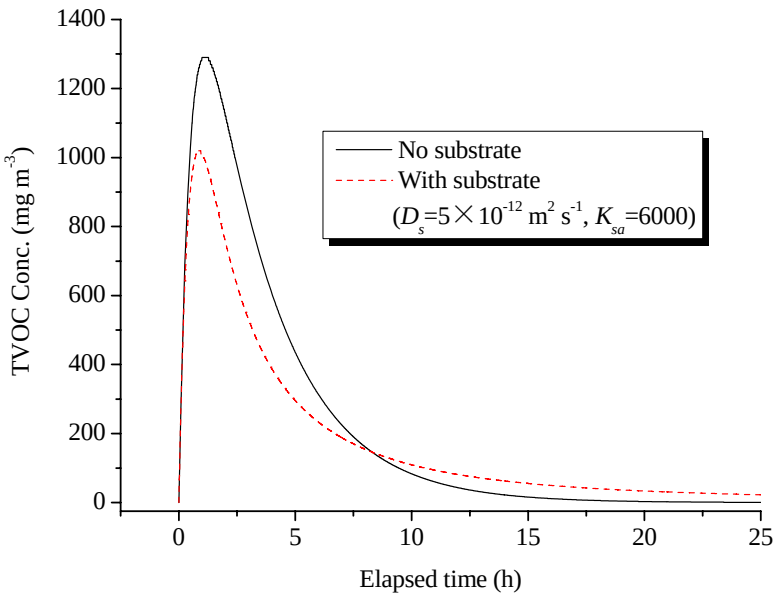

Figure 3.16 Effects of substrate (Cases 2 and 10)

It is known that most VOCs emissions from the paint film occurred in the early stage through an evaporation-like process. However, when the paint is applied on a sorptive substrate, a portion of the VOCs containing in the paint film will first

transport into the substrate through sorption and diffusion processes and later re-emit into the paint film. Such that, in comparison with paint applied on non-sorptive substrate, the indoor VOCs concentration is lower at the early stage and considerably higher at late times for paint applied on sorptive substrate, as shown in Figure 3.16. The extent of the substrate effect is determined by both the diffusion and partition coefficients of the substrate.

3.5.5 Effects of Substrate's Diffusion Coefficient

Larger diffusion coefficient of the substrate results in more VOCs diffuse into the substrate (less VOCs emit to the room air at this stage) and thereafter back into the film (more VOCs emit to the room air at this stage). Figure 3.17 clearly shows this trend. Increase the diffusion coefficient of the substrate results in a lower VOCs concentration at early times but a higher VOCs concentration at late times.

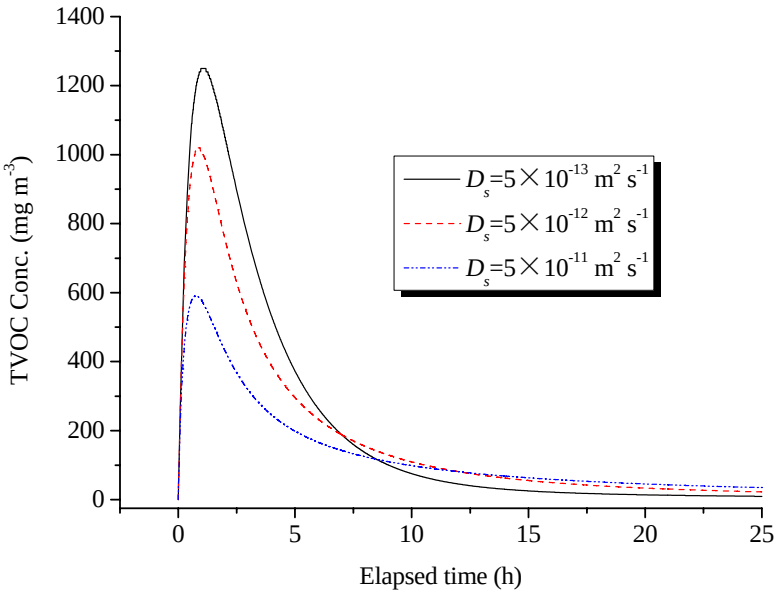

Figure 3.17 Effects of substrate diffusion coefficient (Cases 8, 9 and 10)

3.5.6 Effects of Substrate's Partition Coefficient

How the partition coefficient of the substrate affects the indoor VOCs concentration is evidenced in Figure 3.18. The partition coefficient can be related to the sorption capacity of the material. The larger the partition coefficient of the substrate, the stronger the sorption capacity (ability of holding the VOCs within the material), the more VOCs transported into and held by the substrate material, and thus the less VOCs emitted to the room air. It can be seen that increasing the partition coefficient decreases the emission rate at early times and results in a much slower depletion rate of VOCs; however, the influence of a change in partition coefficient is virtually insignificant below a value of about 1000.

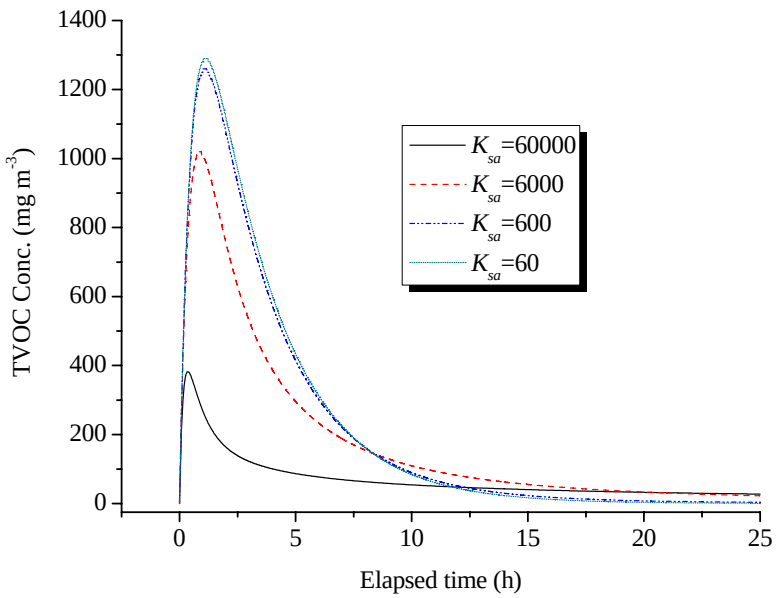

Figure 3.18 Effects of substrate partition coefficient (Cases 10, 11, 12 and 13)

3.5.7 Effects of Ventilation Mode

Figure 3.19 is a comparison of the TVOC concentration resulted from case 10 (continuous ventilation) and 14 (intermittent ventilation). In reality, from the viewpoint of energy saving, HVAC systems are normally operated during working hours and shut off on weekday evenings and during weekends. When no ventilation

is employed, the indoor VOCs concentration is very likely to continuously build up. Consequently, the employees will be exposed to high VOCs concentration in the early morning when they come back to work. In Figure 3.19, it can be seen that for continuous ventilation mode, after about 233 hours' flush-out, the corresponding TVOC concentration is lower than the 600 μg m^{-3} guideline concentration (8-hour average of TVOC level 2 - good level). While for the intermittent ventilation mode, even after the simulation period 240 h (10 days) ends, the TVOC concentration still exceeds 600 μg m^{-3}.

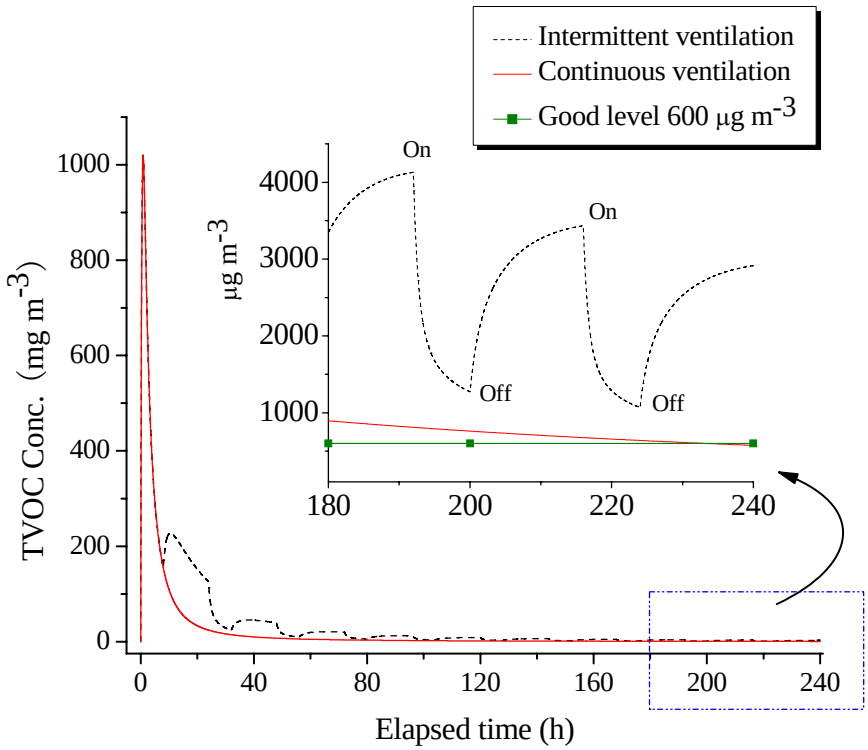

Figure 3.19 Effects of ventilation mode (Cases 10 and 14)

It should be reminded that the indoor VOCs concentration can be very high after renovations for at least several weeks. Recall that increasing the air change rate can result in largely reduced indoor VOCs concentration. A good choice is to maintain a high ventilation rate with 100 percent of outdoor air for several days to weeks to speed up VOCs emissions processes before the occupancy begins in a newly built or

renovated building. In addition, the early morning pre-occupancy ‘flush-out’ is an effective way to quickly reduce the VOCs concentration buildup during an overnight HVAC system’s shutdown after the room is putting into use. The optimal time required for building flush-out and daily early morning flush-out can be estimated using models like the proposed one.

3.6 Summary

Wet coatings like paints are recognized as one of the major sources of VOCs in indoor environment. Commercially available water-based emulsion paint was tested using European standard test method - FLEC. Totally 23 individual VOCs were detected and quantified, the 7 major VOCs were 1-ethyl-3-methylbenzene, followed by 1,2,4-trimethylbenzene, n-hexane, 1,3,5-trimethylbenzene, propylbenzene, o-xylene and toluene. The sum of the amount of these 7 VOCs was 85% of that of the total 23 VOCs detected.

A physically-based model is developed to predict VOCs emissions from paint. Physically speaking, due to the model assumptions it is suggested using the present model for short-term predictions. All the model parameters have clear physical meanings and thus the model is easy to scale up. The emission data of the water-based emulsion paint obtained from FLEC test is used to validate the model. Excellent agreement between experimental data and model predictions is attained.

VOCs emissions from paint can be significantly affected by many factors, which are numerically investigated in this study and some valuable conclusions can be drawn. Increase the air velocity results in an increased peak concentration but a lower concentration at late times. Increase the air change rate reduces the overall indoor VOCs concentration - this leads to the technique of building flush-out to achieve

good air quality in a newly built or renovated building. Source reduction or elimination is the most cost effective way to meet the goal of control strategy. The substrate on which paint is applied first stores VOCs from paint film and re-emits them when the concentration gradient is reversed. The larger the diffusion and partition coefficients of the substrate, the more significant the substrate effect is. The intermittent ventilation strategy is usually adopted for the sake of energy saving, under this circumstance, the indoor VOCs concentration can build up during the HVAC off period. So, pre-occupancy flush-out in the early morning, for example, two hours earlier before the office hours, is a good choice to avoid occupants' exposure to high VOCs concentration.

The present model can be a simple but useful tool to screen how different combinations of decorative materials can affect indoor VOCs concentration and to evaluate the effectiveness of various ventilation control strategies like building pre-occupancy flush-out.

Chapter 4
Inverse Determination of VOCs Diffusion and Partition Coefficients in Dry Building Materials

4.1 Introduction

Volatile organic compounds (VOCs) emitted from building materials are recognized as major problems affecting human comfort, health, and productivity (Huang and Haghighat, 2002). Therefore, it is significant to understand the VOCs emission characteristics of building materials in order to evaluate their impact on the indoor air quality and further to control the level of VOCs concentration in indoor environment.

Due to the costs and limitations of experimental methods, many researchers have switched their focus to numerical methods. Different models, including empirical and mass transfer theory based models have been developed during the past decade. Empirical models based on measurements in environmental chambers have moved towards physically based models involving a variety of phenomena: boundary layer diffusion and convection, diffusion in materials, adsorption/desorption at the material/air interfaces (Little et al., 1994; Yang et al., 2001d; Huang and Haghighat, 2002; Xu and Zhang, 2003; Zhang and Niu, 2003a; Deng and Kim, 2004a; Luo and Niu, 2004). With the known indoor environmental conditions and properties of VOCs/building materials, mass transfer theory based model is capable of predicting the concentration of VOCs in the material and in indoor air. The computation of VOCs concentration in the material and in air, from the knowledge of initial and boundary conditions, as well as the indoor environmental conditions and properties of chemicals and materials appearing in the model, constitutes a direct problem of mass transfer.

Generally, there are four major parameters involved in VOCs emission model, i.e. initial condition C_{m0}, convective mass transfer coefficient h_m, diffusion coefficient D_m and partition coefficient K_{ma}. C_{m0} can be easily measured by using solvents or heat to extract target compounds or by fluidized-bed desorption (FBD) method, while h_m can be estimated through well validated empirical correlations. However, VOCs/material properties like diffusion and partition coefficients are very limited and can rarely be found in literature. Now the true obstacle in the development of models capable of simulating realistic building configurations is the lack of experimental data for the physical parameters involved in the models (Blondeau et al., 2003), because accurate knowledge of parameters appearing in mathematical models used in numerical simulations is of capital importance for the accuracy of the results obtained.

Considering the mass diffusion equation is so similar to the heat conduction equation, and inverse methods (Alifanov, 1994; Ozisik and Orlande, 2000) have been so successfully used in solving heat conduction problems, including the parameter estimation problems, it is logical to use the same procedure to investigate the VOCs diffusion coefficient in building material, with the help of extra condition available, i.e. the VOCs concentration measurements in chamber air against time. Furthermore, the inspiring thing is that not only diffusion coefficient but also partition coefficient might be estimated by using inverse method if certain criterions are satisfied. In the present investigation, VOCs diffusion and partition coefficients in building material are simultaneously estimated by solving the inverse problem of the one-dimensional unsteady mass diffusion. The model used in this investigation considers both diffusion and convection. As a pilot study, a pair of diffusion and partition coefficient D_m, K_{ma} is selected as a benchmark, measurement concentrations required

in the inverse analysis are generated by solving the so called direct problem using this pair of coefficients. Using the generated measurements, D_m, K_{ma} can be inversely estimated; then the estimated results are compared with the benchmark values for D_m, K_{ma} to evaluate the accuracy of the estimation.

Although the purposes of the pilot study are to verify the possibility and accuracy of simultaneous estimation of the two coefficients via inverse analysis and subsequently to explore how and to what extent some major factors would affect the accuracy of the estimation. The ultimate goal of the project is to develop experimental method that can be used to accurately determine the parameters and subsequently to enrich the database of D_m and K_{ma} of building materials.

Based on the positive findings in the pilot study, a follow-up study using real measured concentration data to determine diffusion and partition coefficients of selected VOC/material combination was conducted.

4.2 Direct Problem of One-dimensional Unsteady Mass Diffusion

Figure 4.1 depicts a schematic representation of a dry building material placed in a stainless steel environmental chamber. The edges of the material are sealed to avoid VOCs leakage. Concentration gradient is assumed to be the only driving force for VOCs transportation, and there is no chemical reaction inside the material. The lower surface of the material can be considered to be mass-insulation because of extremely low sorption capacity of stainless steel. In addition, convective mass flux can be approximately considered to be uniformly distributed over the emission surface of the material. Therefore, for a dry material with homogeneous diffusivity, transient mass diffusion in the material can be regarded as one-dimensional with the first and third boundary conditions on the emission boundaries.

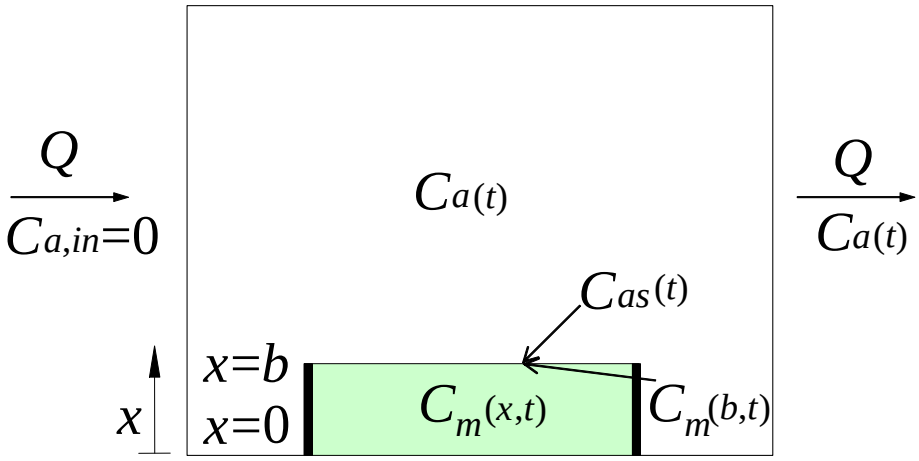

Figure 4.1 Schematic representation of a dry building material slab in an environmental chamber

4.2.1 One-dimensional Transient Mass Diffusion Model

The governing equation describing the one-dimensional transient VOCs diffusion in the material is (Little et al., 1994):

$$\frac{\partial C_m(x,t)}{\partial t} = D_m \frac{\partial^2 C_m(x,t)}{\partial x^2} \tag{4.1}$$

It should be noted that equation (4.1) cannot properly describe the VOCs transport in very porous materials. In case porous materials are studied, multi-phase models (Tiffonnet et al., 2002; Murakami et al., 2003) would be much better candidates. However, it is also found that parameters in continuum model and in multi-phase model for a specific chamber test are convertible as long as the linear sorption isotherm is used in both models (Haghighat et al., 2005). Because most of the existing test data are analyzed by utilizing the continuum model, for the purpose of comparison, the continuum model is also used here.

The material is assumed to be initially at uniform VOCs concentration.

$$C_m(x,t)\big|_{t=0} = C_0\,,\ 0 \le x \le b \tag{4.2}$$

The first boundary condition assumes there is no flux through the bottom of the material, that is:

$$\frac{\partial C_m(x,t)}{\partial x}\Big|_{x=0} = 0\,,\ t > 0 \tag{4.3}$$

A third kind of boundary condition is imposed on the upper surface of the material

$$-D_m \frac{\partial C_m(x,t)}{\partial x}\Big|_{x=b} = h_m\left[C_{as}(t) - C_a(t)\right],\ t > 0 \tag{4.4}$$

where h_m is the mean convective mass transfer coefficient. h_m for laminar flow in an environmental chamber can be estimated using the relationship between Sherwood number (Sh), Reynolds number (Re) and Schmidt number (Sc) (Huang and Haghighat, 2002; Xu and Zhang, 2003; Deng and Kim, 2004a), that is $Sh = 0.664 Sc^{1/3} Re^{1/2}$. Where $Sh = h_m l / D_a$, $Sc = \upsilon / D_a$, $Re = u_m l / D_a$, υ is the kinematic viscosity of the air, u_m is the velocity of the air over the material, l is the characteristic length of the material, and D_a is the diffusion coefficient of VOCs in the air. It should be noted that the relationship is valid only for laminar flow over a flat plate, and it has been used for internal convection mass transfer analysis here, partly because of the insensitivity of the emission rate of dry material to this convection coefficient h_m, as will be analyzed later in this study.

At atmospheric pressure, for low VOCs concentration and isothermal conditions, the equilibrium relation between concentrations of VOCs in the air phase and material phase can be described by the linear isotherm (Little et al., 1994):

$$C_m(x,t)\big|_{x=b} = K_{ma} C_{as}(t) \tag{4.5}$$

where K_{ma} is the partition coefficient. This relationship between material and air phase VOCs concentration has been widely used and well validated by different modelers.

Assume the inlet VOCs concentration is zero, and the VOCs is well mixed in the chamber air, the mass balance of VOCs in the chamber air can be described as:

$$\frac{\partial C_a(t)}{\partial t} = -LD_m \frac{\partial C_m(x,t)}{\partial x}\Big|_{x=b} - NC_a(t) \tag{4.6}$$

Assume that the initial VOCs concentration in the chamber air is zero. That is:

$$C_a(t)\big|_{t=0} = 0 \tag{4.7}$$

Equations (4.1) - (4.7) are referred to as a direct problem when the initial and boundary conditions, as well as all parameters appearing in the equations are known.

4.2.2 Solutions of the Direct Problem

Several analytic solutions for the aforesaid one-dimensional unsteady diffusion model by introducing some simplifications are available now. As a comparison, numerical solution of the direct problem is also given. The errors caused by the unrealistic simplifications will be evidenced and analyzed.

4.2.2.1 Solution Given by Little et al.

By assuming h_m is infinitely large in equation (4.4), i.e. neglecting convective mass transfer resistance, Little et al. (1994) solved the equations (4.1) - (4.3) and (4.5) - (4.7) from an analogous heat transfer analytically. The solutions they obtained are as follows:

$$C_m(x,t) = 2C_{m0}\sum_{n=1}^{+\infty}\frac{\exp(-Dq_n^2 t)(H_1 - H_2 q_n^2)\cos(q_n x)}{\left[b(H_1 - H_2 q_n^2)^2 + q_n^2(b + H_2) + H_1\right]\cos(q_n b)} \tag{4.8}$$

$$C_a(t) = C_m(b,t)/K_{ma} \tag{4.9}$$

where $H_1=N/(LD_mK_{ma})$, $H_2=1/(LK_{ma})$ and q_n (n=1,2,3…) are the positive roots of

$$q_n \tan(q_n b) = H_1 - H_2 q_n^2 \tag{4.10}$$

4.2.2.2 Solution Given by Huang and Haghighat

Huang and Haghighat (2002) solved the equations (4.1) - (4.7) by the method of separation of variables with the assumption that $C_a(t)$ is much smaller than the concentration of VOCs in the near material surface air $C_{as}(t)$, i.e. $C_a(t)=0$ in the equation (4.4). The analytic solutions are:

$$C_m(x,t) = 2C_{m0}\sum_{n=1}^{+\infty}\frac{\sin(q_n b)}{q_n b + \sin(q_n b)\cos(q_n b)}\exp(-D_m q_n^2 t)\cos(q_n b) \tag{4.11}$$

$$C_a(t) = 2C_{m0}LD_m \sum_{n=1}^{+\infty}\frac{q_n \sin^2(q_n b)}{(N - q_n^2 D_m)\left[q_n b + \sin(q_n b)\cos(q_n b)\right]}\left[\exp(-D_m q_n^2 t) - \exp(-Nt)\right] \tag{4.12}$$

where q_n (n=1,2,3…) are the positive roots of:

$$q_n \tan(q_n b) = \frac{h_m}{K_{ma} D_m} \tag{4.13}$$

4.2.2.3 Solution Given by Deng and Kim

Deng and Kim (2004a) solved the equations (4.1) - (4.7) by using the Laplace transformation without any simplifications. The analytic solutions are:

$$C_m(x,t) = 2C_{m0}\sum_{p=1}^{+\infty}\frac{(\alpha - q_p^2)}{A_p}\cos(\frac{x}{b}q_p)\exp(-D_m q_p^2 b^{-2} t) \tag{4.14}$$

$$C_a(t) = 2C_{m0}\beta\sum_{p=1}^{+\infty}\frac{q_p \sin(q_p)}{A_p}\exp(-D_m q_p^2 b^{-2} t) \tag{4.15}$$

where

$$\begin{aligned} A_p = &\left[K_{ma}\beta + (\alpha - q_p^2)K_{ma}H^{-1} + 2\right]q_p^2 \cos q_p \\ &+ \left[K_{ma}\beta + (\alpha - 3q_p^2)K_{ma}H^{-1} + \alpha - q_p^2\right]q_p \sin q_p \end{aligned} \tag{4.16}$$

where $H = h_m b / D_m$, $\alpha = Nb^2 / D_m$, $\beta = Lb$ and q_p (p=1,2,3…) are the positive roots of:

$$q_p \tan q_p = \frac{\alpha - q_p^2}{K_{ma}\beta + (\alpha - q_p^2)K_{ma}H^{-1}} \tag{4.17}$$

4.2.2.4 Finite Difference Method

The direct problem can also be solved numerically by using finite difference method. The fully implicit scheme is used here for its advantage of stability for all sizes of time step. However, the time step must be kept reasonably small to obtain results sufficiently close to the exact solution.

The (x,t) domain is divided into intervals Δx, Δt such that

$x=j\Delta x$ $\quad j=0, 1, 2, \ldots, M$ $\quad$ with $b=M\Delta x$

$t=n\Delta t$ $\quad n=0, 1, 2, \ldots$

and the VOCs concentration in the material $C_m(x,t)$ is represented by $C_m(j\Delta x, n\Delta t)$, the VOCs concentration in the chamber air is represented by $C_a(n\Delta t)$. In this study, the mesh size is chosen to be Δt=0.5 h and M=40. Different mesh size can be used and results can be compared to choose an optimal one. Also the numerical results can be compared with the analytical solution to check the appropriateness of the mesh size chosen. It should be mentioned that when numerical model is used for inverse analysis, smaller mesh size requires larger computation resources, because iterations are involved in inverse analysis. After representing the diffusion equation (4.1) and corresponding boundary conditions in finite differences and rewriting the equations in matrix form, we get:

$$\begin{bmatrix} (1+2r) & -2r & 0 & 0 & \cdots & 0 & 0 & 0 \\ -r & (1+2r) & -r & 0 & \cdots & 0 & 0 & 0 \\ 0 & -r & (1+2r) & -r & \cdots & 0 & 0 & 0 \\ \vdots & & & & & & & \\ 0 & 0 & 0 & 0 & & -r & (1+2r) & -r \\ 0 & 0 & 0 & 0 & \cdots & 0 & -2r & (1+2r+\alpha) \end{bmatrix} \begin{bmatrix} C_{m,0}^{n+1} \\ C_{m,1}^{n+1} \\ C_{m,2}^{n+1} \\ \vdots \\ C_{m,M-1}^{n+1} \\ C_{m,M}^{n+1} \end{bmatrix} = \begin{bmatrix} C_{m,0}^{n} \\ C_{m,1}^{n} \\ C_{m,2}^{n} \\ \vdots \\ C_{m,M-1}^{n} \\ 2C_{m,M}^{n} + \beta \end{bmatrix} \tag{4.18}$$

where $r = \frac{D_m \Delta t}{\Delta x^2}$, $\alpha = 1 + \frac{2h_m \Delta t(1 + N\Delta t)}{K_{ma}\Delta x(1 + N\Delta t + Lh_m \Delta t)}$ and $\beta = \frac{2h_m \Delta t}{\Delta x(1 + N\Delta t + Lh_m \Delta t)} C_a^n$.

Equation (4.18) is M+1 simultaneous algebraic equations for M+1 unknown VOCs concentrations $C_{m,0}^{n+1}, \cdots, C_{m,M}^{n+1}$ at time level n+1 in terms of the M+1 known VOCs concentrations in material $C_{m,0}^{n}, \cdots, C_{m,M}^{n}$ and one known VOCs concentration C_a^n in the chamber air. Utilizing the relations given by equations (4.4) and (4.5), the finite-difference representation of the equation (4.6) is:

$$C_a^{n+1} = \frac{Lh_m \Delta t}{K_{ma}(1 + N\Delta t + Lh_m \Delta t)} C_{m,M}^{n+1} + \frac{1}{1 + N\Delta t + Lh_m \Delta t} C_a^n \qquad (4.19)$$

Based on the initial conditions given by equations (4.2) and (4.7), the VOCs concentrations in the material and in the chamber air can be determined by solving the finite-difference equations (4.18) and (4.19). To solve equation (4.18), an efficient algorithm called Thomas's algorithm can be utilized. Once equation (4.18) is solved, solving equation (4.19) is straightforward.

4.2.3 Assessment of the Direct Problem

Yang et al. (2001d) conducted an experiment on VOCs emission from particle board in a small chamber. The concentration of total volatile organic compound (TVOC) in chamber air was measured. The initial TVOC concentration in the material, the diffusion and partition coefficients of TVOC in the particle board and the experimental conditions were given by Yang et al. (2001d), which are listed in Table 4.1. Another key parameter, the mean convective mass transfer coefficient h_m can be estimated using the correlation $Sh = 0.664 Sc^{1/3} Re^{1/2}$.

Table 4.1 Environmental parameters and material properties [extracted from: (Yang et al., 2001d)]

Temperature (°C)	23±0.5
Relative humidity (%)	50±0.5
Air change rate (h^{-1})	1.0±0.05
Loading ratio (m^2/m^3)	0.729
Diffusion coefficient D_m (m^2/s)	7.65×10^{-11}
Partition coefficient K_{ma}	3289
Initial concentration C_{m0} ($\mu g/m^3$)	5.28×10^{7}

Comparison of the simulated results is presented in Figure 4.2. It is clear that Little et al.'s model and Huang and Haghighat's model greatly overestimate the VOCs concentration especially at the initial stage, which is mainly due to their over simplifications, i.e. neglecting the convective mass transfer resistance for Little et al.'s model and assuming zero VOCs concentration in chamber air for Huang and Haghighat's model, respectively. No significant difference is found between predictions given by Deng and Kim's analytical solution and numerical solution, because this particular analytical method involves no simplifications. It also indicates that the present finite difference method with selected mesh size can provide a reasonable accuracy. Figure 4.3 shows Deng and Kim's model and the numerical model tend to Little et al.'s model when h_m is very large or even infinite.

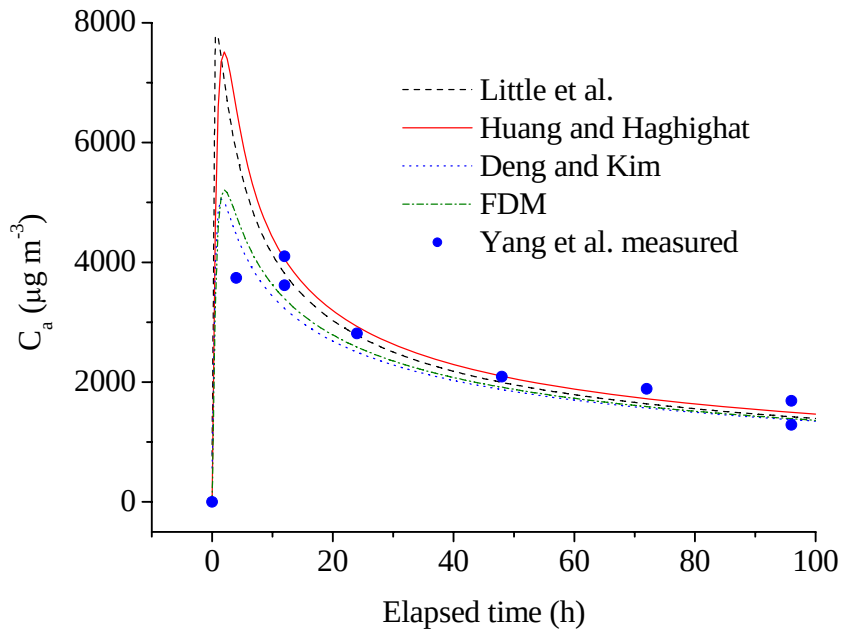

Figure 4.2 Experimental results and model predictions resulted from different models

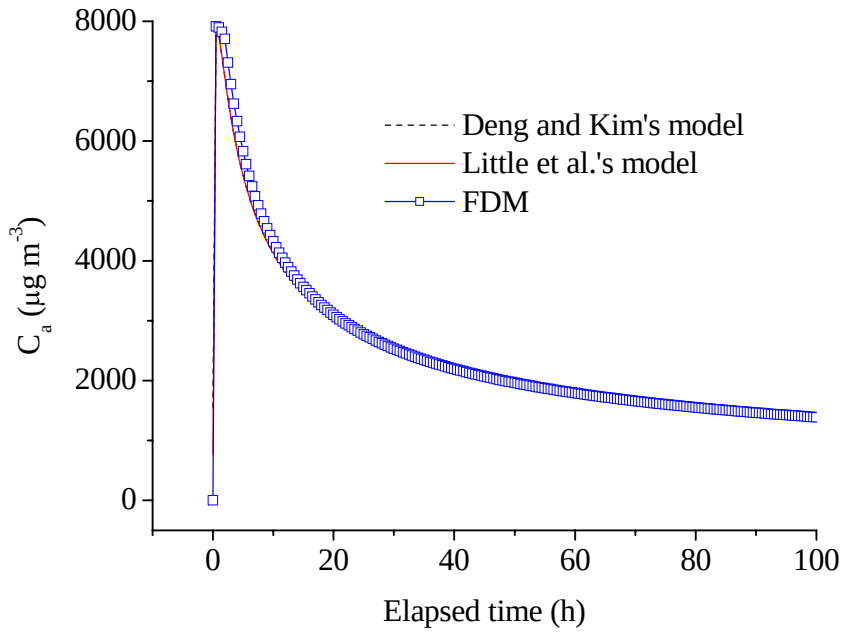

Figure 4.3 Deng and Kim's model and the numerical model tend to Little et al.'s model if h_m is very large

4.2.4 Parametric Study of the Direct Problem

The effects of the four key model parameters on the VOCs concentration in air are examined. Figure 4.4 indicates that C_a is affected by h_m mainly at the early stage. It

can also be found that, for h_m=1×10^{-3} (m/s) and h_m=∝, there is no significant difference between the calculated C_a, even at the initial state. This implies that for relatively large h_m it is reasonable to simply assume h_m is infinite, i.e. neglecting the convective mass transfer resistance. Under this circumstance, Little et al.'s model can be used. It also indicates that, from the viewpoint of energy saving, it is not wisdom to overmuch increase the air velocity or air change rate to flush-out VOCs emitted by dry building materials because as analyzed above, when h_m increases to a certain extent it virtually has no significant effect on VOCs emission from dry materials.

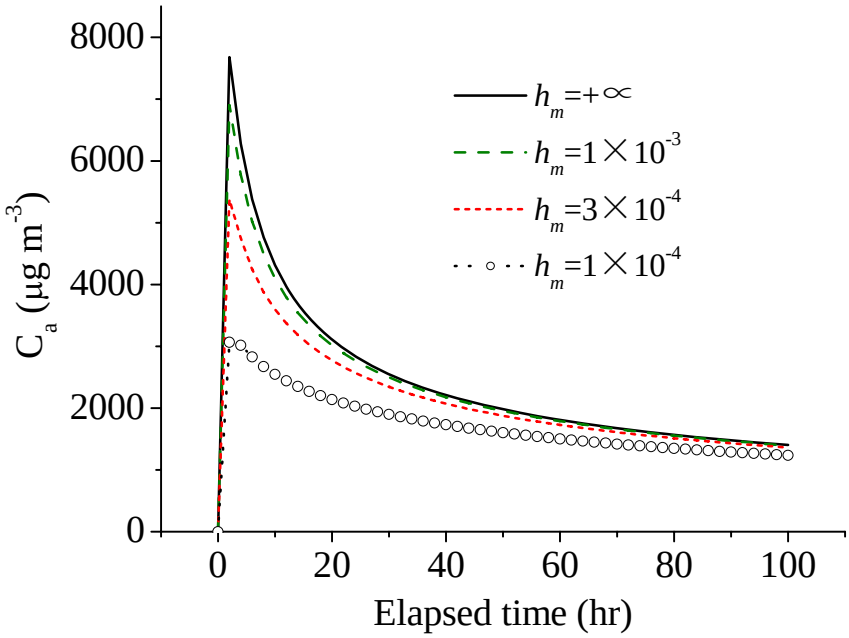

Figure 4.4 Effect of h_m on C_a
(D_m=7.65×10^{-11} m^2/s, K_{ma}=3289 and C_{m0}=5.28×10^7 μg/m^3)

Figure 4.5 shows the effect of C_{m0} on C_a. It is clear that the VOCs concentration in air increases greatly with the increase of C_{m0}. So, probably the most effective way to control the VOCs concentration in indoor air might be reducing the initial VOCs concentration in the material or using so called "green building materials".

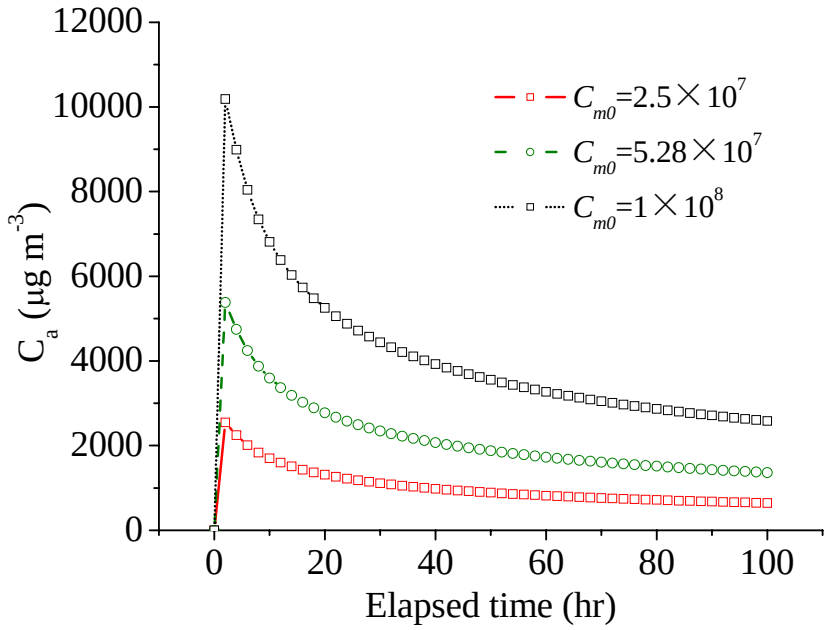

Figure 4.5 Effect of C_{m0} on C_a

(D_m=7.65×10^{-11} m^2/s, K_{ma}=3289 and h_m =3×10^{-4} m/s)

Figure 4.6 shows that increasing D_m results in higher VOCs concentration for the whole test duration.

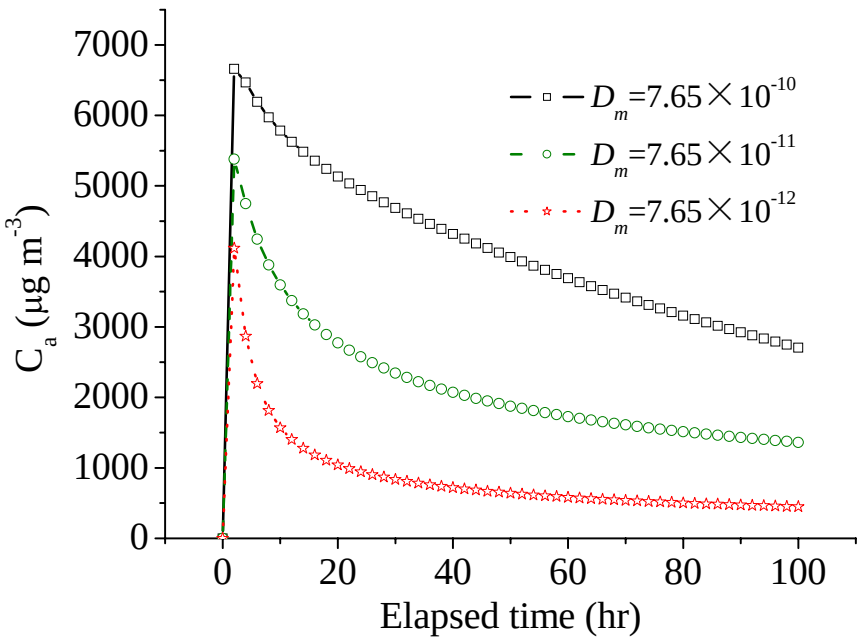

Figure 4.6 Effect of D_m on C_a

(C_{m0}=5.28×10^7 μg/m^3, K_{ma}=3289 and h_m =3×10^{-4} m/s)

This provides another method to reduce the indoor VOCs concentration that is covering the VOCs sources by a less permeable or impermeable material (i.e. material with very small D_m) so that VOCs in the sources are extremely difficult to diffuse out. Under this circumstance, although the total emission time may last longer, the peak VOCs concentration indoors will be lower.

While Figure 4.7 shows increasing K_{ma} only results in a decreased emission rate at the early stage, and eventually almost has no impact on indoor VOCs concentration.

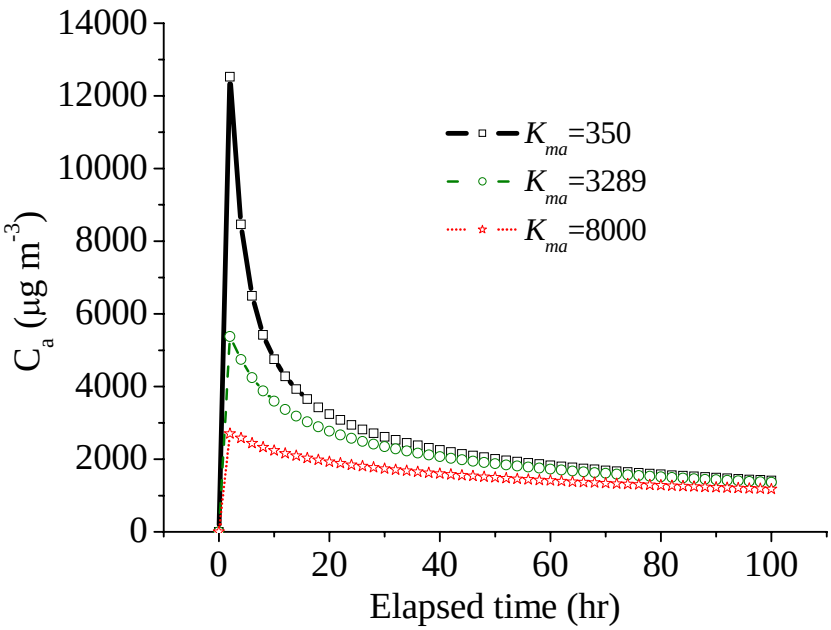

Figure 4.7 Effect of K_{ma} on C_a
(C_{m0}=5.28×10^7 μg/m^3, D_m=7.65×10^{-11} m^2/s and h_m =3×10^{-4} m/s)

4.3 Inverse Problem of the One-dimensional Transient Mass Diffusion

4.3.1 Development of the Inverse Algorithm

The direct problem defined by equations (4.1) - (4.7) is mathematically classified as well-posed, that is, the solution satisfies the requirements of existence, uniqueness and stability with respect to the input data (Alifanov, 1994; Ozisik and Orlande, 2000). On the other hand, the problem given by equations (4.1) - (4.7) with the

diffusion coefficient D_m and partition coefficient K_{ma} unknown is an ill-posed inverse problem (Alifanov, 1994; Ozisik and Orlande, 2000). The additional information obtained from transient VOCs concentration measurements at the chamber outlet is then used for the estimation of the unknown parameters. Several methods of solving this kind of inverse problem, such as the Levenberg-Marquardt method (Marquardt, 1963; Ozisik and Orlande, 2000) used in this research, involve their reformulation in terms of well-posed minimization problems. The Levenberg-Marquardt algorithm has proved to be an effective and popular way to solve nonlinear least squares problems. By assuming additive, uncorrelated and normally distributed random errors, with constant standard deviation and zero mean, the solution of the present parameter estimation problem can be obtained through the minimization of the ordinary least-squares norm. Such a norm can be written as:

$$S(\mathbf{P}) = [\mathbf{Y} - \mathbf{C_a}(\mathbf{P})]^T [\mathbf{Y} - \mathbf{C_a}(\mathbf{P})] \tag{4.20}$$

where the superscript T denotes the transpose, and $[\mathbf{Y} - \mathbf{C_a}(\mathbf{P})]^T$ is defined as:

$$[\mathbf{Y} - \mathbf{C_a}(\mathbf{P})]^T = [Y_1 - C_{a1}, Y_2 - C_{a2}, \cdots, Y_I - C_{aI}] \tag{4.21}$$

where

S is sum of squares errors or objective function

$\mathbf{P} = [P_1, P_2, ..., P_l]^T$, vector of unknown parameters

$\mathbf{Y} = [Y_1, Y_2, \cdots, Y_I]^T$, measured VOC concentration in chamber air

l, total number of unknown parameters

I, total number of measurement, where $I \geqslant l$

$\mathbf{C_a(P)} = [C_{a1}, C_{a2}, \cdots, C_{aI}]^T$, estimated VOC concentration in chamber air

To minimize the least squares norm given by equation (4.20), the necessary condition is:

$$\nabla S(\mathbf{P}) = 2\left[-\frac{\partial \mathbf{C_a^T(P)}}{\partial \mathbf{P}}\right][\mathbf{Y} - \mathbf{C_a(P)}] = 0 \tag{4.22}$$

where

$$\frac{\partial \mathbf{C_a^T(P)}}{\partial \mathbf{P}} = \begin{bmatrix} \frac{\partial}{\partial P_1} \\ \frac{\partial}{\partial P_2} \\ \vdots \\ \frac{\partial}{\partial P_l} \end{bmatrix} [C_{a1}\ C_{a2} \cdots C_{aI}] \tag{4.23}$$

The sensitivity or Jacobian matrix, **J(P)** is defined as the transpose of equation (4.23), that is:

$$\mathbf{J(P)} = \left[\frac{\partial \mathbf{C_a^T(P)}}{\partial \mathbf{P}}\right]^T = \begin{bmatrix} \frac{\partial C_{a1}}{\partial P_1} & \frac{\partial C_{a1}}{\partial P_2} \cdots & \frac{\partial C_{a1}}{\partial P_l} \\ \frac{\partial C_{a2}}{\partial P_1} & \frac{\partial C_{a2}}{\partial P_2} \cdots & \frac{\partial C_{a2}}{\partial P_l} \\ \vdots & \vdots & \vdots \\ \frac{\partial C_{aI}}{\partial P_1} & \frac{\partial C_{aI}}{\partial P_3} \cdots & \frac{\partial C_{aI}}{\partial P_l} \end{bmatrix} \tag{4.24}$$

By using the definition of the sensitivity matrix, equation (4.22) becomes:

$$-2\mathbf{J}^T\mathbf{(P)[Y - C_a(P)]} = 0 \tag{4.25}$$

The present inverse mass diffusion problem is very ill-conditioned, especially near the improper initial guesses used for the unknown parameters. The Levenberg-Marquardt method (Marquardt, 1963; Ozisik and Orlande, 2000) can be used to solve equation (4.25) by utilizing an iterative procedure in the form:

$$\mathbf{P}^{k+1} = \mathbf{P}^{k} + \left[(\mathbf{J}^{k})^{T} \mathbf{J}^{k} + \mu^{k} \Omega^{k} \right]^{-1} (\mathbf{J}^{k})^{T} \left[\mathbf{Y} - \mathbf{C_a}(\mathbf{P}^{k}) \right] \tag{4.26}$$

where μ^k is a positive scalar named damping parameter, and

$$\Omega^{k} = diag\left[(\mathbf{J}^{k})^{T} \mathbf{J}^{k} \right] \tag{4.27}$$

The purpose of the matrix term $\mu^k \mathbf{\Omega}^k$ is to damp oscillations and instabilities due to ill-conditioned character of the problem, by making its components large as compared to those of $\mathbf{J}^T \mathbf{J}$, if necessary. The damping parameter is made large in the beginning of the iterations, since the problem is generally ill-conditioned in the region around the initial guess used for the iterative procedure, which can be quite far from the exact parameters.

With such an approach, the matrix $\mathbf{J}^T \mathbf{J}$ is not required to be non-singular in the beginning of iterations and the Levenberg-Marquardt method tends to the Steep Descent Method (this is straightforward when μ^k approaches infinite in equation (4.26)), which converges slowly but does not require a good initial guess. The parameter μ^k is then gradually reduced as the iteration procedure advances to the solution of the parameter estimation problem, and then the Levenberg-Marquardt method tends to the Gauss Method (this is also straightforward when μ^k approaches zero in equation (4.26)), which converges fast but requires a good initial guess. However, if instabilities are noticed during the minimization procedure, the parameter μ^k is automatically increased by the method.

The iterative procedure is initialized with an initial guess for the unknown parameters, $\mathbf{P}^0$, and new estimates, $\mathbf{P}^{k+1}$, are obtained using equation (4.26) until any of the convergence criteria given in equation (4.28) is satisfied (Ozisik and Orlande, 2000):

$$\begin{cases} S(\mathbf{P}^{k+1}) < \varepsilon_1 \\ \left\| (\mathbf{J}^k)^T \left[\mathbf{Y} - \mathbf{C_a}(\mathbf{P}^k) \right] \right\| < \varepsilon_2 \\ \left\| \mathbf{P}^{k+1} - \mathbf{P}^k \right\| < \varepsilon_3 \end{cases} \tag{4.28}$$

where ε_1, ε_2 and ε_3 are the prescribed tolerances, in the present study they are all taken as 10^{-7}. $\|\cdot\|$ is the vector Euclidean norm, i.e., $\|X\| = (X^T X)^{1/2}$.

4.3.2 Sensitivity Analysis

An important requirement for parameter estimation is that the sensitivity coefficients should not be of small magnitude, and when two or more parameters are estimated simultaneously, their sensitivity coefficients must be linearly independent over the entire experimental time domain (Ozisik and Orlande, 2000). So, before executing any parameter estimation, careful examination of the sensitivity coefficients is imperative (Beck and Arnold, 1977).

The sensitivity coefficient defined by equation (4.24) can be approximated by using central differences in the form:

$$J_{ij} = \frac{\partial C_{ai}(\mathbf{P})}{\partial P_j} \approx \frac{C_{ai}(P_1, P_2, ..., P_j + \varepsilon P_j, ..., P_l) - C_{ai}(P_1, P_2, ..., P_j - \varepsilon P_j, ..., P_l)}{2\varepsilon P_j} \tag{4.29}$$

where ε is chosen as 10^{-7}, i=1, 2, …, I, and j=1, 2, …, l.

In problems involving parameters with different orders of magnitude, like the present problem, the sensitivity coefficients with respect to the various parameters may differ by several orders of magnitude, creating difficulties in their comparison and identification of linear dependence. These difficulties can be alleviated through the analysis of relative sensitivity coefficients defined as:

$$J_{P_j} = P_j \frac{\partial C_a(\mathbf{P})}{\partial P_j} \tag{4.30}$$

Note that the relative sensitivity coefficients have the units of the measured variable C_a, hence they are compared as having the magnitude of C_a as a basis. In order to calculate the relative sensitivity coefficients, approximate values of P_j are needed, which should be close to their exact values and can be obtained from experience or literature.

4.4 Application of the Inverse Method

As stated in the introduction section of this chapter, the study is composed of two stages. The first stage is to theoretically validate the proposed method and to investigate major impact factors on the accuracy of the parameter determination. If satisfying results generated in the first stage study, real measurements of the exhaust air of the Field and Laboratory Emission Cell (FELC) will be utilized to determine parameters of selected VOC/material combinations.

4.4.1 Factors Affecting the Accuracy of Estimates

First of all, sensitivity analysis is required. For simplicity, the exact values (D_m, K_{ma} and C_{m0} are shown in Table 4.1, h_m is calculated based on an empirical correlation.) for the unknowns are used here. The results are plotted in Figure 4.8. The relative sensitivity coefficients for K_{ma} are negative that means an increase in K_{ma} tends to decrease the VOCs concentration in chamber air, while the relative sensitivity coefficients for D_m, C_{m0} and h_m are positive implies that an increase in D_m, C_{m0} or h_m tends to increase VOCs concentration in chamber air. It can also be found that the relative sensitivity coefficients for K_{ma} and h_m are very small (almost equal to zero) at the late stage of the test, which means change of K_{ma} or h_m will have little influence

on the VOCs concentration in chamber at this particular stage compared to that of the initial stage. However, the relative sensitivity coefficients for D_m and C_{m0} remain almost unchanged and keep relatively large values. This implies that change of D_m and C_{m0} will affect the VOCs concentration in the whole test duration. Among the four, relative sensitivity coefficients of C_{m0} are the largest; this explicitly tells that the initial VOCs content in the material is the determinant factor affecting the indoor VOCs concentration. This again shows the importance of the source control strategy in maintaining an acceptable indoor air quality. The above sensitivity analysis is consistent with the conclusions drawn in subsection 4.2.4. A careful check of the relative sensitivity coefficients of D_m and K_{ma} reveals that the magnitudes are large and no linear dependence is found. Thus, it is feasible to simultaneously estimate D_m and K_{ma} with the developed inverse method.

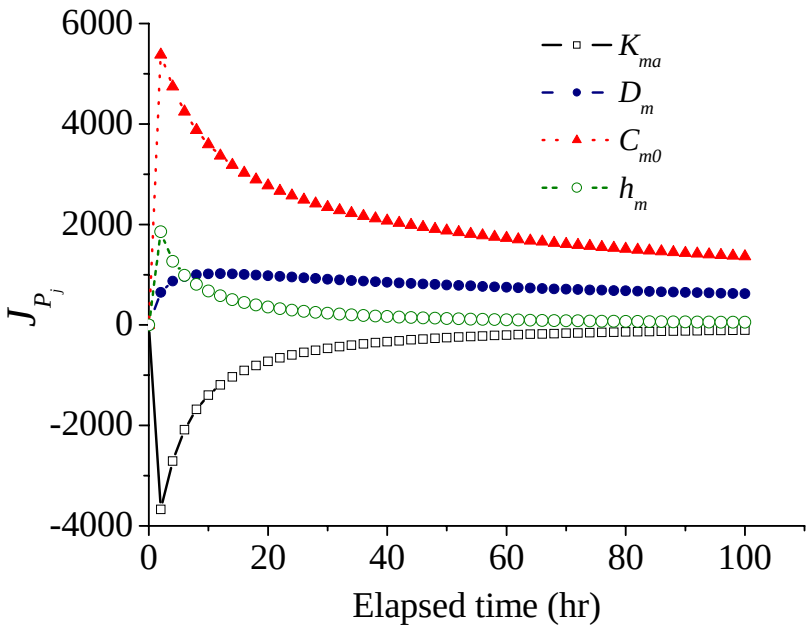

Figure 4.8 Relative sensitivity coefficients

The exact (errorless) measurements of VOCs concentration in chamber air $\mathbf{Y}_{\mathbf{exa}}$ are generated by solving the direct problem with the exact parameters, i.e., K_{ma}=3289,

D_m=7.65×10^{-11} m^2/s, C_{m0}=5.28×10^{7}μg/m^3 and h_m=3×10^{-4} m/s. Measurements containing random errors are simulated by adding an error term to $\mathbf{Y_{exa}}$ in the form:

$$\mathbf{Y} = \mathbf{Y_{exa}} + \boldsymbol{\omega}\sigma \tag{4.31}$$

where σ is the standard deviation of the measurement errors, and $\boldsymbol{\omega}$, random variable with normal distribution, zero mean and unitary standard deviation. For normally distributed random numbers with 99% confidence level, the value of $\boldsymbol{\omega}$ lies in the range -2.576< $\boldsymbol{\omega}$ <2.576.

The initial guesses in the inverse analysis for diffusion and partition coefficients are 3×10^{-13} m^2/s and 1000, respectively. As a matter of fact, different initial guesses covering a wide range of magnitude can be used to repeat the inverse analysis, if the final results are very close to each other, the estimates are considered to be unique and accurate. When real measurements are used to estimate the parameters, the correctness of the estimates can also be evaluated by comparing with the ranges of the values of typical building materials.

4.4.1.1 Effects of Number of Measurements on the Accuracy of Estimation

The effects of number of measurements on the accuracy of estimation are presented in Table 4.2. For a fixed total measuring time of 100 hours, the number of measurements I = 100, 50, 25 and 12 correspond to time steps Δt = 1, 2, 4 and 8 hour, respectively. Clearly, the accuracies of estimations are improved by increasing the number of measurements I or decreasing the measuring time step Δt. However, the improvement is negligible for I >25.

For run 4 in Table 4.2, the results of the estimated parameters are totally not acceptable because the estimated K_{ma} is one order of magnitude smaller than the

exact value due to the large time step used. It seems that 12 measurements are not sufficient to obtain reasonable results.

Nevertheless, in run 5, there is the same number of measurements as in run 4, but variable time steps are adopted. Measurements are taken at t =1, 2, 4, 6, 8, 12, 18, 24, 36, 48, 72 and 96 hour. Significantly improved accuracy of the results has been achieved.

In fact, measurements with variable time steps are commonly adopted during emission/sorption tests, because the concentration of VOCs in the chamber air decays/increases much faster at the initial stage than at the late stage. Basically, more measurements are required to be taken at the initial stage in order not to miss any critical data points on the concentration curve, as Figure 4.9 shows. Some other researchers also called this 'the data abundance' (He and Yang, 2005).

Table 4.2 Effects of the number of measurements on the accuracy of estimation (σ = 0)

Run	I	Δt (hour)	Parameters	Exact	Estimates	Error (%)
1	100	1	K_{ma}	3289	3288.7	-0.009
			$D_m \times 10^{11}$ (m^2/s)	7.65	7.6492	-0.010
2	50	2	K_{ma}	3289	3288.5	-0.015
			$D_m \times 10^{11}$ (m^2/s)	7.65	7.6485	-0.020
3	25	4	K_{ma}	3289	3287.9	-0.033
			$D_m \times 10^{11}$ (m^2/s)	7.65	7.6476	-0.031
4	12	8	K_{ma}	3289	279.8	-91.49
			$D_m \times 10^{11}$ (m^2/s)	7.65	5.0795	-33.60
5	12	variable time step	K_{ma}	3289	3292.1	+0.094
			$D_m \times 10^{11}$ (m^2/s)	7.65	7.5577	-1.207

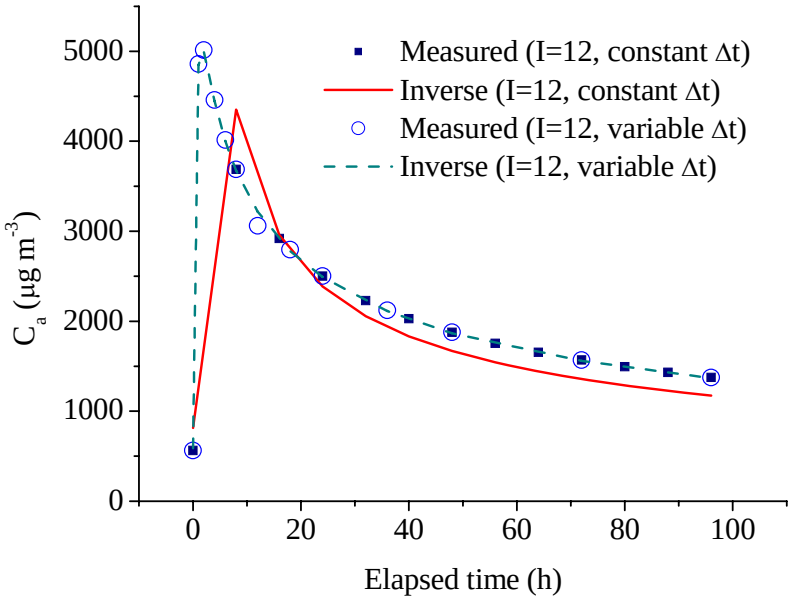

Figure 4.9 Effects of sampling intervals on inverse analysis of VOC concentration in chamber air

4.4.1.2 Effects of Random Measurement Errors in C_a on the Accuracy of Estimation

It can be seen in Table 4.3 that acceptable estimates are obtained, even for measurements containing large random errors. Figure 4.10 shows the agreement between the simulated, inverse estimated and exact VOCs concentration. For the sake of clarity, only two error levels $\sigma = 0.03\mathbf{Y}_{\mathbf{exa,max}}$ and $0.05\mathbf{Y}_{\mathbf{exa,max}}$ are shown. It seems that the random errors involved in the measurements of VOCs concentration have smaller effect on the accuracy of estimated results compared with other determinant factors. In fact, non-uniformly systematic error instead of random error is the major factor which significantly affects the accuracy of estimated D_m and K_{ma}. For example, the measured concentrations of VOCs are always smaller than the real values (Luo and Niu, 2004). This is natural because it is very difficult to collect all the VOCs of interest onto the sorbents of the sampling tube during the sampling period, and also possible loss of VOCs may occur during the period of sample storage and analysis.

Table 4.3 Effects of random measurement errors in C_a on the accuracy of estimation (I=50)

Run	σ	Parameters	Exact	Estimates	Error (%)
6	$0.01\mathbf{Y}_{\mathbf{exa,max}}$	K_{ma}	3289	3290.1	+0.03
		$D_m\times10^{11}$ (m^2/s)	7.65	7.301	-4.56
7	$0.03\mathbf{Y}_{\mathbf{exa,max}}$	K_{ma}	3289	3148.3	-4.28
		$D_m\times10^{11}$ (m^2/s)	7.65	7.3655	-3.72
8	$0.05\mathbf{Y}_{\mathbf{exa,max}}$	K_{ma}	3289	3083.3	-6.26
		$D_m\times10^{11}$ (m^2/s)	7.65	6.5683	-14.14
9	$0.1\mathbf{Y}_{\mathbf{exa,max}}$	K_{ma}	3289	3440.5	+4.59
		$D_m\times10^{11}$ (m^2/s)	7.65	8.1721	+6.82

Note: $\mathbf{Y}_{\mathbf{exa,max}}$ is the maximum simulated errorless VOCs concentration.

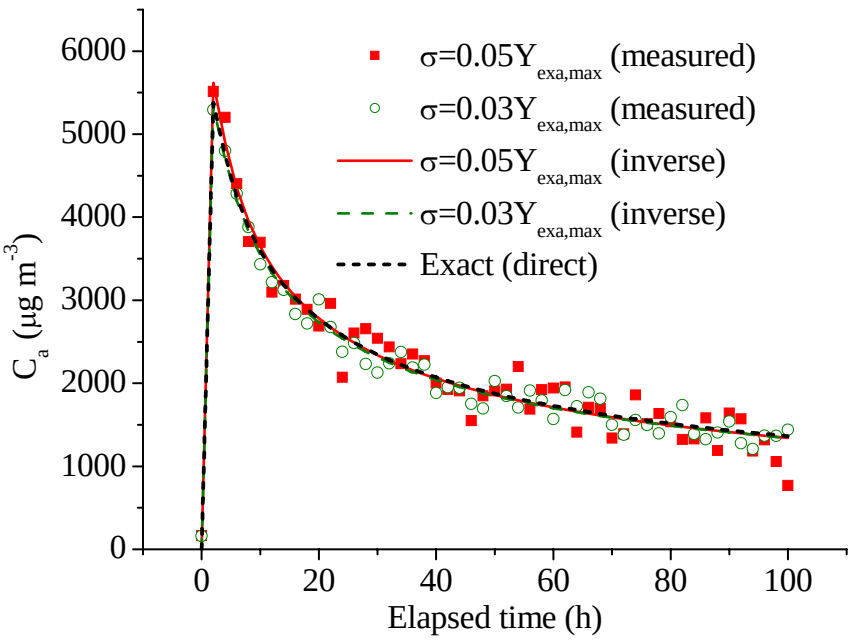

Figure 4.10 Comparison of measured, inverse estimated and exact C_a

4.4.1.3 Effects of Errors in h_m on the Accuracy of Estimation

Here we use $h_{m,cal}$ and $h_{m,exa}$ to standard for the calculated and exact value of h_m for ease of description. Because $h_{m,cal}$ is usually estimated from an empirical equation that rarely fit the experiment data precisely, there might be errors involved, the value of $h_{m,cal}$ is possible of greater or smaller than the exact value $h_{m,exa}$.

We examine the estimated value of diffusion coefficient D_m in Table 4.4. Clearly, the errors in h_m hardly have any influences on the estimation of D_m, in a wide range of $h_{m,cal}$ between zero to infinite, which is consistent to the fact that VOCs emission for dry building material is dominated by internal diffusion. However, the partition coefficient K_{ma} is quite sensitive to the errors in h_m. The smaller $h_{m,cal}$ than $h_{m,exa}$ results in the smaller estimated K_{ma}, the minimum of the estimated K_{ma} is zero when $h_{m,cal}$ approaches zero, however, it should be noted that this is only an extreme case illustration and practically speaking K_{ma} is unlikely to be below 1 (He et al., 2005). On the contrary, estimated K_{ma} increases with the increasing $h_{m,cal}$, when $h_{m,cal}$ is greater than $h_{m,exa}$. Suppose, $h_{m,cal} = \infty$, the estimated parameters can be found in Table 4.4, they are D_m=7.4195×10^{-11} m^2/s and K_{ma}=6212.8. Actually the model tends to Little et al.'s model when $h_{m,cal} = \infty$. So it is clear that if using Little et al.'s model for inverse analysis, the partition coefficient K_{ma} would be largely overestimated with an error of approximately 90%, while the diffusion coefficient D_m can still be accurately estimated.

Table 4.4 Effects of errors involved in h_m on the accuracy of estimation (I=50, σ=0.01 $Y_{exa,max}$)

Run	Error of h_m	Parameters	Exact	Estimates	Error (%)
10	-10%	K_{ma}	3289	3276	-0.395
		D_m×10^{11} (m^2/s)	7.65	7.9164	+3.48
11	-20%	K_{ma}	3289	2975	-9.55
		D_m×10^{11} (m^2/s)	7.65	7.6656	+0.204
12	-50%	K_{ma}	3289	2244.2	-31.77
		D_m×10^{11} (m^2/s)	7.65	7.8296	+2.35
13	-99.9%	K_{ma}	3289	0.0065	-99.99
		D_m×10^{11} (m^2/s)	7.65	7.395	-3.33
14	10%	K_{ma}	3289	3466.7	+5.40
		D_m×10^{11} (m^2/s)	7.65	7.6998	+0.65

15	50%	K_{ma}	3289	3935	+19.64
		$D_m \times 10^{11}$ (m^2/s)	7.65	7.676	+0.34
16	100%	K_{ma}	3289	4404.8	+33.91
		$D_m \times 10^{11}$ (m^2/s)	7.65	7.6599	+0.129
17	200%	K_{ma}	3289	4869.7	+48.06
		$D_m \times 10^{11}$ (m^2/s)	7.65	7.6465	-0.046
18	300%	K_{ma}	3289	5018.2	+52.58
		$D_m \times 10^{11}$ (m^2/s)	7.65	7.4681	-2.38
19	∞	K_{ma}	3289	6212.8	+88.896
		$D_m \times 10^{11}$ (m^2/s)	7.65	7.4195	-3.013

Note: Negative errors mean $h_{m,cal} < h_{m,exa}$, positive errors mean $h_{m,cal} > h_{m,exa}$.

4.4.1.4 Effects of Errors in C_{m0} on the Accuracy of Estimation

Table 4.5 presents the results of estimated parameters with initial concentration C_{m0} involving measurement errors. Since the measured concentrations of VOCs are generally smaller than the real values, we only consider the situations of underestimating the initial concentration.

Table 4.5 Effects of measurement errors in C_{m0} on the accuracy of estimation (I=50, σ=0.01$Y_{exa,max}$)

Run	Relative error in C_{m0} (%)	Parameters	Exact	Estimates	Relative error (%)
20	3%	K_{ma}	3289	3255.2	-1.03
		$D_m \times 10^{11}$ (m^2/s)	7.65	8.313	8.67
21	5%	K_{ma}	3289	3158	-3.98
		$D_m \times 10^{11}$ (m^2/s)	7.65	8.4718	10.74
22	10%	K_{ma}	3289	3059	-6.99
		$D_m \times 10^{11}$ (m^2/s)	7.65	9.7755	27.78
23	20%	K_{ma}	3289	2713.5	-17.5
		$D_m \times 10^{11}$ (m^2/s)	7.65	12.234	59.92
24	30%	K_{ma}	3289	2339.2	-28.88
		$D_m \times 10^{11}$ (m^2/s)	7.65	15.46	102.09
25	50%	K_{ma}	3289	1673.5	-49.12
		$D_m \times 10^{11}$ (m^2/s)	7.65	31.062	306.1

Obviously, underestimating C_{m0} results in underestimated VOCs concentration in chamber air when D_m and K_{ma} are constant. We also know that the VOCs concentration in chamber air increases with the decreasing K_{ma} and increasing D_m when C_{m0} is constant (Little et al., 1994).

So, with the measured VOCs concentration in chamber air, it is natural that the estimated values of D_m should be increased and K_{ma} be decreased to compensate for the underestimation of C_{m0}.

It is also noticed that partition coefficient decreases with the increasing measurement error in C_{m0}; whereas the diffusion coefficient increases rapidly with the increasing measurement error in C_{m0}. When the relative error in C_{m0} is above 20%, the estimated D_m is an order of magnitude larger than its exact value. Figure 4.11 shows the errors in estimated D_m and K_{ma} against the errors in C_{m0}.

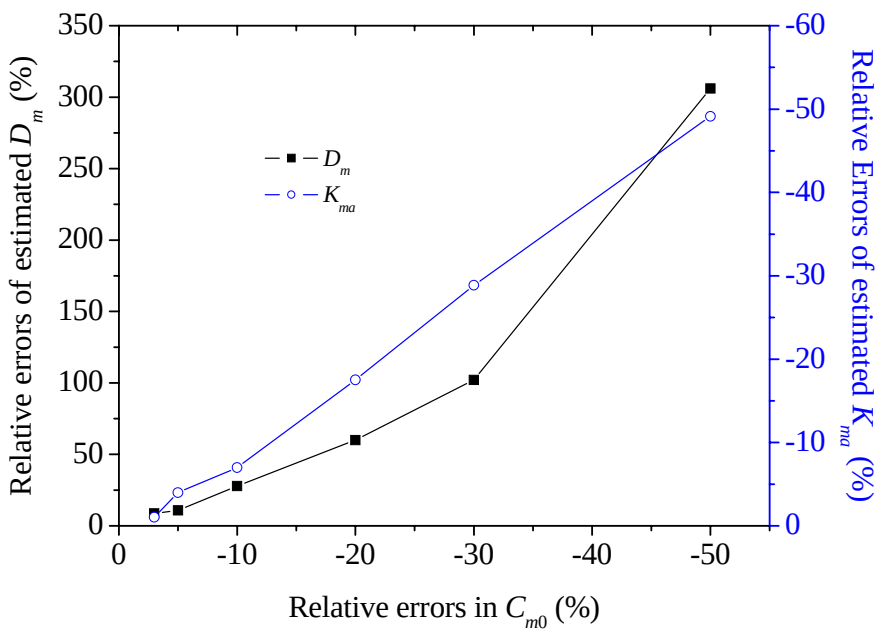

Figure 4.11 Effects of errors in C_{m0} on the accuracy of estimates

4.4.2 Experimental Determination of D_m and K_{ma} of Selected VOC/material Combination

4.4.2.1 Method 1 - Emission Test Using FLEC

A 35 ml mini-environmental chamber - Field Laboratory Emission Cell (FLEC) was used to test VOCs emissions from a typical carpet with 100% polyamide pile yarn and modified bitumen with PP/PES carrier backing. The schematic representation of the test rig is shown in Figure 4.12.

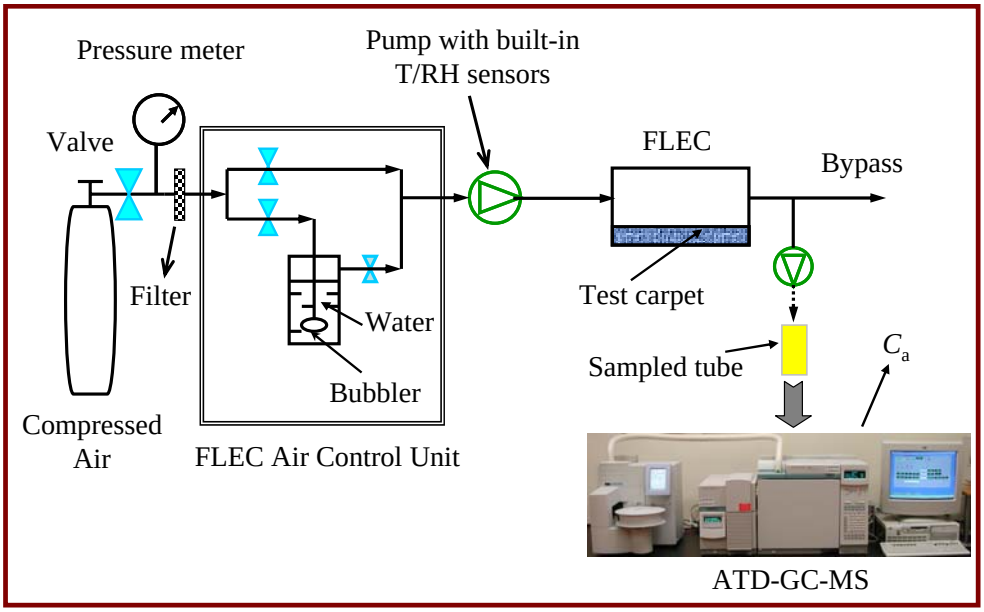

Figure 4.12 Schematic representation of the emission test rig

The new carpet was sealed for three months before testing to achieve uniform VOCs distribution within it and its total thickness was 6.3±0.5 mm. The air flow through FLEC was 100 ml/min which was controlled by FLEC Air Control Unit and measured by an FLEC air pump, relative humidity of the clean air supplied to the FLEC was adjusted to 50% by FLEC air control unit and the test was performed in an air conditioned lab, where the temperature was maintained at 23±1 °C. The measurement accuracies of the sensors were 2% for relative humidity, and 0.2°C for temperature, respectively. The air samples for VOCs at the outlet of the FLEC were

periodically collected on **AirToxics™** sorbent tubes at a flowrate of 66.7 ml/min during the 300-hour test duration. The pumps were checked using SKC INC. ACCUFLOW® Digital Film Calibrator (Serial No. 302988, Cat. No. 712, Range: 5 to 5000 ml/min) before the test. The calibration curves of the FLEC inlet supply pump and outlet sampling pump are shown in Figure 4.13. It can be seen that the relative errors of the flowrate measurements for the inlet supply pump and outlet sampling pump are -1% and -2.8% at their set flow rates, respectively.

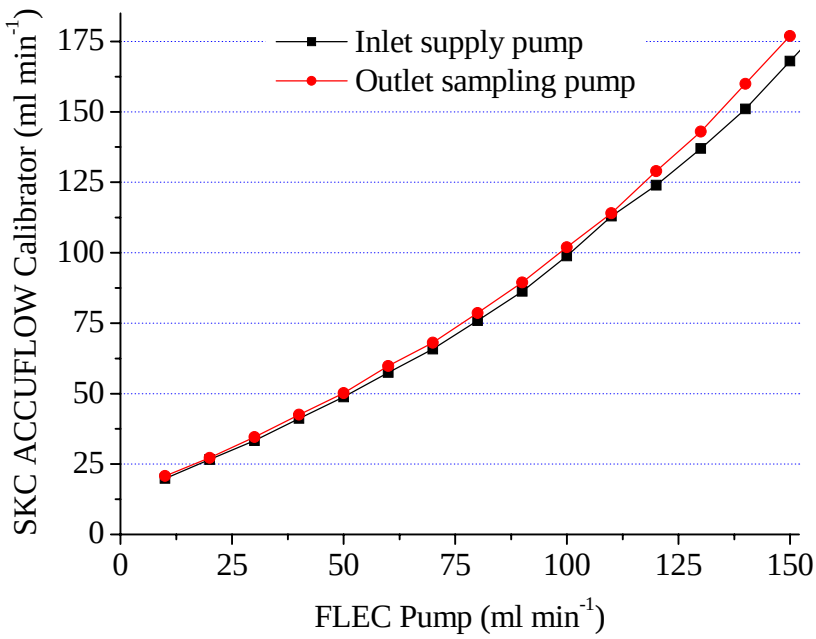

Figure 4.13 Flow correlations of SKC ACCUFLOW Calibrator against FLEC Pumps

The sampled tubes were then desorbed in an automatic thermal desorption system (ATD 400, Perkin-Elmer) followed by gas-chromatography/mass-spectroscopy (6850 GC/5793N MSD, Agilent, Hewlett-Packard) according to the descriptions given in the U.S. Compendium Method TO-17. Among the compounds detected and quantified, styrene was chosen to implement the inverse technique. It should be pointed out that the convective mass transfer coefficient h_m in the FLEC should be calculated using equation (3.11).

The experimental results and inverse estimates are presented in Figure 4.14.

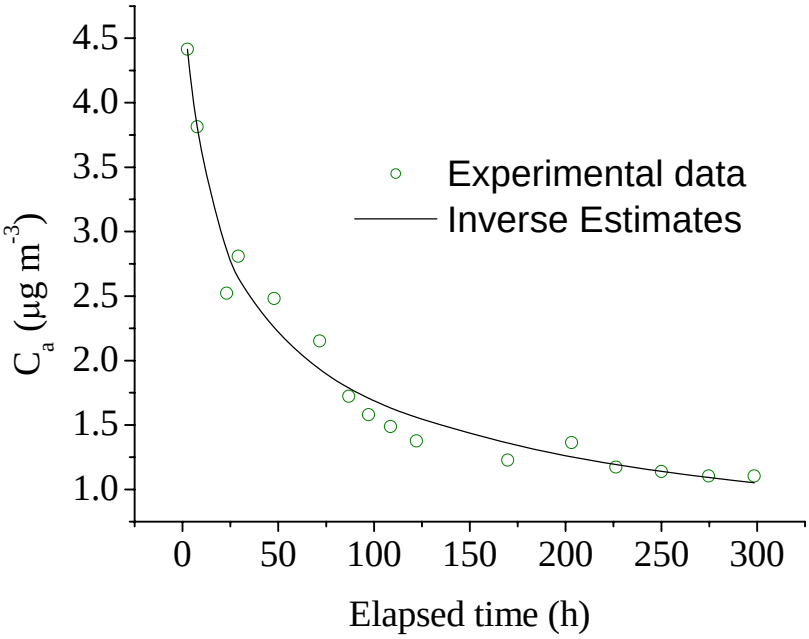

Figure 4.14 Experimental and inverse determined concentration of styrene emitted from carpet in the FLEC against time

The inverse determined diffusion and partition coefficients for styrene in the test carpet were D_m=2.4×10^{-12} m^2/s and K_{ma}=14072, respectively. Little et al. (1994) also determined D_m and K_{ma} for styrene in Carpet 1a (D_m=4.1×10^{-12} m^2/s, K_{ma}=4200), Carpet 1b (D_m=3.6×10^{-12} m^2/s, K_{ma}=6500), and Carpet 3 (D_m=3.1×10^{-12} m^2/s, K_{ma}=5700). Although direct comparison is improper because different types of carpets were tested, however, to some extent, the orders of magnitude of the results show their reasonabilities. In addition, the theoretical validation of the inverse technique in subsection 4.4.1 makes this method convincing.

4.4.2.2 Method 2 - Sorption Test Using FLEC

Although the results obtained from carpet emission test seem to be acceptable, it is known that, the VOC concentration in the FLEC is very low for not strong VOC sources (e.g. aged building materials) or sink materials, even for the newly bought

carpet (which is usually a strong VOCs source material) tested in this study. The reasons may be that most of the VOCs containing in the new carpet have emitted during the periods of transportation and storage. In order to fit into the detection limit of the GC-MS system, the sampling time has to be significantly increased. Because the concentration measured by using sampling method represents the concentration corresponding to the time at the middle of the sampling starting and ending time, this inevitably causes large measurement errors, and consequently may affect the accuracy of the parameter determination. To overcome this problem, an improved test method – sorption test method is developed, which is suitable for sink materials or substrate materials.

4.4.2.2.1 Principle of the Sorption Test

The main procedures are letting the conditioned test material (zero initial VOCs concentration) experience an adsorption period and reach an equilibrium state, and finally a desorption period. A schematic drawing of the principle of the sorption test is shown in Figure 4.15.

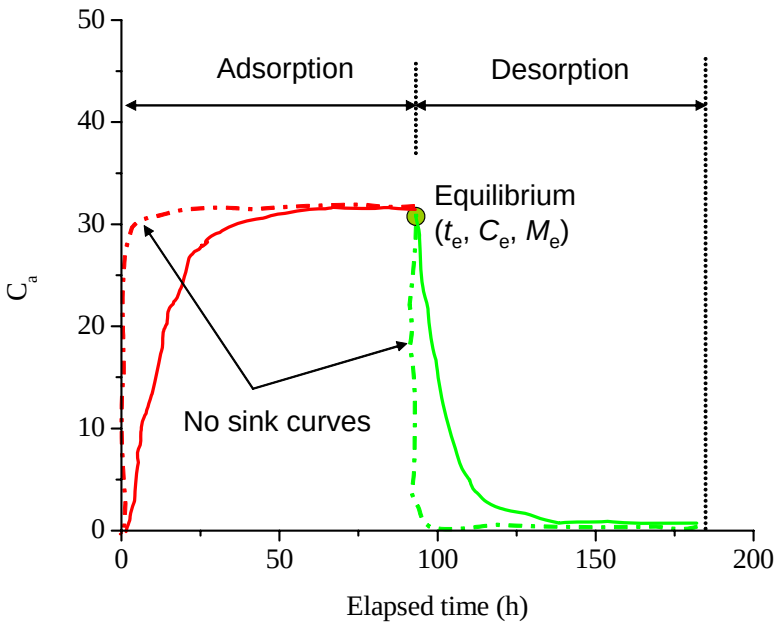

Figure 4.15 Schematic drawing of adsorption/desorption processes

The advantage of this method is capable of artificially elevating the concentration level to increase the accuracy of concentration measurement. The equilibrium VOC concentration can be measured, while the transient adsorbed/desorbed mass and adsorbed mass at the equilibrium state can be calculated using equations (4.32) - (4.36).

$$C^*(t) = C_{in} \cdot (1 - e^{-\frac{Q}{V}t}) \tag{4.32}$$

$$M_{ad}(t) = Q \cdot \int_0^t (C^* - C_a)dt \tag{4.33}$$

$$M_e = Q \cdot \int_0^{t_e} (C^* - C_a)dt \tag{4.34}$$

$$C^{**}(t) = C_e \cdot e^{-\frac{Q}{V}t} \tag{4.35}$$

$$M_{de}(t) = Q \cdot \int_{t_e}^{t} (C_a - C^{**})dt \tag{4.36}$$

where Q is the volumetric flowrate, V the volume of the chamber, C_{in} the inlet VOCs concentration during adsorption period, C_a the transient VOCs concentration at the

outlet, C^* no sink step-up curve, C^{**} no sink decay curve, t time, and t_e equilibrium state time. Based on these equations, sorption capacities of different building materials can be ranked. However, the focus of this study is to determine the diffusion and partition coefficients of building materials utilizing the dynamic concentration curves.

4.4.2.2.2 Test Rig of Sorption Test

The test rig for sorption test is shown in Figure 4.16. The environmental conditions are the same as those in emission tests. The main difference is the air flow loop, for sorption test, a diffusion tube filling with compound of interest is held at a constant temperature by a water bath to maintain a constant VOC generation rate. During the adsorption process, air with a constant VOC concentration is continuously supplied to FLEC (by closing valve A and opening valves B1 and B2), VOC is then adsorbed by test material; samples are carried out onto **Air Toxics™** tubes at the inlet and outlet of the FLEC, when the VOC concentration at the outlet of the FLEC does not change with time, equilibrium is assumed to be achieved and then VOC generation system is shut off, clean air is supplied to the FLEC right away (by closing valves B1 and B2, and opening valve A), from this moment on, desorption process begins, VOC concentration at the FLEC outlet is still sampled. The samples are then analyzed by ATD-GC-MSD system.

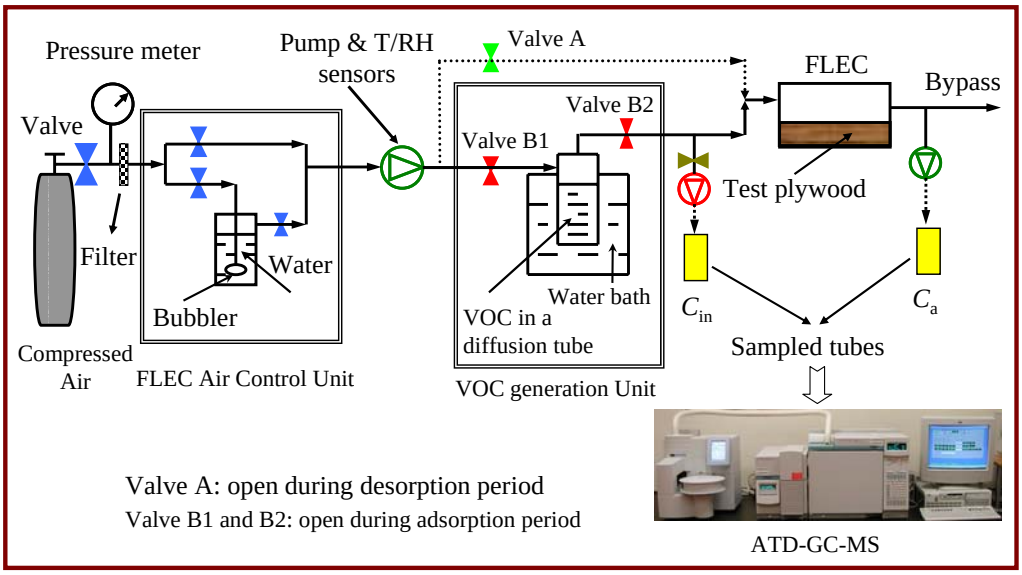

Figure 4.16 Schematic drawing of experimental setup for sorption test

4.4.2.2.3 Test VOC/material and Test Conditions

In this study, toluene is chosen as the compound of interest because toluene is a prevalent indoor air pollutant and is commonly studied in indoor air research as well. Locally bought plywood is chosen as the test material because plywood is widely used indoors and is often used as substrate of paint. The 4mm thick plywood was cut into circular with a diameter 150mm to meet the configuration of the FLEC. The test specimen was first placed in an oven at a temperature of 45°C for two weeks to drive away the residual VOCs. Then it was conditioned with clean humid air (RH=50%) at a flow rate of 100 ml min^{-1} and at a temperature about 23°C for another two weeks before testing.

Because in this test, new FLEC air pumps were bought and to be used, the new pumps were then checked by the SKC INC. ACCUFLOW® Digital Film Calibrator. The curves are shown in Figure 4.17.

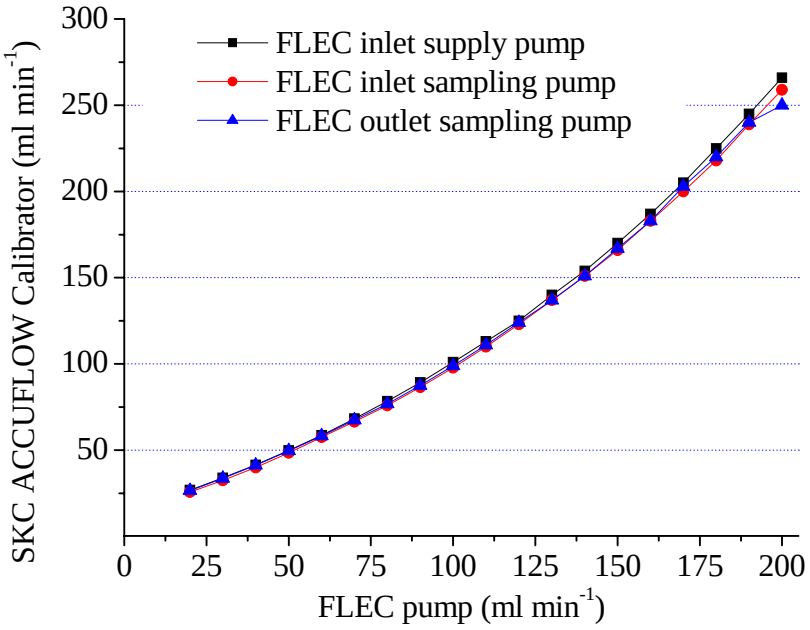

Figure 4.17 Flow correlations of SKC ACCUFLOW Calibrator against FLEC Pumps

The supply air flow rate was 100 ml min^{-1} and the sampling flowrate at the inlet and outlet of the FLEC were 40 ml min^{-1} and 50 ml min^{-1}, respectively. Thus, the relative errors of the flowrate measurements for FLEC inlet supply pump, inlet sampling pump and outlet sampling pump at their set flow rates were 1%, 0%, and -0.6%, respectively.

The dimensions of the diffusion tube were 10cm in length and 1mm in I.D., respectively. During the test, the edges and the bottom of the test specimen were sealed with aluminum foil to meet the boundary conditions defined in the model. The temperature of the water in the water bath was maintained at 26±1°C. Environmental conditions were temperature 23°C and RH 50%.

4.4.2.2.4 Test Results

The monitored inlet toluene concentration is shown in Figure 4.18. It can be seen that the inlet toluene concentration fluctuated within an acceptable range with the mean

value 2763.36 μg m^{-3}. It suggests that the diffusion tube filling with pure liquid VOC can serve as a constant emission source.

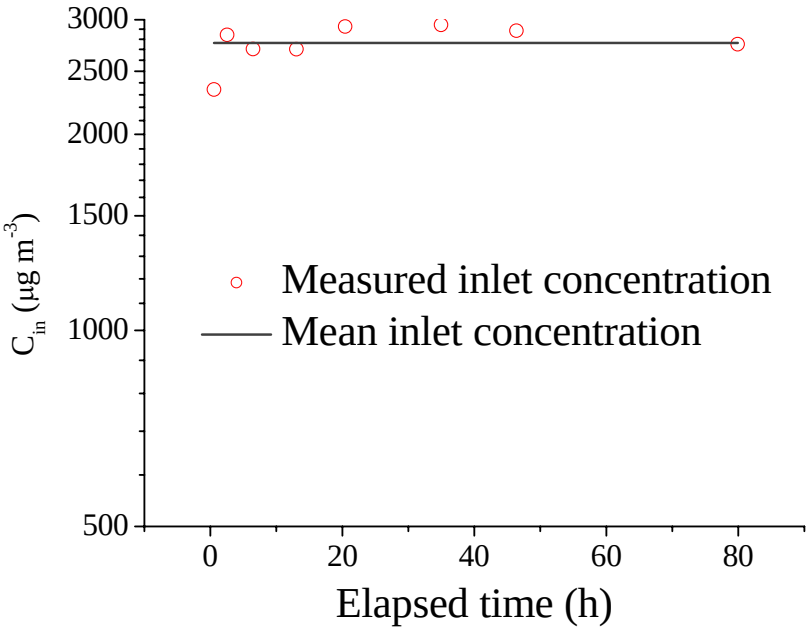

Figure 4.18 Measured toluene concentration at the inlet of the FLEC during adsorption period

The toluene concentration at the outlet of the FLEC was monitored during the whole test period. The measured data are plotted in Figure 4.19. Considering the fact that during adsorption period, the inlet toluene concentration fluctuated and thus introduced a source error. The desorption period would not suffer from this fluctuations since clean air was supplied to the FLEC in this period and was therefore more stable. For this reason, the data in dynamic desorption period was used to obtain the D_m and K_{ma} of toluene/plywood combination.

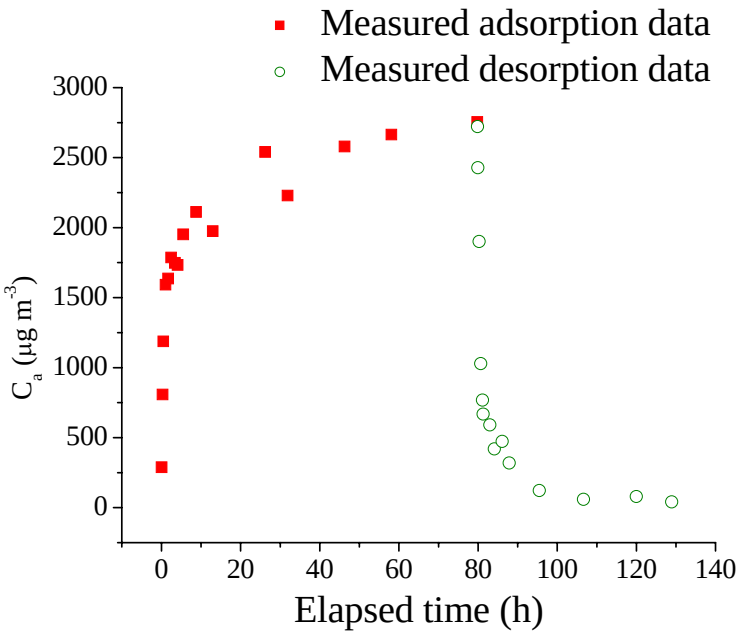

Figure 4.19 Measured toluene concentration at the outlet of the FLEC

The inverse estimated results for toluene/plywood were D_m=2.19×10^{-10} m^2 s^{-1} and K_{ma}=124.67, the wellness of inverse determination can be seen in Figure 4.20.

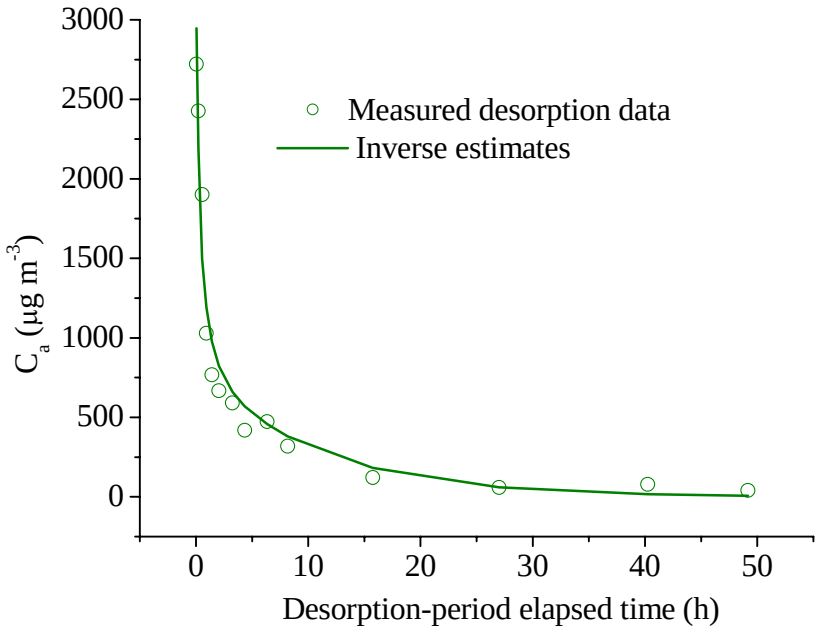

Figure 4.20 Measured and inverse estimated desorption data

Bodalal et al. (2001) also measured diffusion and partition coefficients of toluene/plywood combination by means of diffusionmetric method. The results they

obtained were D_m=1.75×10^{-10} m^2 s^{-1} and K_{ma}=358. However, the model they used neglects the convective mass transfer resistance, which would result in a largely overestimated partition coefficient K_{ma} (Li and Niu, 2005b) and an underestimated diffusion coefficient D_m (Haghighat et al., 2002). As a consequence, the diffusion and partition coefficients of toluene/plywood obtained using proposed method appears more reasonable. It should be pointed out that the discrepancy may be also due to different interior structure of plywood tested.

4.5 Summary

An inverse approach is developed to determine key model parameters. With the use of simulated measurements as input data for the inverse analysis, the existence, stability and uniqueness of the solution of the inverse problem were examined for various levels of measurement errors, by generating measurements with different standard deviations and by comparing the estimated quantities with those used to generate the simulated measurements.

Results show that measurements containing random errors only slightly affect the accuracy of estimation.

Both of the number of measurements I and the time step Δt have significant influences on the accuracy of estimation. Optimizing Δt and increasing I will give rise to more reasonable and unaffected results.

The errors in mean convective mass transfer coefficient hardly have any effects on the estimation of diffusion coefficient D_m, but have substantial impacts on the estimation of partition coefficient K_{ma}. When the calculated $h_{m,cal}$ varies between 0 to ∞, the estimated partition coefficient lies in the range 0 to $K_{ma,max}$, $K_{ma,max}$ is

equivalent to the estimated K_{ma} by inversely solving the Little et al.'s model under the same conditions. Using Little's et al.'s model for inverse analysis will result in an approximate 90% error of K_{ma}, while D_m is still relatively accurate.

The key factor that significantly affects the accuracy of the parameter estimation is the measurement errors in the initial concentration within the material, K_{ma} decreases while D_m increases rapidly with the increasing error of underestimation of C_{m0}. The estimated D_m appears to be one order of magnitude larger than the exact value in case the error in C_{m0} is greater than 20%.

Based upon the theoretical studies, real measured emission data of styrene/carpet combination in FLEC are used, the inverse determined diffusion and partition coefficients for styrene in the test carpet are D_m=2.4×10^{-12} m^2/s and K_{ma}=14072, respectively. Little et al. (1994) also determined D_m and K_{ma} for styrene in Carpet 1a (D_m=4.1×10^{-12} m^2/s, K_{ma}=4200), Carpet 1b (D_m=3.6×10^{-12} m^2/s, K_{ma}=6500), and Carpet 3 (D_m=3.1×10^{-12} m^2/s, K_{ma}=5700). Although different types of carpets tested, the same order of magnitude of the diffusion coefficients shows the validity of the proposed method.

A sorption test rig is developed to determine properties of sink materials or substrate materials which are not strong VOCs sources themselves. Adsorption and desorption behaviors of VOCs on building material can be characterized by conducting sorption tests in the FLEC. The dynamic desorption data are used as the input of the proposed inverse method. A preliminary study of toluene/plywood combination is conducted. The inverse estimated results for toluene/plywood were D_m=2.19×10^{-10} m^2 s^{-1} and K_{ma}=124.67. Bodalal et al. (2000) also measured diffusion and partition coefficients of toluene/plywood combination by means of diffusionmetric method. The results

they obtained were D_m=1.75×10^{-10} m^2 s^{-1} and K_{ma}=358. However, the discrepancy may be partly due to different interior structure of plywood tested. In addition, the D_m they obtained may be underestimated while the K_{ma} may be overestimated due to the neglecting of convective mass transfer resistance in their model (Haghighat et al., 2002; Li and Niu, 2005b). From these perspectives, the diffusion and partition coefficients of toluene/plywood obtained using the proposed method appears more reasonable. More VOCs/material combinations will be tested in the future studies, which would enrich the database of VOCs/material properties and consequently help to implement the mass transfer theory based models.

Chapter 5
Inverse Estimation of the Initial Distribution of Volatile Organic Compounds in Dry Building Material

5.1 Introduction

The quantity of initial condition C_{m0} is an important parameter that will greatly affect the emission characteristics, as has been studied in the previous chapter. Actually the distribution of VOCs within the material is also very important. However, almost all of the existing models assume that the initial VOCs are uniformly distributed within the building material. Obviously, this is a rough hypothesis; it may be true only for thin materials that have been sealed for a long time. For aged materials or materials with one side exposed to the air, the initial concentration of VOCs within the materials might not be uniform. However, very few studies have been conducted and little progress has been made on this aspect, mainly because it is very difficult to determine the initial distribution of VOCs within the material without using special equipments, such as those used by Cox et al. (2002). Even though, the initial distribution obtained was in a rough and discrete form due to the constraints of the technique. Moreover, the experimental method was destructive to the test material and might only be applicable to those homogenous materials like vinyl flooring. When dealing with porous materials, the method would probably fail because of possible loss of VOCs during the period of sample preparation. Xu and Zhang (2004) studied the effects of the initial distribution of VOCs on emission rate by varying the distributions under the condition that the initial amount of VOCs was the same. They found that only for long-term predictions and thin materials with a relatively large diffusion coefficient can the effects of the initial distribution of VOCs on the

emission characteristics be neglected. However, in practice, they were still unable to consider such effects utilizing their model, because, as mentioned before, no information on the distribution of the initial VOCs is readily available. Kumar et al. (2001) assumed that the initial concentration of VOCs was the highest at the bottom of the material and the lowest at the surface. They considered two scenarios: linear decay and exponential decay. However, these assumptions are somewhat too arbitrary and subjective. In order to precisely catch the emission characteristics, methods of finding the initial distribution of VOCs within the material must be developed.

The use of inverse analysis to estimate surface conditions such as temperature and heat flux (Lee and Yang, 2003); to determine temperature-dependent thermophysical properties (Dantas and Orlande, 1996) such as the thermal conductivity and heat capacity of solids; and to estimate initial conditions such as initial temperature profiles (Alifanov, 1994; Ozisik and Orlande, 2000) by utilizing the transient temperature measurements taken within the medium, has numerous practical applications. Since the governing equations of the mass diffusion of VOCs in building material are so similar to those of heat conduction, it is logical to introduce the inverse method to solve various mass diffusion problems.

The major purpose of this study is to develop an inverse method to estimate the initial distribution of VOCs within building material by utilizing transient measurements of VOCs concentration in environmental chamber air. It will be especially useful when modeling the emission of VOCs from building materials under real situations, e.g., in a room. One can cut a small piece of material to conduct a chamber test (if this is not allowable then just simply use the non-destructive in-situ test instrument - FLEC) and perform an inverse analysis. Information on the initial

distribution of VOCs within the material would then be known. With this actual initial information, emissions of VOCs from the materials in the room can be precisely simulated.

The conjugate method of minimization with the adjoint problem (Ozisik and Orlande, 2000) is useful for solving problems of function estimation when no a priori information is available on the functional form. In the present study, this method is developed and used to inversely estimate the initial distribution of VOCs within building material. The basic steps in this method include: the direct problem; the inverse problem; the sensitivity problem; the adjoint problem; the gradient equation, and the algorithm of the solution. Details of the major steps, as applied to the estimation of the unknown initial distribution of VOCs within building material, are described below.

5.2 Development of the Inverse Method

5.2.1 Direct Problem

5.2.1.1 Development of the Direct Problem

Again, we assume that test material is placed in an environmental chamber or an emission cell. This time the test material is an unconditioned one (i.e. the test specimen is not pretreated) and thus the initial VOCs distribution within the material is very likely to be nonuniform. The D_m and K_{ma} of VOCs/material are assumed to be known, or can be determined using the method described in the previous chapter. The test rig is somewhat similar to Figure 4.1 in Chapter 4, and thus is not shown here.

The direct problem of interest here is straightforward based on the knowledge introduced in section 4.2.1. The only difference is the initial condition in the material. The system of equations is given as follows:

$$\begin{cases} \dfrac{\partial C_m(x,t)}{\partial t} = D_m \dfrac{\partial^2 C_m(x,t)}{\partial x^2} \\ \dfrac{\partial C_m(x,t)}{\partial x}\Big|_{x=0} = 0 \\ -D_m \dfrac{\partial C_m(x,t)}{\partial x}\Big|_{x=b} = h_m \left[C_m(x,t)\big|_{x=b} / K_{ma} - C_a(t) \right] \\ C_m(x,t)\big|_{t=0} = f(x) \\ \dfrac{\partial C_a(t)}{\partial t} = -LD_m \dfrac{\partial C_m(x,t)}{\partial x}\Big|_{x=b} - NC_a(t) \\ C_a(t)\big|_{t=0} = 0 \end{cases} \tag{5.1}$$

5.2.1.2 Impacts of Initial VOCs Distributions on Emission Characteristics

The effects of initial VOCs distribution on emission behaviors can be evidenced by varying $C_m(x,t)\big|_{t=0} = f(x)$ while keeping other conditions unchanged. Here the illustrative example used in section 4.2.3 is again utilized. All other conditions are just the same (i.e., the dimensions of the particle board are 0.212×0.212×0.0159 m^3, the dimensions of the chamber are 0.5×0.4×0.25 m^3, the chamber is kept at a temperature of 23±0.5 ^{0}C and RH of 50±0.5%, with an air change rate of 1.0±0.05 h^{-1}, the mean convective mass transfer coefficient is assumed to be 3×10^{-4} m s^{-1}, the diffusion and partition coefficients of the VOCs in the particle board are 7.65×10^{-11} m^2 s^{-1} and 3289, respectively), except that the initial condition in the material is changed for the purpose of this study.

The initial amount of VOCs m_0 in the material is assumed to be 0.0572 g, however, the initial VOCs distribution in the material is varied in order to investigate its effect on the emission characteristics. Six different types of initial VOCs distribution

functional forms are listed in Table 5.1 and the corresponding initial in-material concentration profiles are plotted in Figure 5.1.

Table 5.1 Six different types of initial VOCs concentration distributions

Case	Name	Functional form
1	Cosine curve	$f(x) = 40\cos(2\pi x/b) + 80 \quad 0 \le x \le b$
2	Sine curve	$f(x) = 40\sin(2\pi x/b) + 80 \quad 0 \le x \le b$
3	Linear increase	$f(x) = 40 + 80x/b \quad 0 \le x \le b$
4	Linear decay	$f(x) = 120 - 80x/b \quad 0 \le x \le b$
5	Triangular	$f(x) = \begin{cases} 40 + 160x/b & 0 \le x \le b/2 \\ 200 - 160x/b & b/2 < x \le b \end{cases}$
6	Uniform	$f(x) = 80 \quad 0 \le x \le b$

Where, x is the axial coordinates (m), in the range 0~b, the unit of $f(x)$ is g m^{-3}.

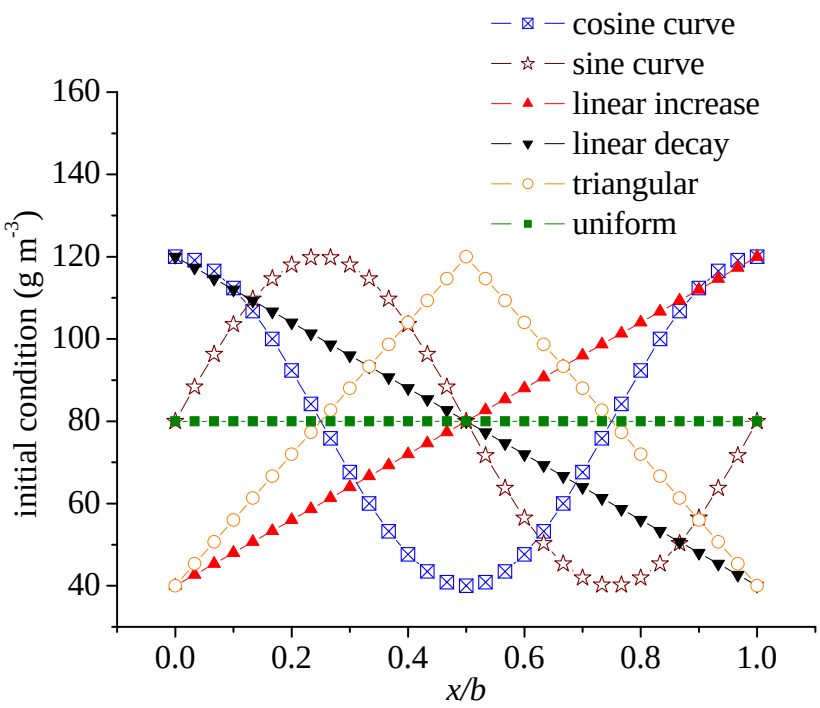

Figure 5.1 Different types of initial VOCs distribution (m_0=0.0572 g)

Finite differencing, with space increment $\Delta x = b/30$, time increment Δt=0.1 hour, final time t_f =300 hours, the direct problem is solved with the given test conditions and

material properties, as well as the six different initial conditions in Table 5.1. Results are shown in Figure 5.2. It is clear that the initial VOCs distribution in material greatly affects the emission characteristics for short-term predictions, say less than 100 hours in this study. While for long-term predictions, if the initial amount of VOCs containing in the material is same, the VOCs concentration in chamber air will not vary much regardless of different initial VOCs distributions. The effects are expected to be more significant for thicker materials with smaller diffusion coefficients.

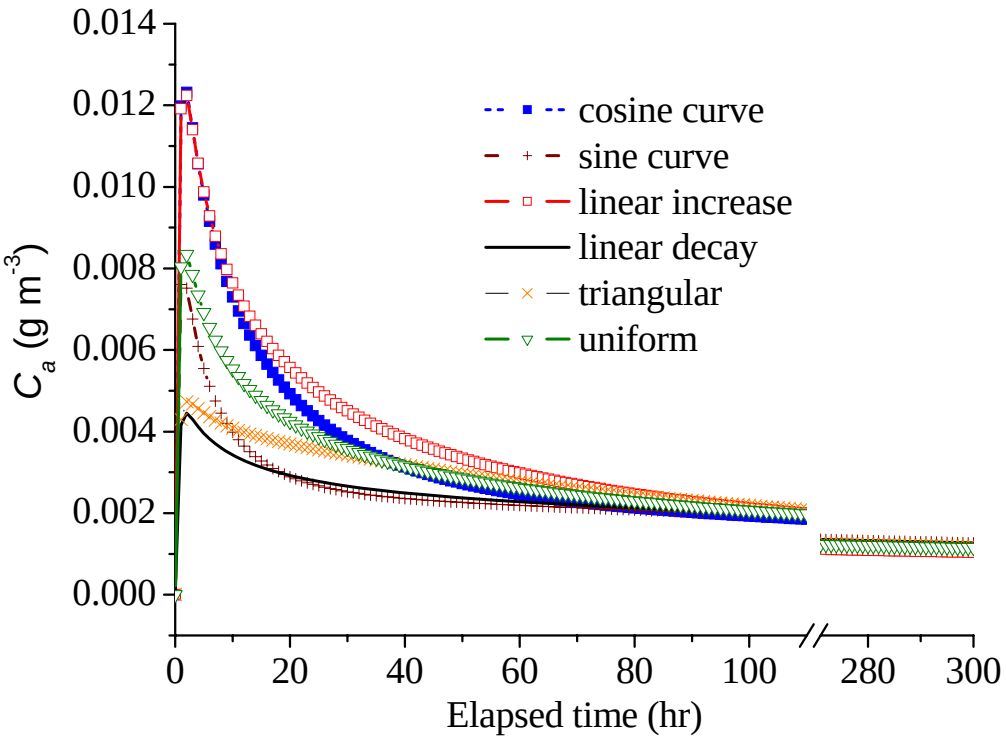

Figure 5.2 Effects of different initial VOCs distributions on emission characteristics (m_0=0.0572 g)

5.2.2 Inverse Problem

Since the initial VOCs concentration distribution does have substantial effects on material emission behaviors, it is worthwhile to develop a method to figure it out, namely the inverse function estimation method. In the inverse problem, the initial

condition $C_m(x,t)\big|_{t=0} = f(x)$ is regarded as unknown, but everything else in the equation (5.1) is known and, in addition, the measurements of the VOCs concentration in the chamber are available. It should be noted that the solution of inverse problem is generally unstable. Therefore, small perturbations in the input data, such as measurement errors inherent to the measurements used in the analysis, can cause large oscillations in the solution (Chiwiacowsky and Velho, 2003). However, the conjugate gradient method with the adjoint problem is an iterative method, in which the regularization is implicitly built in the computational procedure. With a suitable stopping criterion stable solutions can be obtained.

The solution of the present inverse mass diffusion problem involves minimizing the following functional:

$$S[f(x)] = \sum_{i=1}^{I} \left[Y_{mea}(\tau_i) - C_{a,est}(\tau_i; f(x)) \right]^2 \tag{5.2}$$

where τ_i, I, $Y_{mea}(\tau_i)$, and $C_{a,est}(\tau_i; f(x))$ are the sampling time, total number of measurements, and measured and estimated concentrations of VOCs, respectively. For the sake of convenience in the subsequent analysis, the ordinary least squares norm, equation (5.2), can be rewritten as

$$S\left[f(x)\right] = \int_{t=0}^{t_f} \sum_{i=1}^{I} \left[Y_{mea}(t) - C_{a,est}(t) \right]^2 \delta(t-\tau_i)dt \tag{5.3}$$

where t_f is the duration of the experiment and $\delta(\cdot)$ is the Dirac delta function.

In order to apply the conjugate gradient method to minimize the functional (5.3), two auxiliary problems, called the sensitivity and adjoint problems, need to be developed.

5.2.3 Sensitivity Problem

This problem is developed by assuming that when the initial condition $f(x)$ perturbed by $\Delta f(x)$, the VOCs concentration in chamber $C_a(t)$ is perturbed by an amount $\Delta Ca(t)$ and VOCs concentration in the material $C_m(x,t)$ is perturbed by $\Delta C_m(x,t)$. In order to obtain the sensitivity problem, we replace $C_m(x,t)$ by $[C_m(x,t)+\Delta C_m(x,t)]$, $C_a(t)$ by $[C_a(t)+\Delta C_a(t)]$ and $f(x)$ by $[f(x)+\Delta f(x)]$ in the direct problem equation (5.1) and subtract from it the original problem (5.1) (Ozisik, 1993; Ozisik and Orlande, 2000).

The following problem results for the sensitivity problem:

$$\begin{cases} \dfrac{\partial \Delta C_m(x,t)}{\partial t} = D_m \dfrac{\partial^2 \Delta C_m(x,t)}{\partial x^2} \quad \text{in } 0 < x < b;\ \text{for } t > 0 \\ \dfrac{\partial \Delta C_m(x,t)}{\partial x} = 0 \quad \text{at } x = 0;\ \text{for } t > 0 \\ -D_m \dfrac{\partial \Delta C_m(x,t)}{\partial x} = h_m \left[\dfrac{\Delta C_m(x,t)}{K_{ma}} - \Delta C_a(t) \right] \quad \text{at } x = b;\ \text{for } t > 0 \\ \Delta C_m(x,t) = \Delta f(x) \quad \text{for } t = 0;\ \text{in } 0 \le x \le b \\ \dfrac{\partial \Delta C_a(t)}{\partial t} = -LD_m \dfrac{\partial \Delta C(x,t)}{\partial x} - N \Delta C_a(t) \quad \text{at } x = b;\ \text{for } t > 0 \\ \Delta C_a(t) = 0 \quad \text{for } t = 0 \end{cases} \tag{5.4}$$

5.2.4 Adjoint Problem

In the present inverse problem, since the VOCs concentrations in chamber are coupled with the concentrations in material, hence, two constraints need to be satisfied, which are the solutions of the first and fifth equations in the direct problem. Therefore, two Lagrange multipliers (Ozisik, 1993; Alifanov, 1994; Colaco and Orlande, 1999; Woodbury, 2003) come into picture here. To develop the adjoint problem, the first equation in direct problem is multiplied by the Lagrange multiplier $\lambda(x,t)$ and the resulting expression is integrated over the time and space domains.

While the fifth equation in direct problem is multiplied by the Lagrange multiplier $\lambda_a(t)$ and the resulting expression is integrated over the time domain. Then the results are added to the right-hand side of equation (5.3) to yield the following expression for the functional $S[f(x)]$ (Ozisik and Orlande, 2000):

$$
\begin{aligned}
S[f(x)] = & \int_{t=0}^{t_f} \sum_{i=1}^{I} \left[Y_{mea}(t) - C_{a,est}(t) \right]^2 \delta(t-\tau_i) dt \\
& + \int_{t=0}^{t_f} \int_{x=0}^{b} \lambda(x,t) \left[\frac{\partial C_m(x,t)}{\partial t} - D_m \frac{\partial^2 C_m(x,t)}{\partial x^2} \right] dx dt \\
& + \int_{t=0}^{t_f} \lambda_a(t) \left[\frac{\partial C_a(t)}{\partial t} + N C_a(t) + L D_m \frac{\partial C_m(x,t)}{\partial x} \Big|_{x=b} \right] dt
\end{aligned}
\tag{5.5}
$$

The variation $\Delta S[f(x)]$ is obtained by perturbing $C_m(x,t)$ by $\Delta C_m(x,t)$, $C_a(t)$ and $C_{a,est}(t)$ by $\Delta C_a(t)$ in equation (5.5), subtracting from the resulting expression the original equation (5.5) and neglecting second-order terms. We obtain:

$$
\begin{aligned}
\Delta S[f(x)] = & \int_{t=0}^{t_f} \sum_{i=1}^{I} 2 \left[C_{a,est}(t) - Y_{mea}(t) \right] \Delta C_a(t) \delta(t-\tau_i) dt \\
& + \int_{t=0}^{t_f} \int_{x=0}^{b} \lambda(x,t) \left[\frac{\partial \Delta C_m(x,t)}{\partial t} - D_m \frac{\partial^2 C_m(x,t)}{\partial x^2} \right] dx dt \\
& + \int_{t=0}^{t_f} \lambda_a(t) \left[\frac{\partial \Delta C_a(t)}{\partial t} + N \Delta C_a(t) + L D_m \frac{\partial \Delta C_m(x,t)}{\partial x} \Big|_{x=b} \right] dt
\end{aligned}
\tag{5.6}
$$

In equation (5.6), the last two integral terms are integrated by parts; the initial and boundary conditions given by the second, third, fourth and sixth equations in the sensitivity problem equation (5.4) are utilized and then let the terms containing $\Delta C_m(x,t)$ and $\Delta C_a(t)$ go to zero (Ozisik, 1993; Alifanov, 1994; Colaco and Orlande, 1999; Woodbury, 2003). The vanishing of the integrands containing $\Delta C_m(x,t)$ and $\Delta C_a(t)$ leads to the following adjoint problem for the determination of the Lagrange multipliers $\lambda(x,t)$ and $\lambda_a(t)$:

$$
\begin{cases}
\dfrac{\partial \lambda(x,t)}{\partial t} + D\dfrac{\partial^2 \lambda(x,t)}{\partial x^2} = 0 \quad \text{in } 0 < x < b;\ \text{for } 0 < t < t_f \\
\dfrac{\partial \lambda(x,t)}{\partial x} = 0 \quad \text{at } x = 0;\ \text{for } 0 < t < t_f \\
-D_m \dfrac{\partial \lambda(x,t)}{\partial x} = \dfrac{h_m}{K_{ma}}[\lambda(x,t) - L\lambda_a(t)] \quad \text{at } x = b;\ \text{for } 0 < t < t_f \\
\lambda(x,t) = 0 \quad \text{for } t = t_f;\ \text{in } 0 \le x \le b \\
\dfrac{\partial \lambda_a(t)}{\partial t} = \left(N + Lh_m\right)\lambda_a(t) - h_m \lambda(x,t) \\
\qquad\qquad + 2\displaystyle\sum_{i=1}^{I}[C_a(t) - Y_{mea}(t)]\delta(t - \tau_i) \quad \text{at } x = b;\ \text{for } 0 < t < t_f \\
\lambda_a(t) = 0 \quad \text{for } t = t_f
\end{cases}
\tag{5.7}
$$

5.2.5 Gradient Equation

In the process of obtaining the adjoint problem, the following integral term is left:

$$
\Delta S[f(x)] = -\int_{x=0}^{b} \lambda(x, t=0)\Delta f(x)dx \tag{5.8}
$$

By using the assumption that $f(x)$ belongs to the Hilbert space of square integrable functions (Colaco and Orlande, 1999; Ozisik and Orlande, 2000) in the domain $0 < x < b$, we can write:

$$
\Delta S[f(x)] = \int_{x=0}^{b} \nabla S[f(x)]\Delta f(x)dx \tag{5.9}
$$

Comparing equations (5.8) and (5.9), it is easy to obtain the gradient equation for the functional as:

$$
\nabla S[f(x)] = -\lambda(x, t=0) \tag{5.10}
$$

5.2.6 Iterative Procedures

The computational procedure is summarized in the following algorithm:

Step 1: Choose an initial guess $f^0(x)$, e.g. $f^0(x) = 0$.

Step 2: Solve the direct problem given by equation (5.1) to obtain the estimated VOCs concentration $C_a(\tau_i)$.

Step 3: Solve the adjoint problem defined by equation (5.7) to obtain the Lagrange multiplier $\lambda(x,t)$. Then compute the gradient of the functional $\nabla S\left[f^k(x)\right]$ from equation (5.10).

Step 4: Compute the conjugate coefficient:

$$\gamma^k = \frac{\sum_{i=1}^{I}\left\{\nabla S\left[f^k(x)\right]\right\}^2}{\sum_{i=1}^{I}\left\{\nabla S\left[f^{k-1}(x)\right]\right\}^2} \tag{5.11}$$

Step 5: Calculate the direction of descent:

$$d^k(x) = \nabla S\left[f(x)\right] + \gamma^k d^{k-1}(x) \tag{5.12}$$

Step 6: Set $\Delta f(x) = d^k(x)$, then solve the sensitivity problem given by equation (5.4) to obtain $\Delta C_a(\tau_i)$.

Step 7: Compute the search step size

$$\beta^k = \frac{\sum_{i=1}^{I}\left[C_{a,est}(\tau_i; f(x)) - Y_{mea}(\tau_i)\right]\Delta C_a(\tau_i; d^k(x))}{\sum_{i=1}^{I}\left[\Delta C_a(\tau_i; d^k)\right]^2} \tag{5.13}$$

Step 8: Update the initial guess

$$f^{k+1}(x) = f^k(x) - \beta^k d^k \tag{5.14}$$

Step 9: Repeat the iteration until stopping criterion based on discrepancy principle is met (Ozisik and Orlande, 2000).

5.2.7 Solution of the Direct, Sensitivity and Adjoint Problems

The direct, sensitivity, and adjoint problems described by equations (5.1), (5.4) and (5.7), respectively, are so similar except that in the adjoint problem, the conditions (the fourth and sixth equations in adjoint problem) are the values of the functions $\lambda(x,t)$ and $\lambda_a(t)$ at the final time t_f. In the conventional initial value problem, the value of the function is specified at time $t=0$. However, the final value adjoint problem (5.7) can be transformed to an initial value problem by defining a new time variable given by $\zeta = t_f - t$. The direct, sensitivity and adjoint problems can then be easily solved by using the fully implicit finite difference method.

5.3 Application of the Inverse Function Estimation Approach

Since the initial distribution of VOCs is very important to the accuracy of the predictions of the source/sink models, it would be gratifying if the present inverse method is proven effective.

In order to validate this method, simulated measurements are used instead of real test data. This is because, with the use of simulated measurements as the input data for the inverse analysis, the solutions of the function estimation can be compared with the pre-defined functional forms (which, however, are unavailable when using real test data) to see how well the initial distributions of VOCs are recovered.

We are now trying to recover the six different types of initial distributions of VOCs defined in subsection 5.2.1.2 using the proposed inverse algorithm. Errorless simulated measurements $\mathbf{Y}_{\mathbf{exa}}$ are generated by solving the direct problem with the known initial conditions listed in Table 5.1. Measurements containing measurement errors are generated by adding an error term to $\mathbf{Y}_{\mathbf{exa}}$, i.e. $\mathbf{Y} = \mathbf{Y}_{\mathbf{exa}} + \boldsymbol{\omega}\sigma$, where σ is

the standard deviation of the measurement errors, and $\boldsymbol{\omega}$ is the random variable with a normal distribution, zero mean, and unitary standard deviation. For normally distributed random numbers with a 99% confidence level, the value of $\boldsymbol{\omega}$ lies in the range -2.576< $\boldsymbol{\omega}$ <2.576 (Ozisik and Orlande, 2000). For the sake of simplicity, we do not lose any generality by generating equally spaced measurements with a time interval of 1 hour. The initial guess for each case is always set to be $f^0(x) = 0$.

The results obtained through inverse analyses are presented in Figure 5.3 - Figure 5.8. In Figure 5.3 - Figure 5.8, it can be noticed that good agreements between the exact and estimated values are achieved, even for case 5, which shows a function exhibiting a sharp corner, which is generally difficult to be recovered by inverse analysis. The present inverse method has proven to be most effective. However, it should be noted that measurements containing large errors might lead to inaccurate results because as mentioned before, inverse problems are generally ill-conditioned.

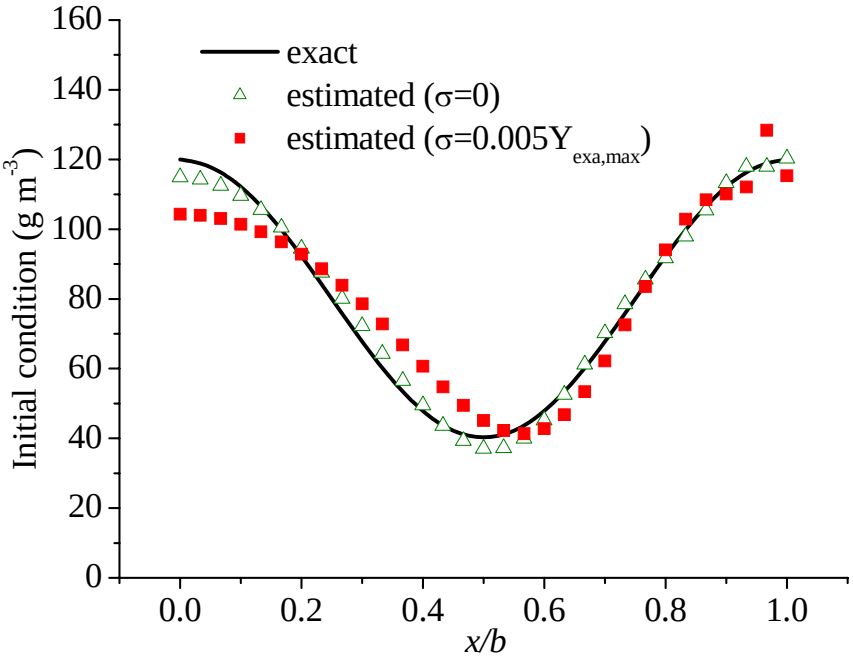

Figure 5.3 Recovered initial condition for case 1 (cosine curve)

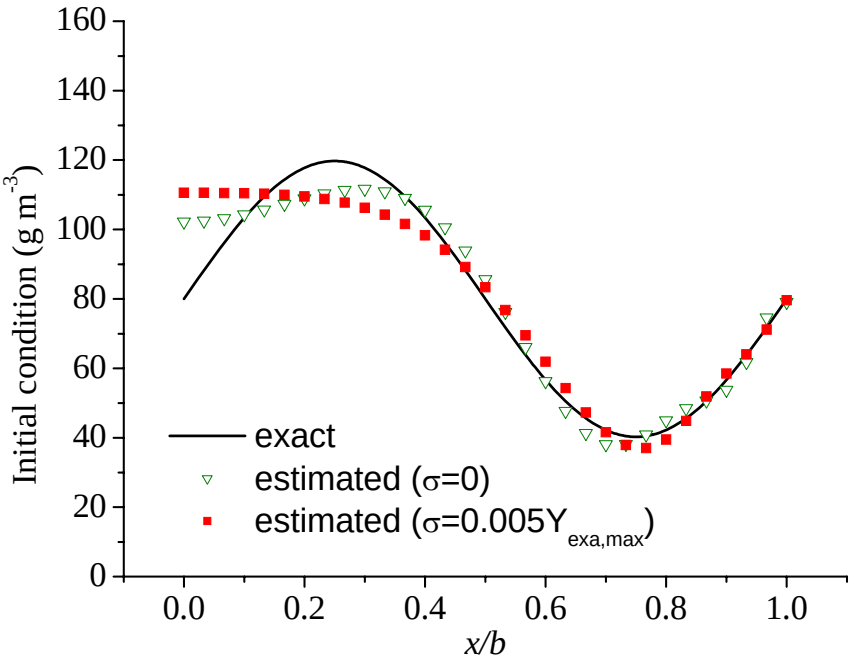

Figure 5.4 Recovered initial condition for case 2 (sine curve)

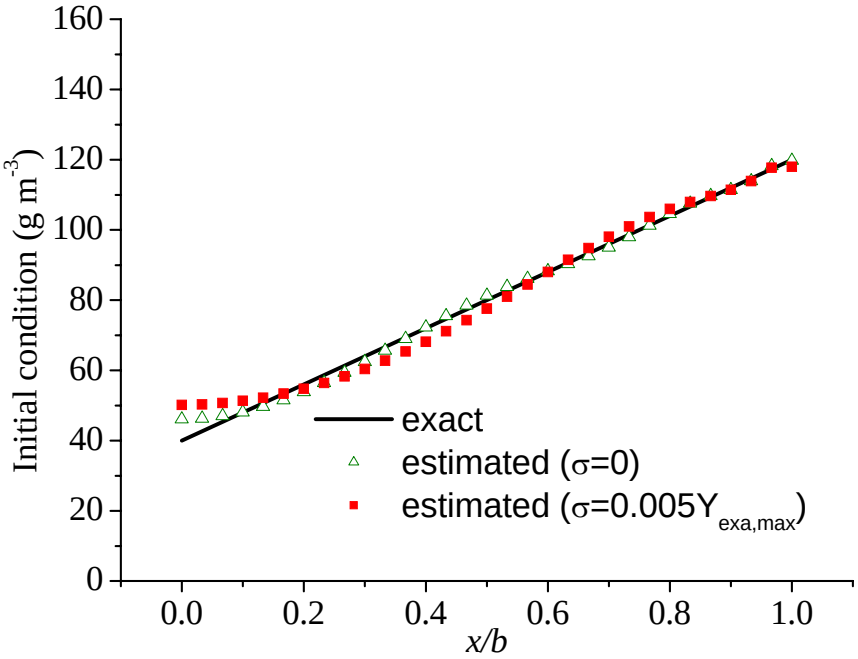

Figure 5.5 Recovered initial condition for case 3 (linear increase)

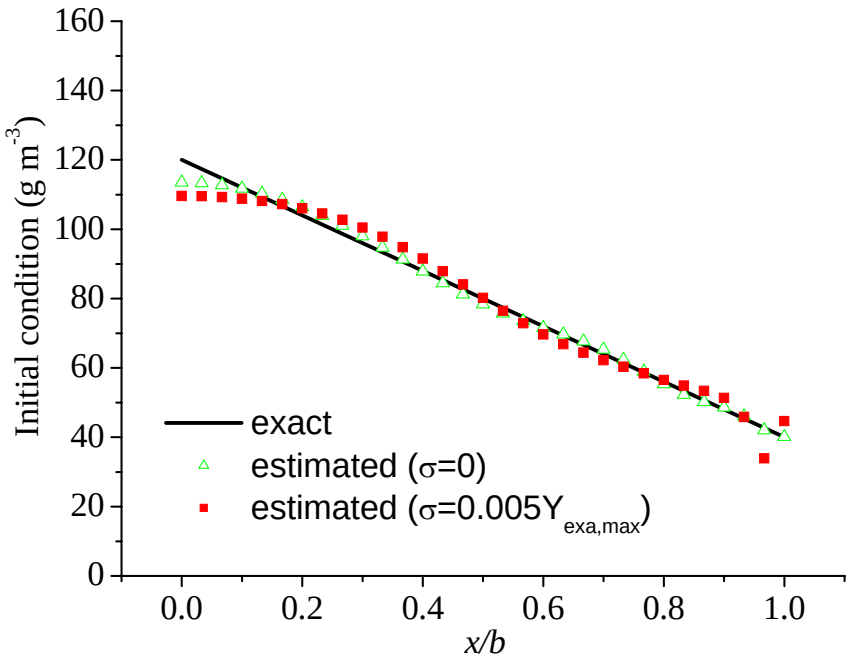

Figure 5.6 Recovered initial condition for case 4 (linear decay)

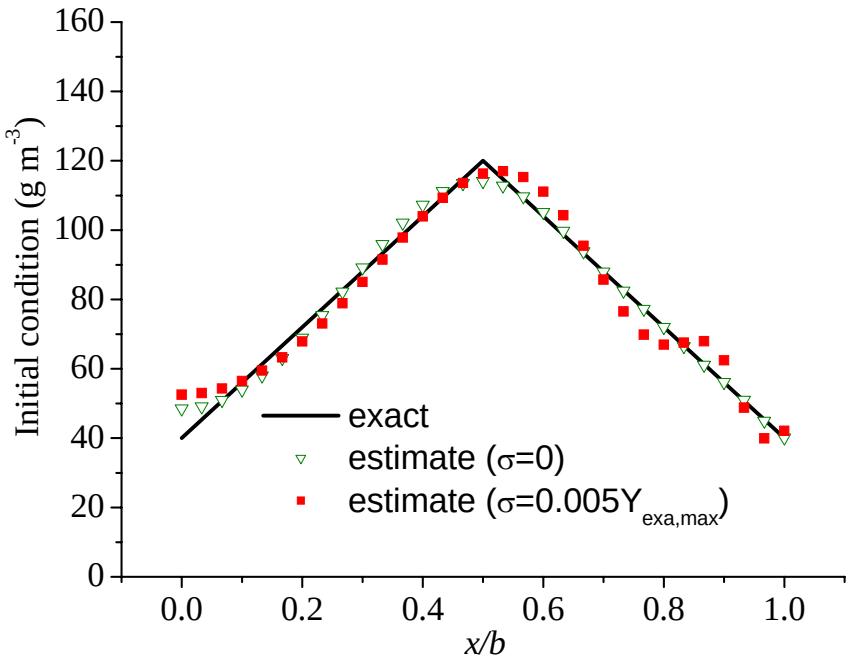

Figure 5.7 Recovered initial condition for case 5 (triangular ramp)

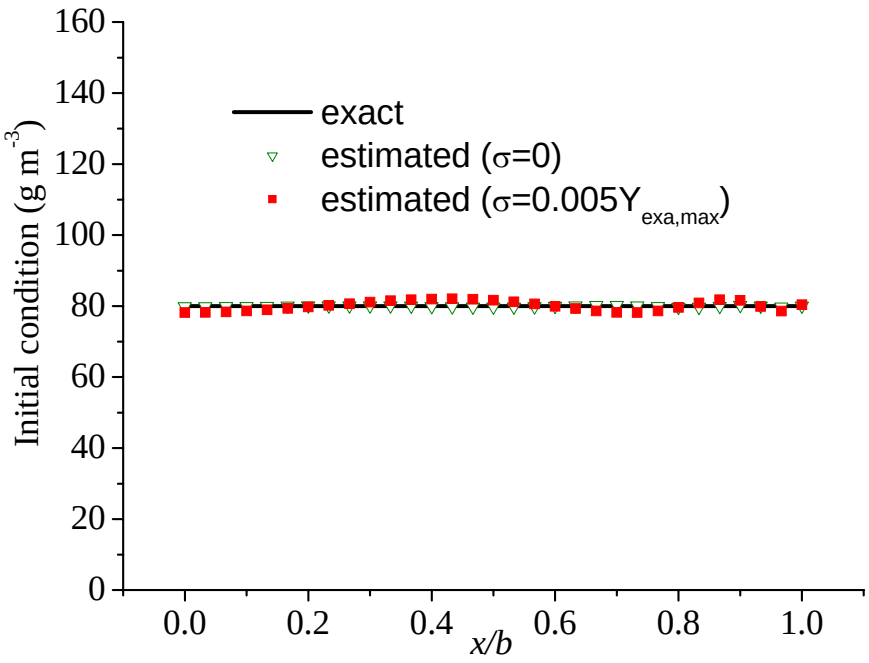

Figure 5.8 Recovered initial condition for case 6 (uniform distribution)

Noticeable deviations between the exact and recovered distributions near the bottom (x=0) of the material can be found in Figure 5.3 - Figure 5.8. This is because data on the concentration of VOCs in the chamber air are less sensitive to the initial VOCs conditions in the deep of the material (especially for thick materials). It is easy to see, both physically and mathematically, why this is the case. The closer the sensor is to the active surface, the greater will be the sensor's response (output) to a change in the surface conditions (input) (Woodbury, 2003). The sampling tube and ATD-GC-MS system can be alternatively regarded as the sensor in our cases. Obviously, the 'sensor' is closer to the upper surface of the test material. Improving the experimental design may help to solve this problem. The two-chamber or two-FLEC method, which uses two identical chambers with the material specimen placed between them, can be used. Both chambers are supplied with clean air and the concentrations of VOCs in individual chambers are monitored. Thus, more information on the initial condition near the bottom of the material will be collected

by measuring the concentration data in the additional chamber, and, consequently, be recovered by inverse analysis. It is certain that the accuracy of the inverse estimation will be improved through the use of the two-chamber method, although the forward and inverse problems will become somewhat more complicated.

Another important issue may be how much time is required to accurately identify the initial distribution of VOCs within the material. Although it depends on the properties of the VOC/material combination (e.g., b, D_m, and K_{ma}), as well as on test conditions, a method called sensitivity analysis introduced by Bendada and Nguyen (1999) can be used to approximately choose t_f for a specific case. The main procedures are: first, suppose an initial VOCs profile. Let this profile be approximated by piecewise constant VOCs concentrations. Then, calculate the relative sensitivity coefficients with respect to individual piecewise constants and find the value of t_c which is defined as follows: beyond t_c, the relative sensitivity coefficients become linearly dependent or extremely small. Finally, the test duration are determined to be no shorter than t_c, because measurements taken within 0~ t_c are pivotal to the accurate identification of the initial distribution of VOCs. In this study, a sensitivity analysis shows that t_c is around 150 h for the particular VOC/material combination used here.

5.4 Summary

A study of a certain building material based on the condition that it initially contains the same amount of VOCs for each type of initial distribution of VOCs reveals that for short-term predictions the effect of different types of initial distributions of VOCs on the concentration in the chamber air cannot be neglected, while for long-term predictions the effects are negligible.

If the effects cannot be neglected, say, for short-term predictions, it is natural that the initial distribution must be known. But the fact is that this information is hardly available. The present conjugate method with the adjoint problem for estimating the initial distribution of VOCs in dry building material fills this gap. Different types of initial distributions of VOCs with no a priori information on the functional form can be recovered using the present inverse method. This inverse technique has proven to be highly effective and is non-destructive to test materials in conjunction with FLEC cells and is believed to be applicable to all types of dry building materials.

There is much work to be done. Future research work should concentrate on such matters as developing an inverse technique for the two-chamber or two-FLEC test method to improve the accuracy of estimating and investigating the initial distribution of VOCs within some typical building materials at various real applications in buildings to aid in simulating VOCs emissions from these materials.

Chapter 6
Numerical Simulation of VOCs Emissions from a Multi-layer Porous/non-porous Building Material Assembly

6.1 Introduction

Building materials usually appear in the composite forms, such as floor assembly, wall assembly and ceiling assembly. Previous models can only handle single layer situations. Until recently, the double-layer analytical model (Kumar and Little, 2003a) and multi-layer model (Haghighat and Huang, 2003; Zhang and Niu, 2004) have been developed. It is known that almost all of the building materials are porous. However, all of the existing multi-layer models belong to the so called continuum models, i.e. one-phase models, which treat both non-porous and porous materials as homogenous mediums. In fact, porous materials are usually void and solid overlapping mediums and both gas phase and adsorbed phase VOCs existing within them. Obviously, this is an oversimplified assumption because mass transport within porous materials is far more complicated than within non-porous materials. The continuum models may be correct for non-porous or microporous building materials. For mesoporous or macroporous materials, multi-phase models may be better candidates.

In the existing multi-layer models, oversimplification of the ventilation system has been made by assuming a constant air change rate, e.g. 1 h^{-1}, which is not the case in reality, even for natural ventilation, the air change rate is different for the situations of opening/closing doors/windows. Practically, for mechanically ventilated rooms, for the sake of energy saving, HVAC systems are normally operated during working hours and shut off during off-work hours. In addition, the supply air of the

ventilation system usually comprises an airflow rate Q_{OA} of outdoor air, plus a recirculation airflow rate Q_R of air removed from the room.

A generally applicable IAQ model must take these aspects into consideration.

6.2 Model Development

A schematic representation of a single-zone room is shown in Figure 6.1. Unlike in the existing models, in the proposed model the supply air is the resultant of mixing the outdoor air with a portion of the return air. An in-duct filter is installed to prevent VOCs containing in the re-circulated air from re-entering into the room. The model also considers the effect of air infiltration/exfiltration, the infiltration rate can be predicted based on building leakage information and the measured indoor/outdoor temperature difference and wind speed, for simplicity, in this research the infiltration rate is assumed to be equal to the exfiltration rate and is always constant.

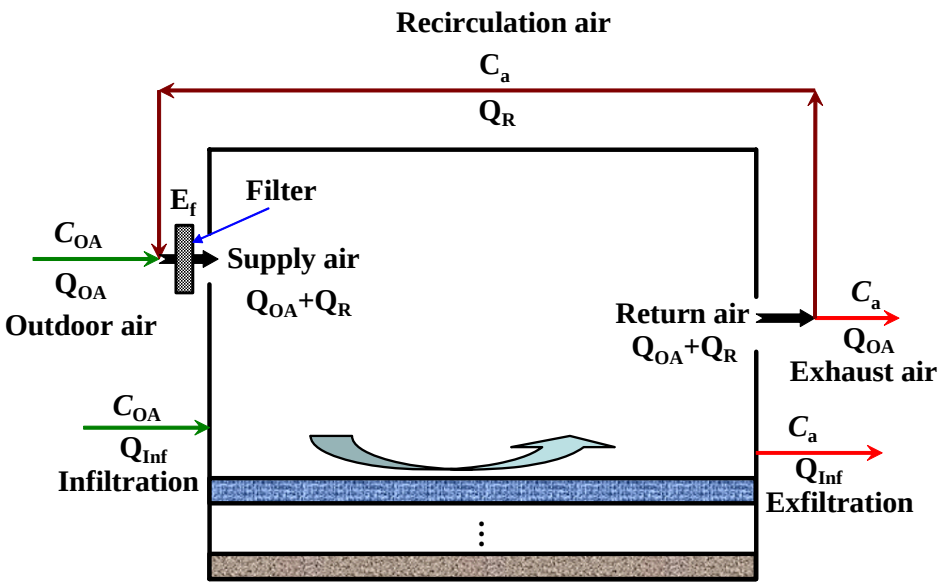

Figure 6.1 Schematic representation of a building material assembly in a well-mixed room

The building materials composing the multi-layer structure can be either non-porous materials or porous materials or a combination of them, as shown in Figure 6.2. The number of the layers of the assembly is *n*. The chamber air passes through the surface of the top layer.

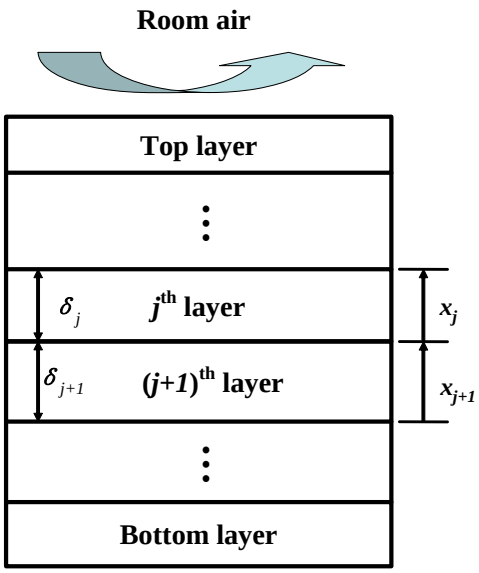

Figure 6.2 Schematic drawing of a multi-layer building material assembly

6.2.1 VOCs Diffusion within the Building Materials

(a) For non-porous layers:

Fick's second law is often used to describe the material phase diffusion within the material. The transient material-phase VOCs diffusion can be described by a one-dimensional diffusion equation (Crank, 1975; Little et al., 1994):

$$\frac{\partial C_{m,j}}{\partial t} = D_{m,j} \cdot \frac{\partial}{\partial x_j}\left(\frac{\partial C_{m,j}}{\partial x_j}\right) \tag{6.1}$$

where the subscript *j* means the jth layer; *t* is time; *x* is the distance from the bottom to the top of individual layers; C_m is the material phase VOCs concentration and D_m is the material phase diffusion coefficient.

(b) For porous layers:

By assuming surface and adsorbed phase diffusion are both negligibly small; the adsorbed phase concentration remains in linear equilibrium with the porous gas phase concentration (i.e., $C_{ad} = K_s \cdot C_g$), the gas phase VOCs diffusion equation becomes (Tiffonnet et al., 2002; Lee, 2003; Lee et al., 2005):

$$\frac{\partial C_{g,j}}{\partial t} = \frac{D_{e,j}}{\varepsilon_j + K_{s,j}} \cdot \frac{\partial}{\partial x_j}\left(\frac{\partial C_{g,j}}{\partial x_j}\right) \tag{6.2}$$

where D_e (m^2 s^{-1}) is the effective diffusion coefficient of porous materials; ε (m^3 air/m^3 material) is the porosity; K_s (m^3 air/m^3 material) is the interior sorption property.

6.2.2 Boundary Conditions

Several assumptions are made here: (i) for non-porous materials, at the material surface, the material-phase VOCs concentration at the material side is always in equilibrium with the gas phase VOCs concentration at the air side; (ii) for porous materials, the gas phase VOCs concentration is continuous at the material surface; (iii) there is no loss of mass at the layer/layer interfaces.

(1) Boundary conditions at the interfaces of jth and $(j+1)^{th}$ layers (j=1, …, n-1)

There are four possibilities to be considered:

(a) Both of the two adjacent j^{th} and $(j+1)^{th}$ layers are non-porous materials:

$$C_{m,j}\Big|_{x_j=0} = \left(K_{ma,j} / K_{ma,j+1}\right) \cdot C_{m,j+1}\Big|_{x_{j+1}=\delta_{j+1}} \tag{6.3}$$

$$-D_{m,j}\frac{\partial C_{m,j}}{\partial x_j}\Big|_{x_j=0} = -D_{m,j+1}\frac{\partial C_{m,j+1}}{\partial x_{j+1}}\Big|_{x_{j+1}=\delta_{j+1}} \tag{6.4}$$

where K_{ma} is the surface partition coefficient of non-porous materials; δ is the thickness of the material layer.

(b) Both of the two adjacent j^{th} and $(j+1)^{th}$ layers are porous materials:

$$C_{g,j}\Big|_{x_j=0} = C_{g,j+1}\Big|_{x_{j+1}=\delta_{j+1}} \tag{6.5}$$

$$-D_{e,j}\frac{\partial C_{g,j}}{\partial x_j}\Big|_{x_j=0} = -D_{e,j+1}\frac{\partial C_{g,j+1}}{\partial x_{j+1}}\Big|_{x_{j+1}=\delta_{j+1}} \tag{6.6}$$

(c) The jth layer is non-porous material and the $(j+1)^{th}$ layer is porous material:

$$C_{m,j}\Big|_{x_j=0} = K_{ma,j}\cdot C_{g,j+1}\Big|_{x_{j+1}=\delta_{j+1}} \tag{6.7}$$

$$-D_{m,j}\frac{\partial C_{m,j}}{\partial x_j}\Big|_{x_j=0} = -D_{e,j+1}\frac{\partial C_{g,j+1}}{\partial x_{j+1}}\Big|_{x_{j+1}=\delta_{j+1}} \tag{6.8}$$

(d) The jth layer is porous material and the $(j+1)^{th}$ layer is non-porous material:

$$C_{m,j+1}\Big|_{x_{j+1}=0} = K_{ma,j+1}\cdot C_{g,j}\Big|_{x_j=\delta_j} \tag{6.9}$$

$$-D_{e,j}\frac{\partial C_{g,j}}{\partial x_j}\Big|_{x_j=0} = -D_{m,j+1}\frac{\partial C_{m,j+1}}{\partial x_{j+1}}\Big|_{x_{j+1}=\delta_{j+1}} \tag{6.10}$$

(2) Boundary conditions at the surface of the top layer (two possibilities):

(a) If the top layer is non-porous material:

$$C_{m,1} = K_{ma,1}C_{as,1} \tag{6.11}$$

$$R = -D_{m,1}\frac{\partial C_{m,1}}{\partial x_1} = h_m(t)\cdot(C_{as,1} - C_a(t)) \tag{6.12}$$

(b) If the top layer is porous material:

$$C_{g,1} = C_{as,1} \tag{6.13}$$

$$R = -D_{e,1}\frac{\partial C_{g,1}}{\partial x_1} = h_m(t)\cdot(C_{as,1} - C_a(t)) \tag{6.14}$$

where C_{as} kg m^{-3} is the gas-phase VOCs concentration in the boundary layer, and R kg m^{-2} s^{-1} is the VOCs emission rate between the surface of the top layer and room air; $h_m(t)$ m s^{-1} is the transient convective mass transfer coefficient, which can be estimated by using an well validated empirical formula (Axley, 1991).

(3) Boundary conditions at the bottom of the last layer (two possibilities):

VOCs mass insulation is assumed at the bottom of the last layer.

(a) If the bottom layer is non-porous material:

$$-D_{m,n}\frac{\partial C_{m,n}}{\partial x_n} = 0 \tag{6.15}$$

(b) If the bottom layer is porous material:

$$-D_{e,n}\frac{\partial C_{g,n}}{\partial x_n} = 0 \tag{6.16}$$

(4) Boundary conditions at the air inlet:

$$C_{OA}(t) = f_{OA}(t) \tag{6.17}$$

which means that the outdoor air can be not fresh and the outdoor air VOCs concentration can vary with time.

6.2.3 Initial Conditions

Initial VOCs concentration in the chamber:

$$C_a(t)\big|_{t=0} = C_{a0} \tag{6.18}$$

Initial VOCs concentration profiles in the building materials

(a) For non-porous materials:

$$C_{m,j}(x_j,t)\big|_{t=0} = f_{m,j}(x_j) \tag{6.19}$$

(b) For porous materials:

$$C_{g,j}(x_j,t)\big|_{t=0} = f_{g,j}(x_j) \tag{6.20}$$

It can be seen that this model can handle non-uniform initial VOCs concentration scenarios.

6.2.4 VOCs Mass Conservation in the Chamber Air

A mass balance equation of VOCs in the chamber air can be written as:

$$\begin{aligned} V\frac{dC_a}{dt} &= Q_{Inf}\cdot(C_{OA}-C_a)+(Q_{OA}C_{OA}+Q_RC_a)(1-E_f) \\ &\quad -(Q_{OA}+Q_R)C_a + A\cdot R \end{aligned} \tag{6.21}$$

where V m^3 is the room volume; Q_{Inf} m^3 s^{-1}, infiltration airflow rate (assuming exfiltration flow rate is equal to infiltration flow rate); Q_{OA} m^3 s^{-1}, the outdoor airflow rate; Q_{R} m^3 s^{-1}, recirculation airflow rate; C_{OA} kg m^{-3}, the outdoor air VOCs concentration; E_{f}, the VOCs removal efficiency of the filter, and A m^2, the surface area of the material assembly exposed to room air.

6.3 Model Assessment

Kumar and Little (2003a) developed a double-layer continuum analytical model. Table 6.1 lists the baseline parameter values they used for one of the cases they calculated. It can be seen that $D_{m,1}$=1.2×10^{-11} m^2 s^{-1} and is two orders of magnitude larger than $D_{m,2}$. Under this circumstance, it is better to consider the top layer material as a porous material. Before applying the proposed model, the properties of

the top layer given in material-phase should be converted into gas-phase, following the rules given by (Lee, 2003; Haghighat et al., 2005), i.e. $D_e=D_m\times K_{ma}$, $K_{ma}=(\varepsilon+K_s)$, and $C_{g0}=C_{m0}/K_{ma}$.

Table 6.1 Baseline parameter values used in Kumar and Little's model (Kumar and Little, 2003a) (In the brackets are the corresponding gas-phase values converted from material-phase)

Volume of room, V	20 m^3
Surface area of VF exposed to air, A	9 m^2
Flow rate through room, Q_s	20 m^3 h^{-1}
Partition coefficient of first layer, $K_{ma,1}$	120,000 (ε_1+K_{s1}=120,000)
Diffusion coefficient of first layer, $D_{m,1}$	1.2×10^{-11} m^2 s^{-1} ($D_{e1}=1.44\times10^{-6}$ m^2 s^{-1})
Initial concentration of first layer, $C_{m0,1}$	200 g m^{-3} ($C_{g1,0}$=1.67 mg m^{-3})
Thickness of first layer δ_1	0.0002 m
Partition coefficient of second layer, $K_{ma,2}$	120,000
Diffusion coefficient of second layer, $D_{m,2}$	1.2×10^{-13} m^2 s^{-1}
Initial concentration of second layer, $C_{m0,2}$	200 g m^{-3}
Thickness of second layer δ_2	0.0018 m

The predictions resulted from both models are plotted in Figure 6.3. It is clear that Kumar and Little's model significantly overestimates the early stage VOCs concentration, whose peak concentration is more than three times that of the proposed model. This is because at the early stage, the emissive power of the material is strong, both convection and diffusion dominate the mass transfer processes. As time goes by, diffusion controls the emission rate. So, as Lee (2003) demonstrated that for solid materials with large diffusion coefficients, i.e., porous materials, convection effect should not be ignored. Generally speaking, with the

exception of the early stage data, the predictions given by the two different models agree well with each other.

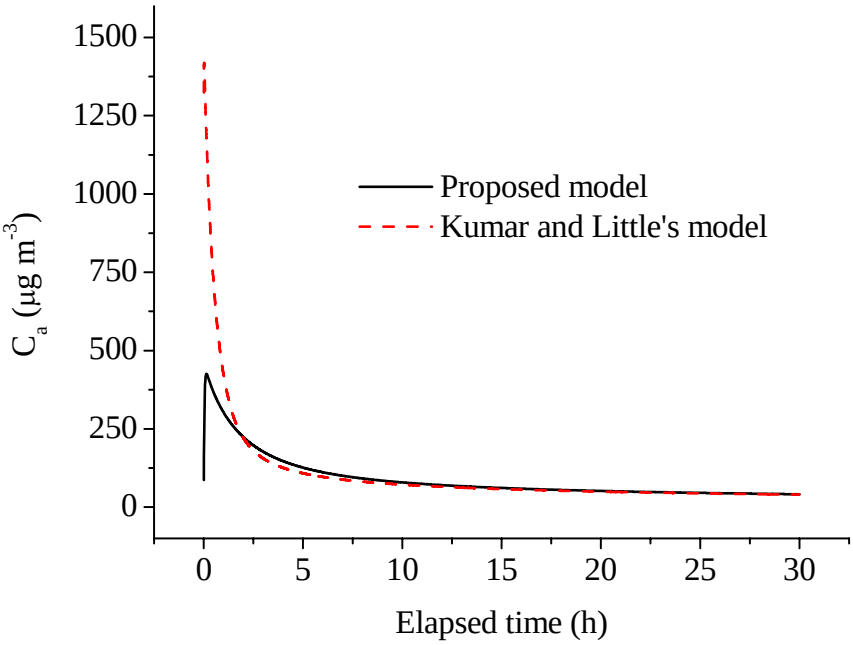

Figure 6.3 Comparison of predictions resulted from proposed and Kumar and Little's model

6.4 Model Applications

6.4.1 Impact of Barrier Layer on VOCs Concentration

The effect of a barrier layer on reducing the emission rate and consequently lowering the gas-phase indoor VOCs concentration can be demonstrated by using the proposed model. As has been shown in Table 6.1, layer1 can be regarded as a porous material while layer2 can be taken as a non-porous material. Although both of the two layers initially have the same VOCs concentrations, significantly different indoor VOCs concentration will be resulted by changing the sequence of the two layers, i.e., the first scenario - layer1 is the uppermost layer; the second scenario - layer1 becomes the bottommost layer. In the second scenario, the less permeable material layer2 is expected to act as a barrier layer to reduce the overall indoor gas phase VOCs

concentration. Utilizing the parameters given in Table 6.1 as the inputs of the proposed model, the results of the two scenarios are shown in Figure 6.4. The effect is clearly evidenced.

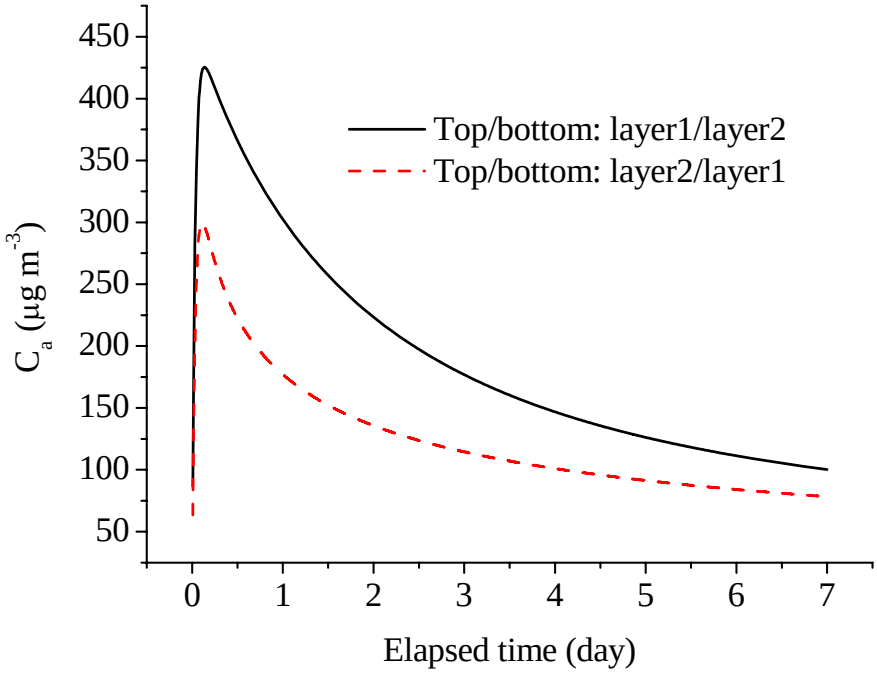

Figure 6.4 The effect of barrier layer on indoor VOCs concentration

In order to strengthen the barrier layer effect, a smaller diffusion coefficient of the barrier layer is preferred. It is explicit that more significant effects can also be achieved by reducing the initial VOCs content in the barrier layer. It should be mentioned that special attention should be paid to the moisture conditions of the materials under the barrier layer when implementing this method. Because on one hand too high moisture content may do damages to the materials under the barrier layer, on the other hand how the moistures in materials affect VOCs transportation are still not very clear.

6.4.2 Impact of Ventilation Strategies on VOCs Concentration

Now, let's consider a mechanically ventilated office room. Define the recirculation air fraction as the ratio between recirculation airflow rate and total supply airflow

rate: $f = Q_R/(Q_R + Q_{OA})$. The material properties remain unchanged as shown in Table 6.1. For intermittent operation, the HVAC system is assumed to operate on weekdays from 8:00 AM to 20:00 PM and to be off during the off-work hours and weekends. It is assumed that the infiltration rate is always 0.2 h^{-1}. The in-duct filter is only in effect when ventilation system is on. Simulations are performed over seven days, starting 8:00 AM Monday morning and ending the following Sunday 20:00 PM.

Indoor VOCs concentrations resulted from continuous and intermittent ventilation are investigated. Suppose *f*=0, i.e., 100 per cent of the supply air is outdoor air. The simulation results are plotted in Figure 6.5.

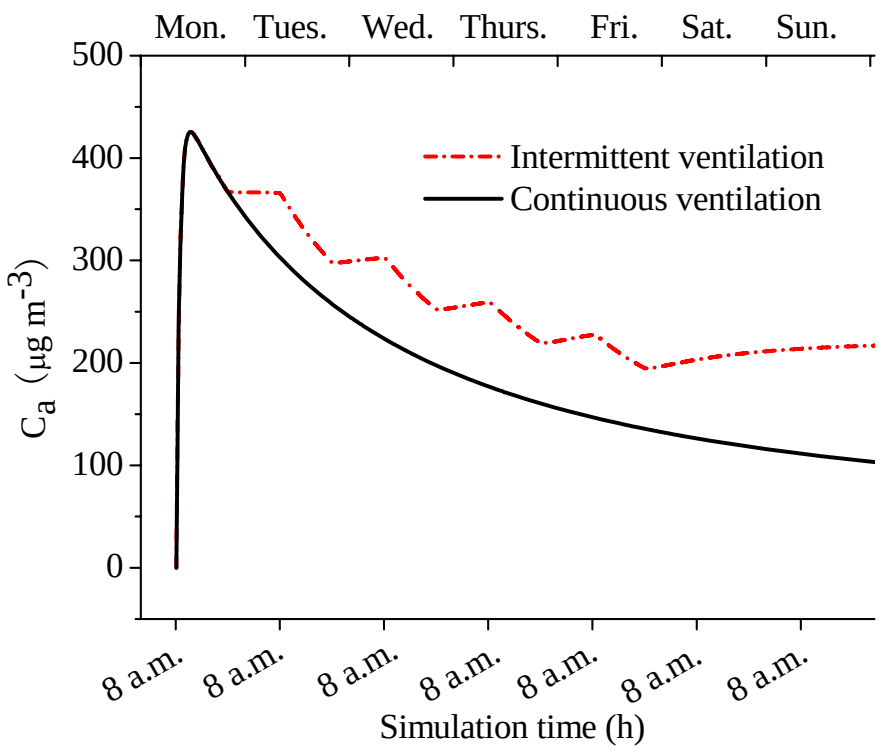

Figure 6.5 Impacts of ventilation modes on VOCs concentration (*f*=0)

It is apparent that the indoor VOCs concentration resulted from intermittent ventilation is much higher. Practically speaking, indoor VOCs emission models should take ventilation modes into account for accurate predictions, subsequently for

decision-making of indoor VOCs control strategies. It should be noted that when no ventilation is employed during off-work hours, whether the indoor VOCs concentration would build up or decrease is determined by many factors, such as infiltration rate, material properties and their initial conditions etc. If the total effect makes the right hand side of equation (6.21) greater than zero, then the indoor VOCs concentration builds up, otherwise decreases. Generally speaking, in most cases, the contaminants generated by the building accumulate during this no ventilation period.

6.4.3 Impact of Filtration Efficiency on Indoor VOCs Concentration

Figure 6.6 shows the impacts of filtration efficiency on indoor VOCs concentration at a fixed recirculation air fraction f=0.5. It is clear that the higher the efficiency, the more contaminant removed from airflow by the filter and thus the lower indoor VOCs concentration resulted.

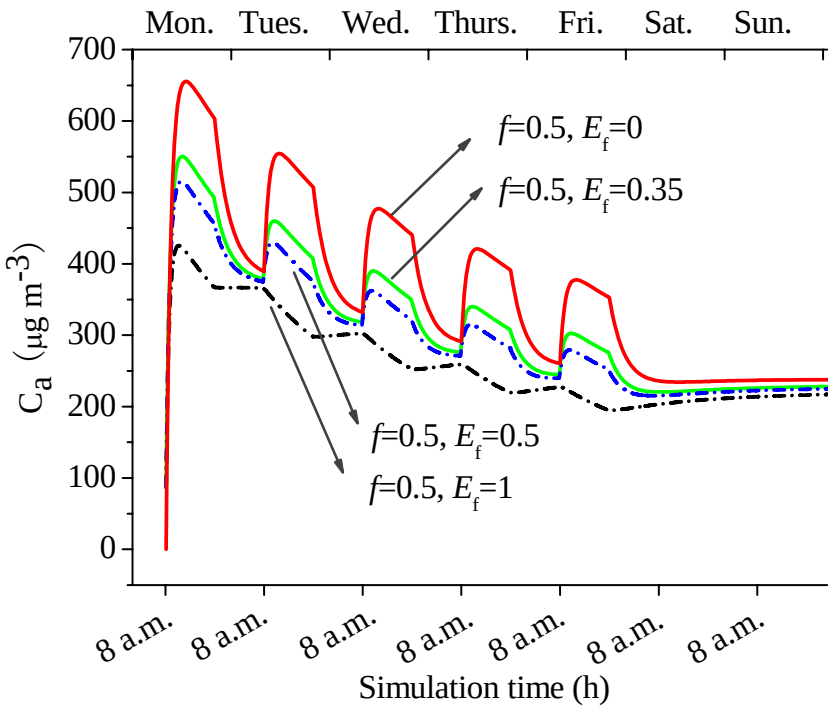

Figure 6.6 Effect of filtration efficiency on VOCs concentration

Observing Figure 6.5 and Figure 6.6, for intermittent ventilation, the same indoor VOCs concentration level is obtained for two different intermittent ventilation strategies: f=0 and f=0.5, E_f=1 (practically no filter has so high efficiency, especially in removing gases and vapors, the value is used just for ease of demonstration). It means that the combination of re-circulated air and filter can on one hand control indoor VOCs concentration at an acceptable level and on the other hand save energy (because less outdoor air needs to be treated when recirculation air is employed). It can also be noticed in Figure 6.6 that high filter efficiency can also dampen the oscillations of the concentration curve caused by the on/off operations of the ventilation system and the employment of recirculation air. It should be noted that when recirculation air is employed, the required outdoor airflow rate should be carefully determined to maintain acceptable indoor air quality.

6.5 Summary

The proposed single-component multi-layer multi-phase model is assessed by comparing the predicted results with Kumar and Little's double-layer analytical model for a same case. Results show that neglecting convection term will result in an overestimated concentration at the early stage, in particular the peak concentration. A possible way of indoor VOCs control is applying a barrier layer tightly above the source material. Selection of barrier layer with small diffusion coefficient, as well as reduction of initial VOCs content in the barrier layer plays an important role on the successfulness of implementing this method. Significant impacts of ventilation strategies on VOCs concentration are demonstrated by comparing two ventilation modes, i.e. continuous and intermittent ventilation, respectively. The overall concentration level resulted from intermittent ventilation is much higher due to no

ventilation provided when the HVAC system is off. Effects of in-duct filter filtration efficiency on indoor VOCs concentration are also investigated, the higher the filter efficiency at a fixed recirculation air fraction, the lower overall indoor concentration resulted. From the point of view of both IAQ control and energy saving, high efficiency filter is recommended for use in case recirculation air is employed. The studies reported in this chapter are mainly to validate the applicability and to demonstrate the flexibility of the developed model. The proposed model proves to be a step forward in modeling VOCs emission from building material assembly under real room/building scenarios. In the next chapter, more sophisticated situations will be considered and more quantitative analysis will be presented.

Chapter 7
Development of an Integrated Model for Characterizing VOCs Source/Sink Behaviors of Building Materials in a Room

7.1 Introduction

In the previous chapter, a single-component multi-layer multi-phase model was developed. The model can conveniently handle different scenarios: non-porous, porous materials co-existing; natural or mechanical ventilation; continuous or intermittent ventilation; re-circulation air and installation of VOCs filter etc. The imperfection of this model lies in that only one component is considered existing in the 'room'. The 'room' is thus more like an environmental chamber. In real buildings, the situation is more complex, there are different building components in a real room, such as the wall assemblies, the floor assembly and the ceiling assembly (Zhang and Niu, 2004), and each component is composed of different layers of porous or non-porous materials. Furthermore, in the presence of other components, the interactions of VOCs with different components would be more complicated. Some components may act as VOCs sources, while others may act as sinks of VOCs and temporarily adsorb compounds and re-emit them afterwards depending on the concentration gradient between the components and indoor bulk air.

Air cleaners may be an important part of IAQ control, but cannot adequately remove all of the pollutants typically found in indoor air. Air cleaners should only be considered as an adjunct measure to source control and ventilation. Air cleaners that have high filter efficiency and are designed to handle large amounts of air are the best choice for use in office or residential buildings. A comprehensive model must

also be able to consider the effects of in-duct filters or portable air cleaners on indoor VOCs concentration.

In terms of modeling VOCs concentration in a room, usually there are three methods: single zone method, zonal method and CFD method. The selection of what kind of method to use depends on the purposes of researches. If the information of the distribution of VOCs in the room is required, then the zonal or CFD method may have to be employed. However, CFD method generally requires huge computational resources and an experienced specialist operator to perform the modeling to obtain accurate results (Ellacott and Reed, 1999; Haghighat et al., 2005). Although the zonal model is somewhat simpler than CFD model, it is still too expensive and time consuming to be used as routine tool for predicting indoor VOCs concentration. Actually, most of the time, people are more interested in the overall indoor VOCs concentration level than in the excessively detailed results such as air flow pattern, temperature pattern and VOCs distributions. For those non-specialists, the simplest is the best - the well-mixed single zone method meets their demands.

The one component single-zone model developed in the previous chapter will be further developed and extended to a multi-component model to be able to model real room scenarios. The assumptions made in developing the one component single-zone model still hold in this chapter.

7.2 Model Development

The schematic drawing of a typical air-conditioned office room is shown in Figure 7.1.

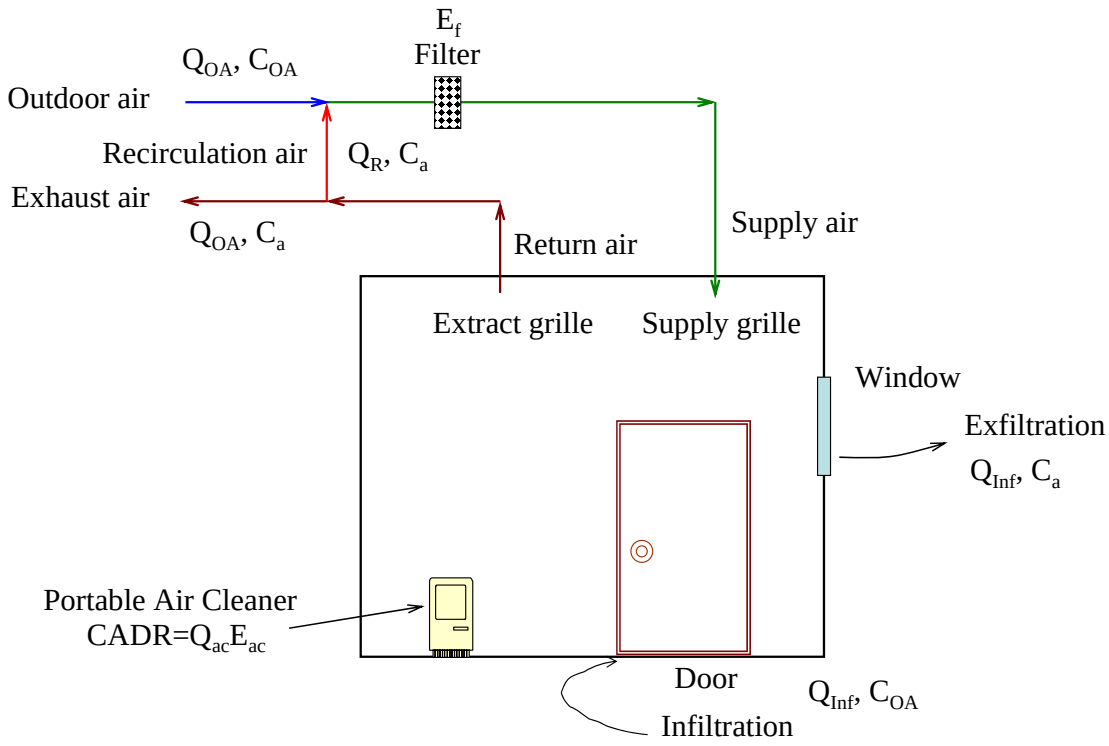

Figure 7.1 Schematic drawing of a typical air-conditioned office room

There may be infiltration and exfiltration through the door and windows or other openings; the HVAC system may work only during working-hours; recirculation air may be applied in order to save energy; there may be a portable air cleaner in the room.

A variety of building materials may exist in the room, some of them may be porous materials, and others may be less porous materials which sometimes can be regarded as non-porous materials for the sake of simplicity. The mass transfer mechanisms for VOCs in the porous and non-porous materials are significantly different. For non-porous materials, material phase VOCs diffusion, surface partitioning (equilibrium between material phase surface concentration and gas phase concentration in the boundary), and surface convection are the major processes involved, while for porous materials, gas phase VOCs diffusion (surface diffusion and adsorbed phase diffusion can normally be neglected), sorption on pore surfaces (equilibrium between

gas phase VOCs concentration and adsorbed phase VOCs concentration), and surface convection are the three main processes. Although the corresponding forms of governing equations, boundary conditions and initial conditions, as well as the variables in the equations may be different for non-porous and porous materials; a universal form should be written to make the model solvable.

For ease of description, let's define that the numbered components can be denoted by i (i=1, 2,…, 6), with i=1 for ceiling component, i=2, 3, 4, 5 for sidewall components, and i=6 for floor component; the numbered layers of ith component can be denoted by j (j=1, 2,…, n_i), where n_i is the total number of layers of ith component; the numbered nodes of ith component jth layer can be denoted by k (k=1,2…$m_{i,j}$), where $m_{i,j}$ is the total number of nodes of the ith component jth layer. The details of the model development are as following.

7.2.1 Governing Equation

The modified Fick's second law can be used to describe VOCs diffusion in building materials:

$$(\varepsilon_{i,j} + K_{s,i,j})\frac{\partial C_{i,j}}{\partial t} = D_{i,j}\frac{\partial^2 C_{i,j}}{\partial x_{i,j}^2} \tag{7.1}$$

Where, for non-porous materials, $\varepsilon = 0$, $K_s = 1$, C is material phase concentration, D is material phase diffusion coefficient; for porous materials, ε is the porosity, K_s is the internal linear sorption isotherm, C is gas phase VOCs concentration, D is effective diffusivity for gas-phase diffusion. The subscripts i and j stand for wall numbers (1: ceiling, 2-5: sidewall, 6: floor) and layer numbers, respectively. If not additionally noted, these descriptions hold throughout this chapter.

7.2.2 Boundary Conditions

7.2.2.1 At the Surface of the Uppermost Layers

An equilibrium relationship at the surface of the uppermost layers (exposed to room air) can be written:

$$C_{s,i,1} = K_{ma,i,1} C_{as,i,1} \tag{7.2}$$

Where, C_{as} is the gas phase VOCs concentration in the boundary layer near the surface; for porous materials, C_s is the gas phase surface VOCs concentration, $K_{ma} = 1$ (which means gas phase VOCs concentration is continuous at the surface); for non-porous materials, C_s is the material phase surface VOCs concentration, K_{ma} is the surface partition coefficient. If no additional notes, these descriptions hold throughout this chapter.

When air passes over the material surface, a mass boundary layer exists between the material surface and the main flow. VOCs mass transfer in the boundary layer can be expressed as:

$$R_{i,1} = -D_{i,1} \frac{\partial C_{i,1}}{\partial x_{i,1}}\bigg|_{x_{i,1}=\delta_{i,1}} = h_m(t)(C_{as,i,1} - C_a) \tag{7.3}$$

7.2.2.2 At the Material/Material Interfaces

It is assumed that there are no losses of mass at the material/material interfaces:

$$-D_{i,j} \frac{\partial C_{i,j}}{\partial x_{i,j}}\bigg|_{x_{i,j}=0} = -D_{i,j+1} \frac{\partial C_{i,j+1}}{\partial x_{i,j+1}}\bigg|_{x_{i,j+1}=\delta_{i,j+1}} \tag{7.4}$$

Meanwhile, the two corresponding surface concentrations of the two adjacent layers are assumed to be always in equilibrium with gas phase concentration:

$$C_{s,i,j}\Big|_{x_{i,j}=0} = K_{ma,i,j} C_{as,i,j\&j+1}$$
$$C_{s,i,j+1}\Big|_{x_{i,j+1}=\delta_{j+1}} = K_{ma,i,j+1} C_{as,i,j\&j+1} \tag{7.5}$$

7.2.2.3 At the Bottom of the Bottommost Layers

It is assumed that there is no VOCs mass transfer through the bottom of the last layer material:

$$-D_{i,n_i} \frac{\partial C_{i,n_i}}{\partial x_{i,n_i}}\Big|_{x_{i,n_i}=0} \tag{7.6}$$

7.2.2.4 At the Fresh Air Intake

$$C_{OA}(t) = f_{OA}(t) \tag{7.7}$$

The outdoor air may be contaminated and the outdoor air VOCs concentration can be a function of the time.

7.2.3 Initial Conditions

Initial VOCs concentration in the room:

$$C_a\Big|_{t=0} = C_{a0} \tag{7.8}$$

Initial VOCs concentration in each layer can be nonuniform:

$$C_{i,j}(x_{i,j},t)\Big|_{t=0} = f_{i,j}(x_{i,j}) \tag{7.9}$$

7.2.4 VOCs Mass Conservation in the Room

The system of the equations is not closed so far. An additional equation should be given, i.e. mass conservation of VOCs in the room air:

$$\begin{aligned} V\frac{dC_a}{dt} = &\left[(Q_{OA}C_{OA} + Q_R C_a)(1-E_f) + Q_{Inf}C_{OA}\right] - (Q_{OA} + Q_R + Q_{Inf})C_a \\ &- Q_{ac}E_{ac}C_a + \sum_{i=1}^{6} A_{i,1}\cdot R_{i,1} \end{aligned} \tag{7.10}$$

where Q_{ac} is the airflow rate through the air cleaner, E_{ac} is the average single pass efficiency of the air cleaner (Reed et al., 2002). Q_{ac} can be measured, E_{ac} is usually empirically determined with a single zone mass balance model in association with environmental chamber test.

In practice, the effectiveness of air cleaners in removing pollutants from the air depends on both the efficiency of the device itself (e.g., the percentage of the pollutant removed as it goes through the device) and the amount of air handled by the device (EPA, 1990).

Several investigators of portable air-cleaning units have expressed their results as a "clean air delivery rate" or CADR, e.g. (Foarde et al., 1997; Niu et al., 1998; Chen et al., 2005). The CADR is the product of the unit efficiency and the air flow rate through it. CADR is also known as effective cleaning rate (ECR) (Reed et al., 2002).

7.3 Model Solution

Implicit finite volume method can be used to solve the model. Detailed discretization processes are shown in the following. A schematic drawing of one of the discretized components is given in Figure 7.2, the black dots are the centers of the individual control volumes.

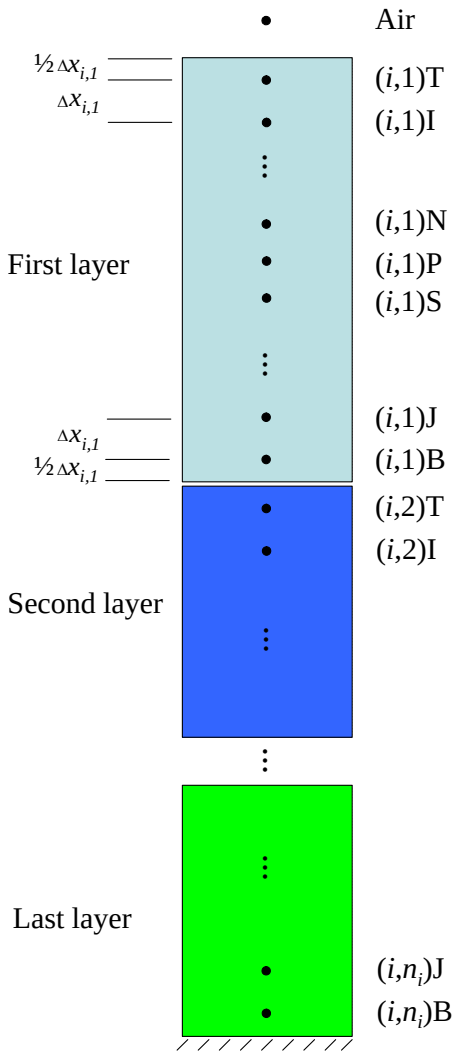

Figure 7.2 Illustration of the discretization of the building components

7.3.1 The First Control Volume of the Uppermost Layer

Consider the first control volume of the uppermost layer as shown in Figure 7.3, whose center is denoted as (i,1)T, based on equations (7.2) and (7.3), the gas phase VOCs concentration near the surface can be expressed as:

$$C_{as,i,1} = \frac{\dfrac{D_{i,1}}{0.5\Delta x_{i,1}} C_{i,1}^{T} + h_m C_a}{\dfrac{D_{i,1}}{0.5\Delta x_{i,1}} K_{ma,i,1} + h_m} \tag{7.11}$$

Integrating equation (7.1) over the control volume, we get:

$$(\varepsilon_{i,1}+K_{s,i,1})\frac{C_{i,1}^{T}-C_{i,1}^{T^0}}{\Delta t}\Delta x_{i,1}=D_{i,1}\frac{\partial C_{i,1}}{\partial x_{i,1}}\bigg|_{x_{i,1}=\delta_{i,1}}-D_{i,1}\frac{C_{i,1}^{T}-C_{i,1}^{I}}{\Delta x_{i,1}} \tag{7.12}$$

Substituting equation (7.3) into (7.12), and then substituting equation (7.11) into the obtained new equation, after re-arrangement, one can have:

$$a_{P,i,1,1}C_{i,1}^{T}=a_{N,i,1,1}C_{a}+a_{S,i,1,1}C_{i,1}^{I}+a_{P,i,1,1}^{0}C_{i,1}^{T^0} \tag{7.13}$$

where,

$$a_{P,i,1,1}^{0}=\frac{\Delta x_{i,1}}{\Delta t}(\varepsilon_{i,1}+K_{s,i,1}) \tag{7.14}$$

$$a_{N,i,1,1}=\frac{\dfrac{D_{i,1}}{0.5\Delta x_{i,1}}h_m K_{ma,i,1}}{\dfrac{D_{i,1}}{0.5\Delta x_{i,1}}K_{ma,i,1}+h_m} \tag{7.15}$$

$$a_{S,i,1,1}=\frac{D_{1,i}}{\Delta x_{i,1}} \tag{7.16}$$

$$a_{P,i,1,1}=a_{P,i,1,1}^{0}+a_{S,i,1,1}+{a_{N,i,1,1}}/{K_{ma,i,1}} \tag{7.17}$$

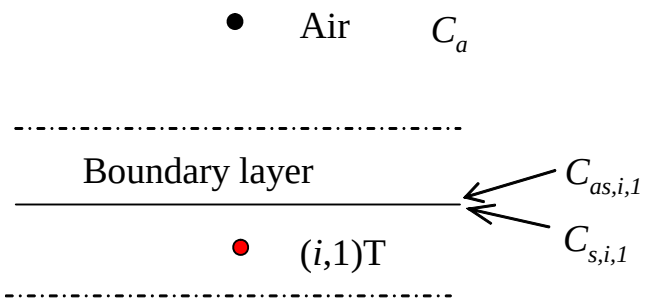

Figure 7.3 The first control volume of the uppermost layer

7.3.2 The Last Control Volume of the Bottommost Layer

Now we consider the last control volume of the bottommost layer as shown in Figure 7.4, whose center is denoted as (i,n_i)B. Integrating equation (7.1) over this control volume, we get:

$$(\varepsilon_{i,n_i} + K_{s,i,n_i})\frac{C^B_{i,n_i} - C^{B^0}_{i,n_i}}{\Delta t}\Delta x_{i,n_i} = D_{i,n_i}\frac{C^J_{i,n_i} - C^B_{i,n_i}}{\Delta x_{i,n_i}} - D_{i,n_i}\frac{\partial C_{i,n_i}}{\partial x_{i,n_i}}\bigg|_{x_{i,n_i}=0} \tag{7.18}$$

Substituting equation (7.6) into (7.18), after re-arrangement, one can get:

$$a_{P,i,n_i,m_{i,j}} C^B_{i,n_i} = a_{N,i,n_i,m_{i,j}} C^J_{i,n_i} + a^0_{P,i,n_i,m_{i,j}} C^{B^0}_{i,n_i} \tag{7.19}$$

where,

$$a^0_{P,i,n_i,m_{i,j}} = (\varepsilon_{i,n_i} + K_{s,i,n_i})\frac{\Delta x_{i,n_i}}{\Delta t} \tag{7.20}$$

$$a_{N,i,n_i,m_{i,j}} = \frac{D_{i,n_i}}{\Delta x_{i,n_i}} \tag{7.21}$$

$$a_{P,i,n_i,m_{i,j}} = a^0_{P,i,n_i,m_{i,j}} + a_{N,i,n_i,m_{i,j}} \tag{7.22}$$

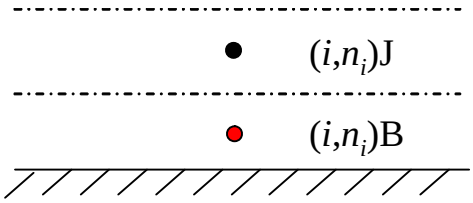

Figure 7.4 The last control volume of the bottommost layer

7.3.3 The Last Control Volume of Layers Other Than the Bottommost Layer

The last control volume of layers other than the bottommost layer means $j \le n_i - 1$ and $k = m_{i,j}$. Considering two adjacent layers as shown in Figure 7.5,

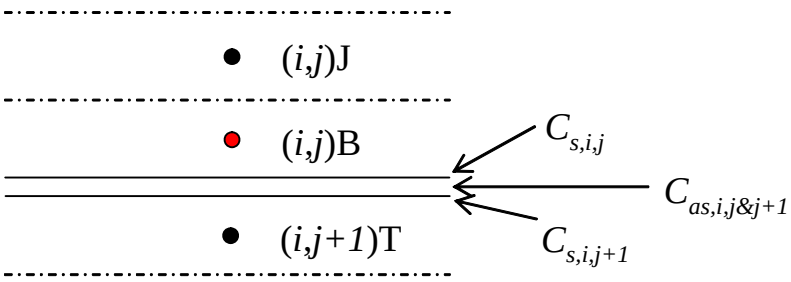

Figure 7.5 The interface of the two adjacent layers

utilizing equations (7.4) and (7.5), the following equations are resulted:

$$C_{s,i,j}\Big|_{x_{i,j}=0} = \frac{\dfrac{D_{i,j}}{0.5\Delta x_{i,j}} C_{i,j}^{B} + \dfrac{D_{i,j+1}}{0.5\Delta x_{i,j+1}} C_{i,j+1}^{T}}{\dfrac{D_{i,j}}{0.5\Delta x_{i,j}} K_{ma,i,j} + \dfrac{D_{i,j+1}}{0.5\Delta x_{i,j+1}} K_{ma,i,j+1}} K_{ma,i,j} \tag{7.23}$$

$$C_{s,i,j+1}\Big|_{x_{i,j}=\delta_{i,j+1}} = \frac{\dfrac{D_{i,j}}{0.5\Delta x_{i,j}} C_{i,j}^{B} + \dfrac{D_{i,j+1}}{0.5\Delta x_{i,j+1}} C_{i,j+1}^{T}}{\dfrac{D_{i,j}}{0.5\Delta x_{i,j}} K_{ma,i,j} + \dfrac{D_{i,j+1}}{0.5\Delta x_{i,j+1}} K_{ma,i,j+1}} K_{ma,i,j+1} \tag{7.24}$$

Integrating equation (7.1) over the control volume near the bottom of layer *j*, we get:

$$(\varepsilon_{i,j} + K_{s,i,j}) \frac{C_{i,j}^{B} - C_{i,j}^{B^0}}{\Delta t} \Delta x_{i,j} = D_{i,j} \frac{C_{i,j}^{J} - C_{i,j}^{B}}{\Delta x_{i,j}} - D_{i,j} \frac{C_{i,j}^{B} - C_{s,i,j}\Big|_{x_{i,j}=0}}{0.5\Delta x_{i,j}} \tag{7.25}$$

Substituting equation (7.23) into (7.25) and re-arranging the new equation, one can have:

$$a_{P,i,j,m_{i,j}} C_{i,j}^{B} = a_{N,i,j,m_{i,j}} C_{i,j}^{J} + a_{S,i,j,m_{i,j}} C_{i,j+1}^{T} + a_{P,i,j,m_{i,j}}^{0} C_{i,j}^{B^0} \tag{7.26}$$

where,

$$a_{P,i,j,m_{i,j}}^{0} = (\varepsilon_{i,j} + K_{s,i,j}) \frac{\Delta x_{i,j}}{\Delta t} \tag{7.27}$$

$$a_{N,i,j,m_{i,j}} = \frac{D_{i,j}}{\Delta x_{i,j}} \tag{7.28}$$

$$a_{S,i,j,m_{i,j}} = \frac{\dfrac{D_{i,j}}{0.5\Delta x_{i,j}} \cdot \dfrac{D_{i,j+1}}{0.5\Delta x_{i,j+1}} \cdot K_{ma,i,j}}{\dfrac{D_{i,j}}{0.5\Delta x_{i,j}} K_{ma,i,j} + \dfrac{D_{i,j+1}}{0.5\Delta x_{i,j+1}} K_{ma,i,j+1}} \tag{7.29}$$

$$a_{P,i,j,m_{i,j}} = a_{P,i,j,m_{i,j}}^{0} + a_{N,i,j,m_{i,j}} + \frac{D_{i,j}}{0.5\Delta x_{i,j}} - a_{S,i,j,m_{i,j}} \frac{D_{i,j}}{D_{i,j+1}} \frac{\Delta x_{i,j+1}}{\Delta x_{i,j}} \tag{7.30}$$

7.3.4 The First Control Volume of Layers Other Than the Uppermost Layer

The first control volume of layers other than the uppermost layer means $j \neq 1$ and $k = 1$. Referring Figure 7.6,

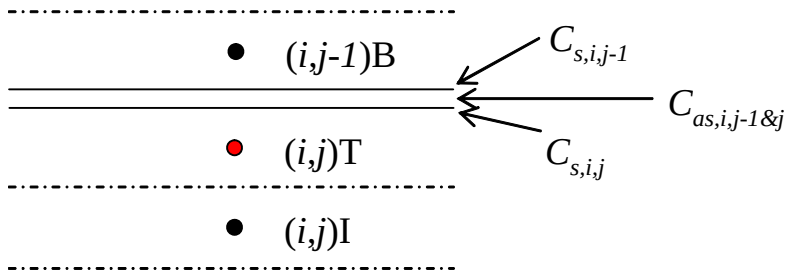

Figure 7.6 The first control volume of layers other than the uppermost layer

and integrating equation (7.1) over the control volume near the upper surface of layer *j*, we get:

$$(\varepsilon_{i,j}+K_{s,i,j})\frac{C_{i,j}^{T}-C_{i,j}^{T^0}}{\Delta t}\Delta x_{i,j}=D_{i,j}\frac{C_{s,i,j}\Big|_{x_{i,j}=\delta_{i,j}}-C_{i,j}^{T}}{0.5\Delta x_{i,j}}-D_{i,j}\frac{C_{i,j}^{T}-C_{i,j}^{I}}{\Delta x_{i,j}} \qquad (7.31)$$

Substituting equation (7.23) into (7.31) and re-arranging the new equation, one can have:

$$a_{P,i,j,1}C_{i,j}^{T}=a_{N,i,j,1}C_{i,j-1}^{B}+a_{S,i,j,1}C_{i,j}^{I}+a_{P,i,j,1}^{0}C_{i,j}^{T^0} \qquad (7.32)$$

Where,

$$a_{P,i,j,1}^{0}=(\varepsilon_{i,j}+K_{s,i,j})\frac{\Delta x_{i,j}}{\Delta t} \qquad (7.33)$$

$$a_{N,i,j,1}=\frac{\dfrac{D_{i,j-1}}{0.5\Delta x_{i,j-1}}\cdot\dfrac{D_{i,j}}{0.5\Delta x_{i,j}}\cdot K_{ma,i,j}}{\dfrac{D_{i,j-1}}{0.5\Delta x_{i,j-1}}K_{ma,i,j-1}+\dfrac{D_{i,j}}{0.5\Delta x_{i,j}}K_{ma,i,j}} \qquad (7.34)$$

$$a_{S,i,j,1}=\frac{D_{i,j}}{\Delta x_{i,j}} \qquad (7.35)$$

$$a_{P,i,j,1}=a_{P,i,j,1}^{0}+a_{S,i,j,1}+\frac{D_{i,j}}{0.5\Delta x_{i,j}}-a_{N,i,j,1}\frac{D_{i,j}}{D_{i,j-1}}\frac{\Delta x_{i,j-1}}{\Delta x_{i,j}} \qquad (7.36)$$

7.3.5 Internal Control Volumes of Each Layer

By saying internal control volumes of each layer means $k\neq 1$ and $k\neq m_{i,j}$ Integrating equation (7.1) over the control volume whose center is denoted by (*i*,*j*)P as shown in Figure 7.7,

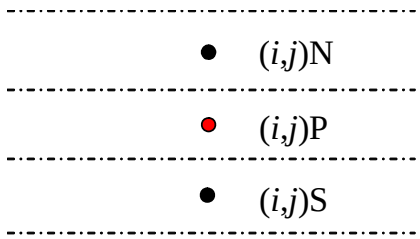

Figure 7.7 Three consecutive internal control volumes in a material layer

we get:

$$(\varepsilon_{i,j} + K_{s,i,j})\frac{C_{i,j}^{P} - C_{i,j}^{P^0}}{\Delta t}\Delta x_{i,j} = D_{i,j}\frac{C_{i,j}^{N} - C_{i,j}^{P}}{\Delta x_{i,j}} - D_{i,j}\frac{C_{i,j}^{P} - C_{i,j}^{S}}{\Delta x_{i,j}} \tag{7.37}$$

Re-arranging the above equation, one can have:

$$a_{P,i,j,k}C_{i,j}^{P} = a_{N,i,j,k}C_{i,j}^{N} + a_{S,i,j,k}C_{i,j}^{S} + a_{P,i,j,k}^{0}C_{i,j}^{P^0} \tag{7.38}$$

where,

$$a_{P,i,j,k}^{0} = (\varepsilon_{i,j} + K_{s,i,j})\frac{\Delta x_{i,j}}{\Delta t} \tag{7.39}$$

$$a_{N,i,j,k} = a_{S,i,j,k} = \frac{D_{i,j}}{\Delta x_{i,j}} \tag{7.40}$$

$$a_{P,i,j,k} = a_{P,i,j,k}^{0} + a_{S,i,j,k} + a_{N,i,j,k} \tag{7.41}$$

7.3.6 The Discretization of VOCs Mass Conservation Equation in the Room Air

Substituting equation (7.11) into (7.3), the VOCs emission rates from/into different components can be expressed as:

$$R_{i,1} = h_m\left(\frac{\dfrac{D_{i,1}}{0.5\Delta x_{i,1}}}{\dfrac{D_{i,1}}{0.5\Delta x_{i,1}}K_{ma,i,1} + h_m}C_{i,1}^{T} - \frac{\dfrac{D_{i,1}}{0.5\Delta x_{i,1}}K_{ma,i,1}}{\dfrac{D_{i,1}}{0.5\Delta x_{i,1}}K_{ma,i,1} + h_m}C_a\right) \tag{7.42}$$

Substituting equation (7.42) into (7.10), re-arranging the new equation, it is easy to obtain:

$$V\frac{dC_a}{dt}=\left[(Q_{OA}C_{OA}+Q_RC_a)(1-E_f)+Q_{Inf}C_{OA}\right]$$
$$-(Q_{OA}+Q_R+Q_{Inf})C_a-Q_{ac}E_{ac}C_a \tag{7.43}$$
$$+\sum_{i=1}^{6}A_{i,1}\cdot h_m\left(\frac{\frac{D_{i,1}}{0.5\Delta x_{i,1}}}{\frac{D_{i,1}}{0.5\Delta x_{i,1}}K_{ma,i,1}+h_m}C_{i,1}^T-\frac{\frac{D_{i,1}}{0.5\Delta x_{i,1}}K_{ma,i,1}}{\frac{D_{i,1}}{0.5\Delta x_{i,1}}K_{ma,i,1}+h_m}C_a\right)$$

The discretization form of equation (7.43) is:

$$\left\{\frac{1}{\Delta t}+\frac{Q_RE_f+Q_{Inf}+Q_{OA}+Q_{ac}E_{ac}}{V}+\sum_{i=1}^{6}\frac{A_i}{V}\frac{\frac{D_{i,1}}{0.5\Delta x_{i,1}}K_{ma,i,1}h_m}{\frac{D_{i,1}}{0.5\Delta x_{i,1}}K_{ma,i,1}+h_m}\right\}C_a$$
$$=\frac{C_a^0}{\Delta t}+\frac{Q_{Inf}+Q_{OA}(1-E_f)}{V}C_{OA}+\sum_{i=1}^{6}\frac{A_i}{V}\frac{\frac{D_{i,1}}{0.5\Delta x_{i,1}}h_m}{\frac{D_{i,1}}{0.5\Delta x_{i,1}}K_{ma,i,1}+h_m}C_{i,1}^T \tag{7.44}$$

With the above discretization equations and the well defined initial conditions, the system of discretized equations can be readily solved by programming utilizing the mathematical software packages such as MATLAB®.

7.4 Model Assessment

In order to assess the proposed model, the simulation case used in the multi-component multi-layer continuum model developed by Zhang and Niu (2004) is used for the purpose of comparison. A typical small office room with the dimensions of 3×3×3 m^3 is considered. The detailed schematic drawing of the structures is shown in Figure 7.8.

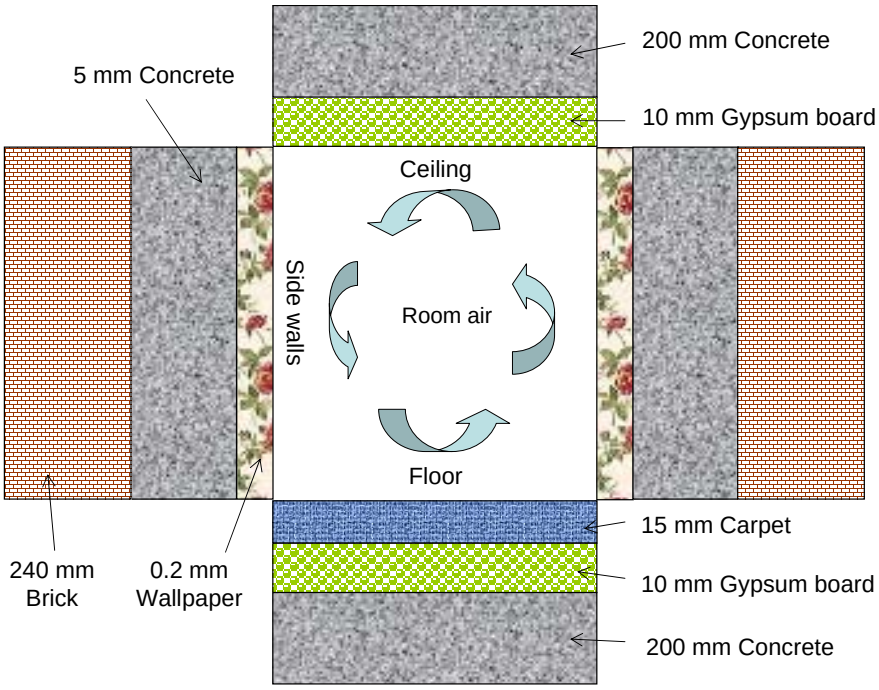

Figure 7.8 Structures of sidewalls, ceiling and floor

The structures of the construction: the sidewalls are composed of three layers, from outermost layer to innermost layer, 240 mm brick, 5 mm concrete, and 0.2 mm wallpaper; the ceiling is composed of two layers, from uppermost layer to bottommost layer, 200mm concrete and 10mm gypsum board; the floor is composed of three layers, from uppermost layer to bottommost layer, 200 mm concrete, 10 mm gypsum board, and 15 mm carpet.

Most of the input data originate from (Meininghaus et al., 2000a), except those who are additionally clarified. The material properties are shown in Table 7.1. Ethyl acetate is selected as a model substance. The compound has comparatively low boiling point, which means the compound evaporates easily at room temperature and whose vapor is readily inhaled by occupants. The chemical and physical properties of ethyl acetate are listed in Table 7.2. The effective diffusion coefficients and sorption coefficients of the selected VOC/material combinations measured by Meininghaus et al. (2000a) are presented in Table 7.3.

Table 7.1 Densities and porosities of materials

Material	Density (kg m^{-3})	Porosity (%)
Wallpaper with paste	1300	10
Carpet with SBR backing	295.29	15
Solid concrete	2298	10.4
Brick wall	1680	17.1
Gypsum board	774.4	28

Table 7.2 Chemical and physical properties of ethyl acetate

VOCs properties	Ethyl acetate
Molecular formula	$CH_3COOC_2H_5$
Molecular weight (g mol^{-1})	88.1
Boiling point (°C)	77.1
Polarity (10^{-24} m^3)	9.7
CAS number	141-78-6

Table 7.3 The effective diffusivities and sorption coefficients for selected VOC/material

Material	Effective diffusivity (m^2 s^{-1})	Sorption coefficient (m^3 air/m^3 material)
Wallpaper with paste	8.33×10^{-9}	3000
Carpet with SBR backing	4.52×10^{-7}	42.2
Solid concrete	5.06×10^{-8}	1140.69
Brick wall	4.74×10^{-7}	182.33
Gypsum board	1.13×10^{-6}	86.65

It has been demonstrated that the value of the porosity (within the range 0~1) itself has little impact on the resultant indoor VOCs concentration curve if the effective diffusivity and sorption coefficient are fixed (Haghighat et al., 2005). So, the reference values of the porosities of solid concrete, brick wall, and gypsum board shown in Table 7.1 are extracted from (Blondeau et al., 2003), while the porosities of

wallpaper with paste and carpet with SBR backing are factitiously assigned since no corresponding information can be found in public literature. The sorption coefficients in Table 7.3 are converted from the partition coefficients measured by Meininghaus et al. (2000a) with the aid of the information of material density in Table 7.1 and air density (at 1 atm, 24 °C - test conditions). An exception is the sorption coefficient in wallpaper with paste which was not given in (Meininghaus et al., 2000a) and thus the value given in (Zhang and Niu, 2004) is adopted (the authors didn't indicate how this value was obtained, it was likely an estimated one) and converted from material phase to gas phase value.

The initial condition given in (Zhang and Niu, 2004) was that: the carpet in the room was the only VOCs source, the material-phase concentrations of ethyl acetate in the carpet was 0.01 kg m^{-3}. The initial material-phase concentration divided by the corresponding sorption coefficient yields the initial gas-phase concentration value $C_{6,1}(x_{6,1},t)\big|_{t=0} = 236.97$ mg m^{-3}.

Because most of the material properties were obtained under 1 atm, 24 °C, the simulation is carried out at the same pressure and temperature conditions. The air change rate (100 per cent fresh air) in (Zhang and Niu, 2004) was 1.0 h^{-1}, this can be achieved by setting $Q_{Inf} = 0$, $Q_R = 0$, and $Q_{OA} = 27$ m^3 h^{-1} in the proposed model. Since no filter or air cleaner appeared in (Zhang and Niu, 2004), $E_f = 0$, and $Q_{ac}E_{ac} = 0$ are then assumed. All the parameters required for the simulation are ready now. Simulation is carried out for the period 0~50 hours, approximately two days since the completion of the installation of the materials. The results are compared with those given by (Zhang and Niu, 2004), the predicted indoor ethyl acetate concentrations are given in Figure 7.9, while the emission factors from/into different

components of the room are shown in Figure 7.10, surprisingly good agreements are achieved.

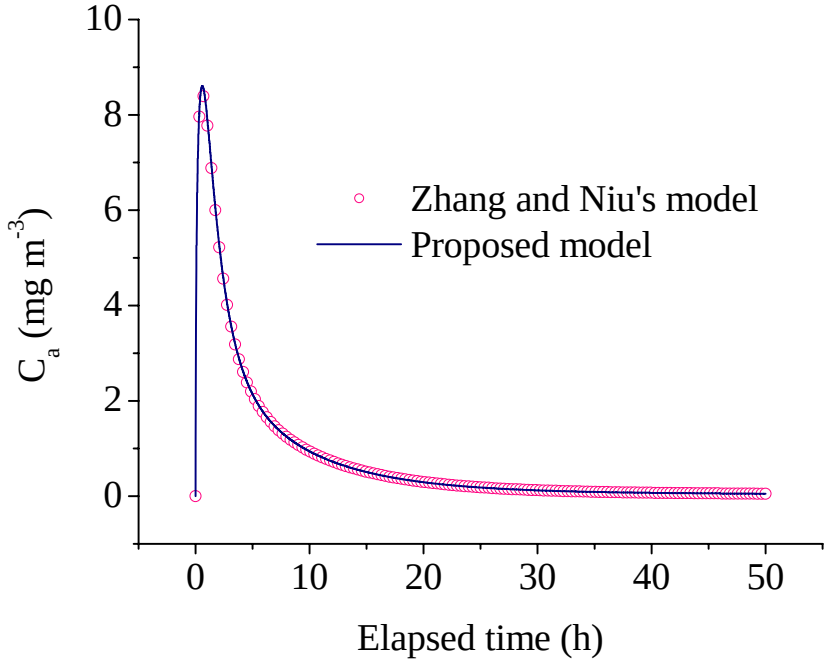

Figure 7.9 Comparison of predicted indoor ethyl acetate concentrations resulted from Zhang and Niu's model and proposed model

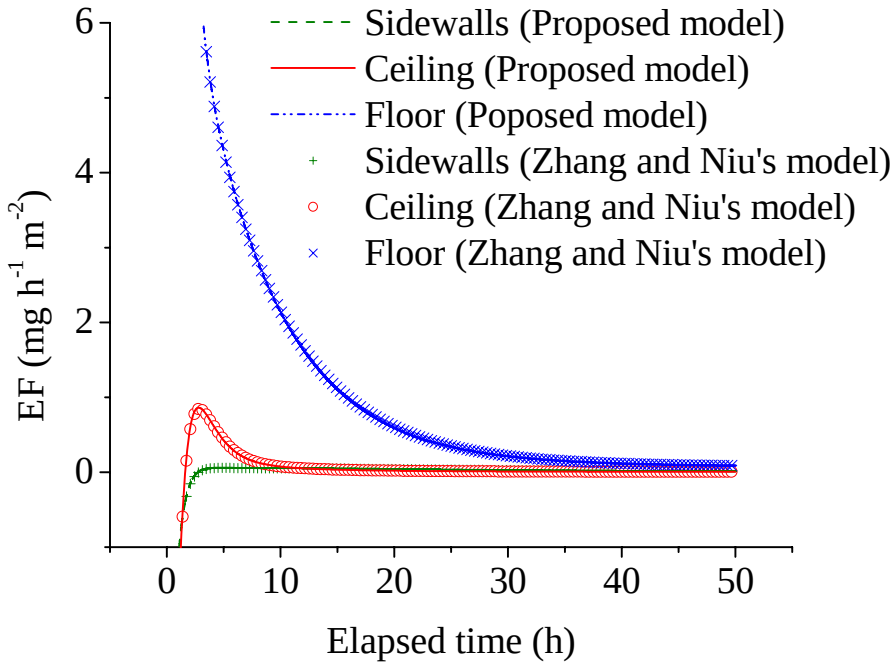

Figure 7.10 Emission factors of ethyl acetate from different components

In Figure 7.9, it can be seen that the indoor ethyl acetate concentration reaches its maximum within the first hour, and then decays rapidly in the first day, it decays relatively slowly in the second day and afterwards.

The sink effect is evidenced in Figure 7.10. It is noticed that the values of emission factors of the sidewalls and ceiling are negative at the beginning of the simulation and become positive afterwards, while that of floor is always positive. The negative values of the emission factors mean the corresponding components act as sinks, while the positive values represent that the corresponding components act as sources. It can also be noticed in Figure 7.10 that the ceiling can temporarily be a relatively strong source of pollutants, e.g. during 1.6 ~ approximately 10 hours, while the sidewalls steadily re-emit the compounds adsorbed at a very slow rate. The difference can be ascribed mainly to the large differences existing in the effective diffusivities and sorption coefficients of materials, as well as the environmental conditions. The materials directly contact with the room air are gypsum board for the ceiling and wallpaper for the sidewalls. It is clear in Table 7.3 that the order of magnitude of the effective diffusivity of gypsum board is several orders larger than that of wallpaper, and the sorption coefficient of gypsum board is much smaller than that of wallpaper. The larger effective diffusivity results in that the compounds are more easily to diffuse into/out of the material; the smaller sorption coefficient results in the weak ability of holding the compounds within the material. In all, this phenomenon is the combined effects of several factors; special attention should be paid to the sink effect to prevent potential negative impacts on indoor air quality.

The normalized cumulative removed mass of ethyl acetate VS the elapsed time is shown in Figure 7.11, where m_r is the cumulative removed mass of ethyl acetate and

m_0 is the initial mass of ethyl acetate contained in the carpet. It can be seen that more than 75 per cent of the compound initially containing in the carpet is removed within the first day, and only less than 5% is further removed from the indoor space during the second day, which is consistent with the trends behaved in Figure 7.9 and Figure 7.10. The removal of pollutant is the result of dilution because no other means such as gaseous air filter or portable air cleaner exist.

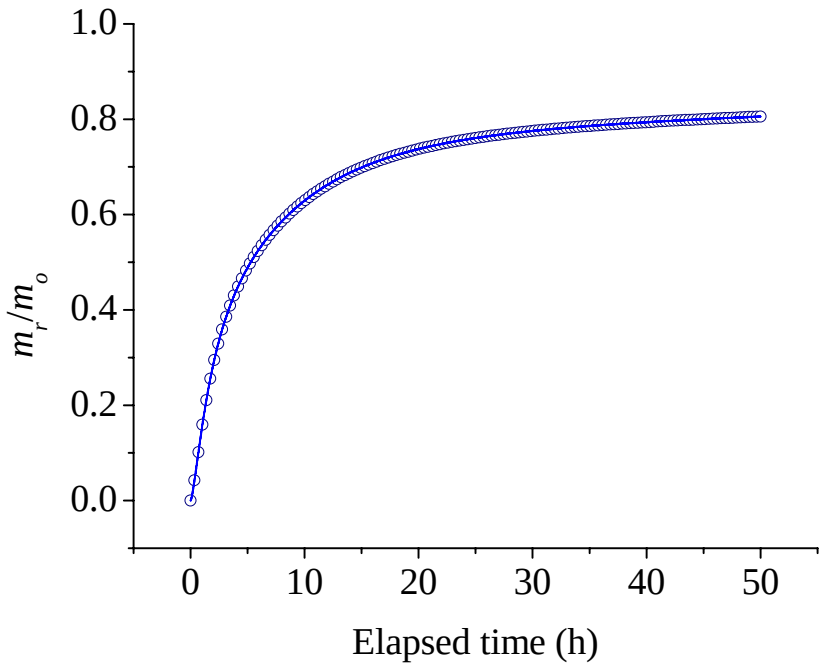

Figure 7.11 Normalized cumulative removed mass of ethyl acetate against elapsed time

7.5 Model Application

In order to investigate the impact of various ventilation strategies on indoor VOCs emission/sorption behavior, the proposed model is used to predict the hourly VOCs concentrations for the aforementioned 3×3×3 m^3 small office room. Assume one occupant occupies this room. The room is mechanically air-conditioned by a constant volume system delivering supply air at the rate of 18 L/s. The infiltration airflow rate is kept at 0.75 L/s, which is equivalent to an infiltration air change rate

of 0.1 h^{-1}, the value is chosen based on the real measurements done by American researchers in Building and Fire Research Laboratory NIST. The in-duct filter is in effect when the HVAC system is working, since the effect of filter efficiency on indoor VOCs concentration has been investigated in the previous chapter, here its efficiency is assumed to be 35%. For intermittent ventilation, the HVAC system is assumed to work from 8:00 AM to 20:00 PM during the work-hours and to shut off during off-work hours and weekends. The removal of VOCs by portable air cleaner will also be investigated because it is an important component of VOCs control strategy. The CADR of the air cleaner is assumed to be 10 L/s (21.2 CFM). The efficiencies of the in-duct filter and portable air cleaner are chosen on the basis of the results of efficiencies measured for different in-duct filters and portable air cleaners by different researchers (Niu et al., 1998; Reed et al., 2002; Chen et al., 2005). A variety of ventilation strategies shown in Table 7.4 will be modeled and evaluated. The simulation period is 0:00AM Monday ~ 23:59PM Sunday.

Table 7.4 Various ventilation strategies modeled and evaluated

Strategy	Mode	Q_{OA} (L s^{-1} per person)	Lag time (h)	Lead time (h)	CADR (L s^{-1})
A	Continuous	7.5	-	-	-
B	Intermittent	7.5	-	-	-
C	Intermittent	7.5	-	2	-
D	Intermittent	7.5	-	2*	-
E	Continuous	10	-	-	-
F	Intermittent	10	-	-	-
G	Intermittent	10	2	-	-
H	Intermittent	7.5	-	-	10
I	Continuous	18	-	-	-

*Note: Q_{OA} is doubled during this period

Figure 7.12 shows the effect of continuous building flush-out on the indoor air VOCs concentrations. An examination of Figure 7.12 reveals that continuous provision of ventilation significantly reduces the indoor VOCs concentration within a couple of days. The more outdoor air supplied to the room by the air conditioning system, the shorter time required to reach a desired concentration level. It is thus suggested that newly built or renovated buildings conduct flush-out with maximum outdoor air supplied to minimize the risk of exposure to high level of VOCs concentration.

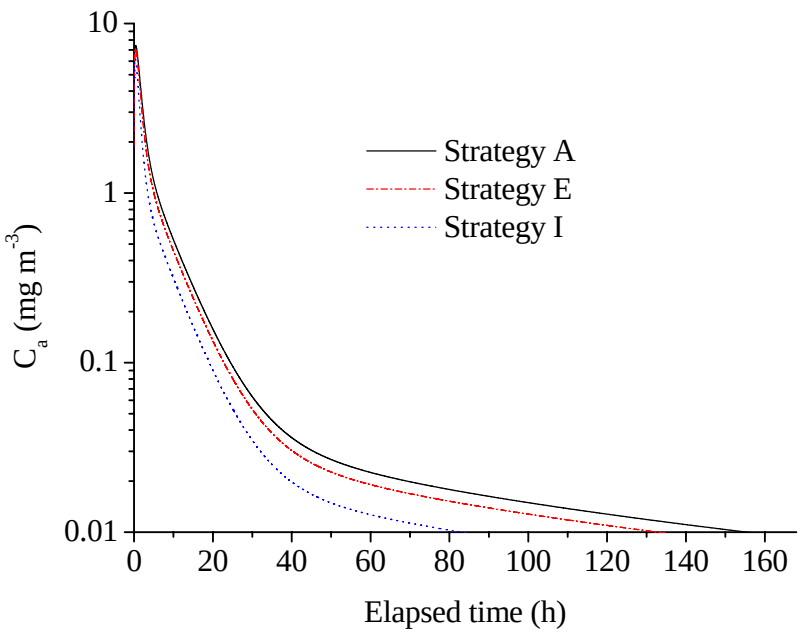

Figure 7.12 Pre-occupancy 'flush-out' at different outdoor airflow rates

However, if there is no ample time for such a period of pre-occupancy building flush-out, and the air conditioning system is operating intermittently like the strategy B or F, the resulted overall indoor VOCs concentration would be much higher throughout the time. Figure 7.13 and Figure 7.14 show two examples of the large differences in the concentrations under different ventilation schemes during the simulation period (one week since the completion of construction or renovation).

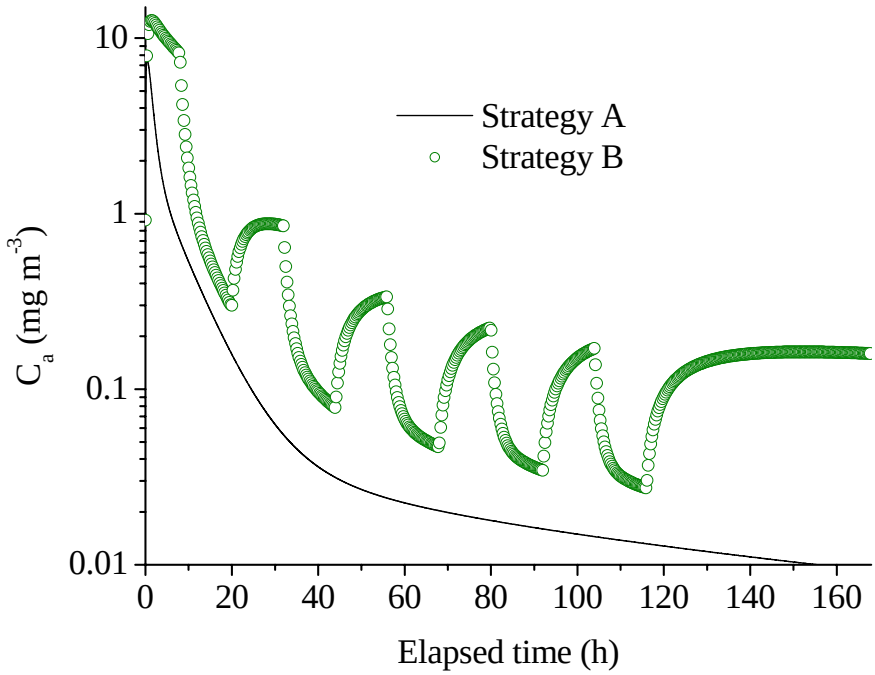

Figure 7.13 Indoor VOCs concentration behaviors under continuous (strategy A) and intermittent ventilation (strategy B)

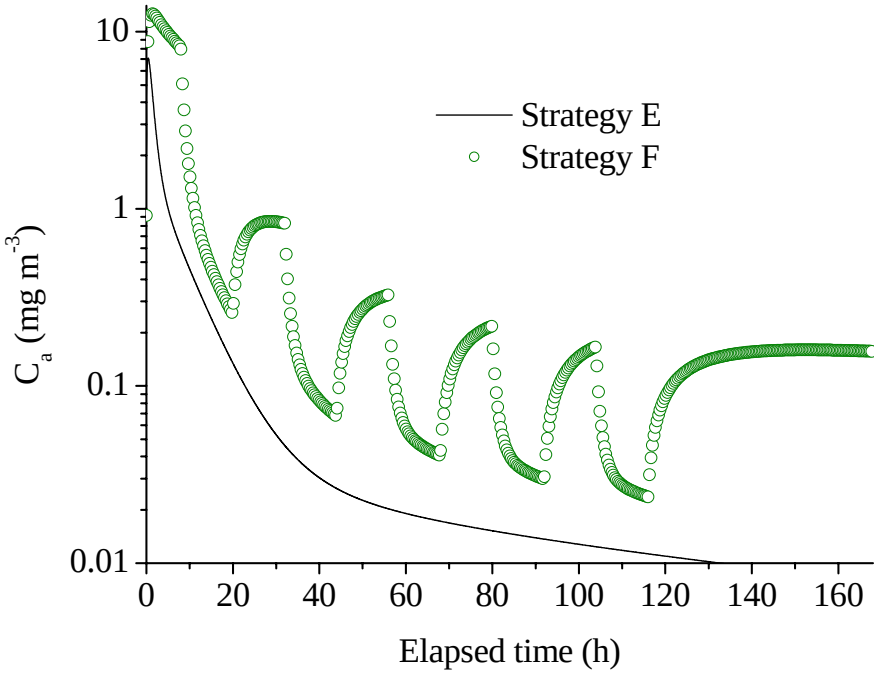

Figure 7.14 Indoor VOCs concentration behaviors under continuous (strategy E) and intermittent ventilation (strategy F)

In the absence of ventilation during the off-work hours, the infiltration flow rate is not sufficient to dilute the indoor VOCs and thus they continue to accumulate during this period, which can be seen in Figure 7.13 and Figure 7.14. The extent of

contaminant buildup depends on the source strength, sorption capacity of building materials, the infiltration rate and also the environmental conditions. The VOCs concentration is likely to be at a substantially elevated level before occupancy begins in the next morning.

Recently, a newly renovated room was monitored in terms of TVOC concentration by a part-time student from BSE department. The measured data is presented in Figure 7.15.

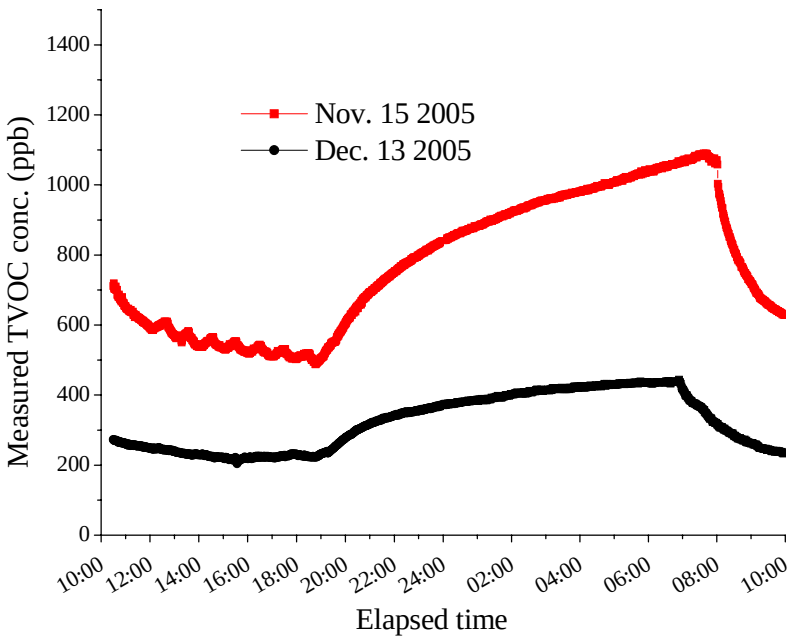

Figure 7.15 TVOC concentration measured in the selected room

Measurements were conducted by utilizing ppbRAE, which logged every 1-minute, and thus the TVOC concentration in the room could be continuously measured within the period of interest. The operation period of the HVAC system in the room was 8:00 AM - 7:00 PM (Monday to Saturday). It can be seen in Figure 7.15 that the behaviors of the measured TVOC concentrations are consistent with the numerical studies.

The extent of the improvement of IAQ by increasing the outdoor airflow rate from 7.5L/s to 10L/s is shown in Figure 7.16.

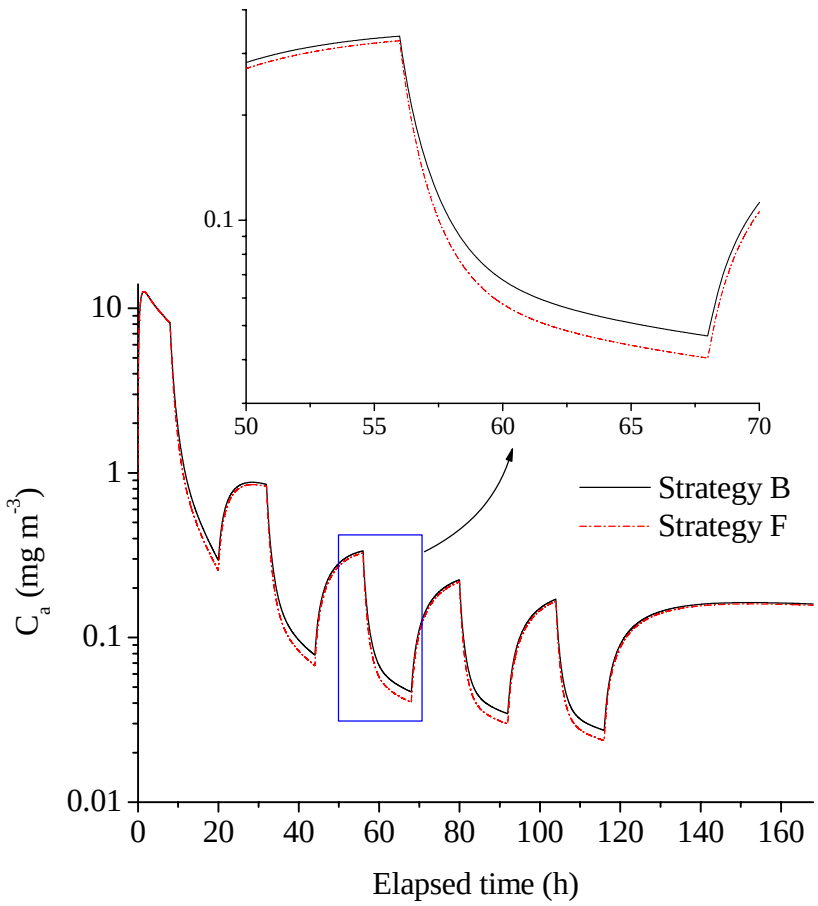

Figure 7.16 Comparison of indoor VOCs concentrations resulted from strategy B and strategy F

It can be noticed in Figure 7.16 that the VOCs concentrations during the working hours are moderately lower for strategy F than B. Though there are some improvements in indoor air quality by increasing the outdoor airflow rate, the energy consumption increases accordingly, especially during hot and cold spells because it is costly to heat cold winter air and to cool hot summer air, thus the amount of outdoor air brought into the system is often reduced by the building engineers during these two spells. Moreover, Zhang and Niu (2004) concluded that when the fresh air change rate is larger than 2 h^{-1}, it has little potential in further reducing VOCs

concentration in a room. So that, the rate of outdoor airflow supplied to a room should be optimized from the point of views of IAQ control and energy saving.

As discussed earlier, elevated VOCs concentration is likely to be encountered in the early morning due to the absence of ventilation during the past night. A morning pre-occupancy flush-out may be helpful in lessening this phenomenon. Therefore, it is necessary for the HVAC system to operate before occupancy begins in the morning. Figure 7.17 shows the concentration curves resulted from ventilation strategies B and C, respectively.

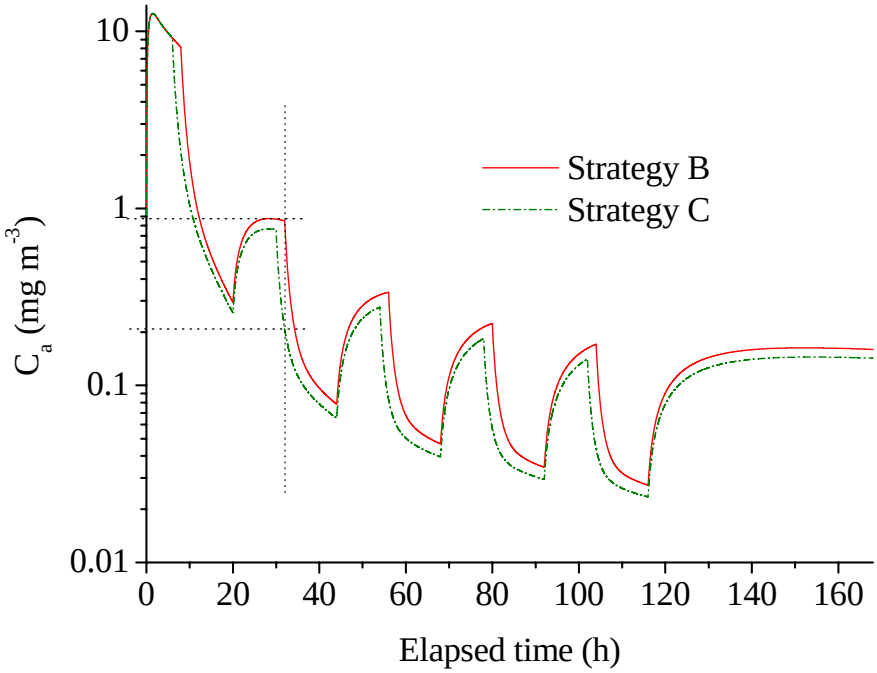

Figure 7.17 Effect of lead-time provision of ventilation on indoor VOCs concentration

It can be seen that a 2 h lead-time provision of ventilation significantly reduces the concentration level from the time occupancy begins in the working day.

Since the lead-time provision of ventilation can successfully reduce the risk of exposure to high level of contaminant concentration for the occupants during the working hours. It would be a worthwhile job to investigate the strategy D on the

indoor air quality. Compared with strategy C, the outdoor airflow rate is doubled (15 L/s) during the 2 h lead-time operation for strategy D. It is expected that a further reduction of indoor VOCs concentration can be achieved when the occupancy begins. The simulation results are presented in Figure 7.18. It can be seen in Figure 7.18 that increasing the outdoor airflow rate during the lead-time ventilation (strategy D) does further reduce the indoor VOCs concentration at the time when occupancy begins. In addition, the concentration during the working-hours for strategy D is considerably lower compared with strategy C. So, it can be a good practice to maximize the outdoor airflow rate during the morning lead-time ventilation.

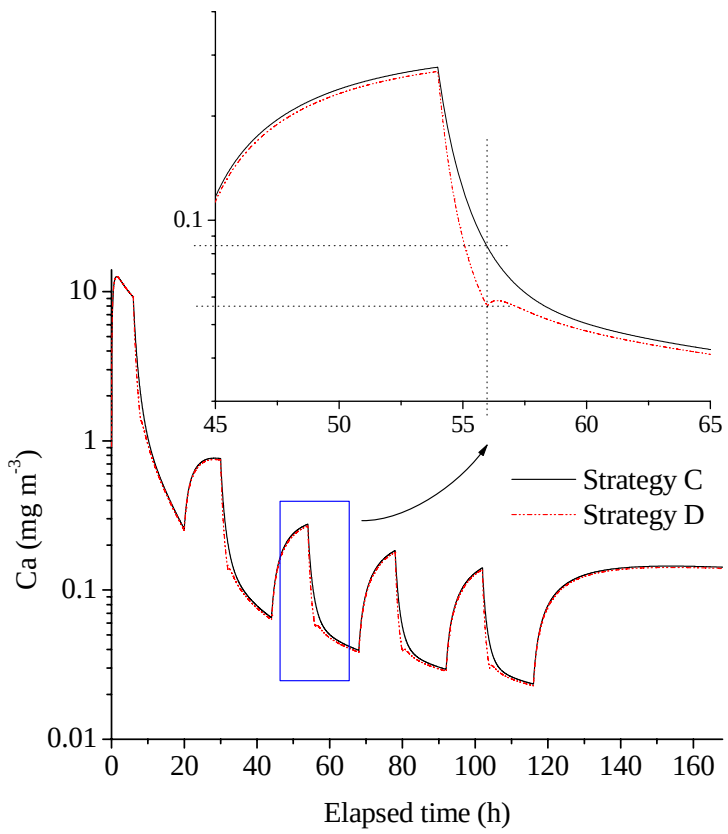

Figure 7.18 Effect of outdoor airflow rate during lead-time operation on indoor VOCs concentration

On the contrary, another interesting question is what will happen if the provision of ventilation is delayed after the commencement of occupancy? The question is answered in Figure 7.19.

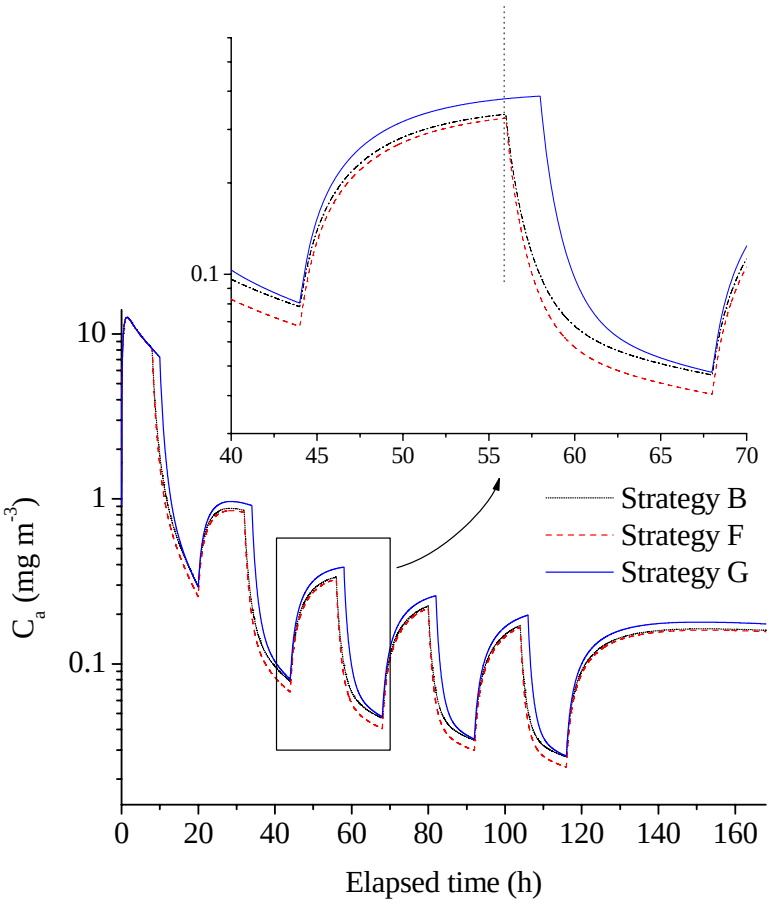

Figure 7.19 Effect of lag-time provision of ventilation on indoor VOCs concentration

Strategy G is almost the same as strategy F, except employing a 2-hour lag-time. It can be found that the delay makes the resultant indoor VOCs concentration the highest during the working-hours among strategies B, F and G, though the outdoor airflow rate for strategy G (10 L/s) is larger than that for strategy B (7.5 L/s). This reminds us that when implementing ventilation strategies like lag-time provision of ventilation based on monitored indoor CO_2 concentration (occupant related source), special attention should be paid to the concentration of other contaminants like VOCs (mainly building related source) because the concentrations of the building related sources may continuously build up during the lag time. An energy efficient ventilation strategy should assure the concentrations of both types of contaminants below the recommended levels. Considering the health effects of many VOCs found

indoors are incompletely understood, and the guidelines for individual VOCs are not available, the TVOC concentration can be used as the other simple indicator of the indoor air quality with cautions, though there are still some debates with respect to the applications of the TVOC concept (Molhave and Nielsen, 1992; Wolkoff and Nielsen, 2001).

It is known that the emission rate or emission factor of VOCs from building material firstly increases to a peak and then decays continuously when constant flowrate of outdoor air is provided. How the behavior of emission factor would change with the circulation of on/off scheme of HVAC system is an interesting question. Since the behaviors of emission factors for different intermittent ventilation strategies are similar, for instance, emission factors from sidewalls, ceiling and floor for strategy B are computed. The results are presented in Figure 7.20. It can be seen that all the indoor surfaces present sudden increases in emission factor at the starting-up of the air conditioning system in the early morning. This may be caused by the sudden provision of ventilation - consequently relatively large convective mass transfer coefficient is resulted. In contrast, opposite phenomenon is observed when the HVAC system is switched from state ‘on’ to ‘off’.

It can also be found that most of the indoor surfaces become VOCs sources after the starting-up of the HVAC system, and some of the sorptive components may re-adsorb VOCs during the HVAC shut-off period. Actually, the interactions between the indoor air and the indoor surfaces are very complicated. The operation of the building, the pollutant sources and the physical and chemical processes affecting the pollutants all affect the efficacy of ventilation for controlling VOCs concentrations. Source control measures, in addition to adequate ventilation, are required to limit concentrations of VOCs in indoor environment (Hodgson et al., 2003).

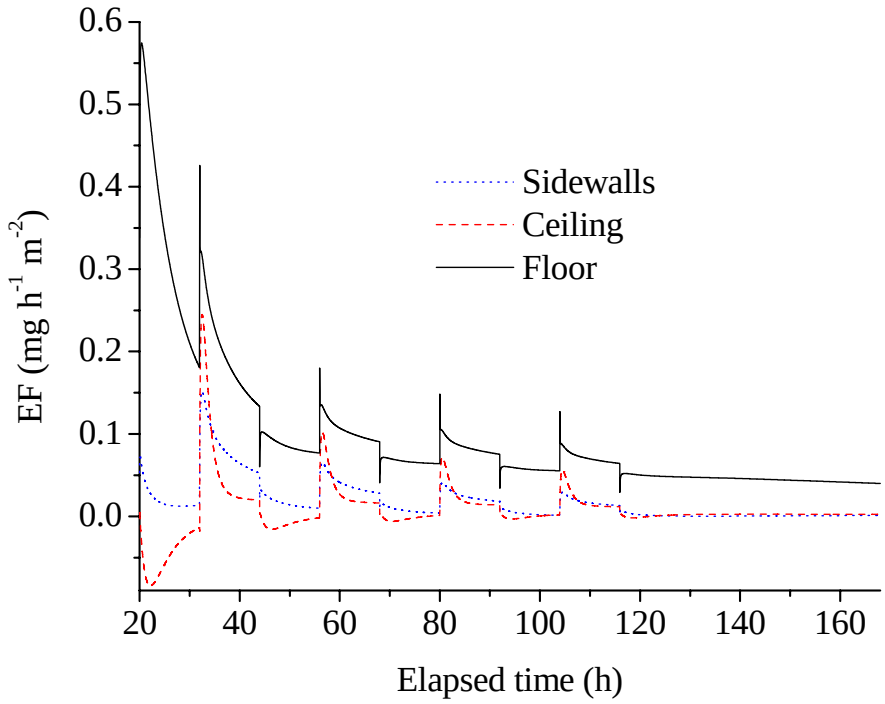

Figure 7.20 Behaviors of emission factors under intermittent ventilation mode (e.g. strategy B)

Pollutant emission control strategies cannot rely solely on mechanical ventilation to achieve acceptable indoor air quality, as an increase in fresh air change rate is not necessarily accompanied by a corresponding decrease in indoor pollutant concentrations. The air cleaner may serve as a supplement to source control and ventilation. Figure 7.21 is a simulation result of the effect of gaseous air cleaner on indoor VOCs concentration, where a constant efficiency of the air cleaner is assumed. The air cleaners for removing particles are usually very effective, while the efficiencies of those designed for removing gaseous pollutants vary greatly from product to product and from VOC to VOC, limited test data can be found in (Niu et al., 1998; Chen et al., 2005). In general, the effectiveness of the existing gaseous air cleaners is unsatisfactory. In addition, no air-cleaning systems are expected to totally eliminate all hazards from gaseous pollutants and these systems may have a limited lifetime before replacement is necessary (EPA, 1990). There is still a long way for

the designers to go to design gaseous air cleaners that have high efficiencies and are designed to handle large amounts of air, yet have longer lifetime.

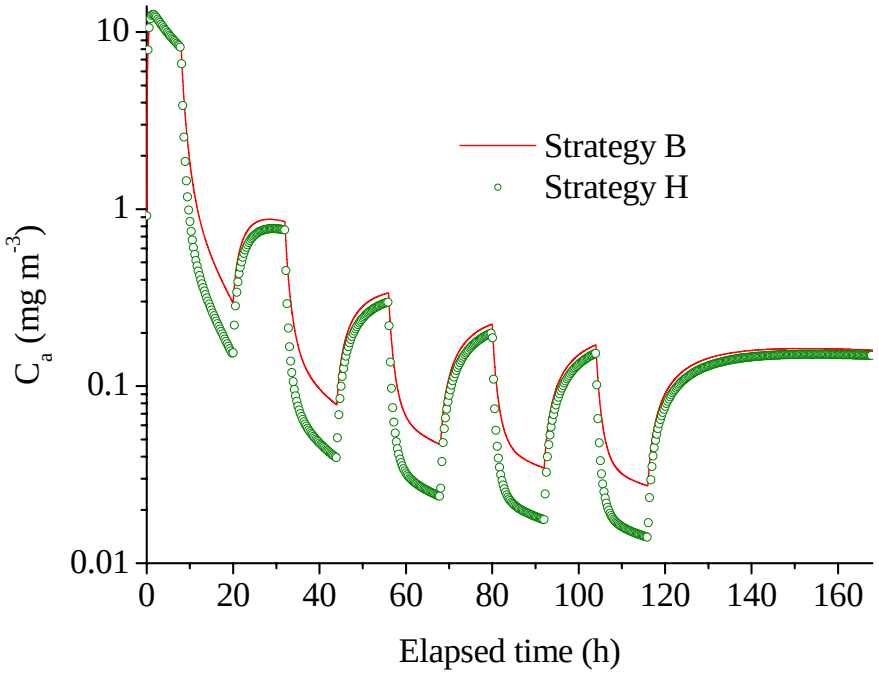

Figure 7.21 Effect of gaseous air cleaner on indoor VOCs concentration

7.6 Summary

There used to be two branches in modeling indoor VOCs concentrations. One typical method is simply assuming a constant VOCs emission rate from building materials and the focus is put on the ventilation side. In contrast, other models concentrate more on the emission mechanisms; this type of model is originally developed for environmental chamber study and usually assumes a constant air change rate. Considering the real situations in a room, it is easy to see both methods have their limitations. A conjunction of the two types of models would be a better choice. In this study, a comprehensive model based on fundamental mass transfer theories is developed. The model can be used to simulate VOCs emissions from building materials in their actual use conditions. The variation of the indoor VOCs concentration against the time is the result of diffusion/sorption within individual

layers of materials and interaction of the indoor air with interior building material surfaces under a certain ventilation scheme. Sometimes, an air cleaner may be used indoors to further reduce the VOCs concentration; the model also takes this aspect into consideration.

Numerical studies reveal that the required indoor VOCs concentration can be achieved by different ventilation strategies but the corresponding energy consumption may vary widely. Improper provision pattern of ventilation would put people at far greater risk of SBS or BRI. Pre-occupancy flush-out after construction or renovation can sharply reduce the building related contaminants' concentration. Provision of ventilation several hours before the occupancy in the morning is another effective way to provide people with good indoor air. The proposed model is useful in analyzing the levels of contaminant buildup that would occur during no ventilation period for intermittent ventilation situations and in determining the amount of outdoor air and the lead-time hours required to flush out the contaminants to attain an acceptable level prior to occupancy. Portable air cleaner is also a valuable supplemental equipment to further reduce the indoor VOCs concentration, providing that difficulties in high efficiency, capable of handling large amounts of air and long lifetime can be addressed successfully.

Chapter 8
Conclusions and Recommendations

8.1 Conclusions

A simplified yet mass transfer theory based model is developed for the prediction of VOCs emissions from wet materials like paints. Good agreement is found between experimental data and model predictions. Numerical studies show that: 1) when the air change rate is kept constant, increasing the air velocity over the material surface results in an increased peak VOCs concentration but a lowered VOCs concentration at late times; 2) when the local air velocity is kept unchanged, increase the air change rate causes sharply reduced VOCs concentration, especially in the first day or so, the effect is insignificant thereafter; 3) it is no doubt that source control is the most cost-effective way to reduce indoor VOCs concentration; 4) substrate effect makes the indoor VOCs concentration firstly decreased and then elevated compared with no substrate situations. The larger the diffusion and partition coefficients, the more significant the substrate effect is. The influence of a change in partition coefficient is virtually insignificant below a value of 1000; 5) indoor VOCs concentration is very likely to build up during the time of no ventilation provided. In addition, the overall indoor concentration resulted from intermittent ventilation is much higher than that from continuous ventilation. For the latter case, the indoor TVOC concentration is lower than the guideline good level after 233 hours' flushing, while for the former case, the indoor TVOC concentration is still well above that level beyond the simulation period (240 hours). Thus it is recommended that pre-occupancy flush-out after building construction and daily in the early morning be conducted to attain an acceptable VOCs concentration level when the occupancy begins.

An inverse method for the determination of diffusion and partition coefficients of dry building materials is developed. The stability and uniqueness of the inverse method is investigated by using generated measurements. Factors that affect the accuracy of the determination are parametrically investigated. Results indicate that: 1) measurements containing random errors only slightly affect the accuracy of inverse determination; 2) both of the number of measurements and the intervals of measurements have significant influences on the accuracy of determination. Optimizing the intervals of measurements and increasing the number of measurements will give rise to more accurate results; 3) the error containing in the estimated mean convective mass transfer coefficient hardly has any effects on the accuracy of determining diffusion coefficient but has substantial influences on the accuracy of determining partition coefficient; 4) the error containing in the initial VOCs concentration has greatest impacts on the accuracy of determined parameters. The determined partition coefficient decreases while diffusion coefficient increases rapidly with the increasing error of underestimation of initial VOCs concentration. Two experimental methods - emission test method for source materials and sorption test method for sink materials or substrate materials are developed to determine the two parameters of VOCs/dry building materials. Both tests are conducted in a standard FLEC, VOCs concentration profiles of the exhaust air are then analyzed by the inverse algorithm. The obtained parameters are comparable to those determined by other researchers through other methods and are believed to be more accurate because the model developed here is fully based on fundamental mass transfer theories.

A model taking into account non-uniform initial VOCs concentration in dry building material is developed. Numerical studies show that for thick materials with small

diffusion coefficients the effect of non-uniform distributions can not be neglected, in particular for short-term predictions. Therefore, an inverse function estimation method called conjugate gradient method with adjoint problem is developed to figure out the actual pattern of VOCs within the dry material with the aid of the measured VOCs concentration in bulk air in a chamber or cell. The method is validated by successfully recovering different types of pre-defined distributions. The whole process can be non-destructive when the proposed method is utilized in conjunction with non-destructive test facility - FLEC.

Since building materials usually appear in composite forms, a multi-layer model is developed to predict VOCs emission from a material assembly composed of different layers (either porous or non-porous materials). The model takes HVAC system into consideration, e.g., intermittent or continuous ventilation, recirculation air, in-duct air filtration etc. The model is validated by comparing predictions resulted from the proposed model and a double layer analytical model developed by other researchers. Numerical investigations show that the behavior and overall level of VOCs concentration are totally different for intermittent and continuous ventilation, which, in turn, demonstrates the importance of taking ventilation mode into consideration. At a fixed fraction of recirculation air, the higher the filter efficiency, the lower the level of overall indoor VOCs concentration and the less fluctuant of the VOCs concentration. It is also found that adding a cleaner barrier layer onto the top of the source material layer may greatly reduce the resultant indoor VOCs concentration.

A comprehensive model for the characterization of VOCs source/sink behaviors of building materials is developed. It is an extension of the one component multi-layer model to a multi-component multi-layer model. Thus the model can be used to simulate VOCs emission from building materials in their actual use conditions so

that the impact of material emissions on indoor air quality can be evaluated without doing costly experiments. Numerical studies show that pre-occupancy flush-out after construction or renovation and provision of ventilation several hours before the occupancy in the early morning are promising ways to provide people with good indoor air. The proposed model can also be used to predict the levels of contaminant buildup that would occur during no ventilation period for intermittent ventilation mode. It can also be used to determine the flow rate of outdoor air and the lead-time hours required to flush out the contaminants to an acceptable level prior to occupancy. Portable air cleaner is a valuable supplemental tool in further reducing the indoor VOCs concentration, providing that difficulties in high efficiency, capable of handling large amounts of air and long lifetime can be addressed successfully.

The outcomes of the studies reported in this thesis provide a routine tool for architects, designers, builders, building operators and occupants for indoor VOCs control. Many emission testing data are available from the literature, which can be compiled into a database if the data are normalized using the developed mass-transfer model. The database will provide a reference for the set-up of criteria for screening products. For the manufactures, the effect of the product formulation on the product emission becomes more explicit, which gives a guide on product improvement via reformulation. The effects of various IAQ management strategies can be quantitatively estimated with the potential health impacts assessed at the same time. These will eventually lead to improved IAQ and reduced adverse impacts on people's health and productivity.

8.2 Recommendations

A number of future studies following on the successful competition of the work reported in this thesis are detailed as follows:

More experimental studies for paint are to be conducted, for example the substrate effects and long-term emissions. The model can then be further validated. At this stage, the standard FLEC can still be used. Next, experimental studies should be concentrated on the effects of the presence of other sorptive materials on VOCs emissions from paint to mimic real indoor conditions. At this stage, tests should be conducted in a small-scale chamber or even in a full-scale chamber. Accordingly, mathematical model to be able to simulate this kind of situation would be developed and validated.

Lack of model parameters are the key factor that constraints the use of numerical models. Since there are thousands of different VOCs and building materials, it is almost impossible to experimentally measure the emission parameters for every VOC/material combination. Some researchers have tried to correlate diffusion coefficients with VOC's molecular weight and partition coefficient with VOC's vapor pressure for a same category of building materials. But recent studies show that the microstructures of materials in a same category may vary greatly. Thus the emission parameters in general should be related to both chemical properties of VOC and physical properties of building materials. So, the multi-phase model developed on a microcosmic scale in this thesis appears to be most useful in this aspect. More experimental studies should be conducted. Method capable of analyzing microstructures of building materials should also be adopted. Broad collaborations

with other laboratories are helpful to save both time and expenses by sharing experimental data.

The moisture conditions within the building materials and bulk air have been identified to have great impacts on the emission/sorption of VOCs. As a pilot study, single VOC may be firstly investigated. Experimental studies should be carried out to reveal the mechanisms of combined moisture and VOC mass transport within the building materials. This would be a multidisciplinary work project which may require chemical backgrounds. Then mathematical model is to be developed to quantify the combined moisture and VOC mass transfer. On the basis of the pilot study, further studies may be concentrated on the influence of VOCs mixture on the combined moisture and VOCs mass transfer. Similarly, mathematical model is expected to be proposed to describe the mass transfer processes. So that more accurate predictions of VOCs emission from building materials in their actual use conditions can be available.

Actually, to date, most of the models are developed and validated using small test chambers or FLECs. In order to determine their utilities for predicting indoor concentrations, it is important to validate the models in realistic environments. Scale-up validation process can first be implemented in large chambers and then in test houses. Problems exposed during the two-stage model scale-up validation processes should be resolved before the model can be practically used in reality.

A user-friendly input and output interface of the IAQ model should be developed for ease of applying the model. Common construction materials and their properties, and ventilation strategies should be built-in so that the ordinary users can use it just by

clicking the mouse. The package should also allow adding or customizing items like material properties and ventilation schemes for the expert users.

References

Afshari, A., Gunnarsen, L., Clausen, P. A. et al., 2004. Emission of phthalates from PVC and other materials. Indoor Air 14, 120-128.

Alifanov, O. M., 1994. Inverse Heat Transfer Problems, New York : Springer-Verlag, Berlin.

An, Y., Zhang, J. S., Shaw, C. Y., 1999. Measurements of VOC adsorption/desorption characteristics of typical interior building materials. HVAC and R Research 5, 297-316.

ASTM, 1990. Standard Guide for Small-Scale Environmental Chamber Determinations of Organic Emissions from Indoor Materials/products. ASTM D5116-97.

Axley, J. W., 1991. Adsorption Modelling for Building Contaminant Dispersal Analysis. Indoor Air 1, 147-171.

Axley, J. W., Lorenzetti, D., 1993. Sorption Transport Models for Indoor Air Quality Analysis, In: Modeling of Indoor Air Quality and Exposure, ASTM STP 1205, N. L. Nagda (Ed.), American Society for Testing and Materials, Philadelphia, 105-127.

Bako-Biro, Z., Wargocki, P., Weschler, C. J. et al., 2004. Effects of pollution from personal computers on perceived air quality, SBS symptoms and productivity in offices. Indoor Air 14, 178-187.

Beck, J. V., Arnold, K. J., 1977. Parameter estimation in engineering and science, Wiley, New York.

Bendada, A., Nguyen, K. T., 1999. Estimation of the initial temperature profile and the heat transfer coefficient in polymer processing by an inverse method. In: ASME Proceedings of the International Conference on Inverse Problems in Engineering: Theory and Practice, PortLudlow, WA: 355- 361.

Berglund, B., Johansson, I., Lindvall, T., 1989. Volatile organic compounds from used building materials in a simulated chamber study. Environment International 15, 383-387.

Blondeau, P., Tiffonnet, A. L., Damian, A. et al., 2003. Assessment of contaminant diffusivities in building materials from porosimetry test. Indoor Air 13, 302-310.

Bodalal, A., Zhang, J. S., Plett, E. G., 2000. A method for measuring internal diffusion and equilibrium partition coefficients of volatile organic compounds for building materials. Building and Environment 35, 101-110.

Bodalal, A., Zhang, J. S., Plett, E. G. et al., 2001. Correlations between the internal diffusion and equilibrium partition coefficients of volatile organic compounds (VOCs) in building materials and the VOC properties. ASHRAE Transactions 107, 789-800.

Borazzo, J. E., Davidson, C. I., Andelman, J. B., 1990. Sorption of organic vapours to indoor surfaces of synthetic and natural fibrous materials. In: Proceedings of Indoor Air '90, Ottawa, Canada: Mortgage and Housing Corporation: 3, 617-622.

Bouhamra, W., Elkilani, A., 1999. Development of a Model for the Estimation of Indoor Volatile Organic Compounds Concentration Based on Experimental Sorption Parameters. Environmental Science & Technology 33, 2100-2105.

Brown, S. K., 1999. Chamber Assessment of Formaldehyde and VOC Emissions from Wood-Based Panels. Indoor Air 9, 209-215.

Brunauer, S., 1945. The adsorption of gases and vapors, vol. 1, Princeton University Press, Princeton, NJ.

CEC-Commission of the European Communities, 1998. Building products-determination of the emission of volatile organic compounds--Part2: Emission test cell method. PreENV 13419-2, European Committee for Standardization, Brussels.

Chang, J. C. S., Guo, Z., 1992. Characterization of Organic Emissions from a Wood Finishing Product - Wood Stain. Indoor Air 2, 146-153.

Chang, J. C. S., Guo, Z., 1994. Modeling of Alkane Emissions from a Wood Stain. Indoor Air 4, 35-39.

Chang, J. C. S., Sparks, L. E., Guo, Z. et al., 1998. Evaluation of Sink Effects on VOCs from a Latex Paint. J. Air & Waste Manage. Assoc. 48, 953-958.

Chang, J. C. S., Tichenor, B. A., Guo, Z. et al., 1997. Substrate Effects on VOC Emissions from a Latex Paint. Indoor Air 7, 241-247.

Chau, C. K., Tu, E. Y., Chan, D. W. T. et al., 2002. Estimating the total exposure to air pollutants for different population age groups in Hong Kong. Environment International 27, 617-630.

Chen, W., Zhang, J. S., Zhang, Z., 2005. Performance of Air Cleaners for Removing Multiple Volatile Organic Compounds in Indoor Air. ASHRAE Transactions 111, 635-645.

Chiwiacowsky, L. D., Velho, H. F. d. C., 2003. Different approaches for the solution of a backward heat conduction problem. Inverse Problems in Science and Engineering 11, 471 - 494.

Choy, B., Reible, D. D., 2000. Diffusion models of environmental transport, Lewis Publishers, Boca Raton, Fla.

Christiansson, J., Yu, J.-W., Neretnieks, I., 1993. Emission of VOC's from PVC-floorings - models for predicting the time dependent emission rates and resulting concentration in the indoor air. In: Proceedings of Indoor Air '93: The 6th International Conference on Indoor Air Quality and Climate, 4-8 July 1993, Helsinki, Finland: Vol. 1, 987-992.

Clark, M. M., 1996. Transport Modeling for Environmental Engineers and Scientists, Wiley, New York.

Clausen, P. A., 1993. Emission Of Volatile And Semivolatile Organic Compounds From Waterborne Paints - The Effect Of The Film Thickness. Indoor Air 3, 269-275.

Clausen, P. A., Wolkoff, P., Hoist, E. et al., 1991. Long-term Emission of Volatile Organic Compounds from Waterborne Paints - Methods of Comparison. Indoor Air 1, 562-576.

Colaco, M. J., Orlande, H. R. B., 1999. Comparison of different versions of the conjugate gradient method of function estimation. Numerical Heat Transfer Part A: Applications 36, 229-249.

Colombo, A., Bortoli, M., Knoppel, H. et al., 1993. Adsorption Of Selected Volatile Organic Compounds On A Carpet, A Wall Coating, And A Gypsum Board In A Test Chamber. Indoor Air 3, 276-282.

Colombo, A., De Bortoli, M., Pecchio, E. et al., 1990. Chamber testing of organic emission from building and furnishing materials. The Science of The Total Environment 91, 237-249.

Cox, S. S., Little, J. C., Hodgson, A. T., 2001a. Measuring Concentrations of Volatile Organic Compounds in Vinyl Flooring. Journal of the Air & Waste Management Association 51, 3823-3830.

Cox, S. S., Little, J. C., Hodgson, A. T., 2002. Predicting the emission rate of volatile organic compounds from vinyl flooring. Environmental Science and Technology 36, 709-714.

Cox, S. S., Zhao, D., Little, J. C., 2001b. Measuring partition and diffusion coefficients for volatile organic compounds in vinyl flooring. Atmospheric Environment 35, 3823-3830.

Crank, J., 1975. The mathematics of diffusion, Clarendon Press, Oxford.

Dantas, L. B., Orlande, H. R. B., 1996. A function estimation approach for determining temperature-dependent thermophysical properties. Inverse Problems in Engineering 3, 261-279.

De Bortoli, M., Knoppel, H., Columbo, A. et al., 1996. Attempting to characterize the sink effect in a small stainless stell test chamber, In: Characterizing sources of indoor air pollution and related sink effects, B. A. Tichenor (Ed.), ASTM (STP;1287), West Conshohocken, PA, 305-318.

Deng, B., Kim, C. N., 2004a. An analytical model for VOCs emission from dry building materials. Atmospheric Environment 38, 1173-1180.

Deng, B., Kim, C. N. C. N., 2004b. Physical-based double-exponential model for VOCs emission from carpet. Atmospheric Environment 38, 4085-4089.

Elkilani, A. S., Baker, C. G. J., Al-Shammari, Q. H. et al., 2003. Sorption of volatile organic compounds on typical carpet fibers. Environment International 29, 575-585.

Ellacott, M. V., Reed, S., 1999. Development of Robust Indoor Air Quality Models for the Estimation of Volatile Organic Compound Concentrations in Buildings. Indoor and Built Environment 8, 345-360.

Engvall, K., Wickman, P., Norback, D., 2005. Sick building syndrome and perceived indoor environment in relation to energy saving by reduced ventilation flow during heating season: a 1 year intervention study in dwellings. Indoor Air 15, 120-126.

EPA, 1994. Indoor Air Pollution: An Introduction for Health Professionals. The American Lung Association (ALA), The Environmental Protection Agency (EPA), The Consumer Product Safety Commission (CPSC), and The American Medical Association (AMA).

Fanger, P. O., 2000. Indoor Air Quality in the 21st Century: Search for Excellence. Indoor Air 10, 68-73.

Foarde, K. K., Myers, E. A., Hanley, J. T. et al., 1997. Methodology to Perform Clean Air Delivery Rate Type Determinations with Microbiological Aerosols. Aerosol Science and Technology 30, 235-245.

Girman, J. R., Hodgson, A. T., Newton, A. S. et al., 1986. Emissions of volatile organic compounds from adhesives with indoor applications. Environment International 12, 317-321.

Gudmundsson, K., 2003. An approach to determining the water vapour transport properties of building materials. Nordic Journal of Building Physics 3, 1-10.

Gunnarsen, L., Nielsen, P. A., Wolkoff, P., 1994. Design and Characterization of the CLIMPAQ, Chamber for Laboratory Investigations of Materials, Pollution and Air Quality. Indoor Air 4, 56-62.

Guo, H., Murray, F., 2000. Characterization of total volatile organic compound emissions from paints. Clean Products and Processes 2, 28-36.

Guo, H., Murray, F., Wilkinson, S., 2000. Evaluation of Total Volatile Organic Compound Emissions from Adhesives Based on Chamber Tests. Journal of the Air & Waste Management Association 50, 199-206.

Guo, Z., 2002. Review of indoor emission source models. Part 1. Overview. Environmental Pollution 120, 533-549.

Guo, Z., Chang, J. C. S., Sparks, L. E. et al., 1999. Estimation of the rate of VOC emissions from solvent-based indoor coating materials based on product formulation. Atmospheric Environment 33, 1205-1215.

Guo, Z., Fortman, R., Marfiak, S. et al., 1996. Modeling and VOC emissions from interior latex paint applied to gypsum board. In: Proceedings of the 7th International Conference on Indoor Air Quality and Climate, Nagoya, Japan: Vol.1, 987- 991.

Haghighat, F., Donnini, G., 1993. Emissions of indoor pollutants from building materials - state of the art review. Architectural Science Review 36, 13-22.

Haghighat, F., Huang, H., 2003. Integrated IAQ model for prediction of VOC emissions from building material. Building and Environment 38, 1007-1017.

Haghighat, F., Huang, H., Lee, C.-S., 2005. Modeling Approaches for Indoor Air VOC Emissions from Dry Building Materials - A Review. ASHRAE Transactions 111, 635-645.

Haghighat, F., Lee, C. S., Ghaly, W., 2002. Measurement of diffusion coefficients of VOCs for building materials: review and development of a calculation procedure. Indoor Air 12, 81-91.

Hansson, P., Stymne, H., 2000. Voc Diffusion and Absorption Properties of Indoor Materials - Consequences for Indoor Air Quality. In: Proceedings of Healthy Buildings, Espoo - Finland: 4, 151 - 156.

He, G., Yang, X., 2005. On regression method to obtain emission parameters of building materials. Building and Environment 40, 1282-1287.

He, G., Yang, X., Shaw, C. Y., 2005. Material Emission Parameters Obtained Through Regression. Indoor and Built Environment 14, 59-68.

Hodgson, A. T., Faulkner, D., Sullivan, D. P. et al., 2003. Effect of outside air ventilation rate on volatile organic compound concentrations in a call center. Atmospheric Environment 37, 5517-5527.

Hodgson, A. T., Wooley, J. D., Daisey, J. M., 1993. Emissions of volatile organic compounds from new carpets measured in a large-scale environmental chamber. Journal of the Air & Waste Management Association 43, 316-324.

Huang, H., 2003. Modeling of volatile organic compounds emissions and sinks from building materials. Ph.D. Thesis, Concordia University, Montreal, Quebec,Canada.

Huang, H., Haghighat, F., 2002. Modelling of volatile organic compounds emission from dry building materials. Building and Environment 37, 1127-1138.

James, J. P., Yang, X., 2005. Emissions of Volatile Organic Compounds from Several Green and Non-Green Building Materials: A Comparison. Indoor and Built Environment 14, 69-74.

Jørgensen, R. B., Bjørseth, O., 1999. Sorption behaviour of volatile organic compounds on material surfaces - the influence of combinations of compounds and materials compared to sorption of single compounds on single materials. Environment International 25, 17-27.

Jørgensen, R. B., Bjørseth, O., Malvike, B., 1999. Chamber testing of adsorption of volatile organic compounds (VOCs) on material surfaces. Indoor Air 9, 2-9.

Jørgensen, R. B., Dokka, T. H., Bjørseth, O., 2000. Introduction of a Sink-Diffusion Model to Describe the Interaction between Volatile Organic Compounds (VOCs) and Material Surfaces. Indoor Air 10, 27-38.

Jones, A. P., 1999. Indoor air quality and health. Atmospheric Environment 33, 4535-4564.

Kephalopoulos, S., Knoeppel, H., De Bortoli, M., 1996. Testing of sorption and desorption of selected VOC on/from indoor materials. In: Proceedings of Indoor Air '96: The 7th International Conference on Indoor Air Quality and Climate, July 21-26, Nagoya, Japan: Vol. 2, 61-66.

Kirchner, S., Badey, J. R., Knudsen, H. N. et al., 1999. Sorption capacities and diffusion coefficients of indoor surface materials exposed to VOCs: proposal of new test procedures. In: Proceedings of Indoor Air '99: The 8th International Conference on Indoor Air Quality and Climate, August 8-13, 1999, Edinburgh, Scotland: 1, 430-435.

Kjaer, U., Nielsen, P. A., 1991. Adsorption and desorption of organic compounds on fleecy materials. In: Proceedings of IAQ 91: Healthy Buildings, Atlanta, GA: ASHRAE: Vol. 1, 285-288.

Klepeis, N. E., Nelson, W. C., Ott, W. R. et al., 2001. The National Human Activity Pattern Survey (NHAPS): a resource for assessing exposure to environmental pollutants. Journal of Exposure Analysis & Environmental Epidemiology 11, 231-252.

Knudsen, H. N., Kjaer, U. D., Nielsen, P. A. et al., 1999. Sensory and chemical characterization of VOC emissions from building products: impact of concentration and air velocity. Atmospheric Environment 33, 1217-1230.

Kumar, D., Little, J. C., 2003a. Characterizing the source/sink behavior of double-layer building materials. Atmospheric Environment 37, 5529-5537.

Kumar, D., Little, J. C., 2003b. Single-Layer Model To Predict the Source/Sink Behavior of Diffusion-Controlled Building Materials. Environmental Science & Technology 37, 3821-3827.

Kumar, D., Little, J. C., Cox, S. S., 2001. Modeling the source/sink behavior of diffusion-controlled Materials. In: Proceedings of the Air & Water Management Association's (A&WMA) 94th Annual Conference and Exhibition, Pittsburg, PA: Session No. AB-79.

Lee, C.-S., 2003. A Theoretical Study on VOC Source and Sink Behavior of Porous Building Materials. Ph.D. Thesis, Concordia University, Montreal, Quebec, Canada.

Lee, C.-S., Ghaly, W. S., Haghighat, F., 2003. VOC source and sink behaviour of porous building materials: Part I - model development and assessment. In: Proceedings of Healthy Buildings 2003, December 7-11, Department of Building, National University of Singapore, Singapore: 355-360.

Lee, C.-S., Haghighat, F., Ghaly, W. S., 2005. A study on VOC source and sink behavior in porous building materials - analytical model development and assessment. Indoor Air 15, 183-196.

Lee, H. L., Yang, Y. C., 2003. Function estimation in predicting time-dependent heat flux of an annular fin. IJournal of Thermal Stresses 26, 799-813.

Leovic, K., Whitaker, D., Northeim, C. et al., 1998. Evaluation of a Test Method for Measuring Indoor Air Emissions from Dry-Process Photocopiers. Journal of the Air & Waste Management Association 48, 915-923.

Li, F., Niu, J., 2005a. An inverse approach for estimating the initial distribution of volatile organic compounds in dry building material. Atmospheric Environment 39, 1447-1455.

Li, F., Niu, J., 2005b. Simultaneous estimation of VOCs diffusion and partition coefficients in building materials via inverse analysis. Building and Environment 40, 1366-1374.

Li, H., Yang, M., Zhang, J. S. et al., 2005. Measurements and Modeling of VOC Emissions from a Large Wall Assembly of Typical Wood-Framed Residential Houses. ASHRAE Transactions 111, 210-217.

Little, J. C., Hodgson, A. T., 1996. Strategy for characterizing homogeneous, diffusion-controlled, indoor sources and sinks, In: Characterizing sources of indoor air pollution and related sink effects, B. A. Tichenor (Ed.), ASTM (STP;1287), West Conshohocken, PA, 294-304.

Little, J. C., Hodgson, A. T., Gadgil, A. J., 1994. Modeling emissions of volatile organic compounds from new carpets. Atmospheric Environment 28, 227-234.

Low, J. M., Zhang, J. S., Plett, E. G. et al., 1998. Effects of airflow on emissions of volatile organic compounds from carpet-adhesive assemblies. ASHRAE Transactions 104, 1281-1288.

Luo, R., Niu, J. L., 2004. Determination of water vapor diffusion and partition coefficients in cement using one FLEC. International Journal of Heat and Mass Transfer 47, 2061-2072.

Marquardt, D. W., 1963. An Algorithm for Least-Squares Estimation of Nonlinear Parameters. Journal of the Society for Industrial and Applied Mathematics 11, 431-441.

Masel, R. I., 1996. Principles of adsorption and reaction on solid surfaces, John Wiley & Sons, Inc., New York.

McCrillis, R. C., Howard, E. M., Guo, Z. et al., 1999. Characterization of Curing Emissions from Conversion Varnishes. Journal of the Air & Waste Management Association 49, 70-75.

Meininghaus, R., Gunnarsen, L., Knudsen, H. N., 2000a. Diffusion and Sorption of Volatile Organic Compounds in Building Materials-Impact on Indoor Air Quality. Environmental Science & Technology 34, 3101 - 3108.

Meininghaus, R., Kirchner, S., Maupetit, F. et al., 2000b. Gravimetric Studies on VOC Adsorption by Indoor Materials under Near-Ambient Conditions. Indoor and Built Environment 9, 277-283.

Meininghaus, R., Salthammer, T., Knıppel, H., 1999. Interaction of volatile organic compounds with indoor materials - a small-scale screening method. Atmospheric Environment 33, 2395-2401.

Meininghaus, R., Uhde, E., 2002. Diffusion studies of VOC mixtures in a building material. Indoor Air 12, 215-222.

Mendell, M. J., 1993. Non-Specific Symptoms In Office Workers: A Review And Summary Of The Epidemiologic Literature. Indoor Air 3, 227-236.

Mendell, M. J., 2003. Indices for IEQ and building-related symptoms. Indoor Air 13, 364-368.

Mendell, M. J., Heath, G. A., 2005. Do indoor pollutants and thermal conditions in schools influence student performance? A critical review of the literature. Indoor Air 15, 27-52.

Molhave, L., 1989. The sick buildings and other buildings with indoor climate problems. Environment International 15, 65-74.

Molhave, L., 1991. Volatile Organic Compounds, Indoor Air Quality and Health. Indoor Air 1, 357-376.

Molhave, L., Nielsen, G. D., 1992. Interpretation and Limitations of the Concept "Total Volatile Organic Compounds" (TVOC) as an Indicator of Human

Responses to Exposures of Volatile Organic Compounds (VOC) in Indoor Air. Indoor Air 2, 65-77.

Murakami, S., Kato, S., Ito, K. et al., 2001. Distribution of chemical pollutants in a room based on CFD simulation coupled with emission/sorption analysis. ASHRAE Transactions 107, 812-820.

Murakami, S., Kato, S., Ito, K. et al., 2003. Modeling and CFD prediction for diffusion and adsorption within room with various adsorption isotherms. Indoor Air 13, 20-27.

Neretnieks, I., Christiansson, J., Romero, L. et al., 1993. Modelling of Emission and Re-emission of Volatile Organic Compounds from Building Materials with Indoor Air Applications. Indoor Air 3, 2-11.

Nielsen, P. V., 1974. Flow in air conditioned rooms (model experiments and solution of the flow equation). Ph.D. Thesis, Danish Technical University, Copenhagen, Denmark.

Niu, J. L., Burnett, J., 2001. Setting up the criteria and credit-awarding scheme for building interior material selection to achieve better indoor air quality. Environment International 26, 573-580.

Niu, J. L., Tung, T. C. W., Chui, V. W. Y., 1998. Using large environmental chamber technique for gaseous contaminant removal equipment test. ASHRAE Transactions 104, 1289-1296.

Oliver, L. C., Shackleton, B. W., 1998. The indoor air we breathe: a public health problem of the 90s. Public Health Reports 113, 398-409.

Ozisik, M. N., 1993. Heat Conduction, 2nd. John Wiley & Sons, New York.

Ozisik, M. N., Orlande, H. R. B., 2000. Inverse Heat Transfer- Fundamentals and Applications, Taylor and Francis, New York, USA.

Park, I.-S., Do, D. D., 1996. Measurement of the Effective Diffusivity in Porous Media by the Diffusion Cell Method. Catal. Rev.-Sci. Eng. 38, 189-247.

Peter, G., 1998. Diffusion in natural porous media: contaminant transport, sorption/desorption and dissolution kinetics, Kluwer Academic Publishers, Boston, Mass.

Popa, J., Haghighat, F., 2003. The impact of VOC mixture, film thickness and substrate on adsorption/desorption characteristics of some building material. Building and Environment 38, 959-964.

Rafson, H. J. (Ed.), 1998. Odor and VOC control Handbook, McGraw-Hill, New York.

Reed, C. H., Nabinger, S. J., Emmerich, S. J., 2002. Measurement and simulation of the indoor air quality impact of gaseous air cleaners in test home. In: Proceedings, Indoor Air 2002, 9th International Conference on Indoor Air Quality and Climate, June 30-July 5, Monterey, California: 652- 657.

Salthammer, T., 1997. Emission of Volatile Organic Compounds from Furniture Coatings. Indoor Air 7, 189-197.

Seppanen, O., Fisk, W. J., 2002. Association of ventilation system type with SBS symptoms in office workers. Indoor Air 12, 98-112.

Silva, G. V., Fernandes, E. O., Vasconcelos, M. T. S. D. et al., 2003. Adsorption/Desorption of Volatile Organic Compounds by Uncoated Cork Parquet. In: Healthy Buildings 2003: 7th International Conference Energy-Efficient Healthy Buildings, 7-11th December, School of Design & Environment, National University of Singapore, Singapore: 414-419.

Singer, B. C., Revzan, K. L., Hotchi, T. et al., 2004. Sorption of organic gases in a furnished room. Atmospheric Environment 38, 2483-2494.

Sparks, L. E., 2001. Indoor Air Quality Modeling, In: IIndoor Air Quality Handbook, J. D. Spengler, J. M. Samet and J. F. McCarthy (Eds.), McGraw-Hill, New York,

Sparks, L. E., Guo, Z., Chang, J. C. et al., 1999a. Volatile Organic Compound Emissions from Latex Paint - Part 1. Chamber Experiments and Source Model Development. Indoor Air 9, 10-17.

Sparks, L. E., Guo, Z., Chang, J. C. et al., 1999b. Volatile Organic Compound Emissions from Latex Paint - Part 2. Test House Studies and Indoor Air Quality (IAQ) Modeling. Indoor Air 9, 18-25.

Sparks, L. E., Tichenor, B. A., Chang, J. et al., 1996. Gas-Phase Mass Transfer Model for Predicting Volatile Organic Compound (VOC) Emission Rates from Indoor Pollutant Sources. Indoor Air 6, 31-40.

Tichenor, B. A., 1996. Overview of source/sink characterization methods, In: Characterizing sources of indoor air pollution and related sink effects, B. A. Tichenor (Ed.), ASTM (STP;1287), West Conshohocken, PA, 9-19.

Tichenor, B. A., Guo, Z., Dunn, J. E. et al., 1991. The Interaction of Vapour Phase Organic Compounds with Indoor Sinks. Indoor Air 1, 23-35.

Tichenor, B. A., Guo, Z., Sparks, L. E., 1993. Fundamental Mass Transfer Model for Indoor Air Emissions from Surface Coatings. Indoor Air 3, 263-268.

Tiffonnet, A.-L., Blondeau, P., Allard, F., 2002. Sorption isotherms of acetone on various building materials. Indoor Built Environ 11, 95-104.

Topp, C., Nielsen, P. V., Heiselberg, P., 2001. Influence of local airflow on the pollutant emission from indoor building surfaces. Indoor Air 11, 162-170.

Trikkonen, T., Saarela, K., 1997. Adsorption of VOCs on interior surfaces in full scale building. In: Healthy Buildings/IAQ '97, Washington DC, USA: Blacksburg (VA): 3, 551-556.

Van Der Wal, J. F., Hoogeveen, A. W., Leeuwen, L., 1998. A Quick Screening Method for Sorption Effects of Volatile Organic Compounds on Indoor Materials. Indoor Air 8, 103-112.

Wallace, L. A., Pellizzari, E., Leaderer, B. et al., 1987. Emissions of volatile organic compounds from building materials and consumer products. Atmospheric Environment 21, 385-393.

WHO, 1986. Indoor Air Quality Research, Report on a WHO Meeting, WHO Regional Office for Europe, Copenhagen.

Wieslander, G., Norback, D., Bjornsson, E. et al., 1996. Asthma and the indoor environment: the significance of emission of formaldehyde and volatile organic compounds from newly painted indoor surfaces. International Archives of Occupational and Environmental Health 69, 115-124.

Wolkoff, P., 2001. Where are we with the FLEC? - An overview. In: Proceedings of Second International FLEC Symposium, 6-7th September 2001, Copenhagen, Denmark: National Institute of Occupational Health: 1-8.

Wolkoff, P., Clausen, P. A., Nielsen, P. A., 1995. Application of the Field and Laboratory Emission Cell "FLEC" - Performance Study, Intercomparison Study, and Case Study of Damaged Linoleum in an Office. Indoor Air 5, 196-203.

Wolkoff, P., Clausen, P. A., Nielsen, P. A. et al., 1993. Documentation Of Field And Laboratory Emission Cell "FLEC": Identification Of Emission Processes From Carpet, Linoleum, Paint, And Sealant By Modeling. Indoor Air 3, 291-297.

Wolkoff, P., Nielsen, G. D., 2001. Organic compounds in indoor air--their relevance for perceived indoor air quality? Atmospheric Environment 35, 4407-4417.

Won, D., Corsi, R. L., Rynes, M., 2000. New indoor carpet as an adsorptive reservoir for organic compounds. Environ. Sci. Technol. 34, 4193-4198.

Won, D., Corsi, R. L., Rynes, M., 2001a. Sorptive Interactions between VOCs and Indoor Materials. Indoor Air 11, 246-256.

Won, D., Sander, D. M., Shaw, C. Y. et al., 2001b. Validation of the surface sink model for sorptive interactions between VOCs and indoor materials. Atmospheric Environment 35, 4479-4488.

Woodbury, K. A. (Ed.), 2003. Inverse engineering handbook, Boca Raton, FL : CRC Press.

Xi, Y., Bazant, Z. P., Molina, L. et al., 1994. Moisture diffusion in cementitious materials: moisture capacity and diffusivity. Advanced Cement Based Materials 1, 258-266.

Xu, Y., Zhang, Y., 2003. An improved mass transfer based model for analyzing VOC emissions from building materials. Atmospheric Environment 37, 2497-2505.

Xu, Y., Zhang, Y., 2004. A general model for analyzing single surface VOC emission characteristics from building materials and its application. Atmospheric Environment 38, 113-119.

Yang, X., 1999. Study of Building Material Emissions and Indoor Air Quality. Ph.D. Thesis, Massachusetts Institute of Technology, Cambridge, MA.

Yang, X., Chen, Q., 2001. A Coupled Airflow and Source/Sink Model for Simulating Indoor VOC Exposures. Indoor Air 11, 257-269.

Yang, X., Chen, Q., Bluyssen, P. M., 1998. Prediction of Short-term and Long-term VOC Emissions from SBR Bitumen-Backed Carpet Under DIfferent Temperatures. ASHRAE Transactions 104, 1297-1308.

Yang, X., Chen, Q., Zeng, J. et al., 2001a. Effects of Environmental and Test Conditions on VOC Emissions from "Wet" Coating Materials. Indoor Air 11, 270-278.

Yang, X., Chen, Q., Zeng, J. et al., 2001b. A mass transfer model for simulating volatile organic compound emissions from 'wet' coating materials applied to absorptive substrates. International Journal of Heat and Mass Transfer 44, 1803-1815.

Yang, X., Chen, Q., Zhang, J. S. et al., 2001c. A mass transfer model for simulating VOC sorption on building materials. Atmospheric Environment 35, 1291-1299.

Yang, X., Chen, Q., Zhang, J. S. et al., 2001d. Numerical simulation of VOC emissions from dry materials. Building and Environment 36, 1099-1107.

Yu, C., Crump, D., 1998. A review of the emission of VOCs from polymeric materials used in buildings. Building and Environment 33, 357-374.

Zhang, J., Chen, Q., Zhang, J. et al., 2002a. A Critical Review on Studies of Volatile Organic Compound (VOC) Sorption by Building Materials. ASHRAE Transactions 108, 162-174.

Zhang, J., Zhang, J., Chen, Q., 2002b. Effects of Environmental Conditions on the VOC Sorption by Building Materials-Part I: Experimental Results. ASHRAE Transactions 108, 273-282.

Zhang, J., Zhang, J., Chen, Q., 2003. Effects of Environmental Conditions on the VOC Sorption by Building Materials-Part II: Model Evaluation. ASHRAE Transactions 109, 167-178.

Zhang, J. F., Smith, K. R., 2003. Indoor air pollution: a global health concern. British Medical Bulletin 68, 209-225.

Zhang, J. S., Nong, G., Shaw, C. Y., 1999. Sink characteristics of a full-scale environmental chamber and their impact on material emission testing. ASHRAE Transactions 105, 400-413.

Zhang, L. Z., Niu, J. L., 2003a. Effects of substrate parameters on the emissions of volatile organic compounds from wet coating materials. Building and Environment 38, 939-946.

Zhang, L. Z., Niu, J. L., 2003b. Laminar fluid flow and mass transfer in a standard field and laboratory emission cell. International Journal of Heat and Mass Transfer 46, 91-100.

Zhang, L. Z., Niu, J. L., 2003c. Mass transfer of volatile organic compounds from painting material in a standard field and laboratory emission cell. International Journal of Heat and Mass Transfer 46, 2415-2423.

Zhang, L. Z., Niu, J. L., 2004. Modeling VOCs emissions in a room with a single-zone multi-component multi-layer technique. Building and Environment 39, 523-531.

Zhang, Y., Xu, Y., 2003. Characteristics and correlations of VOC emissions from building materials. International Journal of Heat and Mass Transfer 46, 4877-4883.

Zhao, D., Little, J. C., Cox, S. S., 2003. Sorption/Desorption behaviour of polyurethane foam. In: Healthy Buildings 2003: 7th International Conference Energy-Efficient Healthy Buildings, 7-11th December, School of Design & Environment, National University of Singapore, Singapore: 166-171.

Zhao, D., Little, J. C., Cox, S. S., 2004. Characterizing Polyurethane Foam as a Sink for or Source of Volatile Organic Compounds in Indoor Air. Journal of Environmental Engineering 130, 983-989.

Zhao, D., Little, J. C., Hodgson, A. T., 2002. Modeling the reversible, diffusive sink effect in response to transient contaminant sources. Indoor Air 12, 184-190.

Zhu, J., Newhook, R., Marro, L. et al., 2005. Selected volatile organic compounds in residential air in the city of Ottawa, Canada. Environmental Science and Technology 39, 3964-3971.

Zhu, J., Zhang, J., Shaw, C.-Y., 1999a. Chemical composition analysis and its application in estimation of VOC emission rates from hydrocarbon solvent-based indoor materials. Chemosphere 39, 2535-2547.

Zhu, J. P., Magee, R. J., Zhang, J. S. et al., 1999b. Characterization of emissions of aliphatic aldehydes and monoterpenes from wood-based building materials using small dynamic environmental test chamber. In: Proceedings of Air and Waste Management Association's 92th Annual Meeting and Exhibition, 14-18 June 1999, St. Louis, MO, USA: 74-99.